

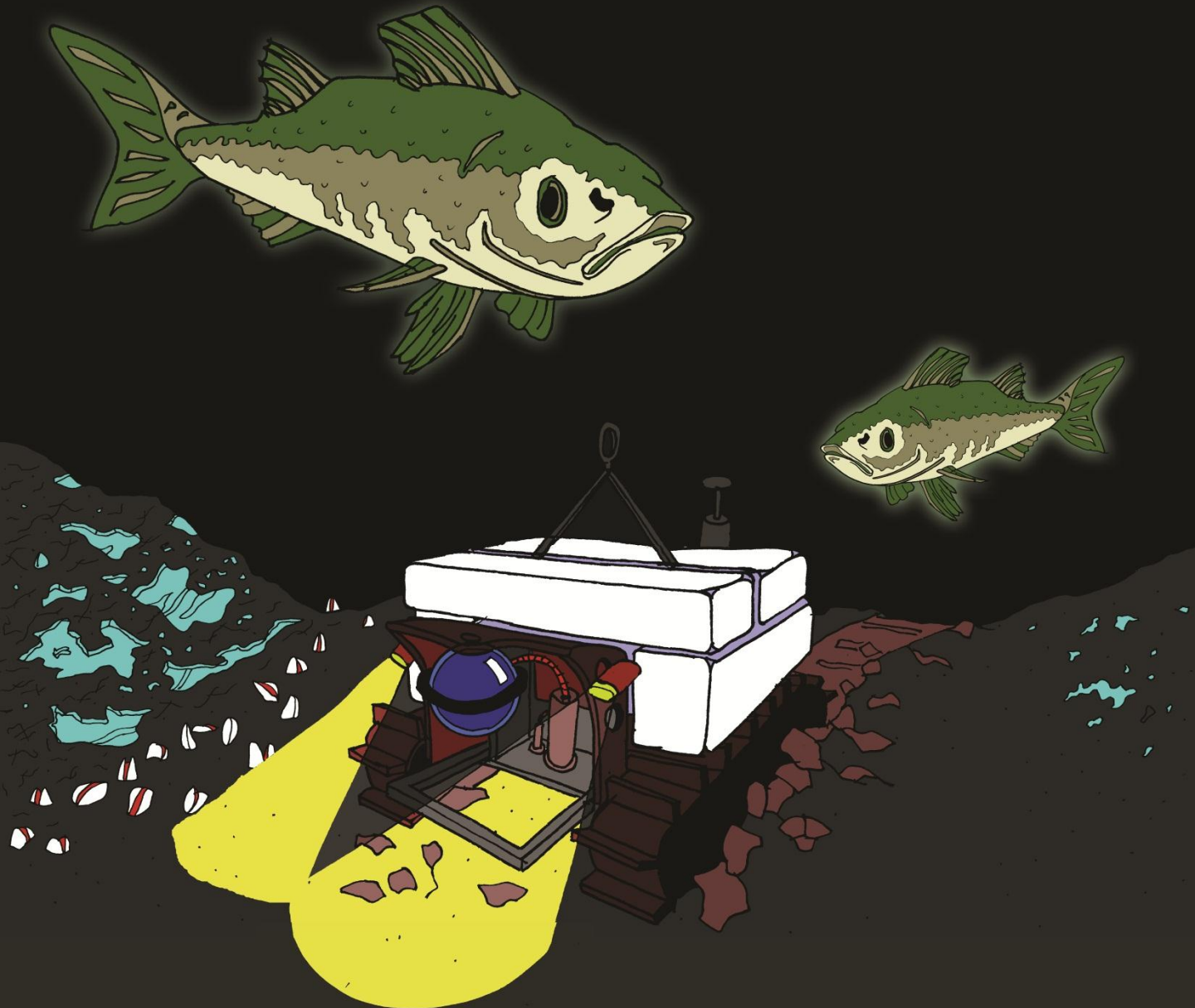
The use of new multiparametric observatory platforms
for the remote monitoring and exploration
of deep-sea ecosystems
at day-night and seasonal temporal scales



Carolina Doya Le Besnerais

SUPERVISOR :
DR. JACOPO AGUZZI

CO-SUPERVISOR:
DR. JOAN BAPTISTA
COMPANY I CLARET





The use of new multiparametric observatory platforms for the remote monitoring and exploration of deep-sea ecosystems at day-night and seasonal temporal scales

Carolina Doya Le Besnerais

ADVERTIMENT La consulta d'aquesta tesi queda condicionada a l'acceptació de les següents condicions d'ús: La difusió d'aquesta tesi per mitjà del repositori institucional UPCommons (<http://upcommons.upc.edu/tesis>) i el repositori cooperatiu TDX (<http://www.tdx.cat/>) ha estat autoritzada pels titulars dels drets de propietat intel·lectual **únicament per a usos privats** emmarcats en activitats d'investigació i docència. No s'autoritza la seva reproducció amb finalitats de lucre ni la seva difusió i posada a disposició des d'un lloc aliè al servei UPCommons o TDX. No s'autoritza la presentació del seu contingut en una finestra o marc aliè a UPCommons (*framing*). Aquesta reserva de drets afecta tant al resum de presentació de la tesi com als seus continguts. En la utilització o cita de parts de la tesi és obligat indicar el nom de la persona autora.

ADVERTENCIA La consulta de esta tesis queda condicionada a la aceptación de las siguientes condiciones de uso: La difusión de esta tesis por medio del repositorio institucional UPCommons (<http://upcommons.upc.edu/tesis>) y el repositorio cooperativo TDR (<http://www.tdx.cat/?locale-attribute=es>) ha sido autorizada por los titulares de los derechos de propiedad intelectual **únicamente para usos privados enmarcados** en actividades de investigación y docencia. No se autoriza su reproducción con finalidades de lucro ni su difusión y puesta a disposición desde un sitio ajeno al servicio UPCommons. No se autoriza la presentación de su contenido en una ventana o marco ajeno a UPCommons (*framing*). Esta reserva de derechos afecta tanto al resumen de presentación de la tesis como a sus contenidos. En la utilización o cita de partes de la tesis es obligado indicar el nombre de la persona autora.

WARNING On having consulted this thesis you're accepting the following use conditions: Spreading this thesis by the institutional repository UPCommons (<http://upcommons.upc.edu/tesis>) and the cooperative repository TDX (<http://www.tdx.cat/?locale-attribute=en>) has been authorized by the titular of the intellectual property rights **only for private uses** placed in investigation and teaching activities. Reproduction with lucrative aims is not authorized neither its spreading nor availability from a site foreign to the UPCommons service. Introducing its content in a window or frame foreign to the UPCommons service is not authorized (*framing*). These rights affect to the presentation summary of the thesis as well as to its contents. In the using or citation of parts of the thesis it's obliged to indicate the name of the author.



**UNIVERSITAT POLITÈCNICA
DE CATALUNYA
BARCELONATECH**



The use of new multiparametric observatory platforms for the remote monitoring and exploration of deep-sea ecosystems at day-night and seasonal temporal scales

**Uso de la nuevas plataformas de observación submarinas para el monitoreo
remoto y exploración de los ecosistemas del mar profundo a escalas temporales
de día-noche y estacionales**

Carolina Doya Le Besnerais

Tesis presentada para la obtención del título de Doctora por la Universitat
Politécnica de Catalunya (UPC)

Programa de Doctorado de Ciencias del Mar 2017

Director:

Dr. Jacopo Aguzzi

Co-director:

Dr. Joan Baptista Company y Claret

Dept. Recursos Marinos Renovables,
Instituto de Ciencias del Mar (ICM) del Consejo Superior de Investigaciones Científicas (CSIC)

“The use of new multiparametric observatory platforms for the remote monitoring and exploration of deep-sea ecosystems at day-night and tidal temporal scales”

The author has been financed by a FPI pre-doctoral grant from April 2012 to April 2015 (BES-2010-042728). The research presented in this Ph.D. Thesis was carried out in the framework of the project RITFIM (CTM2010-16274).

The graphic art in the cover is a reproduction of the original work by ©Autun Purser
Barcelona, May 2017

Abstract

Traditional sampling technologies such as trawling but also novel ones as ROV surveying are oriented toward a high spatial coverage without repeating data collection at fixed seabed windows. The temporal repetition is often neglected so any reported difference in sampling among sites or studies may potentially be confounded with time-induced variations as a product of rhythmic population displacements within the continental margin seabed and water column 3D scenarios. Behaviour is an important life trait conditioning our perception of deep-sea biodiversity, being its rhythmic expression upon different diel (i.e. 24-h based day-night and tidal cycles) poorly known. In this context, technological step forward must be taken in order to observe community changes in deep-sea areas as a product of population behavioural patterns. Here, I studied how activity rhythms of benthic species within deep-sea communities modulate their composition, species abundances, richness, biodiversity and other life-history trait information in representative deep-sea environments through the use of multiparametric video-fixed cabled and non-cabled stations plus moving platforms. At the same time, I provided new methodological sampling hints on data collection protocols and analyses specifically tuned to the different characteristic of each observatory platform. I shed new light on the regulation that environmental cycles exert on animals' rhythmic behavior, revealing that the main environmental rulers affecting deep-sea benthic communities are still day-night indirect or more direct tidal-oriented cycles which act on endobenthic, benthopelagic, and nektobenthic migrations.

Keywords: behavioral rhythms, tidal cycles, day-night cycles, observational technologies, cabled observatories, time-lapse imaging, rovers, landers, day-night and tidal rhythms, richness, biodiversity, benthopelagic coupling, nektobenthic migrations.

Resumen

Las tecnologías de muestreo tradicionales, como la pesca de arrastre, pero también las nuevas, como los trabajos con ROV, están orientadas hacia una elevada cobertura espacial sin necesariamente repetir la recopilación de datos en ventanas fijas de los fondos marinos. Esa repetición temporal es a menudo obviada por lo que cualquier diferencia en el muestreo entre sitios o estudios puede quedar enmascarada por las variaciones a escala temporal como resultado de los desplazamientos rítmicos de la población dentro del margen continental marino y el volumen tridimensional de columna de agua. El comportamiento en los animales es un rasgo importante que condiciona nuestra percepción de la diversidad biológica de los fondos marinos, siendo su expresión rítmica diaria (es decir, ciclos día-noche y mareales) mal conocida. En este contexto, hay una necesidad de avance tecnológico y metodológico que permita la observación de las variaciones en las comunidades del mar profundo en las zonas de aguas profundas como producto de los patrones de comportamiento poblacional. Aquí estudié cómo los ritmos comportamentales de las especies bentónicas y bentopelágicas modulan composición, abundancia de especies, riqueza, diversidad biológica y otra información del ciclo biológico de dichas especies y comunidades dentro de ecosistemas representativos del mar profundo mediante el uso de sistemas de cableado submarino multiparamétrico, plataformas submarinas no cableadas y plataformas submarinas móviles. Al mismo tiempo, aporté nuevas recomendaciones metodológicas sobre protocolos de recolección y análisis de datos específicamente ajustadas a las diferentes particularidades y necesidades de las susodichas tecnologías de observación submarina. Los resultados de este trabajo han ayudado a comprender mejor la regulación que los ciclos ambientales ejercen sobre el comportamiento rítmico de los animales, revelando que los principales factores ambientales que gobiernan las comunidades bentónicas de aguas profundas siguen siendo el ciclo día-noche de forma indirecta y el mareal de forma más directa que actúan modulando los desplazamientos endobentónicos, bentopelágicos y migraciones nektobentónicas.

Palabras clave: ritmos de comportamiento, ciclos mareales, ciclos día-noche, tecnologías de observación submarina, observatorios cableados, imágenes en tiempo transcurrido, rovers, landers, ritmos diurnos y de marea, riqueza, biodiversidad, acoplamiento bentopelágico, migraciones nektobentónicas.

Preface

*“ Les bateaux, les engins, l’argent, les hommes, moi-même,
tout ça c’est de la quincaillerie.*

*Ce qui compte, c’est l’œuvre accomplie: dans un siècle on nous aura oublié,
mais on se souviendra encore de ce que nous avons filmé et dit”*

Jacques-Yves Cousteau

Als meus pares i germans...
A mis padres y hermanos...
À mes parents et frères...
To my parents and brothers...

Table of contents

Abstract.....	i
Resumen.....	ii
Preface	iii
Table of contents.....	v
List of Figures	viii
List of Tables	xiv
List of Appendix	xv
Agraïments/Agradecimientos/Remerciements/Acknowledgements.....	xix
Introduction. State of the art, hypotheses and objectives.....	1
1. Ocean services, major pressures, and motivation for Seafloor Observatories	3
2. Temporal bottleneck in marine sampling strategies.....	4
3. Activity rhythms in the three-dimensional marine scenario	5
4. New seafloor monitoring technologies	6
5. Imaging as strategic monitoring approach linking animal behavior to ecosystem functioning	7
6. Current cabled observatory network initiatives worldwide	8
7. Limitations to the ecological monitoring by cabled observatories imaging in the deep sea and envisaged solutions	10
8. Thesis hypotheses and objectives.....	12
Chapter 1. Diel behavioral rhythms in sablefish (<i>Anoplopoma fimbria</i>) and other benthic species, as recorded by the deep-sea cabled observatories in Barkley canyon (NEPTUNE-Canada).....	15
1.1 Abstract	17
1.2 Introduction	18
1.3 Material and methods	19
1.3.1 Cabled network specifications	19
1.3.2 Data acquisition and time series processing.....	20
1.3.3 Size-frequency distribution	21
1.3.4 Light effects	22
1.4 Results	23
1.4.1 Faunal remarks.....	23
1.4.2 Time series analysis	24
1.4.3 Class-size frequency distribution	31
1.4.4 Light effects	31
1.5 Discussion	33
1.5.1 Sablefish behavioral rhythms.....	33
1.5.2 The hagfish and crab behavior	36
1.5.3 The population structure of sablefish.....	36
1.5.4 Biases in cabled observatory video recording.....	37
1.6 Conclusions	38
1.7 Acknowledgments	39
Chapter 2. The seasonal use of small-scale space by benthic species in a transiently hypoxic area....	41
2.1 Abstract	43
2.2 Introduction	44
2.3 Materials and methods.....	45
2.3.1 The platform, the study area, and data acquisition.....	45
2.3.2 Data treatment.....	47

2.3.3	Oxygen relationships	49
2.4	Results	50
2.4.1	Time series analysis	50
2.4.2	Intraspecific dispersion and spatial autocorrelation	53
2.4.3	Interspecific relationships in space use	55
2.4.4	The segregation index (S)	56
2.4.5	Correlation with oxygen.....	57
2.5	Discussion	59
2.5.1	Use of space by <i>Munida</i>	60
2.5.2	Use of space by <i>Lyopsetta</i>	62
2.5.3	Methodology remarks	63
2.6	Conclusions	64
2.7	Acknowledgements	64
Chapter 3.	Seasonal monitoring of deep-sea megabenthos in Barkley Canyon cold seep by Internet Operated Vehicle (IOV).....	65
3.1	Abstract	67
3.2	Introduction	67
3.3	Materials and Methods	70
3.3.1	The NEPTUNE network and the Barkley Canyon node.....	70
3.3.2	The ‘Wally I’ crawler deployment, connectivity, operations and sensor systems	72
3.3.3	Faunal data collection and treatment	73
3.3.4	Analysis of the community structure linkage with oceanographic variables	74
3.3.5	Ethological remarks	75
3.4	Results	76
3.4.1	Seasonal patterns.....	76
3.4.2	Analysis of the community structure linkage with oceanographic variables	80
3.4.3	Ethological remarks	84
3.5	Discussion	85
3.5.1	Seasonal patterns and the oceanographic influences	85
3.5.2	Methodological remarks	88
3.6	Acknowledgements	90
Chapter 4.	Faunal activity rhythms influencing early community succession of an implanted whale carcass offshore Sagami Bay, Japan	91
4.1	Abstract	93
4.2	Introduction	94
4.3	Materials and Methods	96
4.3.1	The study site and the experimental setting	96
4.3.2	Data analysis	99
4.4	Results	101
4.4.1	Benthic and scavenger community composition.....	101
4.4.2	Time series analysis outputs	103
4.4.3	Multivariate analysis outputs	107
4.5	Discussion	111
4.6	Acknowledgements	115
Discussion.....		117
1.	Internal and external validity of the thesis	120
1.1	First objective:time as ruler of deep-sea community changes	120

1.2 The Second objective: community composition, dynamics and behavior of species in deep-sea environments.....	122
1.3 Third objective: methodology remarks	123
2. Recommendations and future researches	126
Conclusions.....	129
References.....	133
Appendix.....	159
Credits.....	179

List of Figures

Figure I. Seafloor video-observatory networks that has been or are being implemented at different depths of the continental margin, from coastal areas to the deep sea, having the chance to be used to monitor different areas experiencing anthropic impacts (from Danovaro et al. 2017)..... 8

Fig.1. Coarse bathymetric map of the Barkley canyon site, showing the locations of video-stations POD 1, POD 3 and POD 4, as part of NEPTUNE-Canada seafloor observatory infrastructure. Camera platforms (black dots) are powered by a local node (black triangle) through extension cables. Isobaths (dashed lines; in meters) account for the local canyon morphology 19

Fig.2. 14th October to 14th November 2011 time series in visual counts for the three most abundant taxa (i.e. sablefish, hagfish and crabs), as reported by summing data of the three cameras deployed in Barkley canyon by NEPTUNE-Canada. These fluctuations have been reported along with fluctuations in the northerly and easterly components of the tidal currents (gray, north–south; black, east–west). These currents, made up of the combined effect of the K1, M2, N2, and S2 tidal constituents, are considered markers for the local mixed diurnal/semidiurnal tidal regime. Note the differences in fluctuation amplitude of both tidal components and in the abundance values for the three analyzed taxa. Vertical lines delimit consecutive 24-h cycles..... 26

Fig.3. Periodogram analysis outputs on time series of visual counts for the three taxa, as obtained from video recording with the three NEPTUNE-Canada cameras within Barkley canyon. Periodogram results for the time series of Fig. 2 are to the left. For the much abundant sablefish this analysis was repeated for each camera separately (on the right), which showed different significant rhythmicity (reported in min by the percentage of variance peak crossing the significant threshold set at $p < 0.05$). 27

Fig.4. Waveform analysis output plots for visual counts and oceanographic time series for the three taxa, as obtained from video recording with the three NEPTUNE-Canada cameras within Barkley canyon. Results for species depicted in Fig. 2 (in black) and for current velocities (along the significant tidal North–south component U; in gray) account for the absence of any strong diel fluctuation in the former. Only sablefish seems to present a bimodal pattern, with a major and a minor peak (i.e. values above the MESOR) at night-time and in antiphase with water speed increases. MESOR values (dashed lines) account for the overall differences in the abundance of the three taxa and are equal to 5.06 for sablefish, 0.23 for hagfish and 0.14 for crabs. The gray square accounts for the average night duration during the month of October..... 29

Fig.5. Waveform analysis output plots on visual count time series for sablefish separately for each NEPTUNE-Canada camera within Barkley canyon (i.e. POD 1, POD 3 and POD 4). Again, MESOR

values (dashed lines; POD 1 = 1.7; POD 3 = 1.1; POD 4 = 2.3) account for markedly different abundances and timing of phases, shifting from uni-modal at night-time (POD 1) to crepuscular bimodal (POD 4) or arrhythmic (POD 1). 30

Fig.6. Class-size frequency distribution representing total body length of measured sablefish (N = 195) at the three NEPTUNE-Canada cameras installed in Barkley canyon. That class-size analysis has been repeated by representing total body length of measured sablefish separately for each POD camera. The average length (\pm SD) was 63.6 ± 10.4 cm and the three frequency distributions showed similar shapes. 31

Fig.7. Linear regressions depicting the light effect on reported visual counts of sablefish during footage acquisition, as observed in 15 videos randomly selected from those acquired by the three NEPTUNE-Canada cameras (i.e. POD 1, POD 3, and POD 4) during the first five days of experiment. The regression has been obtained after dividing each video recording length in two intervals (i.e. 0–25 and 26–50 s). 32

Fig.8. Modelled typologies of rhythmic displacement of sablefish within the Barkley canyon, as reported by coupling wave form analysis of data sets from the three NEPTUNE-Canada cameras located respectively at the outer canyon flank (POD 3), the inner canyon flank (POD 4) and the deeper canyon axis (POD 1). Apparently, fish perform benthopelagic displacements within the water column (vertical gray-night and white-day arrows) as well as deeper nektobenthic displacements (same type of arrows) back and forth between canyon flank and axis. Waveforms analysis output plots (on the right; adapted from Fig. 5) present a timing shift in rhythm phase (i.e. values above the MESOR), which seems to be related to depth variations in the location of the cameras. 35

Fig.9. Map of Saanich Inlet, showing the location of the camera, as part of the VENUS Cabled Observatory infrastructure (black triangle). 46

Fig.10. The selected VENUS camera field of view, with individuals for the three groups: large (A) and small *M. quadrispina* (B) plus *L. exilis* (C). The main seabed structures within the area are the PVC scale and the sponges (indicated by the arrows). The image was taken at 18:48 h UTC, on September 29, 2012. 47

Fig.11. The field of view used at VENUS, subdivided by the digital grid (red lines) drawn a posteriori and used as a reference system of coordinates to calculate exact animal positioning. The PVC black and white frame was briefly deployed by ROV to calculate the field of view surface and the correction factor. 48

Fig.12. One-year time series (from 2nd March 2012 to 26th February 2013) of visual counts per image for the three groups studied (large and small *M. quadrispina* plus *L. exilis*), along with the

dissolved oxygen concentration. The dashed vertical lines correspond to the 1st of each month. The y-axis scale differs between the three groups.51

Fig.13. The massive aggregation of *M. quadrispina* observed at VENUS during the first 10 days of June. This image was taken at 10:16 h UTC on June 05 2012.52

Fig.14. Year-long relative density maps present the averaged distribution of the three groups (large and small *M. quadrispina* plus *L. exilis*), using the gray scale as a proxy for the number of counts (black and white parcels indicate the highest and the zero counts of animals, respectively). The significant differences in occupation levels are also presented (over-occupied and under-occupied parcels are in yellow and red, respectively). In the schematic map (upper left corner), positions of relevant areas within the field of view are indicated by black crosses (sponges), the black bar (the PVC pipe), and ellipses (where seabed is particularly rough).53

Fig.15. Moran's I correlogram for the number counts of A. large *M. quadrispina*; B. small *M. quadrispina*; and C. *L. exilis*. Black dots represent spatial autocorrelation coefficients significant at the $\alpha=5\%$ level, before applying the Bonferroni correction; white dots are nonsignificant values. Coefficients for the larger distance values (grey zones in correlograms) should not be interpreted, because they are based on a small number of pair (test with low power) and only include the pairs of points bordering the surface. The horizontal red line helps to identify the sign of the spatial autocorrelation coefficient.55

Fig.16. Segregation index (S) over time for each group of animals with respect to the nearest: A. large *M. quadrispina*; B. small *M. quadrispina*; and C. *L. exilis*. On each graph, large *M. quadrispina* (dark gray line), small *M. quadrispina* (light gray) and *L. exilis* (black) are shown. Gaps in S time series represent absence of intraspecific neighbors.57

Fig.17. Linear regression depicting the effect of oxygen levels on the monthly S index for the small—large *M. quadrispina* pair at VENUS during the study.58

Fig.18. Cross-correlation between: A. SFL; B.SFF; C.SSF; D.SSL and oxygen concentrations. The maximum (or minimum if the signals are negatively correlated) of the cross-correlation function indicates the point in time where the signals are best aligned. The blue dashed line represents the confidence intervals of the cross-correlation.59

Fig.19. Overview map of the cold-seep site in Barkley Canyon (northeast Pacific, Canada). (A) The cabled observatory network, The Barkley Canyon node, site of Wally I crawler deployment is highlighted by a black dot. (B) High-resolution bathymetric map showing the region of Barkley Canyon investigated in the current study. The black dots within the canyon axis represent the crawler node with the nearby mid-canyon POD4 platform and other deeper nodes. (C) Image demonstrating the crawler Field Of View (FOV) as used to acquire the faunal data. (D) Map showing position of navigation

waypoints arranged around the hydrate outcrop, the crawler (near waypoint no. 12 in this schematic) and the route from waypoint no. 10 to 14, representing the survey transect analysis area. The cold seep community was distributed on a soft bottom zone with no apparent emerging rocks. At the end of the transect analysis area, a 5 m depth cliff (dashed grey line) separated our study area from a from the gas-hydrate mound (E) The crawler in operation. 71

Fig.20. Visual counts time series (i.e. from 14th February 2013 to 14th April 2014) for the 7 most abundant megafaunal species and the particular case of the grooved tanner crab, as reported by crawler video-imaging. Average values (the grey dots) have been reported in order to better highlight the occurrence of seasonal trends. From left to right and from top to bottom taxonomic units are: Rockfish (i.e. Sebastidae); Sablefish (*Anoplopoma fimbria*); Hagfish (*Eptatretus stoutii*); Buccinid (Neptunidae); Small crab; Grooved tanner crab (*Chionnecetes tanneri*); Ctenophore (*Bolinopsis infundibulum*); and finally, Scyphomedusa (*Poralia rufescens*). Horizontal blue dashed lines correspond to the Midline Estimated Statistic of Rhythm (MESOR) and horizontal blue lines identify significant seasonal increases visual counts increases. Blue asterisks correspond to a month with no data due technical problems. 77

Fig.21. Oceanographic parameters time series (i.e. from 14th February 2013 to 14th April 2014), as recorded by crawler and the nearby POD4 platform within the Barkley Canyon. Average values (the grey dots) have been reported in order to better highlight the occurrence of seasonal trends. Gaps in data acquisition were due to instrument malfunctioning or downtime for the cabled infrastructure. These parameters are: (A) Velocity; (B) Water Density; (C) Temperature; (D) Turbidity; (E) Bakun Index; and finally, (F) Oxygen. We used up-looking and down-looking arrows to highlight upwelling and downwelling periods respectively. 79

Fig.22. Results of fitting environmental variables onto species ordination. The increasing gradient of the environmental variable is indicated by the vector direction. The vector length is proportional to the correlation between the variable and the ordination pattern of the species. Species abbreviations are (taxonomical order; see S1 Table): Eel (*Eelpout*, *Licenchelys* spp.); Dov (Dover sole, *Microstomus pacificus*); Dee (Deep sea sole, *Embassichthys bathybius*); Pac (Pacific halibut, *Hippoglossus stenolepis*); Rat (Rattail, *Coryphaenoides* spp.); Roc (Rockfish, i.e. Sebastidae); Bac (Blackfin poacher, *Bathyagonus nigripinnis*); Sab (Sablefish, *Anoplopoma fimbria*); Hag (Hagfish *Eptatretus stoutii*); Sal (Salp, Salpidae); Dum (Dumbo octopus, *Grimpoteuthis* sp.); Squ (Squid *Gonopus* sp.); Buc (Buccinids, Neptunidae); Bri (Brittle star, Ophiuroidea); Sf1 (Starfish, *Asteroidea*); Sf2 (Starfish, *Zoroasteridae*); St3 (*Hippasteria* sp.); Hol (Holoturian, Holoturoidea); Her (Hermit crab, *Diogenidae*); Sca (Scarlet king crab, *Lithodes couesi*); Gro (Grooved tanner crab, *Chionnecetes tanneri*); Sma (Small crabs); Cte (Ctenophore, *Bolinopsis infundibulum*); Scy (Scyphomedusa, *Poralia rufescens*); Din (Dinner plate jelly, *Solmissus* sp.); Tra (Traquimedusa, *Voragonema pedunculata*). 81

Fig.23. Biodiversity, richness and megafaunal species visual counts (i.e. from 14th February 2013 to 14th April 2014) time series, as reported by crawler video-imaging. Biodiversity have been reported as mean per month Shannon Index (C) and Simpson Index (A). Similarly, we reported the species richness (D). Abundance (B) was normalized for the maximum transects of the study period (i.e. 48). Horizontal dashed lines correspond to the Midline Estimated Statistic of Rhythm (MESOR)..... 83

Fig.24. Map showing the deployment site of the juvenile sperm whale SW off Sagami Bay (empty triangle) at 500 m depth and in relation to the seafloor cabled video observatory (filled triangle) at 1100 m depth (Aguzzi et al. 2010). The deployment site was about. B. 3D laser scan image of the deployment site shows the whale carcass relative to the ballast used to sink it, the camera and ADCP instrumented landers (courtesy of B. Thorton and A. Bodemann). 97

Fig. 25. Images of the taxonomical units as components of the local megafaunal assemblage detected at whale carcass positioning by time-lapse camera imaging (see also Appendix G): A. *Pannychia moseleyi*; B. *Echinothurioida*; C. *Solaster paxillatus*; D. *Ophiurida*; E. *Buccinum yoroianum*; F. *Bathynomus doederleini*; G. *Macrocheira kaempferi*; H. *Hexanchus griseus*; I. *Cephaloscyllium umbratile*; L. *Coelorinchus* sp.; M. *Pterothrissus gissu*; N. *Zoarcidae*; O. *Physiculus japonicus*; P. *Simenchelys parasiticus*; Q. *Helicolenus hilgendorffi*; and finally, R. *Eptatretus deani*..... 101

Fig.26. Temporal changes in the whale carcass positioning with respect to the camera field of view as detected by time-lapse imaging. A. 06.15.2012 to 07.15.2012; B. 07.15.2012 to 07.26.2012; C. 07.26.2012 to 08.07.2012; and finally, D. 08.07.2102 to 08.24.2012. In A, two individuals of *Solaster paxillatus*, and single individuals of *Echinothurioida*, *Ophiuridea*, and *Buccinum yoroianum* are visible. In C and D, two ribs appear on the seafloor..... 102

Fig.27. Temperature at sea bottom, water pressure, vertical and East-West current component as recorded over 72 days by ADCP close to the whale carcass deployment. Whale carcass position changes (see Figure 25) are indicated by vertical light grey dotted lines. 104

Fig.28. Waveform analysis outputs for the visual count time series of those species showing significant 24 hrs. periodicity patterns in the periodogram analysis (see Appendix G for A. *S. parasiticus*, B. *M. kaempferi*, and C. *P.gissu*). Note the varying Y-axis abundance scales. Up and down arrows indicate onset and offset of significant increments in abundance peaks, respectively. They also indicate the first and last calculated mean abundance values above the Midline Estimated Statistic Of Rhythm (MESOR as dashed horizontal lines) line as re-average of all waveform data. MESORs are: A, 4.76; B, 1.18; C, 0.46. The correspondent integrated diurnal displacements (m) along the E-W axis, computed from the FFT results, are superimposed, showing a 2 hrs. delay in the animal periodicity. 106

Fig.29. Cluster analysis of the mean abundance values by day of species recorded at the whale fall for factor “week”. Black lines indicate significant separation at $p < 0.05$ according to SIMPROF test;

B. Bubble nMDS plots with over imposed cluster analysis results (at 60% of resemblance level) of two of the dominant taxa of each phase (weeks 1-6 vs. 7-11): *Macrocheira kaempferi* and ophiuroids..... 108

Fig.30. Scatter plot of the first two axes of the CANOCO. Species and trophic categories (i.e. scavengers, predators, and detritivores) were represented by black points and environmental variables were represented by red vectors. Environmental variables considered are: Date of the observation as “Date”, spatial components of current velocity as “EW_Comp_V” and “Vert_Comp_V”, as well as Depth, Temperature and the time shifted. B, Bar chart of the loadings relative to the first latent vector (explained variance = 77.44%) for both environmental and species blocks (no. 1 and 2, respectively). . 110

List of Tables

Table 1 Complete list of faunal observations (number plus relative percentages) as reported by NEPTUNE-Canada color video cameras installed in Barkley canyon, including the targeted species. That list is complete only for platforms POD 1 and POD 3 on the canyon flank. Such a list is incomplete for platform POD 4, given the lower resolution of its video camera, which in most cases prevented the identification of smaller animals.....	24
Table 2. Interspecific dominance relationships, presented as the percentage of significantly more (+) or less (-) occupied parcels over the total (i.e., 81), as observed over a month. All significant (*) comparisons ($p < 0.0001$) are indicated	56
Table 3: Kruskal-Wallis test among the 14 months of the study for the 8 most abundant species with 13 degrees of freedom.....	80
Table 4 Results of the SIMPER analysis carried out on the two periods (weeks 1-6 vs. 7-11) evidenced by multivariate analysis	109

List of Appendix

Appendix A. Annual Pearson's goodness of fit test for each of the three groups under the null hypothesis of equal probability of parcel occupation. Only significantly more occupied parcels (critical value ($p = 0.001$) = $\sqrt{X_{20.001, 80/81}} = 1.24$) are shown.	161
Appendix B. Monthly heat maps calculations for the three groups of benthic animals. See Figure 6 for specifications on grey scale (i.e. occupation) and on red and yellow outlining (occupation significance).	162
Appendix C. Monthly Segregation Index (S) values between pairs of groups (F, slender sole; L - S, large and small squat lobsters, respectively). Missing values occurred when one of the species was absent. In bold are reported intraspecific S values representing the degree of aggregation between conspecifics, whereas normal-text S values reports the degree of segregation between different groups	165
Appendix D. Monthly total visual counts and percentages for the different megafaunal species studied during the 14 months of video acquisition.	166
Appendix E. Date and time of the reported ethological remarks. (A) Rockfish (Sebatidae) agonistic display against the crawler (i.e. approaching the camera with the open mouth and then escaped). (B) Sablefish (<i>Anoplopoma fimbria</i>) swimming close to the crawler. (C) Male scarlet king crab (<i>Lithodes couesi</i>) feeding behavior and agonistic interaction with a grooved tanner crab. (D) Grooved tanner crab (<i>Chionoecetes tanneri</i>) agonistic display against the (i.e. an elevated body posture and chelipeds forward projection). (E) Grooved tanner crab reproduction behaviour. (F) Female grooved tanner crabs carrying eggs.	167
Appendix F. Photo-mosaic of all species portrayed with the camera installed on the crawler during the 14 months of video acquisition. Individuals in images are: (A) Eelpout (<i>Licenchelys</i> spp.). (B) Dover sole (<i>Microstomus pacificus</i>). (C) Deep sea sole (<i>Embassichthys bathybius</i>). (D) Pacific halibut (<i>Hippoglossus stenolepis</i>). (E) Rattail (<i>Coryphaenoides</i> spp.). (F) Rockfish (Sebastidae). (G) Rockfish (Sebastidae). (H) Rockfish (Sebastidae). (I) Blackfin poacher (<i>Bathyagonus nigripinnis</i>). (J) Sablefish (<i>Anoplopoma fimbria</i>). (K) Hagfish. (L) Dumbo octopus (<i>Grimptoteuthis</i> spp.). (M) Squid. (N) Buccinids (<i>Neptunidae</i>). (O) Brittle star (<i>Ophiuroidea</i>). (P) Starfish (Asteroidea). (Q) Holoturian. (R) Hermit crab. (S) Scarlet king crab. (T) Grooved tanner crab (<i>Chionoecetes tanneri</i>). (U) Male (left) and female (right) of grooved tanner crab facing each other as a part of their reproduction behaviour. (V) Male (left) carrying out a female (right) of grooved tanner crab as a part of their reproduction behaviour. (W) Small crabs, probably small individuals of grooved tanner crab. (X) Ctenophore (<i>Bolinopsis infundibulum</i>). (Y) Scyphomedusa (<i>Poralia rufescens</i>). (Z) Dinner plate jelly (<i>Solmissus</i> spp.). (AA) Traquimedusa (<i>Voragonema pedunculata</i>).	168

Appendix G. Taxonomical assemblage detected over 72 days starting on 14 June 2012 are hierarchically listed by phylogeny and grouped according to behavioral traits (type of movement and life habit as relationship with the seabed), along with bibliographic sources used to derive such an information. The number of individuals per species (N), their relative abundances (%), periodogram analysis outputs as significant ($p < 0.05$) periodicities(P) in minutes (min) and hours (hrs.) are reported along with periodogram peak variance (Var., %) as proxy of rhythm strength. In the periodicity column, we also reported in parenthesis significant sub-periodicities as a proxy of weak tidal patterning. Total animal abundance by functional groups with respect to the 3 trophic groups is also provided..... 169

Appendix H. Seventy-two days-time series of visual counts for the different macrofauna taxonomical units identified during the scavenging process of the sunken whale carcass (following the same taxonomical order of Figure 2). Vertical dashed grey lines are the whale change positioning (see Figure 3)..... 171

Appendix I. Time series of horizontal current data from the ADCP, at 5 m, 32 m, 62 m and 92 m above sea bottom, applying a 25 hrs. moving average window. Red and blue lines represent North-South and East-West component respectively. Black lines show the fluctuations of current velocity. 172

Appendix J. Stick diagrams of horizontal current data from the ADCP, at 5 m, 32 m, 62 m and 92 m above sea bottom, applying a 25 hrs. moving average window. Southeastward flows are dominant in the first 30 m above the sea bottom, whereas northwestward flow characterizes the water column from 32 m to 92 m above the sea bottom, creating a two-layer system. 173

Appendix K. Time series of vertical current data from the ADCP, at 5 m, 32 m, 62 m and 92 m above sea bottom, applying a 25 hrs. moving average window. Dominant negative values indicate prominent downward flow in each layer, especially close to the bottom. 174

Appendix L. Power Spectra of water temperature, East-West, North-South and Vertical components of the velocity current data from the ADCP, at 5 m above sea bottom. Spectra of current data clearly show peak periods for 24, 12, and 6 hrs., whereas peaks for temperature data are only evident at 12 and 6 hrs. The flow near the sea bottom is affected by tidal periodicity. This rhythm may affect the behavior of marine organism 175

Appendix M. Waveform analysis outputs for ADCP data. Time series in A. have been partitioned in 12 hrs. segments, while time series in B. are at 24 hrs. length to show both diurnal and semidiurnal tides. The MESOR is the dashed horizontal line. The semidiurnal and diurnal Fourier component curves are superimposed for vertical and East-West current components (the dash-dotted lines), showing general accordance with the waveform analysis. 176

Appendix N. Waveform analysis outputs for visual counts time series of A. scavengers (and facultative predators), B. detritivores, and C. predators, indicating the occurrence of significant time

shifted peaks (i.e. values above the MESOR; as horizontal dashed line) in the former (i.e. nocturnal) and the latter group (i.e. diurnal). Conversely, detritivores do not show any defined tendency (although a weak peaking occurs in the morning). MESORs are: A. 6.48; B. 0.99; C. 0.97..... 177

Agraïments/Agradecimientos/Remerciements/Acknowledgements

Recordaré siempre la primera vez que vi un ctenóforo en mis vídeos. Sus cepillos iridiscentes ondulando al unísono y su baile etéreo recordando a una bailarina de vals en sus mejores galas mientras se adentraba en lo impreso de la oscuridad absoluta. Ahí entendí que esto iba a ser una aventura y que me atraparía irremediabilmente por su enigmática y bella naturaleza. En esta aventura me han acompañado muchas personas a las que quisiera mencionar. Seguramente olvide alguna, espero no hacerlo.

Primeramente, quisiera agradecer a mi director Dr. Jacopo Aguzzi y mi co-director Dr. Joan Baptista Company (Batis), la oportunidad que me disteis de entrar en el fascinante mundo de la ecología marina y de las nuevas tecnologías de observación submarina. Vuestra ayuda ha sido inestimable. A Jacopo, los conocimientos que me has transmitido, a nivel científico y existencial. Gracias por tu paciencia, sentido del humor, energía y disponibilidad. A Batis, gràcies pel teu pragmatisme, empatia i per estirar del braç en els moments difícils. També voldria agrair a en Dr.Domènec Lloris, el meu primer contacte a l'ICM, el que sempre estigués disponible per orientar-me des de aquell dia que vaig demanar-li assessorament per meu treball de final de carrera.

I would like to thank all the researchers that I met during my short stays in Canada and Japan. My first contact and supervisor during my stay in Department of Biology of the University of Victoria, BC; Canada, Prof. Verena Tunnicliffe, not only for the astonishing knowledge she shared with me but the way she does it by pointing the finger to the correct doors without opening them. I would like to thank you to be an example of woman in science because of your personality and values. Thanks to the Biology Department team to make feel like home in Victoria. In this context, I would like to specially mention Dr. Jackson Chu and Amalis. Thank you Prof. Kim Juniper to open the doors of the Ocean Networks Canada (ONC) during my stay in Victoria and to invite me to the expedition Wiring the Abyss in which I could understand for real the tools and habitats I was working on. Also thank your advice about how to cope with my wallyland study. The friends I make during the cruise, especially to Maëva and Reyna. That was a gift! I am also enormously grateful to my supervisor during my stay in Japan, Dr. Yoshihiro Fujiwara for his helpfulness during my stay in Japan. Many thanks for your kind assistance in all the aspects, for willing to listen and advice and for all the received knowledge about whale-fall ecosystems. Thank you to give me the opportunity to ship and collaborate in your deep-sea shark project. I keep in mind this moment as a treasure as the bird shooting in Aveiro. Thanks to all the BioGeoscience team of the Japan Agency for Marine Sciences (JAMSTEC) to share great after-work moments and guide me in the amazing Japanese culture and country. I also would like to especially thank you to my dear friends Mitsuko, Kumiko and Yoshie.

Me gustaría dar las gracias a todos los investigadores y estudiantes con los que he tenido la suerte de colaborar. Gracias a M.S. María Pardo por tantas horas invertidas contando bichitos y el trabajo

bien hecho. Gracias al Damianos, por darme la oportunidad de ser su codirectora de tesis de máster, por su sentido del humor y por darme la alegría de un buen resultado. ¡Gracias por las horas invertidas en este proyecto y por los paseos para airear las ideas que siempre terminaban en un “Eureka!”. Al Dr. Nixon Bahamon, por toda la ayuda que me ha brindado con sus amplios conocimientos en estadística que me ayudaron a domesticar el deep sea. Sorprende la modestia, se agradece la amabilidad y disponibilidad para las largas charlas al teléfono. Thank you Dr. Corrado Costa for your help in statistics too. A special thank you to Prof. Laurenz Thomsen to give to me the opportunity to drive your crawler “Wally I and have faith in our project”. It has been one of the best experiences of my Ph.D. Thank you Autun Purser to teach me how to drive the crawler and for your helpfulness from the sampling to the publishing process and of course for the amazing cover that you draw for this thesis. Thanks to my co-authors Fabio De Leo, Marjolaine Matabos, Steve Mihaly, Miquel Canals, Emanuela Faneli, Tiziana Ciuffardi, Antonio Schirone, Masaru Kawato, Makoto Miyazaki and Furushima Yasuo for your valuable help.

Agradecer también al resto de personas del Instituto de Ciencias del Mar que han contribuido a que en mi estancia en el Departamento me haya sentido tan a gusto: la Isabel i el seu somriure, sempre disposada a un consell o un cop de mà i el Miquel Àngel que m’ha tret les castanyes del foc quan l’ordenador ha fet de les seves. La Nuria Angosto i la Conchita Borrueal por su disponibilidad y profesionalidad. No puedo dejar de mencionar a mis compañeros de pasillo y departamento (becarios, técnicos, personal laboral, estudiantes de máster y grado), por todos los momentos vividos a nivel profesional (presentaciones, consejos, cables) como en nuestros fuera del instituto (cervezas, almuerzos, cenas, calçotades, escapadas): Aihnoa, Alba, Alejandro, Alfredo, Amalia, Anabel, Ariadna, Catarina, Chiara, Claudio, Cristina, Dafni, Dani, Daniela, David, Federico, Fernando, Iván, John, José Antonio, Laia, Marta, Morane, Noelia, Paula, Sonia, Susana, Tabita, Ulla, Valeria, Vanesa, Xavi...hicisteis que esta estancia fuera para recordar y me llevo buenas amistades y recuerdos increíbles! Quisiera mencionar especialmente a mis compañeros de despacho Giulia, no sólo compañera de despacho, también de maullidos gatunos y de aventuras varias y a Valerio por ser ejemplo a seguir en tantos aspectos. También a los que los han sustituido, Marta, Marina y Marc por acompañarme último período con su buen humor. A los científicos deportistas con los que hemos compartido grandes momentos: Raquel, Marta, María, Angel, Pau, Raül, y Teresa.

Quisiera también agradecer a mi tutor de la UPC, Dr. Vicente Gracia, el haber aceptado tutelar mi tesis, y al coordinador del programa de doctorado de Ciencias del Mar, Dr. Agustín Sánchez-Arcilla y a Genoveva Comas, por su disponibilidad y por toda la ayuda proporcionada

Ya fuera del ambiente laboral, quisiera agradecer a mis amigos. Gracias Walter por aguantarme con paciencia de santo. A mi compañero de piso y amigo John, Ava y Rachel por los momentos de relax de copa de tinto en terraza, las escapadas, salidas, vuestro sentido del humor y el compañerismo. Gracias por hacer que la casa fuera un hogar. A totes les amistats universitàries que s’han mantingut tants anys, pels plans junts i els bons consells, mercès Albert Fernández, Albert Rivas, Alejandro, Cidalina i Joan.

Als meus amics de tota la vida, mercès pel vostre exemple i pels moments de tant necessària desconexió: Felip, Jess, Marta i Nuria. Ester, mercès tot això i pel cop de mà amb el formatat de la tesis.

I finalment, als meus pares, Josep Lluís i Martine, pel vostre recolzament incondicional, pels valors que m'heu après i per creure en mi. Gracies per mostrar-vos sempre orgullosos de la vostra filla. Merci pour vos conseils et encore merci pour m'aider à faire réalité mon rêve. Al meu germà, Pau, per fer màgia amb la teva agenda i ser la meva línia telefónica resuelve-marrones 24/24h. Mercès per aquestes sorpreses que em fas quan no m'ho espero. Merci à ma sœur Eva, pour nos rires, pour être un exemple de sœur, femme et amie, agencia de viajes Salazar i coach. I també a la Ruth i al Marc, dos amores de mis amores. Sense vosaltres això no hagués estat possible, per això aquesta tesis també és molt vostra. Mencionar als Doya et aux Le Besnerais pour être toujours là bien sûr.

A todos y todas: ¡Muchas gracias! Moltes Mercès! Thank you! Merci!

Introduction. State of the art, hypotheses and objectives

The society is more than ever concerned over the potential impacts of global change according to the World Economic Forum ([Global Risk Report, 2016](#)). This consciousness-raising of society promoted the interest in long-term ecosystems monitoring. There is an increasing demand of services provided by these ecosystems and the natural limits to their supplying still remains unclear. Yet, the collapse threshold of four planetary boundaries (climate change, biosphere integrity, land-system change, and altered biogeochemical cycles) has already been surpassed ([Steffen et al. 2015](#)). The ocean represents the most widespread habitat on Earth's, occupying approximately 75% of the planet the bigger services supplier although surprisingly, only a 5% of the ocean has been explored ([Mora et al. 2011](#)). In this PhD. Thesis, I address this lack of ecological knowledge by using a novel *in situ* observational technology developed in the past 30 years.

1. Ocean services, major pressures, and motivation for Seafloor Observatories

The services that ocean brings to the economy cover several ranges of activities (e.g. fishery, mineral, hydrocarbon, novel molecule extraction and ecotourism). Fishery is one of the principal services that ocean provides to the society. According to the United Nations Food and Agriculture Organization ([FAO 2014](#)), 1 billion people in the planet rely on fish as their primary source of protein. In the past 30 years, fish production and consumption have risen to the point that an important fraction of fisheries are on the verge of collapse or already overexploited ([Worm et al. 2009](#), [Worm and Branch 2012](#), [Watson et al. 2013](#), [FAO, 2016](#)). The aquaculture's sector may be developed as subsidiary protein service source but it also may represent an important pollution agent impoverishing at the same time the genetic pool of harvested species ([Naylor et al. 2000](#)). An emerging interest is also increasing incessantly in relation to the exploitation of "dark energy" (methane and hydrogen sulfide) and mineral resource extraction (e.g. gold, zing and cooper; [Van Dover 2011](#)). Oceans strong potential for new species also represents a vast genomic, molecules repository and a pool of potential biomaterials and medicines ([Kim et al. 2015](#)). Ecotourism is a great source of incomes for an important number of countries although a sustainable managing of this activity is still to be developed properly. Other cultural services are education, the more purely aesthetic and inspirational services such as poetry, entertainment and well-being.

In addition to primary services, the ocean provides also subsidiary services, with its unique biodiversity and ecological functions in relation to chemosynthetic primary production (vents and seeps), which covers a paramount significance in global geochemical cycles (i.e. iron, oxygen, carbon), global temperature changes mitigation as well as provides waste detoxification through biotic and abiotic processes ([Thurber et al. 2014](#)).

Persistent climatic or human-induced environmental changes can produce long-lasting modifications in species behavior, with pervasive effects on population distributions and abundances ([Peer and Miller 2014](#)). Such environmental changes may be observed in time series data recorded at a changing location as fauna respond to modifications in key habitat parameters ([Holyoak et al. 2008](#)).

Changes in the distribution of organisms (leading to observed shifts in community structure) are among the most readily detectable and emerging biotic effects of global warming (Parmesan and Yohe 2003; Parmesan 2006, Ehrlén and Morris 2015). The scarce available information about threats and poor quantification of ocean services limits leads to a lack of scientific framework that prevent from design adequate policy strategies to protect ocean ecosystems.

The deep sea, defined here as ocean environments below ≈ 200 m depth (Danovaro et al. 2014) has been traditionally seen as an immutable silent and quiet fraction of oceans. These old paradigms are quickly being re-evaluated thanks to new observational technologies that begin to demonstrate that deep sea is a very heterogeneous and dynamic landscape. The half of the ocean is below 3000 m depth and only the 0.01% of the deep-sea floor has been surveyed in detail (Ramirez-Llodra et al. 2010) although it occupies more than 66% of our planet's surface (Mercier et al. 2011). Consequently, there is an enormous part of the planet that remains unknown including the potential services this fraction of the Earth is able to provide.

The marine benthic realm is tightly coupled to pelagic one, implying deep-sea functioning to be influenced by shallower depths (Thurber et al. 2014, Aguzzi et al. 2015a, Glover et al. 2010). The deep sea is affected by pulses of marine snow, volcanic eruptions, toxic seeps, carcass-falls (e.g. sometimes as big as whales), shifts in ocean currents and temporally hypoxic conditions (Glover et al. 2010, Danovaro et al. 2014). In this sense, the planning of ocean functioning studies, especially in the case of the deep sea, must pay attention to the most relevant sampling frequencies to best monitor all these phenomena. Only in that manner, we will be able to properly manage the potential changes in ecosystems due to the actual course of threats to oceans.

2. Temporal bottleneck in marine sampling strategies

Limited access to the ocean for the observation of marine organisms, communities, and the reciprocal interrelationship (i.e. as proxy of ecosystem functioning) and the response to the surrounding physical environment presents difficulties for the advancement of marine ecology not present in the respective terrestrial discipline (Underwood 2005, Menge et al. 2009, Webb 2012). Much of the paradigms about the oceans results from ship-based expeditions (Favali and Beranzoli 2006; Danovaro et al. 2014) that date back from the 19th century. While habitat mapping and surveys remains essential in elucidating the stage for processes-oriented studies, a sustained time series high-frequency approach is required to truly comprehend earth and ocean science (Favali and Beranzoli 2006, Glover et al. 2010). The areas of study likely to benefit the most from this approach are, from one hand, those involving time-dependent processes or episodically triggered events (e.g. earthquakes, submarine slides, tsunamis, benthic storms, pollution, gas hydrate release). From the other hand, those requiring long-term data sets (i.e. temperature changes, hypoxia, acidification, biodiversity changes). Such an effort is required to disentangle current community changes due to species adaptation to infrannual changes (e.g. species

composition changes due to reproductive, growth, and migration seasonally-oriented patterns) from trends of change through consecutive years due to climate shift and more direct anthropic impacts (Aguzzi et al. 2015a).

Marine sampling programs often lack of this temporal approach, with high-frequency and prolonged sampling strategies difficult to carry out with traditional ship-assisted methodologies. Repetition of trawling, Remotely Operated Vehicle (ROV) or Autonomous Underwater Vehicle (AUV) inspecting are deeply conditioned by unpredictable environmental conditions as well as challenging deployment locations (e.g. canyons, seamounts, slumps, outcrops), all being associated to the high costs of the oceanographic campaigns (Langlois et al. 2010, Watson et al. 2010). Additionally, the sampling of communities is influenced by species rhythmic and synchronic movements within the water column and across continental margin shelves and slopes, adding to unpredicted temporal variability to the already spatially contemplated one.

Trawling is still one of the most effective and more economically feasible methods of sampling of continental margin and deep-sea benthic communities (Raffaelli et al. 2003, Sardà et al. 2004) and is commonly used in pluriannual studies, repeating data collection at certain depth strata or strategic areas (Bertrand et al. 1997, 2002). The studies using this technique are broadly conducted over large seabed surfaces for the assessment of the distribution and demography of populations (e.g., stock assessment), as well as for overall biodiversity evaluations. Nevertheless, significant errors in these assessments may occur if timing of sampling is not considered since species present rhythmic populational displacements into the marine three dimensional scenarios (Aguzzi and Company 2010). In addition to that, trawling exerts big impacts on deep-sea bottom communities (Puig et al. 2012, Watling 2014)

3. Activity rhythms in the three-dimensional marine scenario

Biological clocks generate rhythms at all level of life complexity (e.g. from gene expression to behavior of individuals and their synchronous activation into populations and in relation or other species within a community; (Kronfeld-Schor and Dayan 2003, Aguzzi et al. 2012). Clocks evolved in all phyla as a product of adaptation of life to a deterministically changing environment, as a product of the rotation of the earth on its own axis and in relation to the sun and the deterministic changes in light intensity and photophase duration (at day-night and seasonal scales) as well as in hydrodynamism (tidal bulges). Animal need to cope with temporally predictable changes in habitat key drivers for their survival by preparing their internal physiological activity with an anticipation to the insurgence of that potentially harmful change, being this mechanism known as the “synchronization” (Refinetti 2006, Naylor et al. 2000).

The environmental factors triggering the function of these clocks are known as *Zeitgebers*. Changes in light intensity and spectral quality are well known *Zeitgebers* in oceanic photic and disphotic

(i.e. twilight) zones (Daan and Aschoff 2001, Sbragaglia et al. 2015). But as sunlight disappears (i.e. below the twilight zone end) with last photons being detected as deep as 1 km depending from local oligotrophic conditions (Herring 2002), other geophysical cycles are expected to govern these clocks (Aguzzi et al. 2010). Tides are known to be important synchronizers in certain marine species and depths (Sbragaglia et al. 2015). In spite of that, the transmission of energy from shallower winds and tides in a complex manner due to the effect of frictional dragging with seafloor geomorphologies (Garrett 2003, Babanin 2009) in the deep sea give origin to inertial waves (with or without tidal frequency). Complex hydrodynamics may be an important synchronizer in the deep sea (Aguzzi 2009) but the knowledge of their effects on animals is still insufficient.

Populations react to those deterministic changes by performing rhythmic displacements in a tridimensional space. Diel vertical migrations (DVM) represent the biggest animal migration on Earth in terms of biomass (Hays 2003). Animals travel up from deeper zones into worldwide richer shallower waters. When these bathymetric migrations take place along the seabed those are known as nektobenthic displacements. Lastly, endobenthic movements consist in periodic concealment and emergence from the sediment (Aguzzi et al. 2010). Thus, marine communities present rhythmic composition changes that imply a modification in intra and interspecific relationships, which ends up into spatio (depth) -temporal (tidal, day-night and seasonal) modifications in ecosystem functioning, redistribution of nutrients and organic matter in the ocean.

4. New seafloor monitoring technologies

There is the need of new monitoring technologies adding a solid temporal dimension to marine discovery and monitoring. Most of nowadays multiparametric platforms used for marine exploration bear video cameras as items that can approach the study of ecosystems at the complexity level of fauna (Board 2000, Favali and Beranzoli 2006, Matabos et al. 2017). Platforms such as ROVs, AUVs and landers lack of unlimited power autonomy to sustain a broad set of sensors, large imaging and environmental data storage capacity, as well as real-time inspection possibility, all features needed to monitor ecosystems at 360 degrees over long-term scales encompassing months, seasons, and consecutive years.

During the last 30 years, we have witnessed the appearance of cabled seafloor observatories all around the world, as platforms able to overcome the limitations of other ship-assisted sampling methods. A seafloor observatory is defined as a multiparametric platform at a fixed site, feed of power and supply command, control and communications to sensors located above, on or below the seabed itself, as well as spreading with a cluster of other interconnected stations into a geographic network (NRC 2000, Favali and Beranzoli 2006). The observatory node may also support mobile vehicles, such as Rovers as benthic mobile robots (Thomsen et al. 2015). Among these, there are the crawlers which represent one of the newest Internet Operated Vehicles [IOV] which are tethered to a cabled node, allowing higher spatial coverage around it (Purser 2015, Thomsen et al. 2015).

Cabled observatories are vocationally interdisciplinary, integrating biological, geological, and oceanographic sensors (Favali and Beranzoli 2006; Lampitt et al. 2010), all specifications that make of them potentially important tools for the study of behavioral rhythms in association of concomitant environmental changes (Aguzzi et al. 2012). Their monitoring capacity is sustained by continuous data flow and sufficient power to operate environmental sensors at a high frequency (seconds) over prolonged durations (from days to years) in a remote and real-time fashion. This interdisciplinary monitoring approach would then allow to efficiency scale marine community composition changes at different temporal scales down to the behavioral response of individuals to cyclic and stochastic changes in their eco-field (Danovaro et al. 2017).

5. Imaging as strategic monitoring approach linking animal behavior to ecosystem functioning

Observatory imaging capacities can be used to highlight the relationships between rhythmic behavior of species and community composition spatiotemporal changes. The chance of observing an individual of a species within the framework of a fixed camera fluctuates in response to changes in its rate of displacement activity (which include several behavioral motivations such as for example, feeding, mating, territorial control and homing). In time-lapse photography and footage acquisition, fluctuations in visual counts are proxies of the animals' behavioral rhythms (Costa et al. 2009, Chabanet et al. 2012; Doya et al. 2014). Accordingly, there is a direct correlation between visual counts at a fixed camera field of view and changes in local population abundance due to rhythmic water column seabed displacements (Aguzzi et al. 2010). Thus visual counts monitoring represents a straight ahead method detecting rhythmic behaviours although not the only one. Virtually, any visually detectable rhythmic behavior can be monitored with time-lapse photography any footage acquisition.

When cameras are added to other environmental monitoring sensors, one can use an observatory, not only to properly monitor the response of species and communities to environmental changes (Aguzzi et al. 2012, Condal et al. 2012, Matabos 2012), but also to monitor other interesting behavior such as intra and interspecific interactions. Imaging is therefore a powerful tool of abiotic factors and global change research, and the procedures for best image data analyses will likely be a trending line within future developments of cabled observatory technology (Vardaro et al. 2013).

Time-lapse image capture should ideally be designed at temporal frequencies that maximize the detection of the entire range of species behavior we are interested in. Particularly, such methodology allows discerning between short-term variations in behavior (and local abundance) due to diel and seasonal rhythms from other more long-lasting trend of change for the progressive adjustment of biotic communities to a shifting climate. When data are collected through enough consecutive years, animals'

responses to ongoing local and global changes can be disentangled from infrannual cycles (Glover et al. 2010).

6. Current cabled observatory network initiatives worldwide

A network of cabled video-observatories dispersing across different marine areas of the world brings new possibilities to track large-scale changes in the marine environment. Many large-scale projects have implemented permanent seafloor networks at International level. Canada, Europe, Japan, and USA are the major actors (Fig. I). Those initiatives increase the number of worldwide connected camera nodes, providing progressively higher geographic and bathymetric coverage. Improved access to study real-time or near-real time data (open data policy) of a wide variety of sensors will provide synergy to the researchers' efforts anywhere in the world to understand ocean functioning promoting the interdisciplinary collaborations worldwide. Concomitantly, a wide range of opportunities to public access and participation to the ongoing science and raw data would increase education and public environmental awareness (Matabos et al. 2017).

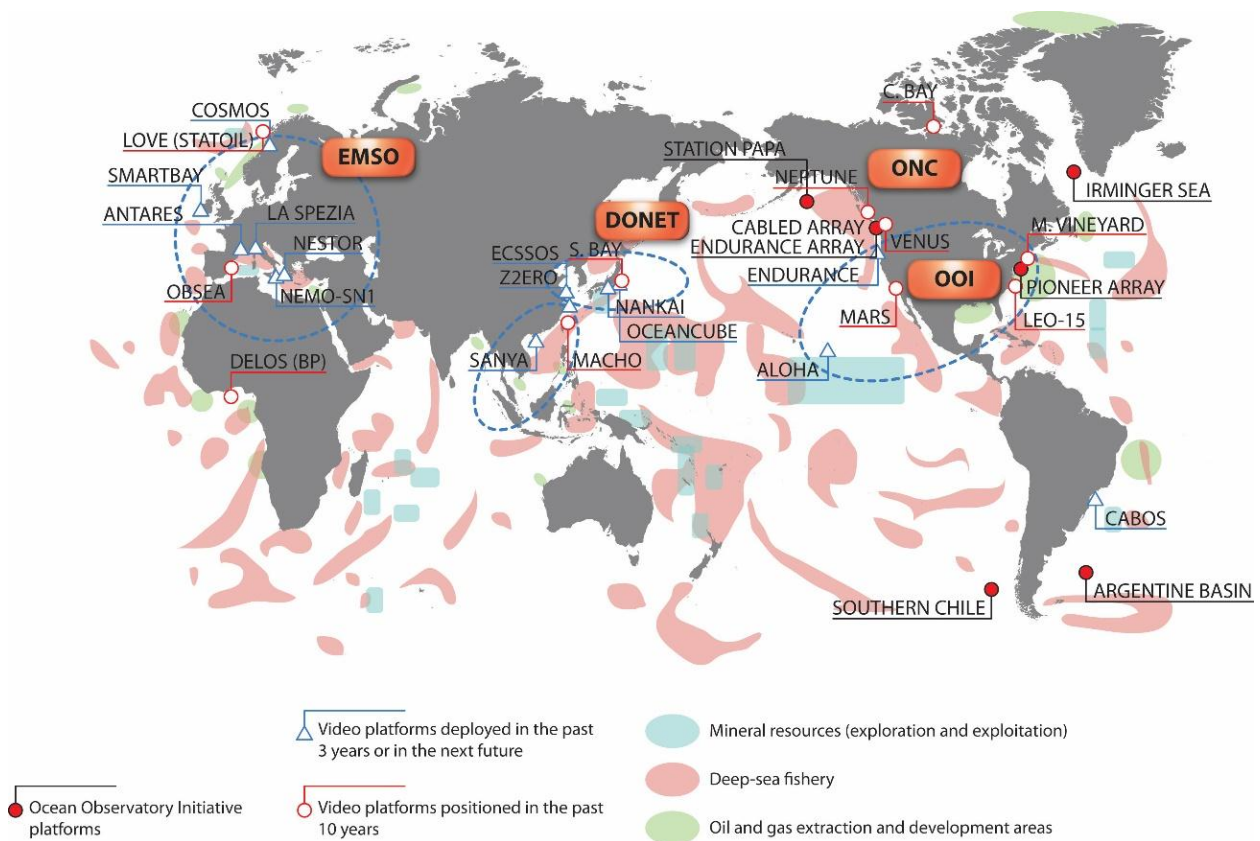


Figure I. Seafloor video-observatory networks that has been or are being implemented at different depths of the continental margin, from coastal areas to the deep sea, having the chance to be used to monitor different areas experiencing anthropic impacts (from Danovaro et al. 2017).

The main efforts in the implementation of ocean observatories are led by the ONC (<http://www.oceannetworks.ca>), an initiative of the Victoria University (British Columbia). The major components are NEPTUNE (North East Pacific Time-series Underwater Networked Experiments, <http://www.neptunecanada.ca>) and VENUS (Victoria Experimental Network Under the Sea, <http://www.oceannetworks.ca/installations/observatories/venus-salish-sea>). VENUS is located in a seasonally hypoxic fjord in Vancouver Island and was the first of his kind in the country. NEPTUNE is a plate-scale multidisciplinary video-observatory network on the Juan de Fuca Plate, located off the west coast Vancouver Island. NEPTUNE is the largest of his kind worldwide and aims to solve a wide span of research questions, such as earthquake dynamics and tsunami hazards, fluid fluxes in the ocean crust and sediments, gas hydrate deposits; ocean and climate dynamics, acidification, nutrient fluxes and impacts on biota; deep-sea ecosystems dynamics; and applied engineering and computer science research (Barnes et al. 2013; Favali 2015). VENUS houses ocean and biological and delta dynamics studies in waters to 300-m depth (Barnes et al. 2013).

OOI US initiative sponsored by the National Science Foundation (NSF) is also an ambitious monitoring program already encompassing or aiming to install cabled observatories from the high latitudes of the North Pacific Station Papa, the North Atlantic component into the Irminger Sea, the Southern Chile and the Argentine Basin Array through the Pioneer located off the coast of New England, south of Martha's Vineyard and the Endurance Array into the coastal upwelling region of the Oregon and Washington coasts (<http://oceanobservatories.org/>). Out of the umbrella of the OOI, the Monterey Accelerated Research System (MARS; <http://www.mbari.org/at-sea/cabled-observatory/>), and the University of Hawaii ALOHA Cabled Observatory(ACO; <http://aco-ssds.soest.hawaii.edu/>) are two cabled observatories also sponsored by the NSF.

Japan its cabled seafloor observatories are not yet fully devoted to the ecological monitoring since chiefly used as seismic and tsunami warning system (Aguzzi et al. 2012). At present, the DONET (Dense Ocean floor Network system for Earthquakes and Tsunamis; <http://jamstec.go.jp/donet>), managed by JAMSTEC (Japan Agency for Marine-Earth Science and TEChnology) is chiefly represented by observing points in the Nankai trough seismogenic zone, and includes several seismometers and pressure gauges in its sensors. DONET has anyway a cabled video-station, in Sagami bay (1100 m depth) to be used for studies on reproductive behavior of *Calypptogena* clam fields in hydrocarbon seepages(Fujiwara et al. 1998). The sole other but shallower cabled video-platform is the reef observing OCEANCUBE held by theOkinawa Institute of Science and Technology (OIST) in Okinawa at 20 m depth.

In Europe, the European Multidisciplinary Seafloor and water-column Observatory (EMSO, <http://www.emso-eu.org/>; Best et al. 2014)is a transnational infrastructure aiming to long-term monitoring the interaction between the geosphere, biosphere, and hydrosphere. It is composed of several stations deployed in geologically or ecologically relevant shallow and deep-sea areas, from the Arctic to the Atlantic, through the Mediterranean, to the Black Sea.

The Center for Ocean, Seafloor, and Marine Observing Systems (COSMOS) located in the Norwegian margin is the northern EMSO video-observatory. Near this observatory there is the LOVE deployed by Statoil ASA and the Institute of Marine Research (IMR) bearing a still camera. Of particular relevance are the sole shallow waters two platforms bearing cameras: the OBSEA (<http://www.obsea.es/www.obsea.es>) and the SMARTBAY subsea real-time observatory (<http://www.smartbay.ie>), both deployed at 20 m depth. Other, much deeper platforms bear special imaging equipment that could be indirectly used for the study of behavioral rhythms and communities' turnover, but whose primary vocation is related to particle physics. These are Neutrino telescopes endowed with photomultiplier tubes capable of detecting not only the passage of quantum sub-atomic particles but also bioluminescence. The ANTARES (Astronomy with a Neutrino Telescope and Abyss environmental RESearch; <http://antares.in2p3.fr/>) at 2300 m depth off Marseille, the NEutrino Mediterranean Observatory (NEMO), off Capopassero (Catania) at 2200 m depth as well as the Neutrino Extended Submarine Telescope with Oceanographic Research (NESTOR) to be installed off Pylos (Greece), at similar depth, represent the protagonist of the Kilometer Cube Network (KM3-NeT).

7. Limitations to the ecological monitoring by cabled observatories imaging in the deep sea and envisaged solutions

Fixed cameras installed on cabled observatories are only capable of imaging a relatively small area of the marine ecosystem, usually a few square meters of seafloor and overlying water column (Aguzzi et al. 2011). This spatial coverage limitation prevents from extrapolating abundance data to larger areas (Assis et al. 2013). Because of these spatial limitations, researchers need to rely on bibliography or perform laboratory tests to determine if peaks in visual counts at specific locations correspond to peaks in activity (Aguzzi et al. 2015). For example, an increase in visual counts for a certain species may be a proxy of a decrease in the rate of swimming rather than an increase in species activity. This often occurs in species that aggregate close to observatory structures (and therefore observatory cameras) during daytime. Seafloor observatories would greatly benefit from the spatial extension of their monitoring borders by establishing spatial network of functionally coordinated nodes (Aguzzi et al. 2012).

Videoining and time-lapse monitoring permit to analyze a wide range of behaviours, including those with an associated periodicity (Aguzzi et al. 2012) but special care must be done with their intrinsic limitations. Powerful lights are needed to illuminate in oligophotic or aphotic depths. Previous studies found out that these lights can attract some fishes biasing animal counts (Longcore and Rich 2004). A solution to consider in certain cases can be the use of infrared light which is not detectable by most marine organisms. Unfortunately, its use is only possible when distances to be enlightened are short due to the rapid attenuation of this wavelength within saltwater (Widder et al. 2005). Biases in animals' counts can also occur as product of recounting the same individuals as they swim in and out of the field of

view, or when the same individual lingers within the field of view in different images or video frames (Mazzei et al. 2014). Time-lapse image acquisition, at minute and hourly frequencies mitigates this problem somewhat, though for species prone to resident behavior (e.g., scorpaenids) observations might still produce erroneously high estimations of abundance.

The technical constraints in time-lapse image monitoring, combined with the bias caused by attraction of some species to the artificial observatory structures, reduce the applicability of using cabled observatories to record unbiased abundance data, but does not wholly prevent their use in the study of activity rhythms (and community changes). Recounting of individuals may be proportional to the differential rate of swimming, and therefore correlate with activity and passivity behavioral phases (Aguzzi et al. 2010). Downward-oriented cameras provide a more uniform field of view for animal counting than oblique imaging (Smith et al. 1993) which would be appropriate for the detecting of walkers and crawlers but would be less advantageous in capturing and identifying active and passive swimming species (Matabos et al. 2014).

A strong variability in overall species abundance may also be the result of habitat heterogeneity (Harvey et al. 2012). At a local scale of meters, different animal counts with the same camera, depending on the field of view to which the camera is aimed (e.g., toward a rocky zone rather than to the adjacent water column; Condal et al. 2012, Purser et al. 2013). Therefore, the careful selection of the appropriate field of view and consideration of potential over or under abundance estimations are required. Other solutions, such as the use of cameras equipped with pan/tilt solutions, require the programming of operational routines for rotatory image acquisition and the standardization of counts across local habitat heterogeneity (Pelletier et al. 2012, Mallet et al. 2014).

ROV-video transects should ideally be conducted around observatory still camera systems to evaluate the effect of habitat heterogeneity on locally detected species assemblages. ROV surveys focus on spatial rather than temporal abundance variability, allowing large areas of the seabed to be investigated though the surveys are often short and sporadic (De Leo et al. 2010, Grange and Smith 2013). Despite the clear advantage in terms of spatial coverage provided by moving imaging techniques, such photographic or video censuses are not necessarily more reliable for estimation of fish population densities than observations from fixed camera systems.

Cumulated multiparametric data produced over long periods of time demand Artificial Intelligence advances for the statistical treatment to reduce human-based time processing costs (Costa et al. 2011). Unfortunately, universal customization of automated video-imaging scripts is highly improbable (Aguzzi et al. 2015) since automated species recognitions depend in too many particular case factors such local species (Aguzzi et al. 2012), heterogeneous background and illumination (Beauxis-aussalet et al. 2013). Citizen Science represents an alternative to overcome this issue (Matabos et al. 2017). This term refers to the participation of the public in scientific programs taking advantage of new

technologies, such as the Internet, for easy data collection and sharing (Del Rio et al. 2013) with volunteers who collect and/or process data (Silvertown 2009, Dickinson 2010).

8. Thesis hypotheses and objectives

Oscillations as biological rhythms are a pervasive phenomenon in nature (Patel et al. 2015). In extreme environments, such as those of the deep-water continental margin and the deep sea activity rhythms are poorly known. I proposed here three hypotheses dedicated to filling the gap of knowledge on important life traits for species such as behaviour and its spatiotemporal modulation resulting in community changes that will be discussed throughout the work:

1. Tidal, day-night and seasonal behavioral rhythms can result in spatial shifts in populations distributions, and therefore on measurable faunal composition, richness, species abundances and evenness.
2. Inclusion of behavioral components in the spatiotemporal analysis of a community can alter the communities composition, based on species alternations at different continental margin locations, being this phenomenon of paramount importance to understand ecosystem functioning.
3. New multiparametric video-observatory platforms represent a relevant tool to improve the overall knowledge several still unknown life traits of deep-water and deep-sea species.

To prove these hypotheses, the general objective of this Ph.D. project was focused to evidence how complex populational rhythms can biases our perception of the composition of local communities faunal composition, richness, species abundances and evenness, through the use of novel but to date still underused observational technologies. The specific aims are:

1. Examine the interplay between diel, tidal and seasonal cycles in regulating rhythmic behavior of animals with different locomotor behavior and life stages.
2. Provide valuable ecological information about community composition, dynamics and behavior of species residing deep-sea environments, as a validation of observational technologies and methodologies used here.
3. Provide methodological solutions to the intrinsic and actual limitations of fix cameras to assess animal counting.

In my Thesis, I highlight the importance and expand the knowledge on behavioral rhythms in different depth strata and deep-sea ecosystems. To do so, I took notice on three relevant deep-water and deep-sea environments (i.e. a canyon, a hypoxic fjord and a whale-fall) and carried out studies spanning from few months up to a year with the use of different observational technologies. In addition, I provided new information on how behavioral rhythms may affect community dynamics. Finally, I specifically tuned protocols for data collection according to the different technical character of platforms

(fixed or mobile) highlighting methodological requirements and mentioning constraints for the appropriate measurement of species behavior over various tidal, day-night and seasonal temporal scales. In this context, I contribute with new directions for the appropriate use and development of observatory technology in relevant deep-sea environments.

Chapter 1. Diel behavioral rhythms in sablefish (*Anoplopoma fimbria*) and other benthic species, as recorded by the deep-sea cabled observatories in Barkley canyon (NEPTUNE-Canada)

1.1 Abstract

Recent advances in cabled observatory video-imaging now enable faunal monitoring over extended periods of time. These platforms can be used to avoid biases in population and biodiversity assessments due to behavioral rhythms (i.e. massive population displacements). In this study we used video monitoring to examine the interplay between day–night and internal tidal cycles in regulating the behavior of sablefish (also referred to as black cod; *Anoplopoma fimbria*), hagfish (*Eptatretus* spp.) and crabs. We counted the number of animals in 50 s video-recordings taken at 30 min intervals with 3 NEPTUNE-Canada cameras located in Barkley canyon at approximately 1000 m depth (one in the axis and two on the wall of the canyon). Current data just above the seafloor was recorded as an indicator of the local internal tidal regime. Chi-Square periodogram analysis did not show significant ($p < 0.05$) day–night or tidal-based rhythms for the three species. The same analysis conducted for the sablefish (i.e. the most abundant) at each camera separately revealed different and significant ($p < 0.05$) 12- and 24-h based periods. Waveform analysis for these time series showed a temporal phase shift among cameras, suggesting diel displacements within the canyon axis. Our results highlight how some deep-sea fish may present diel rhythmic displacements along canyons according to the day–night and internal tidal temporization. In this context, bathymetric networks of cabled video-stations can be an effective sampling tool to monitor this kind of behavior.

Keywords: Sablefish; NEPTUNE-Canada; Behavioral rhythms; Internal tides; Barkley canyon; Nekto-benthic Introduction

1.2 Introduction

The deep sea is the vastest ecosystem on Earth, with depths below 200 m representing 65% of the total surface of the planet (Ramirez-Llodra et al. 2010), but faunal exploration is still at its early stages (Gage and Tyler 1991, Jamieson et al. 2011, Yeh and Drazen 2009). As a result of technological advances, new observational tools provide important data on faunal composition and behavior of species residing in different deep-sea benthic ecosystems such as canyons, cold seeps and hydrothermal vent fields (Glover et al. 2010). Traditional sampling methods such as trawling are progressively being replaced by direct means of visual observation. Imaging systems on technological platforms can be broadly subdivided into mobile (i.e. Remotely Operated and Autonomous Underwater Vehicles — ROVs and AUVs), semi-fixed (i.e. deployable landers with different degrees of temporal autonomy), and fixed (i.e. cabled observatories) systems (reviewed by Aguzzi et al. 2012).

While mobile and semi-fixed platforms allow higher spatial coverage with a reduced observational frequency, the reverse is true for cabled observatories. These platforms are bearing new video-imaging based technologies and other habitat sensors that are providing a new horizon of data collection on the ecology of deep-sea species, especially in relation to behavior. For example, recent studies with video-imaging systems installed on cabled observatories are showing the occurrence of population activity rhythms at a diel (i.e. 24-h based) scale in the aphotic deep sea (reviewed by Aguzzi et al. 2011). Unexpectedly, these rhythms seem to be ruled by both internal tidal and inertial (i.e. atmospheric driven) currents (Aguzzi et al. 2010). These data are promising from the perspective of chronobiology (i.e. the science that studies biological rhythms), since they are extending our knowledge of the biological clocks of marine species from shallow waters to the deep sea. In addition, these data will allow quantifying potential sampling-related biases in our perception of marine communities' composition (Naylor 2005). On the other hand, variations in the rate of activity of deep-sea animals may in turn affect the chance of observing a species at any given location (Bahamon et al. 2010). Massive population displacements occur in benthic and pelagic taxa at different strata depths of the water column and the continental margin, in response to regulatory mechanisms and changes in habitat conditions that are still poorly described (reviewed by Naylor et al. 2000).

In deep-sea species, the study of rhythmic behavior at diel scale requires coupled acquisition of videos/images and environmental parameters at high frequency, over larger periods of time. In this study, we used three deep-sea NEPTUNE-Canada cameras located within the Barkley canyon at aphotic depths, in order to study the rhythmic behavior of sablefish (*Anoplopoma fimbria*) and other abundant and video-discernible species. For the sablefish, we also explored the use of such video-technology for the measurement of class-size frequency distribution as a replacement to more destructive and traditional sampling systems (i.e. trawling or creeling). Finally, we attempted an evaluation of biasing errors in animal counting due to intermittent illumination exposure during image acquisition.

1.3 Material and methods

The North-East Pacific Time-Series Undersea Networked Experiments NEPTUNE Canada (<http://www.neptunecanada.ca>), as part of the Ocean Networks Canada Observatory, located off Vancouver Island (British Columbia, Canada), is currently one of the most advanced technological multiparametric cabled platforms for deep-sea ecological studies (Barnes et al. 2011). Its deployment occurred within a strategic global effort for the continuous and prolonged monitoring of deep-sea communities and associated oceanographic dynamism (Priede and Solan 2003). Installed sensors allow linking animal behavior (and hence rhythms) with concomitant habitat variations. The network includes five main nodes deployed at different depths (Fig. 1) within a diversified set of geologically active and ecologically relevant sites, including a submarine canyon (Barnes and Tunnicliffe, 2008). These nodes are powered and linked together by over 800 km of electro-optic cables, covering part of the Juan de Fuca plate (Northeast Pacific).

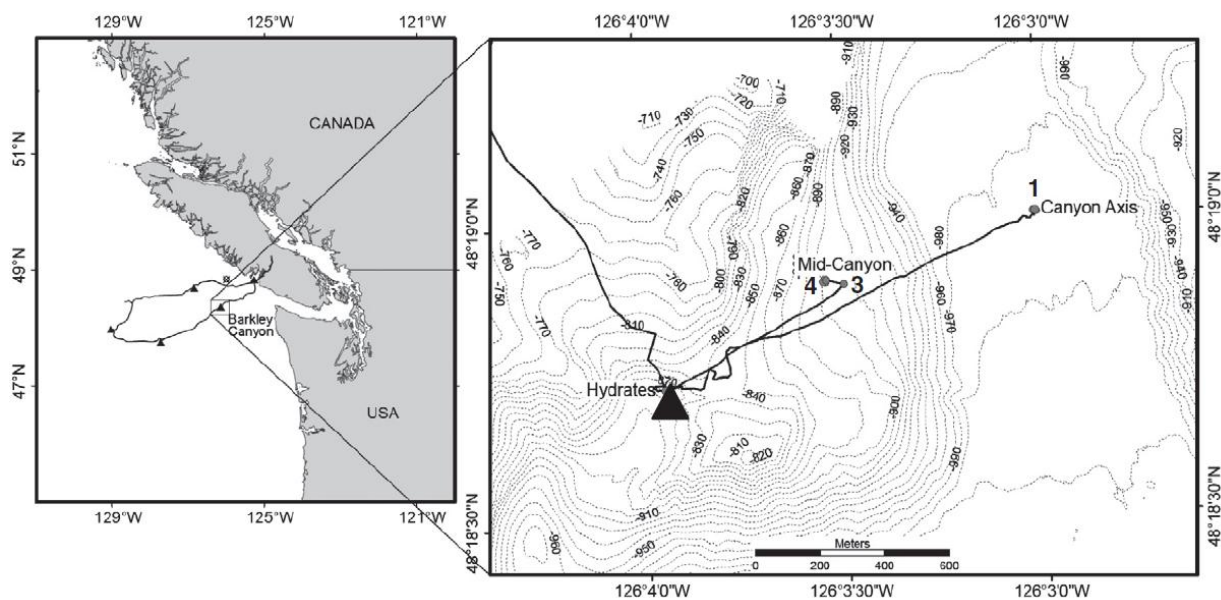


Fig.1. Coarse bathymetric map of the Barkley canyon site, showing the locations of video-stations POD 1, POD 3 and POD 4, as part of NEPTUNE-Canada seafloor observatory infrastructure. Camera platforms (black dots) are powered by a local node (black triangle) through extension cables. Isobaths (dashed lines; in meters) account for the local canyon morphology

1.3.1 Cabled network specifications

Synchronous videos were acquired using three different instrument platforms in the Barkley canyon area. POD 1 was located in the canyon axis (latitude: $48^{\circ}19.0027'N$, longitude: $126^{\circ}03.0077'W$, depth: 987 m), while POD 3 (latitude: $48^{\circ}18.9052'N$, longitude: $126^{\circ}03.5252'W$, depth: 892 m) and POD 4 (latitude: $48^{\circ}18.8923'N$, longitude: $126^{\circ}03.4804'W$, depth: 896 m) were located on the canyon flank (at North West of POD 1), in the vicinity of an outcropping gas hydrate field. Horizontal reciprocal distances

of these platforms, knowing their coordinates were: POD1–POD3, 670 m; POD1–POD4, 675 m; and finally, POD3–POD4, 50 m.

On POD 1 images were acquired with a black and white Multi-Sea Cam 1060 low-light (0.01 lx) video camera. POD 3 bore a 5 Megapixel Axis P1347 color network camera. POD 4 was equipped with a 470 Line ROS Inspector color zoom low-light camera equipped with a 10× optical zoom. For all cameras light was available on demand from two 100 W bulbs (deep-Sea Power&Light) with adjustable intensity. Two 10 mW red lasers provided a 10 cm separation scale to the video-images. In order to link activity rhythms to internal tides, oceanographic sensors on Pod 1 were used to represent the three different study locations. A high resolution bottom-mounted upward-looking 2 MHz ADCP was used to determine the near sea-floor currents. Current velocities from a depth 20 cm above the seabed were harmonically analyzed for the significant tidal constituents (i.e. K1, M2, N2, and S2).

1.3.2 Data acquisition and time series processing

We acquired 50 s duration videos inMP4 format at 30 min intervals over a month (12:00 on 14th October to 00:00 on 14th November, 2011, Canadian local time). The cameras were fixed in a downward orientation at 45° in order to record a constant field of view of approximately 2 m² of seabed.

Observed animals were classified according to the lowest taxonomic level possible using the NEPTUNE-Canada Faunistic Guide (Gervais et al. 2012). For each video-segment, we recorded the number of individuals of the most abundant and discernible species (i.e. depending on the resolution of the camera and the distance from the camera lens). In those time intervals where videos were missing because of technical problems, we replaced data gaps with a 3-step moving-average (i.e. by averaging the values immediately before and after the gap). That procedure was used since periodogram analysis (see below) requires continuous data collected at a constant sample interval (Refinetti 2006).

Current direction and speed were recorded every 10 s, we binned these data into 1-h averages to match the frequency of video observations. The East–west (U) and North–south (V) current velocities were then harmonically analyzed to identify the major tidal constituents. These constituents could then be used to reconstruct the tidal current influence in the overall current regime.

Subsequently, all the biological and oceanographic data sets were equally binned at 1-h frequency in order to highlight rhythmic fluctuations, thus reducing the underlying noise typical of field studies (Levine et al. 2002). Biological data sets for each selected species were first binned for the three cameras together and the resulting data sets plotted over the entire month of observation. In that way, a first and overall screening of the quality of population rhythms was performed. We added to the resulting plots vertical lines delimiting consecutive 24-h cycles, as well as current speed data as markers of the local internal tidal regime.

The occurrence of significant diel periodicities (i.e. day-night or internal tidal associated) was studied using Chi-Square periodogram analysis (Sokolove and Bushell 1978), which is sensitive enough to detect rhythmicity in time series with many scattered animal counts (Refinetti 1992). The periodogram was run with 660 and 1500 min (equals to 11-h and 25-h, respectively) as range of screening frequencies. The periodogram analysis was performed with El Temps software (Diez-Noguera, University of Barcelona, <http://www.el-temps.com>). In the periodogram output plots, the highest peak exceeding the significant ($p < 0.05$) threshold represents the maximum percentage of total data variance explained by the inherent dominant periodicity.

A waveform analysis (Chiesa et al. 2010) was carried out on the biological and oceanographic data sets in order to estimate the phase relationship between the rhythm of visual counts and oscillations in the hydrodynamic regime. Each time series was partitioned into 24-h segments. These were then averaged at 1-h intervals, thus obtaining a mean fluctuation plot. Phase duration and timing were statistically assessed using the Midline Estimating Statistic Of Rhythm (MESOR) (Aguzzi et al. 2006). This is a threshold value used to assess any significant increment in waveform values as representative of the rhythm phase (i.e. peak) (Refinetti 2006). Significant increments in visual counts (i.e. defining the phase duration) were identified from waveform values above the MESOR. This parameter was estimated by re-averaging all waveform values and representing the resulting mean as a horizontal threshold line on the waveform plots.

In order to establish a cause–effect relationship between biological and environment factors, the waveforms for the different species were all represented with overlaid waveforms for current velocity data. We also plotted waveforms by considering the monthly averaged scotophase duration, approximated at the frequency of data acquisition (i.e. from 17:00 to 8:00), as indicative of the day-night cycle.

1.3.3 Size-frequency distribution

The size frequency distribution of sablefish was obtained by measuring the body length of fish in the video images using the laser pointers as the reference scale. The length between the mouth tip and the very end of the upper lobe of the caudal fin was used as in previous deep-sea imaging studies (e.g. Priede et al. 1994, 2003, Shaw and McFarlane 1997). In order to obtain reliable estimates, we selected only images of fish (extracted by footages) that were orthogonal to the viewing direction (i.e. fully showing the lateral line) and approximately at the same distance from the observer's point of view. These individuals had their bodies fully included within the field of view and if not, an easy point of reference was used to finish the measurement when the rest of the animal appeared on the screen. A 5 cm class-size distribution was then composed by summing together the records obtained at the location of each of the three cameras.

1.3.4 Light effects

The presence of lighting may potentially alter the behavior of deep-sea fishes, sablefish in particular (Widder et al. 2005), although usually it does not impair the successful detection of population rhythms (Aguzzi et al. 2010) and behavior (Aguzzi et al. 2012). In order to evaluate the potential perturbing effect of punctual lighting during the footage acquisition, a regression analysis was carried out on fish counted at the POD 1, POD 3 and POD 4 in relation to time. This analysis was performed by subdividing the video recording time in two standard halves: 0–25 s and 26–50 s. We randomly selected 15 sequences taken during the first five days of the survey from the three cameras and summed together for each recording half the counted animals per second. We then did separate regression analysis for the number of observed animals in each standard recording half against the observation duration with the software SPSS 20.0.0.

1.4 Results

We obtained a total of 1487 videos for POD 1 within the canyon axis and 1462 for both POD 3 and POD 4 on the canyon flank. Excluding missing videos due to lighting malfunction, the studies were carried out for 97.7% of POD1 videos and 98.1% of both POD 3 and POD 4 videos.

1.4.1 Faunal remarks

Sablefish was the most abundant species observed, with a total number of 1246, 786, and 1735 individuals counted at POD 1, POD 3, and POD 4, respectively. Two other taxa showed relatively high abundances, although much reduced in comparison to the sablefish. Hagfish, *Eptatretus* spp., total count values were 52, 62, and 50 at POD 1, POD 3, and POD 4, respectively. Crabs, with no taxonomic distinction between species, occurred in lower but still appreciable number, with 27, 63, and 9 individuals at POD 1, POD 3, and POD 4, respectively. We observed other benthopelagic and benthic species that are listed in [Table 1](#).

Table 1 Complete list of faunal observations (number plus relative percentages) as reported by NEPTUNE-Canada color video cameras installed in Barkley canyon, including the targeted species. That list is complete only for platforms POD 1 and POD 3 on the canyon flank. Such a list is incomplete for platform POD 4, given the lower resolution of its video camera, which in most cases prevented the identification of smaller animals

Location	Species	Common name	N	%
POD 1	<i>Anoplopoma fimbria</i>	Sablefish	1246	76.2
	<i>Eptatretus</i> spp.	Hagfish	52	3.2
	<i>Brachyura</i>	Crabs	27	1.7
	<i>Glyptocephalus zachirus</i>	Rex sole	1	0.1
	<i>Bathyagonus nigripinnis</i>	Blackfin poacher	8	0.5
	<i>Lycenchelys</i> spp.	Eelpouts	206	12.6
	<i>Coryphaenoides</i> spp.	Rattail	2	0.1
	Neptunidae	Neptunid	59	3.6
	Ophiuroidea	Brittle star	1	0.1
	Cnidaria	Jellyfish	30	1.7
	Diogenidae	Hermit crab	4	0.2
		Total	1636	
POD 3	<i>Anoplopoma fimbria</i>	Sablefish	786	25.5
	<i>Eptatretus</i> spp.	Hagfish	62	2
	<i>Brachyura</i>	Crabs	63	2
	<i>Bathyagonus nigripinnis</i>	Blackfin poacher	2	0.1
	<i>Lycenchelys</i> spp.	Eelpouts	87	2.8
	<i>Coryphaenoides</i> spp.	Rattail	1	0
	Salpidae	Salps	3	0.1
	Neptunidae	Neptunid	42	1.4
	Asteroidea	Sea stars	2	0.1
	Caridean	Shrimp	1896	61.5
	Diogenidae	Hermit crab	18	0.6
	Octopoda	Octopus	1	0
	<i>Bolinopsis infundibulum</i>	No common name	31	1
	Cnidaria	Jellyfish	88	2.9
		Total	3082	
POD 4	<i>Anoplopoma fimbria</i>	Sablefish	1375	96.7
	<i>Eptatretus</i> spp.	Hagfish	50	2.8
	<i>Brachyura</i>	Crabs	9	0.5
		Total	1434	

1.4.2 Time series analysis

We plotted a 1-month time series of visual counts for sablefish, hagfish and crabs determined by summing data for the three cameras (see Fig. 2). While noticeable differences in the overall detected abundance among the selected taxa were readily visible, rhythmic fluctuations were appreciable only for the relatively abundant sablefish. The scarcity of visual observations for the other two groups created excessively intermittent and squared fluctuation patterns, with no apparent defined periodicity. In particular hagfish were often observed as coiled within the camera field of view. By considering the total of animals detected at the three cameras those observed as stationary (i.e. coiled) amounted to 69%, those

drifting (i.e. displacing without active movement) were 23%, and the remaining 8% were observed as actively swimming.

Harmonic analysis of the tidal currents in the Barkley canyon area indicated a mixed diurnal and semidiurnal regime. Fluctuations in the tidal components (Fig.2) showed markedly different amplitude, being larger in the North–south (i.e. V) component than in the East–west (i.e. U) component. The significant tidal components based on signal to noise ratio were: K1 at 0.0417807 c/h (23.9-h); N2 at 0.0789992 c/h (12.6-h); M2 at 0.0805114 c/h (12.4-h); and finally, S2 at 0.083333c/h (12-h).

The periodogram analysis did not detect any significant ($p < 0.05$) diel periodicity in sablefish, hagfish and crab time series (Fig. 3). For hagfish and crabs, this was possibly due to their small abundance (see Figure 2). Since there was no such paucity for sablefish, the periodogram analysis was repeated for this species on the data sets derived from each camera separately (see Figure 3). Results showed the occurrence of population rhythmic activity for POD 1 and POD 4, with percentage of variance levels below 10% while, again, no rhythmicity was visible at POD 3. At POD 4, mixed diel rhythmicity occurred with a day–night or diurnal tidal-based periodicity of about 1440 min (24-h), along with a weaker one at a semidiurnal frequency of about 750 min (12.4-h). This tidal signal was also present into the periodogram plot, with a non-significant larger periodicity at around 1490 min (~25-h).

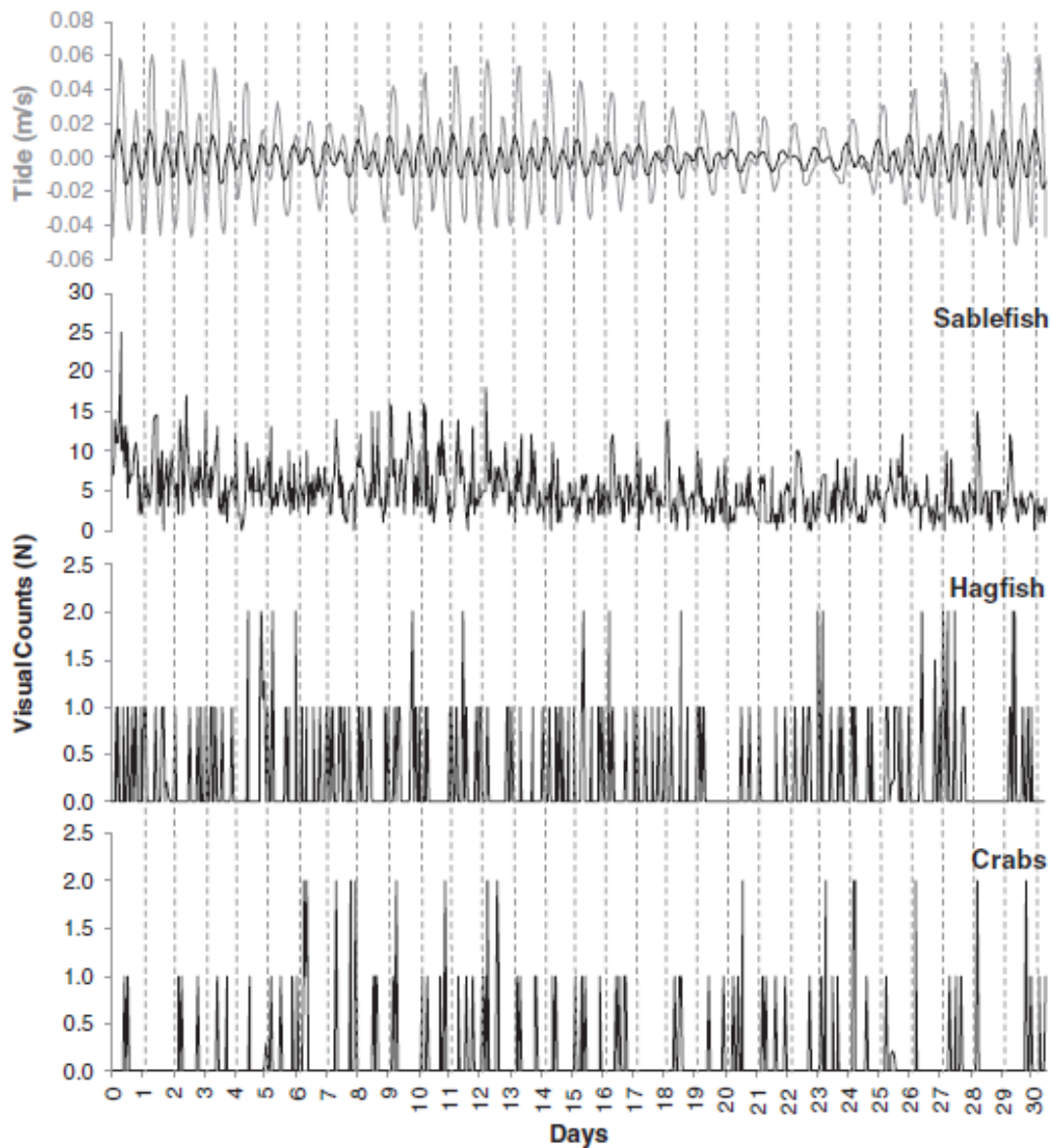


Fig.2.14th October to 14th November 2011 time series in visual counts for the three most abundant taxa (i.e. sablefish, hagfish and crabs), as reported by summing data of the three cameras deployed in Barkley canyon by NEPTUNE-Canada. These fluctuations have been reported along with fluctuations in the northerly and easterly components of the tidal currents (gray, north-south; black, east-west). These currents, made up of the combined effect of the K1, M2, N2, and S2 tidal constituents, are considered markers for the local mixed diurnal/semidiurnal tidal regime. Note the differences in fluctuation amplitude of both tidal components and in the abundance values for the three analyzed taxa. Vertical lines delimit consecutive 24-h cycles.

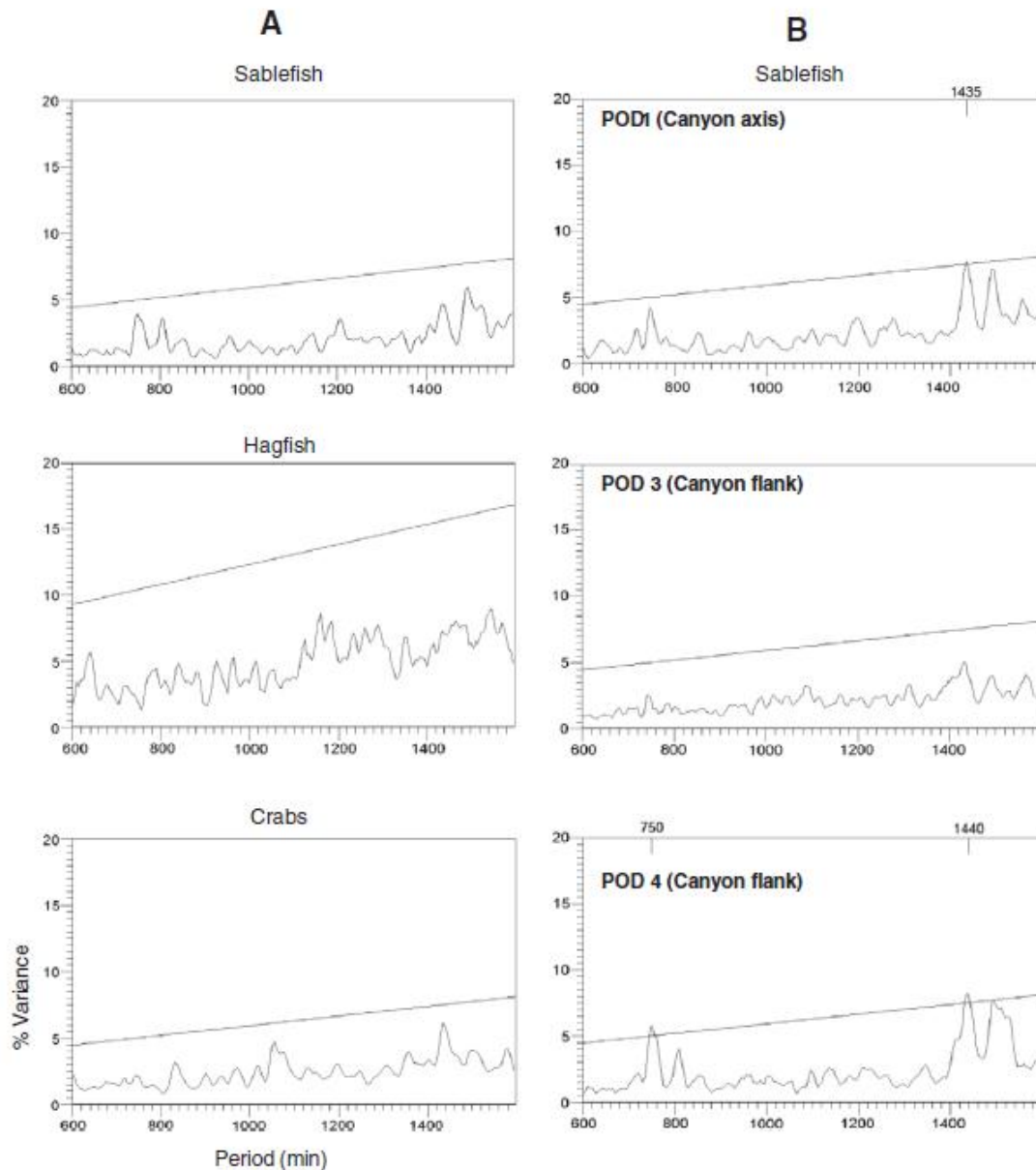


Fig.3. Periodogram analysis outputs on time series of visual counts for the three taxa, as obtained from video recording with the three NEPTUNE-Canada cameras within Barkley canyon. Periodogram results for the time series of Fig. 2 are to the left. For the much abundant sablefish this analysis was repeated for each camera separately (on the right), which showed different significant rhythmicity (reported in min by the percentage of variance peak crossing the significant threshold set at $p < 0.05$).

Waveform analysis (Fig. 4) for visual count time series for the three species summed over the three cameras showed small phase amplitudes in agreement with periodogram results (see Figure 3). Sablefish displayed a bimodal and nocturnal phase with two main peaks (i.e. values above the MESOR) near sunset and sunrise (respective maxima at 18:00 and 7:00). Conversely, for hagfish there was no

discernible diel pattern in their visual count fluctuation, since several peaks appeared at both day and nighttime. Crabs showed a sparse nocturnal increase, with a main peak observed after sunset (centered at 20:00) and other two maxima prior to sunrise (at 3:00 and 8:00).

Waveform analysis outputs for water speed data (Fig. 4) were obtained only for the significant North–south tidal component (i.e. V), since it showed the strongest oscillations (see Figure 2). Water speed showed a mix of diurnal and semidiurnal oscillations, with a larger nocturnal phase (maximum at 2:00) and a smaller peaking at daytime (maximum at 14:00). The superposition of waveforms for fish visual counts and water speed seems to indicate that animal detections increase when current velocity decreases. The peak in crab abundance occurred in a similar way and the peak was also in antiphase with tidal water speed maxima.

For sablefish, waveform analysis was repeated separately for the time series from each camera (Fig. 5). In the canyon axis (POD 1), a single nocturnal peak at 22:00 was observed in the visual counts. Whereas at POD 3 on the canyon flank, no phase appeared, this result could be attributable to a lowering of signal to noise ratio due to weaker currents and lower animal counts relative to the canyon axis. At POD 4, also in the canyon flank, a different rhythmicity occurred, with a bimodal waveform phase, showing temporal shifts with respect to POD 1. At the location of POD 4, two peaks were visible, a broad one at sunset (18:00) and a smaller one during the day (7:00).

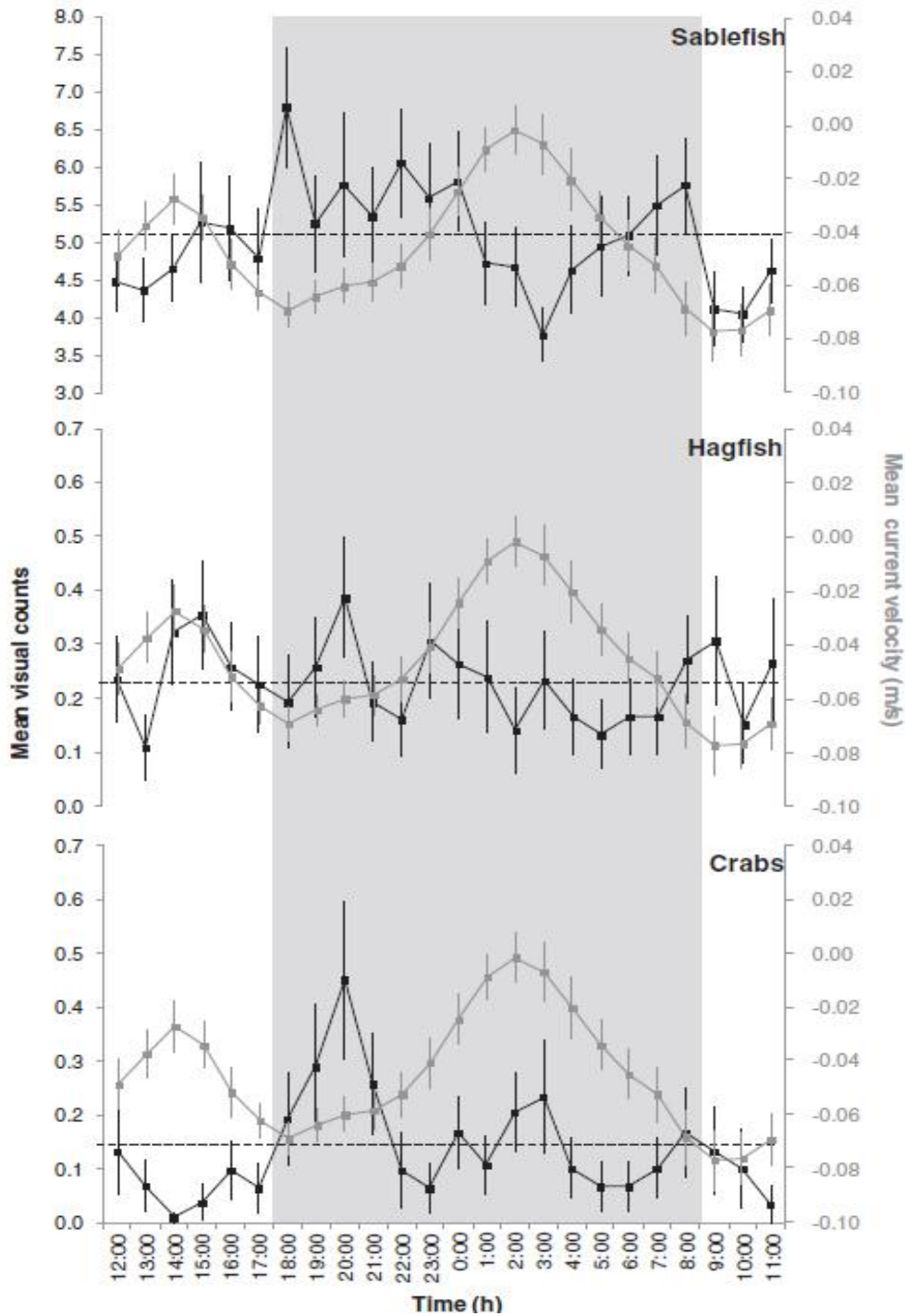


Fig.4. Waveform analysis output plots for visual counts and oceanographic time series for the three taxa, as obtained from video recording with the three NEPTUNE-Canada cameras within Barkley canyon. Results for species depicted in Fig. 2 (in black) and for current velocities (along the significant tidal North–south component U; in gray) account for the absence of any strong diel fluctuation in the former. Only sablefish seems to present a bimodal pattern, with a major and a minor peak (i.e. values above the MESOR) at night-time and in antiphase with water speed increases. MESOR values (dashed lines) account for the overall differences in the abundance of the three taxa and are equal to 5.06 for sablefish, 0.23 for hagfish and 0.14 for crabs. The gray square accounts for the average night duration during the month of October.

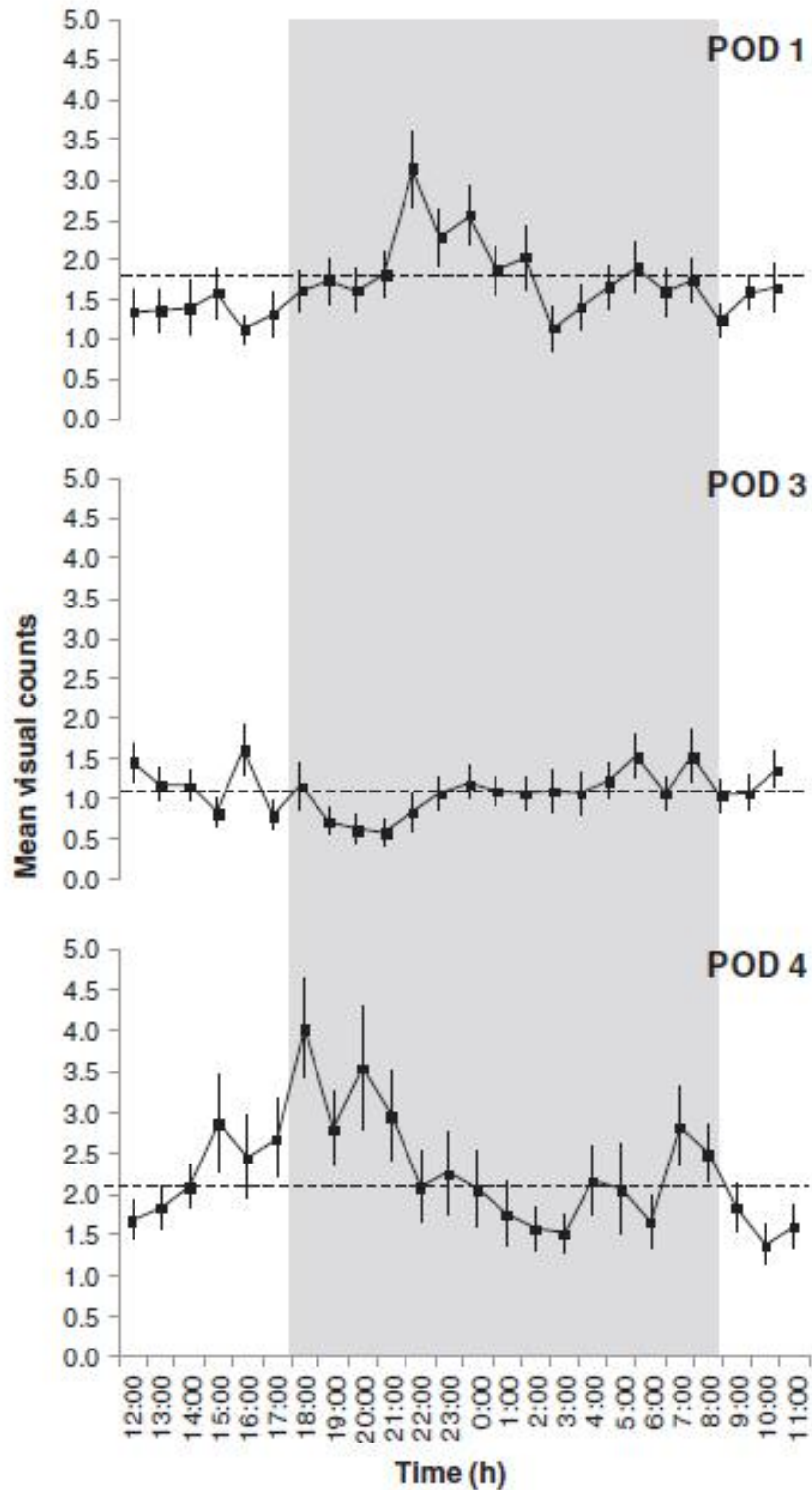


Fig.5. Waveform analysis output plots on visual count time series for sablefish separately for each NEPTUNE-Canada camera within Barkley canyon (i.e. POD 1, POD 3 and POD 4). Again, MESOR values (dashed lines; POD 1 = 1.7; POD 3 = 1.1; POD 4 = 2.3) account for markedly different abundances and timing of phases, shifting from uni-modal at night-time (POD 1) to crepuscular bimodal (POD 4) or arrhythmic (POD 1).

1.4.3 Class-size frequency distribution

195 sablefish were sized during our video recordings (Fig. 6). The total class-size frequency distribution ranged from 35 to 95 cm with a peak at 60–65 cm and average (\pm SD) length of 63.6 ± 10.4 cm. The repetition of this analysis by each POD camera revealed similar class-size frequency shapes. Average length (\pm SD) for these class sizes was: POD1 = 66.9 ± 9.9 ; POD 3 = 62.3 ± 9.1 ; POD 4 = 62.4 ± 10.6 . Although a larger proportion of bigger individuals were reported at the deeper camera (POD 1), no conclusive remark on that difference can be reported given the low sample size.

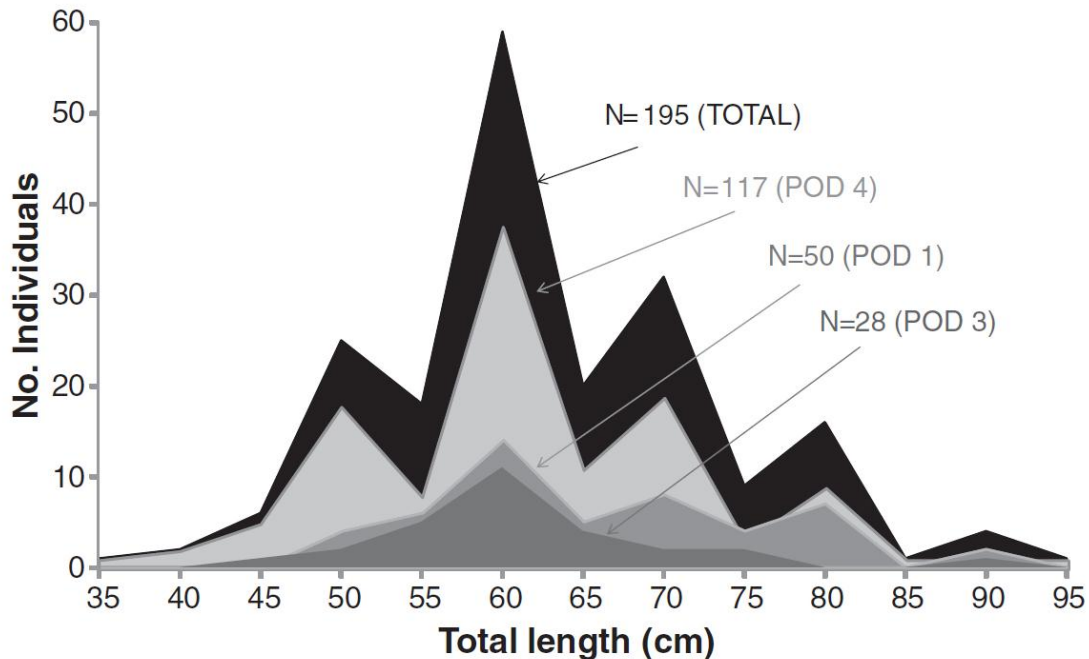


Fig. 6. Class-size frequency distribution representing total body length of measured sablefish ($N = 195$) at the three NEPTUNE-Canada cameras installed in Barkley canyon. That class-size analysis has been repeated by representing total body length of measured sablefish separately for each POD camera. The average length (\pm SD) was 63.6 ± 10.4 cm and the three frequency distributions showed similar shapes.

1.4.4 Light effects

The regression analysis indicated significant perturbing effects of lighting on sablefish visual count (Fig. 7). Considering the 15 randomly selected videos together, we counted in the video recording intervals of 0–25 s and 26–50 s a total of 108 and 68 animals, respectively. This suggests that a significant light attraction effect was reported at the beginning of video recording ($p < 0.005$), followed by a departure ($p < 0.0001$) in the second half of the video sequences.

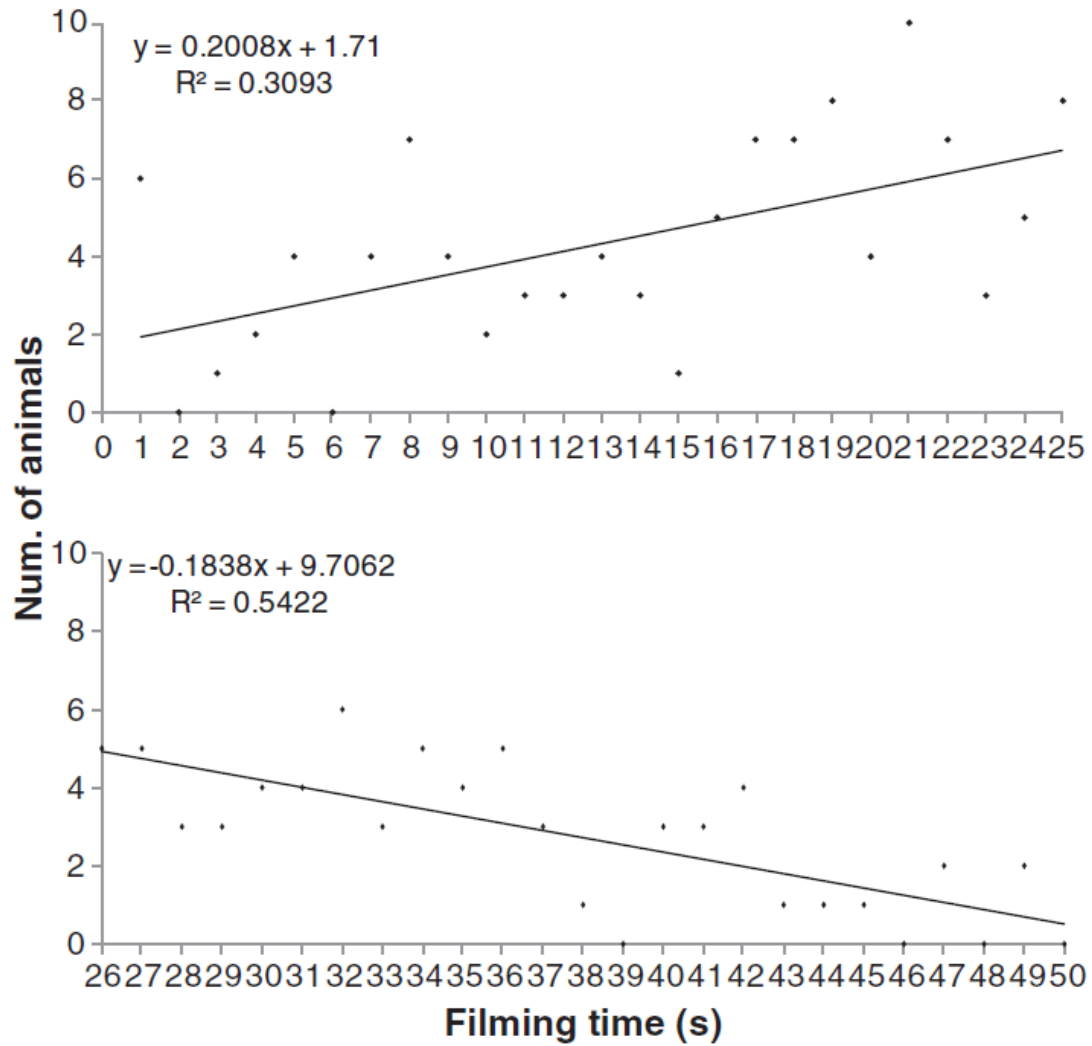


Fig.7. Linear regressions depicting the light effect on reported visual counts of sablefish during footage acquisition, as observed in 15 videos randomly selected from those acquired by the three NEPTUNE-Canada cameras (i.e. POD 1, POD 3, and POD 4) during the first five days of experiment. The regression has been obtained after dividing each video recording length in two intervals (i.e. 0–25 and 26–50 s).

1.5 Discussion

In this study, we combined periodogram and waveform analyses to detect diel rhythmic fluctuations from video counts of a demersal species, the sablefish (*A. fimbria*). In other taxa, hagfish, *Eptatretus* spp., and crabs, which are more confined to the benthos, no discernible temporal pattern of variation was noticed. This was in all likelihood the product of paucity of observations, since at least for crabs a discernible nocturnal phase of activity rhythm was reported in waveform analysis, which was not sustained by periodogram screening. We propose that visual count fluctuations are evidence of population rhythms. Fish rhythms seem to be day–night rather than tidal-driven. Adding the results of our study to those already reported with similar sampling methodology for other deep-sea areas in the Pacific such as Sagami Bay, Japan, at 1100 m depth (Aguzzi et al. 2010), a global scenario of rhythmic regulation at different diel temporal scales at aphotic depths is emerging. These diel rhythms seem to be a widespread phenomenon occurring in the deep waters of all oceans, and are governed either by internal tides or by the day–night cycle especially when species that can attain shallower photic strata in the water column, during their benthopelagic displacements.

1.5.1 Sablefish behavioral rhythms

We are unaware of any temporally scheduled and high frequency (30 min) trawl sampling or video survey study similar to the one we have carried out for sablefish. A previous temporally scheduled ROV video study off Oregon indicated higher numbers of this fish species at night (Hart 2005). Other available behavioral are mostly derived from tagging and recapture studies showing, for example, that continental slope population of sablefish off Vancouver Island is made up mostly of resident individuals (Beamish and McFarlane 1988). Pelagic juveniles chiefly recruit over a broader spatial range involving associated genetic exchange. Large sablefish seem to spend most of their time close to the bottom in order to prey on benthic organisms, while juveniles are more pelagic (Laidig et al., 1997). This behavioral difference is likely to be size–age related, since animals larger than 60 cm (i.e. 6 years old) are mostly observed between 700 and 1000 m of water depth (King et al. 2001, Maloney and Sigler 2008). These data are in agreement with the class-size range observed in our study, where the average body length of animals is 63.6 cm (see Figure6), indicating that our video counts were mostly made on adults.

Sablefish observed at the Barkley canyon seem to follow a diel swimming pattern that modifies the presence (and hence the counts) of animals within the benthic boundary layer. At the camera sites the majority of animals enter in contact with the seabed at sunset, while a minority does so at sunrise (see Figure4). Sablefish diel vertical displacement behavior has been documented for juveniles, which possess pelagic habits, but large adults can have this behavior too (Sogard and Olla 1998). Observations on diel vertical migration patterns for an ecologically similar species, the Atlantic cod (*Gadus morhua*), indicate that animals usually are closely associated to the bottom by day and move off into the water column by night (Adlerstein and Ehrich, 2003, Beamish, 1966, McQuinn et al. 2005). The European hake

(*Merluccius merluccius*) also shows diel vertical migrations, entering in contact with the seabed at 400 m depth during the day (Bozzano et al. 2005). Although the sablefish is not a Gadoid like the cod and hake, our results on rhythmic visual count patterns suggest that their diel vertical migrations are similar with individuals rhythmically entering the benthic boundary layer following benthopelagic displacements (Aguzzi et al. 2010), thus leading to 24-h fluctuations in visual counts.

Diel benthopelagic migrations of fish can result from synchronization of swimming behavior with zooplankton displacements (Andersen and Sardou, 1992, Bergstad et al. 2003, Giske et al. 1990, Mauchline and Gordon 1991, Roe and Badcock 1984). The temporal regulation of these migrations can also be tuned to the temporal activity patterns of visual predators, which in the case of sablefish are mainly marine mammals (see review in Mathias et al. 2012). Accordingly, we propose a hypothesis that accounts for the activity of this species at crepuscular hours in order to maximize chances of feeding whilst at the same time, avoiding predation. By coupling the spatially referenced visual counts time series for two cameras (see Figure 5), one located in the shallower canyon flank (POD 4) and the other deeper in the canyon axis (POD 1), we hypothesize the occurrence of a nektobenthic diel displacement. Since our visual observations mostly involve adults that according to the literature have a preference for the benthos (Laidig et al. 1997), we propose the following: the movement of adults in and out from the canyon axis can account for the different phases detected by waveform analysis in the canyon flank and in the canyon axis (Fig. 8). This displacement may also be accompanied by the regular diel vertical migration within the water column performed by smaller, younger individuals in the shallower video location. This hypothesis fits with the observation of ontogenetic modification of sablefish diet (Laidig et al. 1997). The fish diet varies with length, with smaller individuals chiefly feeding on pelagic small fish and crustaceans whereas the larger individuals feed predominately on benthic organisms.

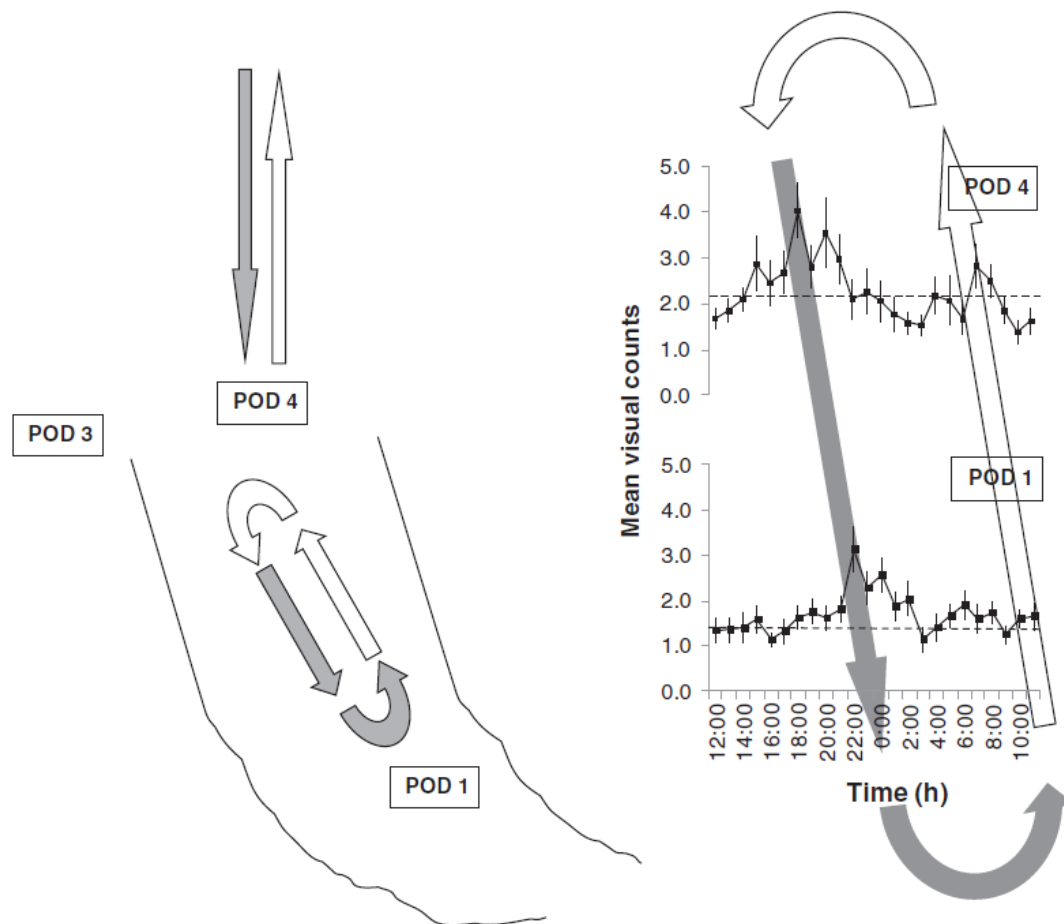


Fig.8. Modelled typologies of rhythmic displacement of sablefish within the Barkley canyon, as reported by coupling wave form analysis of data sets from the three NEPTUNE-Canada cameras located respectively at the outer canyon flank (POD 3), the inner canyon flank (POD 4) and the deeper canyon axis (POD 1). Apparently, fish perform benthopelagic displacements within the water column (vertical gray-night and white-day arrows) as well as deeper nektobenthic displacements (same type of arrows) back and forth between canyon flank and axis. Waveforms analysis output plots (on the right; adapted from Fig. 5) present a timing shift in rhythm phase (i.e. values above the MESOR), which seems to be related to depth variations in the location of the cameras.

Due to the short distance between the cameras in POD 3 and POD 4, we reject the likelihood of relevant ecological difference between the two sites. But so far, there is no clear explanation for the fish observations indicating randomly occurring, but significant lower visual counts at POD 3 over the one-month temporal window. Perhaps the fish simply choose the easiest or more attractive pathway to displace up and down over the canyon flank, passing close to POD 4, avoiding the location of POD 3. Independent of the true reason for the differences detected between these two nearby locations, we think that these results are of relevance as they illustrate that a rather small-scale spatial heterogeneity between two neighboring observational sites may lead to substantially different results in video counting surveys.

1.5.2 The hagfish and crab behavior

The hagfish seen in our videos is likely *Eptatretus stoutii*, which is the most abundant Agatha species in Barkley canyon (Davies et al. 2006). From our observations we cannot detect an activity rhythm in the local population of hagfish. Early laboratory observations on the behavior of another hagfish species (i.e. *Eptatretus burgeri*) by Ooka-Souda et al. (1985) detected the presence of marked nocturnal swimming rhythms in animals exposed to laboratory 12:12 h light-darkness conditions. In a study at 10 m depth in Japanese waters Fernholm (1974) showed that *E. stoutii* remain within a burrow during the day and emerge at night, thus confirming the previous laboratory observations. However, this behavior was not observed in our study, which was conducted in deep waters where hagfish activity is chiefly nocturnal and they have been observed feeding on carrion falls (Davies et al. 2006). We did observe animals coiled onto the seabed when resting (see Section 1.5.4).

Eelpouts show marked hydrodynamically-driven activity rhythms, which are controlled by internal tides (Aguzzi et al. 2010, Cummings and Morgan 2001). The animals orient their body and regulate their swimming activity to adapt to shifting current conditions in terms of strength and direction (see review in Lorance and Trenkel 2006, Trenkel et al. 2004, Uiblein et al. 2002). Possibly, hagfish may also present a swimming behavior influenced somehow by tidal hydrodynamics, though this was not detected in our observations.

We did not detect discernible activity rhythms in the crab group likely made of several species including tanner crab *Chionoecetes tanneri* and scarlet king crab *Lithodes couesi* (Gervais et al. 2012). However, crab species were not taxonomically determined in our video observations, because of the limitations imposed by the small size of the animals and the low resolution of the cameras. In other areas of the Pacific Ocean, deep-sea red crabs *Paralomis multispina* show weak tidally oriented walking rhythms, as observed after a video-sampling methodology similar to ours (Aguzzi et al. 2010). In the deep Mediterranean, decapods show complex regulations of their swimming and walking activity rhythms in response to both day-night and inertial current cycles (Aguzzi et al. 2008, 2008, 2008). Barkley canyon data are not conclusive regarding crabs' activity rhythms. Periodogram analysis did not reveal any significant periodicity even though a major night peak was detected (see Figure 4).

1.5.3 The population structure of sablefish

Sablefish inhabit the shelf and slope waters from central Baja California to the Bering Sea and Japan (DFO, 2009) and support one of the most valuable fisheries in the North Pacific (King et al. 2001; Ryer 2004, Stachura et al. 2012). Therefore, increasing our knowledge about sablefish behavior and population structure with non-invasive sampling methods potentially has socio-economic implications. In our study, the population size structure sample was based on 195 individuals, which, despite being a rather small sample in comparison to the reported total counts, is acceptable according to reference

literature (Priede et al. 1994 2003). At the depth range (892–984 m) within Barkley canyon we observed a sablefish size frequency distribution between 35 and 95 cm, with an average length of ~63 cm (see Section 3.3 and see Figure 6). Such an average size corresponds to an age of 4–5 years (King et al. 2001). We also found percentages of smaller individuals, which were likely younger (35 cm and 1 year). These observations may justify the absence of a long right hand tail in our class-size frequency distribution as there are fewer smaller (younger) individuals than larger (older) ones. Taken together, our results are in agreement with those obtained in the Gulf of Alaska (Maloney and Sigler, 2008), but differ from previous results from our study area. Saunders et al. (1997) reported sablefish aged up to 5 years as occupying shallower depths (640 m), while animals aged 5 to 10 years would occupy mid-depths (641–824 m). Only the oldest animals (≤ 10 years) would be resident in deeper levels (≤ 824 m).

1.5.4 Biases in cabled observatory video recording

We observed a light biasing effect on the detectable number of fishes (see Figure 7). Globally, both attraction and subsequent apparent retreat seem to compensate each other, so an overall biasing may be absent in our particular samples. Attraction to artificial structures either due to the light or other reasons (e.g. bait) is a well-documented phenomenon (Stoner et al. 2008; Trenkel et al. 2004). In particular, studies using baited cameras indicate how fishes arrive, explore and then depart (Farnsworth et al. 2007, Trenkel and Lorange 2011). Although the behavior of sablefish seems to be only minimally affected by artificial lighting (Krieger 1997), attraction to lights has also been described (Harvey et al. 2012). At the “Eye on the Sea” cabled observatory, (Widder et al. 2005) reported an increase in detected sablefish numbers when less visually detectable red light was used. In any case, bright white lighting for video recording does not necessarily impair the detection of population swimming rhythms, as the potential errors due to light attraction or avoidance are constant over the entire sampling time (Aguzzi et al. 2010). It seems that the potential bias in *A. fimbria* behavior that might occur at the Barkley canyon site does not disrupt the analysis of populational rhythms.

1.6 Conclusions

NEPTUNE-Canada video cameras enabled to study the activity rhythms of a sablefish (*A. fimbria*) population in Barkley canyon, west of Vancouver Island. Sablefish is a highly motile marine organism of high ecological and economical relevance in the North Pacific. Synchronous video recording in the canyon axis and flank within the depth range of 892–984 m elucidated a complex behavioral rhythm of displacement for this species that potentially involves these two canyon environments. These results, along with others being obtained in other deep-sea areas of the planet, stress how complex populational rhythms can be, thus deeply biasing our perception of the composition of local communities, especially when sampling technologies and strategies produce too scattered results.

1.7 Acknowledgments

This research was funded by project RITFIM (ref. CTM2010-16274), of the Spanish national RTD program. The Canada Foundation for Innovation and the British Columbia Knowledge Development Fund provided funding for the instrumentation of Barkley canyon. The Spanish DOS MARES project (ref. CTM2010-21810-C03) and Generalitat de Catalunya support to CRG Marine Geosciences (ref. 2009 SGR 1305) are also acknowledged. We thank the ROPOS ROV team and the crews of the CCGS John P. Tully and R/V Thomas G. Thompson for their assistance in the field. J. Aguzzi is a postdoctoral Fellow of the Spanish Ramón y Cajal Program. Ms. Carol Doya is a FPI Ph.D. student. We would like to thank Mrs. V. Radovanovic for editing advice during the manuscript preparation.

**Chapter 2. The seasonal use of small-scale
space by benthic species in a transiently
hypoxic area**

2.1 Abstract

The use of small-scale space by benthos and its variation over the seasons in transiently hypoxic zones is poorly known. In this study, we examined the reciprocal spatial dispersion of the squat lobster (*Munida quadrispina*) and the slender sole (*Lyopsetta exilis*) according to oxygen concentrations at a VENUS platform of Ocean Networks Canada (ONC). This platform is located in a seasonally hypoxic zone at 96m depth in the fjord of Saanich Inlet (British Columbia, Canada). We counted and located small as well as large squat lobsters and slender soles in digital still images during 1 year (2012–2013) also concomitantly obtained oxygen data. Images were subdivided in a squared grid to obtain relative density maps as a proxy for surface occupation and spatial autocorrelation. Pearson's chi-squared tests at a yearly scale, along with Dixon's spatial segregation index (S) for each possible pair among the studied groups, showed a significant absence of overlap. The same analyses by month and cross-correlation between oxygen and S showed that while the dispersion patterns of the large squat lobsters seemed to be driven mainly by the morphology of the seafloor, an effect of hypoxia was found in the small squat lobsters and the slender soles levels of aggregation. Small squat lobster sought seabed protrusions, such as sponges, to reach more oxygenated water. The slender sole's space occupation decreased significantly, being forced to retreat when the squat lobsters' abundance peaked as a result of what appeared to be a seasonal reproduction event in early summer. Our results contribute to the understanding of the ways in which oxygen levels modulate substrate use by benthic species in the framework of a global expansion of hypoxia in coastal and ocean areas.

Keywords: Fjord, Saanich Inlet, *Munida quadrispina*; *Lyopsetta exilis*; Dispersion; Imaging techniques; Hypoxia; Seasonal variations

2.2 Introduction

The study of the ecological niches regarding the fauna of continental margins requires a detailed knowledge of animal presence and activity in space and time (Aguzzi et al., 2013, Kraan et al. 2013). The spacing of individuals affects the population dynamics, genetics, and evolution of species (Brown and Orians 1970, Dixon 2002). Accordingly, it is of special interest to study the spatio-temporal variability of those factors affecting animal spatial dispersion (i.e., as the position of individuals relative to one another; Ricklefs 1979). Dispersion patterns of benthic megafauna at different scales may result from biotic factors such as reproductive processes, intraspecific social behavior, interspecific coactive interactions, abiotic parameters, and stochastic events (Jumars and Eckman 1983). Therefore, animal dispersion patterns in an area should also be studied in an integrated fashion, along with those environmental parameters that play a key role in the spatial and temporal regulation of these patterns. In particular, special attention should be dedicated to the study of those factors affecting the dispersion of dominant species because the niche occupation by the individuals of these species as a response to local environmental changes may directly influence the presence of other subordinate species and the overall diversity of the community (Aiken and Navarrete 2014).

Sediment composition and seabed morphology influence the distribution and abundance of benthos (McArthur et al. 2010). For example, epibenthic walking species are more dependent upon sediment typology than epibenthic swimmers, which are also influenced by currents (Aguzzi and Company 2010, Cnudde et al. 2013, Doya et al. 2014). Such lifestyles would determine the dispersion patterns of deep-water benthos *via* a differential response of animals to biotic factors such as predation pressure (determining an aggregated pattern), territoriality and competition (a regular pattern), or none of the aforementioned (a random pattern) (Brown and Orians 1970). Other putative factors influencing species dispersion could be related to seasonal changes in environmental conditioning, such as, for example, oxygen levels (Riedel et al. 2014). Thus, an analysis of the consequences of the seasonal variability of such factors for the spatial patterns should be conducted in the context of animal-sediment relationships as a core feature of different lifestyles.

In the past years, dissolved oxygen has emerged as a major environmental driver that modulates the presence of benthos in deep-water areas (Levin et al. 2009). According to Grimes (2014), dissolved oxygen concentration is considered an essential ocean variable (EOV) due to the high impact of variation in its concentrations on biotic systems that inform stated scientific and societal issues. Hypoxia is increasing in coastal and oceanic waters (Gilbert et al. 2010, Rabalais et al. 2010), due to eutrophication and global warming (Díaz and Rosenberg 2008, Zhang et al. 2010, Rabalais et al. 2014). Shoaling of hypoxic strata is producing noticeable effects in benthic species such as mass mortality (Breitburg 2002) and shifts in average depths of distribution (Keister and Tuttle 2013, Pihl et al. 1991), posing a threat to marine biodiversity (Díaz and Rosenberg 1995, Kodama et al. 2010). The depth expansion of oxygen minimum zones has been associated with the decline in important fisheries as a result of habitat loss for

targeted species (Craig and Crowder, 2005, Keller et al., 2010). While many studies have addressed the effects of hypoxia on the distribution of benthic communities (Levin et al. 2009), few have focused on effects of oxygen levels on the animals in situ (Villnäs et al. 2012), due to the lack of suitable coordinated image and oxygen sampling.

Cabled seafloor observatories can provide science from high-frequency (minutes) and prolonged (years) datasets on both benthic communities and water characteristics (Aguzzi et al. 2012, Favali and Beranzoli 2006, Puillat et al. 2012). Here, we used the VENUS observatory located in a seasonally hypoxic fjord (Macoun et al. 2010, Tunnicliffe et al. 2003) to test the hypothesis that the dispersion patterns within and between two abundant benthic species, the galatheid squat lobster *Munida quadrispina*, and the slender sole *Lyopsetta exilis*, are random and do not depend on oxygen changes. These species were selected because they dominate the epibenthic community of Saanich Inlet throughout the year and show overall resistance to hypoxia (Dinning and Metaxas 2013, Keller et al. 2010, Matabos 2012). Changes in these dominant and hypoxia-tolerant species are of relevance because they can affect the structure and dynamics of the entire community, and, therefore, strategies of fisheries management and conservation in a scenario of expanding hypoxia. A 1-year time-lapse imaging survey with coordinated dissolved oxygen measurements was designed to assess any changes in the abundance and dispersion patterns of the two selected study species under seasonally transient hypoxia. Only short-range phenomena were examined in detail with statistical tests at small scale to highlight direct inter-individual interactions but also because we were limited by the per-quadrat numbers being generally ones and zeros. Small-scale sampling is of importance for reliably documenting ecologically significant changes at larger geographic scales because mesoscale sampling can miss contrasting environmental shifts at smaller scales (Blanchard and Heder 2014). In literature, small scale is inconsistently defined. In this manuscript, small scale is understood being between 10s of cm and over 100 cm, after Benedetti-Cecchi (2001).

2.3 Materials and methods

2.3.1 The platform, the study area, and data acquisition

The VENUS cabled observatory (<http://www.oceannetworks.ca>) supports a cabled array of instruments in Saanich Inlet (Fig. 9; 48° 39.054' N, 123° 29.203' W; British Columbia, Canada). This siting enables imaging studies of the local benthic community in response to seasonally transient hypoxia (Aguzzi et al. 2011). Saanich Inlet has a maximum depth of 234 m (Herlinveaux 1962) with a shallow sill (70 m) that isolates its basin from the adjacent Satellite Channel. This configuration restricts seasonal renewal of the deep water and promotes oxygen depletion in the basin (Anderson and Devol, 1973, Stucchi and Giovando 1984). Oxygen concentrations < 1.0 ml/l occur below 100 m throughout the year, and the depth and extent of the hypoxic and anoxic interfaces vary over consecutive months (Tunnicliffe 1981).

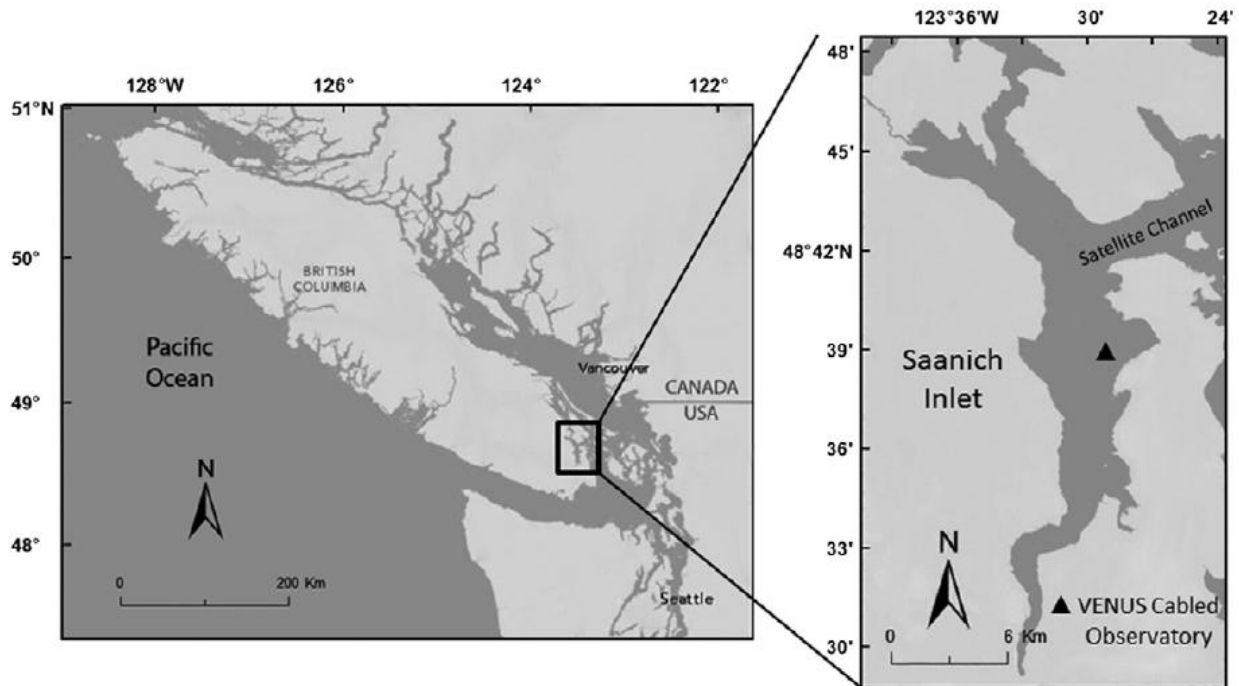


Fig.9. Map of Saanich Inlet, showing the location of the camera, as part of the VENUS Cabled Observatory infrastructure (black triangle).

A 1-year image acquisition program (starting at 00:00 h on March 2, 2012, and continuing until 22:00 h on February 26, 2013; UTC) was conducted with a modified Olympus® C8080 wide zoom camera with a high-resolution (8 megapixels) CCD. A ROS PT-25FB pan and tilt unit allowed the selection of an appropriate field of view. The camera tilt was fixed at 45° to record a constant seabed surface of approximately 7200 cm^2 . The substratum is characterized by consolidated muds around outcropping bedrock in contrast with the predominantly soft substratum, soupy mud of the lower reaches of the bay (Chu and Tunnicliffe 2015). The field of view encompassed a black and white scale bar marked at 10 cm and a large sponge (upper center; Fig. 10). Illumination was not constant but activated only at the camera shooting times *via* Ikelite 200 Ws flashes producing light pulses of 2 ms duration. Image acquisition was automated so that the camera occupied the same position and sampling occurred at preset intervals. The imaging survey was conducted in a time-lapse mode by taking images every 3 days each 2 h (i.e., 12 JPEG images per 24 h).

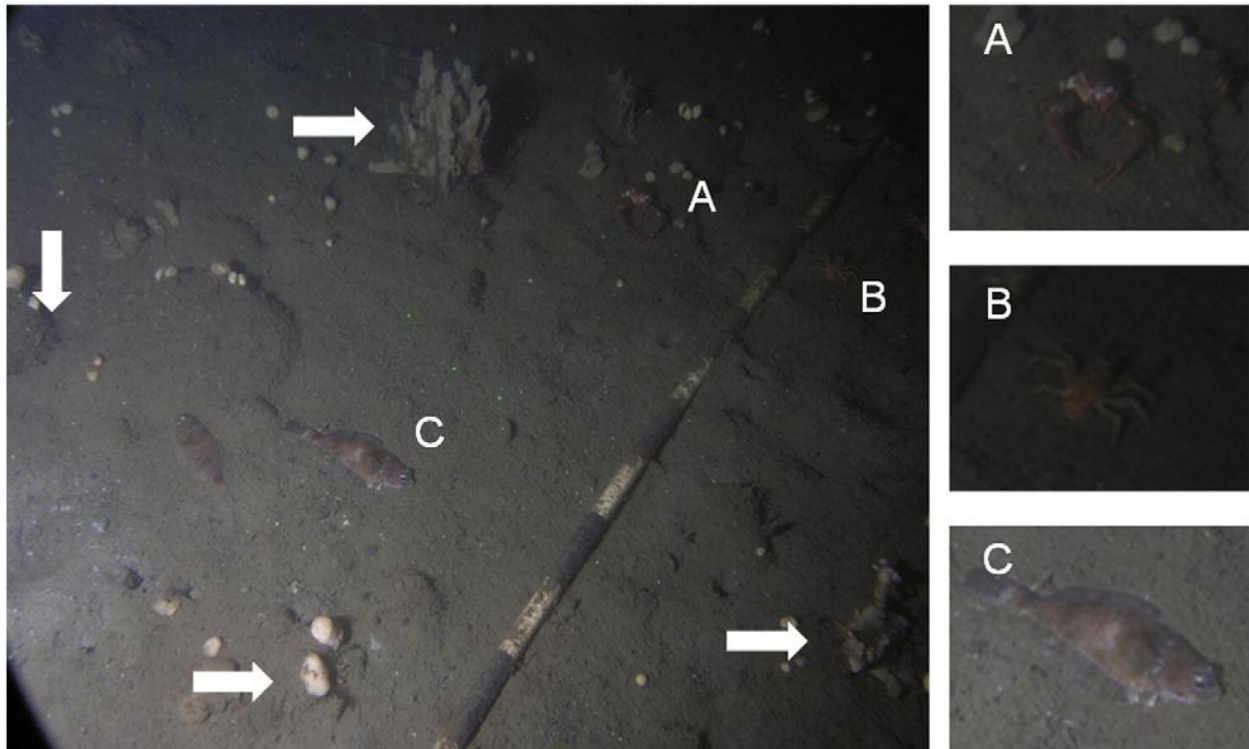


Fig.10. The selected VENUS camera field of view, with individuals for the three groups: large (A) and small *M. quadrispina* (B) plus *L. exilis* (C). The main seabed structures within the area are the PVC scale and the sponges (indicated by the arrows). The image was taken at 18:48 h UTC, on September 29, 2012.

Dissolved oxygen concentrations were measured using an Aanderaa Optode 4175 (S/N 0580) mounted on the camera frame with the sensor head 20 cm above the bottom. This sensor has an accuracy of ± 0.17 ml/l or $\pm 5\%$ (whichever is greater). Oxygen data were taken at 1 Hz.

We focused on the two most abundant, low-oxygen tolerant, epibenthic megafaunal species in the area: the squat lobster *Munida quadrispina* and the slender sole *Lyopsetta exilis*. We considered two size classes (i.e., large and small) of squat lobsters. We used key morphological characteristics (Matabos 2012; see Figure 10) to define these classes: large individuals were greater than 10 cm, and they possessed thick hairs on their chelipeds. Recruits (i.e., individuals with no visible walking legs) were excluded from analysis because they were too small to be properly identified and counted. Slender sole (see Figure 10) were identified based on Eschmeyer et al. (1983).

2.3.2 Data treatment

An overall seasonal screening of biological data was obtained by plotting time series of visual counts for the three groups (i.e., large and small *Munida* and *Lyopsetta*) along with dissolved oxygen concentrations. Oxygen concentration data were averaged at a 2 h frequency for the 2 h prior to image acquisition in order to facilitate the visual interpretation of the time series analysis.

Spatial patterns can be analyzed at 2 levels, either comparing counts of organisms per parcel with random expectation while ignoring their relative locations in space or considering the spatial relationships among individuals with random expectations (Jumars et al. 1977, Sokal and Oden 1978, Legendre and Legendre 2012). In this study, we applied distinct methods covering both levels of spatial patterns.

The exact position of individuals in each image was identified within a system of spatial coordinates. First, a digital marker was placed on each individual, obtaining a pair of x, y coordinates with tpsDig2 (tps free-share software package, version 2.17; <http://life.bio.sunysb.edu/morph/>). To avoid distortions due to the depth of the field of view (i.e., the camera shot at 45°), a correction was applied to the y coordinates using a digital 8 × 8 cm grid (Fig. 11) constructed with GIMP software (free-share version 2.8; <http://www.gimp.org/>). The size of grid subdivisions was calibrated using reference images of a PVC rectangle temporarily placed on site by a remotely operated vehicle. True and image-distorted y-coordinates for grid nodes were regressed, obtaining the angular coefficient as a correction factor ($y_{cor}=1.084 y_{obs}$, where cor and obs are the corrected and the observed coordinates, respectively). Variation in the x-axis along the field of view depth was considered minimal.

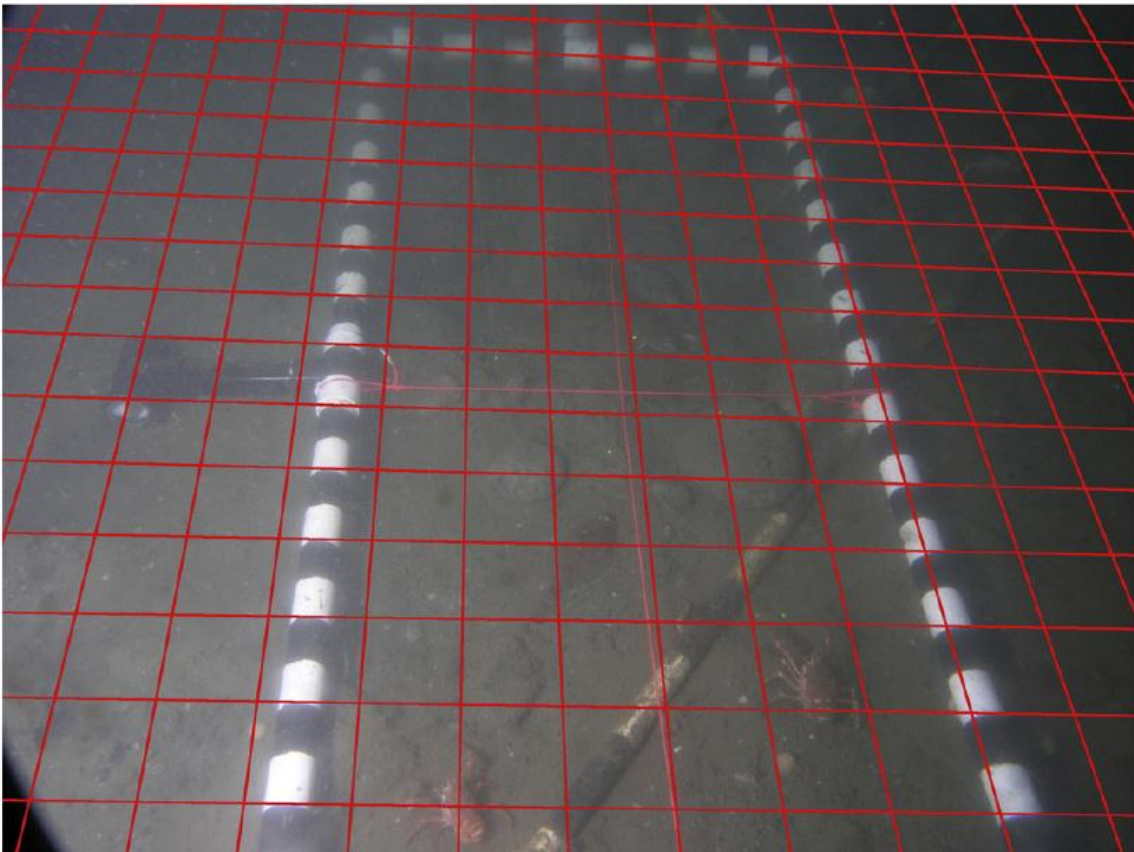


Fig.11. The field of view used at VENUS, subdivided by the digital grid (red lines) drawn a posteriori and used as a reference system of coordinates to calculate exact animal positioning. The PVC black and white frame was briefly deployed by ROV to calculate the field of view surface and the correction factor.

Next, reciprocal Euclidean distances between all individuals in each image were computed with the PAST software (Paleontological STatistics, version 3.01; <http://folk.uio.no/ohammer/past/>; Hammer et al. 2001). The nearest neighbor of each individual was identified, and the resulting data were used for computing a monthly segregation index (S; Dixon 2002). S is used to quantify the tendency of members within a group to be aggregated, regularly or randomly dispersed (Cuvelier et al. 2014). Positive values indicate aggregation; negative values, dissociation; and 0 corresponds to a random dispersion pattern. A time series of the monthly S values between all possible nearest neighbor pairs was plotted for each of the three groups.

The overall spatial arrangement of the three groups was quantified by relative density map analysis. A relative density map is a graphical representation of data, where individual counts contained in a matrix are represented with a gray scale (i.e., the maximum number of counts and 0 counts are shown in black and white, respectively). The field of view was transformed into a second grid of 9×9 parcels (362.67×294.85 pixels) using the corrected y-axis.

To identify the parcel that was occupied most completely by the individuals of a group, a Pearson's goodness of fit test was used (i.e., under the null hypothesis of equal probability of parcel occupation, separately for each species). The results were presented as monthly and annual relative density map outputs. Significantly more or fewer occupied parcels (critical values ($P = 0.001$) = $\sqrt{X^2_{0.001, 80/81}} = 1.24$) were shown with yellow and red margins, respectively, on the plots.

To assess the preponderance of individuals of each group in each parcel, we ran a Pearson's test of independence. Counts for each group were standardized to the most abundant group. The Pearson's test compared standardized abundances per each parcel by month and the whole year, detecting a significant degree of preponderance for any of the groups. The null hypothesis was that the occupation of each parcel by any group was equally probable. Significant differences from the expected values were considered to indicate group dominance in any parcel.

The results were presented as the percentage of parcels over the total (i.e., $N = 81$), where each group was dominant. Finally, the counts data of each group's annual density map were tested for spatial autocorrelation with Moran's I correlograms, using the R package "ncf" (R development Core Team 2013).

2.3.3 Oxygen relationships

We studied the influence of oxygen concentration on the dispersion of each group at a monthly scale. Variation of the spatial relationship among these three groups was screened with a linear regression ($\alpha = 0.05$) of S data against monthly averages of oxygen. Additionally, we cross-correlated the monthly S and oxygen concentration values with the objective of identifying if temporal variability in the former

was significantly dependent upon the temporal variability of the latter. The cross-correlation was implemented through R language functions (R development Core Team 2013).

2.4 Results

2.4.1 Time series analysis

A total of 5776 large *Munida*, 4533 small *Munida*, and 1205 slender sole were counted in 1268 images. Another 160 images were unavailable for counting due to lighting failures at image acquisition, which made the images appear entirely black.

Oxygen showed strong seasonal fluctuation (Fig. 12). Our measurements began on March 2, 2012, with a maximum oxygen concentration of 1.41 ml/l. Oxygen levels appeared to increase progressively throughout late winter, reaching a maximum in mid-March 2012 (3.34 ml/l). Minor peaks occurred until the end of summer but did not prevent an overall oxygen decrease, which continued until the end of September. Near-anoxic conditions prevailed over the succeeding months until mid-January 2013, when oxygen concentration increased again. At that time, these concentrations attained levels similar to those reported at the beginning of our monitoring (maximum 1.78 ml/l).

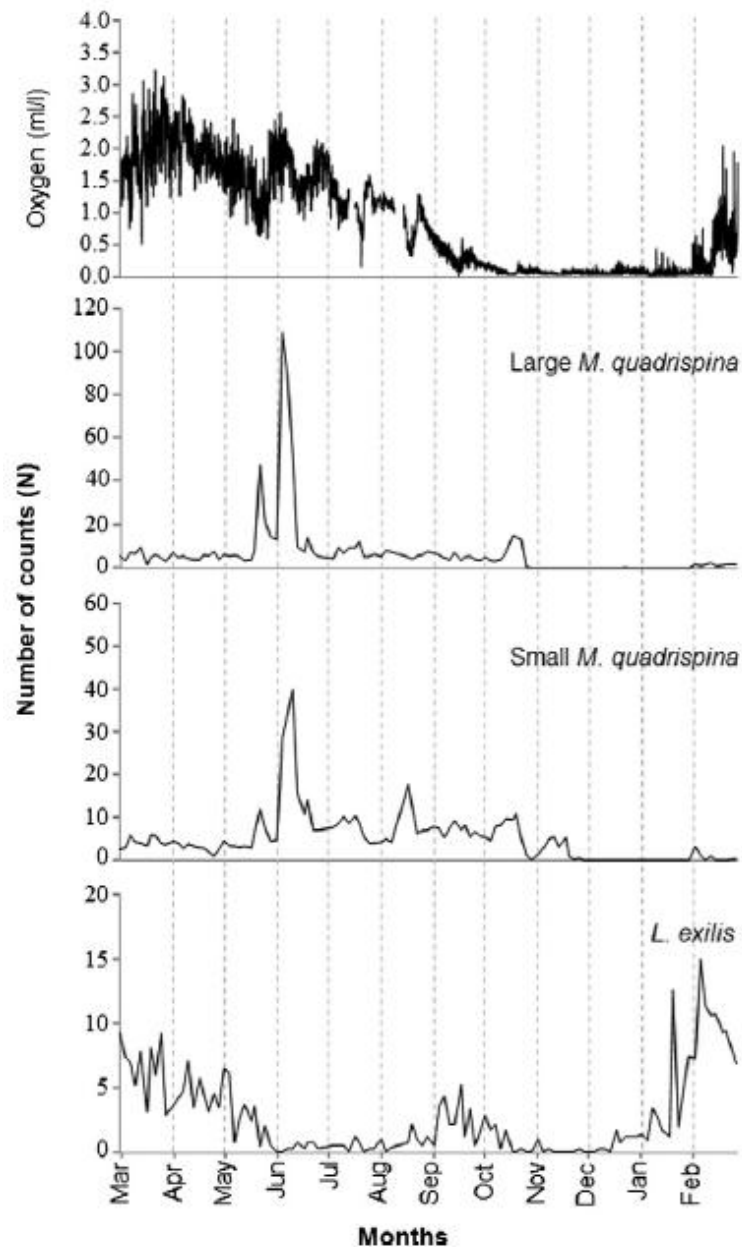


Fig.12. One-year time series (from 2nd March 2012 to 26th February 2013) of visual counts per image for the three groups studied (large and small *M. quadrispina* plus *L. exilis*), along with the dissolved oxygen concentration. The dashed vertical lines correspond to the 1st of each month. The y-axis scale differs between the three groups.

Squat lobsters of both size classes exhibited similar temporal patterns (see Figure 12), although small lobsters were approximately one third as abundant as large lobsters. After the peaks in abundance over the first 10 days of June 2012 (exceeding at times 100 individuals/m²), numerous shed exoskeletons were visible in the images (not quantified here). Squat lobsters also showed a small increase in number in October. In November, large individuals were completely absent, and they were seldom observed until early February. Small individuals followed the same pattern after mid-November. At the time of the squat

lobster peaks, the slender sole generally disappeared. Slenderson counts were, however, higher over the previous months, coinciding with the highest level of oxygen, while the counts of squat lobsters were lower. After a period of slender sole activity in September–October, the fish seldom appeared again until January. Counts in February were the highest for the entire period (peak of 15 individuals occurred in one image on February 14), coinciding with a progressive recovery in oxygen concentrations.

Visual count peaks in large and small squat lobsters coincided with vast aggregations in images (Fig. 13). Individuals ($N = 100$) were often observed in close proximity, even touching each other, occupying all available space.

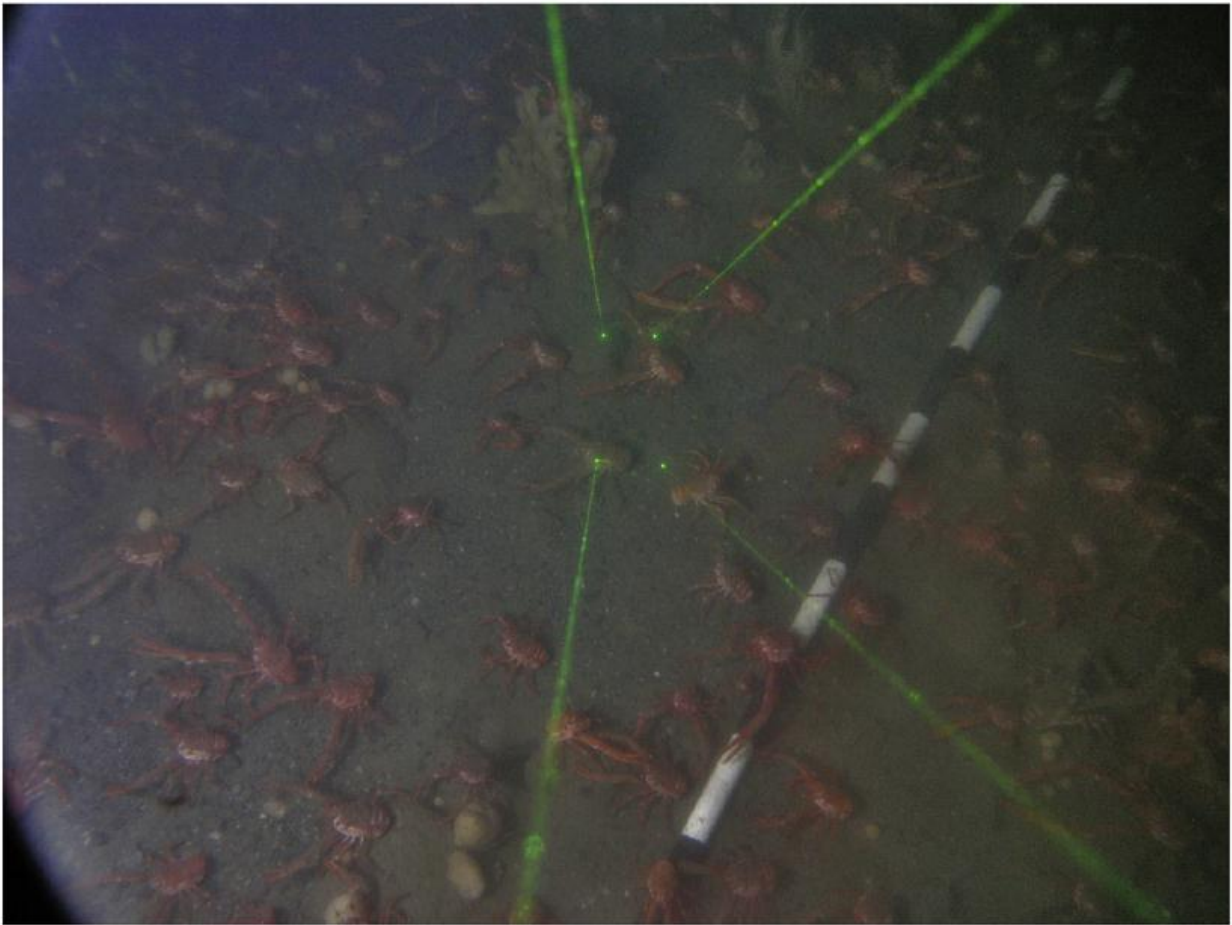


Fig.13. The massive aggregation of *M. quadrispina* observed at VENUS during the first 10 days of June. This image was taken at 10:16 h UTC on June 05 2012.

2.4.2 Intraspecific dispersion and spatial autocorrelation

The general tendency in the occupation of space by each group is evident from the yearly relative density map (i.e., animals per parcel during the whole year; Fig. 14). The outputs of the relative density map calculations showed the most significantly (Pearson test $p=0.001$; Appendix A) occupied areas of the field of view for the three groups.

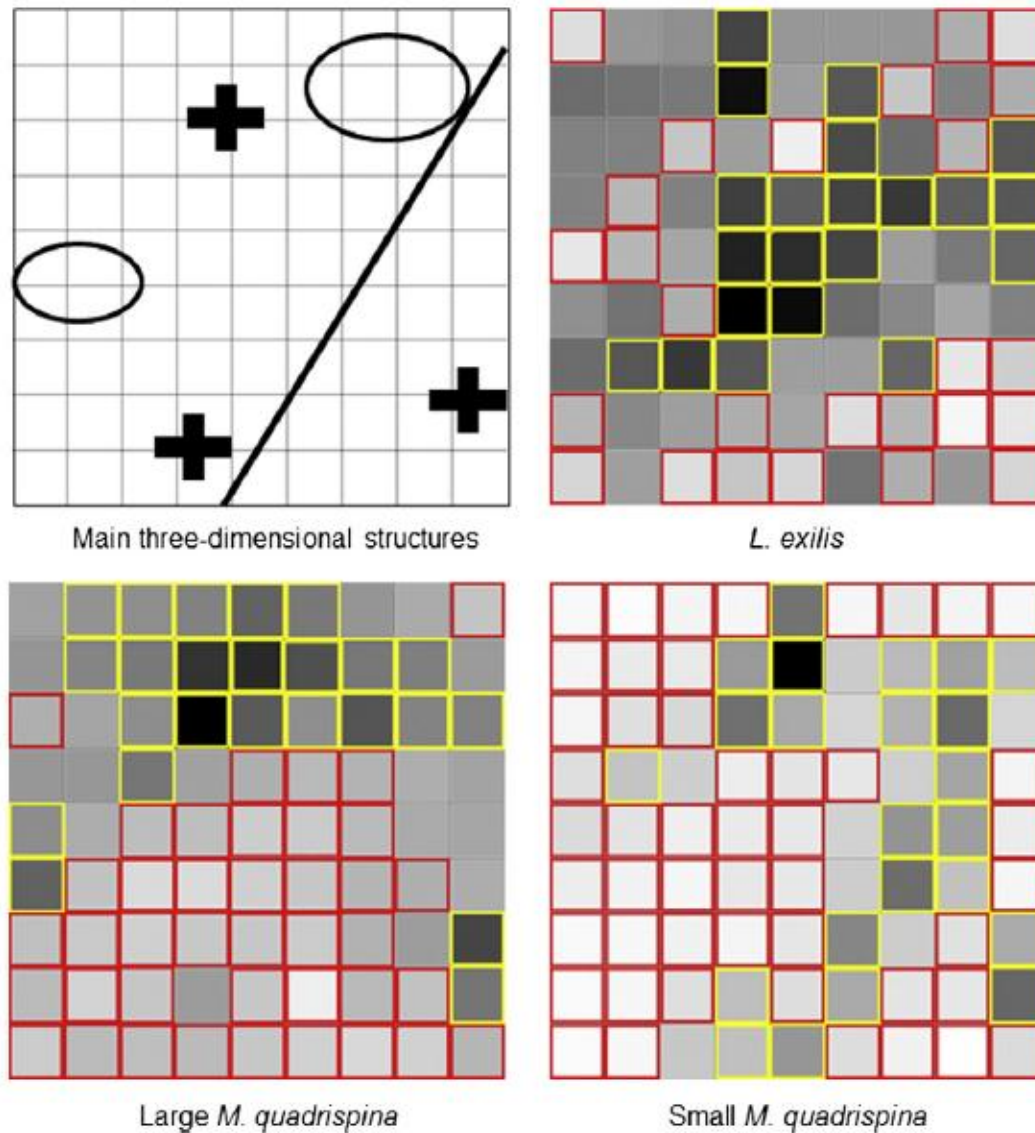


Fig.14. Year-long relative density maps present the averaged distribution of the three groups (large and small *M. quadrispina* plus *L. exilis*), using the gray scale as a proxy for the number of counts (black and white parcels indicate the highest and the zero counts of animals, respectively). The significant differences in occupation levels are also presented (over-occupied and under-occupied parcels are in yellow and red, respectively). In the schematic map (upper left corner), positions of relevant areas within the field of view are indicated by black crosses (sponges), the black bar (the PVC pipe), and ellipses (where seabed is particularly rough).

The relative density map for large squat lobsters (see [Figure 14](#)) showed a significant aggregation in the farthest part of the field of view (i.e., 3 superior parcel rows), coinciding with the location of a sponge and other structures (also visible as a trend in the majority of the monthly relative density map analysis outputs; see [Appendix B](#)). Animals also aggregated in the middle left of the field of view around a rocky complex and in the lower right side, where another isolated sponge is located.

The annual relative density map for the small squat lobsters (see [Figure 14](#)) showed a significant aggregation on two main structures: large sponges and the PVC pipe (see [Figure 10](#)). The monthly relative density maps (see [Appendix B](#)) showed that animals significantly aggregate in high densities along the PVC pipe during the first 3 months of the study (from March to May), when oxygen showed high concentrations (see [Figure 12](#)). In June, the small *Munida* significantly aggregated along the PVC pipe but also around the large sponge. From August to November, and after a sharp reduction of oxygen in August, the occupation displayed by these individuals gradually shifted from the parcels corresponding to the pipe to those in the large sponge area. After this period, no small individual was detected until the next February (see also [Figure 12](#)). The slender sole occupied the flatter central part of the field of view (see [Figure 14](#)), an area bounded by the bar and the sponges (see [Figure 10](#)). However, some of the monthly relative density maps (see [Appendix B](#)), mainly corresponding to months with only a few counts, did not reveal this tendency.

[Fig. 15](#) presents Moran's I spatial autocorrelation for the three faunal groups. There was significantly positive spatial autocorrelation in all cases for distances smaller than 2 density map parcels, thus, patchiness existed in all cases. Spatial autocorrelation was strong for large squat lobsters. Together with that, the first maximum negative Moran's I correlation (which indicates the size of patches, "range of influence" or the distance between zones of high and low concentrations), for large squat lobsters occurred for distances greater than 6 parcels, with the corresponding low for slender sole occurring in a distance class close to 4 parcels. Small squat lobsters did not show any significantly negative spatial autocorrelation. Taken together, these results indicate the more robust shape of the area that large squat lobsters occupied in comparison with the elongated area occupied by small conspecifics and slender sole. These shapes are in agreement with the annual density maps (see also [Figure 14](#)). All correlograms were significant, since none of the coefficients out of the grey area changed in significance after the Bonferroni correction was applied ($\alpha' = 0.00625$).

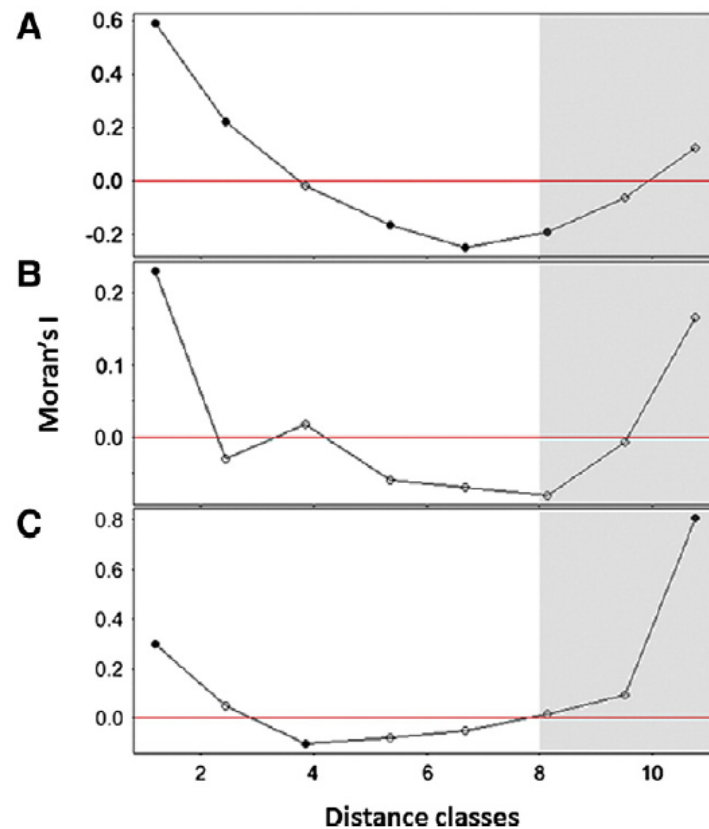


Fig.15. Moran's I correlogram for the number counts of A. large *M. quadrispina*; B. small *M. quadrispina*; and C. *L. exilis*. Black dots represent spatial autocorrelation coefficients significant at the $\alpha=5\%$ level, before applying the Bonferroni correction; white dots are nonsignificant values. Coefficients for the larger distance values (grey zones in correlograms) should not be interpreted, because they are based on a small number of pair (test with low power) and only include the pairs of points bordering the surface. The horizontal red line helps to identify the sign of the spatial autocorrelation coefficient.

2.4.3 Interspecific relationships in space use

The Pearson test of independence examined the degree of dominance in each parcel by each of the groups in relation to the others, highlighting the groups that preferentially occupied given parcels. The results are presented for each group in terms of the percentage of parcels in which the group was significantly ($p < 0.0001$) more or less prevalent (Table 2). From the beginning of our survey until November, the interspecific relationship between the large squat lobsters and the slender sole changed from a significant under-occupation to significant dominance by the latter. However, both groups prevailed significantly against the small squat lobsters during the whole year except in June, when counts of the small squat lobsters peaked.

Table 2. Interspecific dominance relationships, presented as the percentage of significantly more (+) or less (-) occupied parcels over the total (i.e., 81), as observed over a month. All significant (*) comparisons (p < 0.0001) are indicated

Month	<i>L. exilis</i>		Large <i>Munida</i>		Small <i>Munida</i>	
	(+) %	(-) %	(+) %	(-) %	(+) %	(-) %
*Mar	35	22	31	43	23	44
*Apr	33	28	32	31	21	57
*May	31	44	38	31	20	48
*Jun	15	85	67	19	48	30
*Jul	19	77	46	31	32	41
*Aug	27	67	46	28	27	37
*Sep	33	47	43	31	21	54
*Oct	30	47	32	30	35	32
*Nov	7	7	-	-	7	7
Dec	30	4	2	1	1	2
*Jan	48	1	1	48	-	-
*Feb	36	22	27	41	21	58
*Year	49	36	43	32	30	56

2.4.4 The segregation index (S)

In the months when only isolated individuals were observed in all images, pairwise comparison was not possible. Large (L) squat lobsters (Fig. 16A) showed an overall opposite trend compared with their small (S) conspecifics and the slender sole (flatfish; F). The S for large squat lobsters was always close to 0, i.e., they did not show a strong tendency to be distant from or closer to other individuals of any of the groups; thus, they were randomly dispersed. The Segregation Index showed that intraspecific aggregations of small *Munida* (Fig. 16B) occurred throughout the year, with a minimum value observed in August (SSS = 0.29). During this month, the separation of individuals into two groups was more evident as a product of their gradual displacement from the PVC pipe towards the large sponge (see monthly relative density maps in Appendix B). On the other hand, small and large squat lobsters were constantly dissociated (as shown by the negative SSL value obtained throughout the year; see Appendix C). This finding is in agreement with the dispersion pattern of both groups as presented in the annual relative density maps (see Figure 14). Slender sole was spatially aggregated through the year (i.e., SFF = 0), having the highest value in July (SFF=2.75) among all the 9 possible permutations. At that time, individuals occurred as aggregated with small but dissociated from large squat lobsters (SFS = 1.43 and SFL = -1.41, respectively). While SFL and SLF values had similar trends indicating similar reciprocal relations, large squat lobsters more often occurred close to a slender sole than the reverse (having S values closer to 0). In other words, slender sole were less prone to be found near large squat lobsters than the reverse.

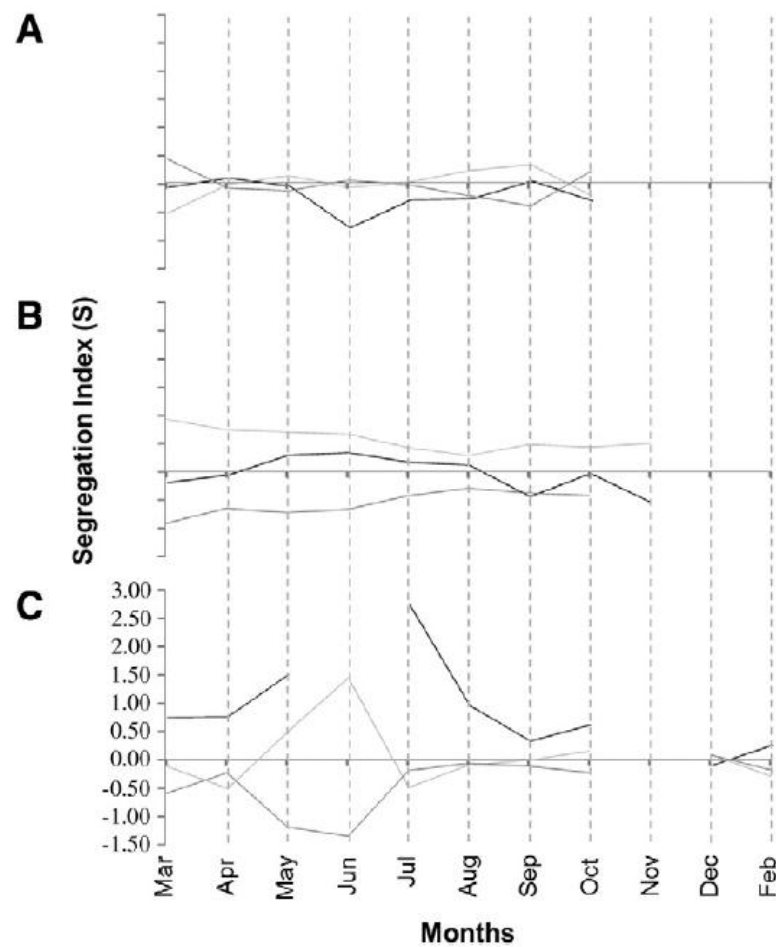


Fig.16. Segregation index (S) over time for each group of animals with respect to the nearest: **A.** large *M. quadrispina*; **B.** small *M. quadrispina*; and **C.** *L. exilis*. On each graph, large *M. quadrispina* (dark gray line), small *M. quadrispina* (light gray) and *L. exilis* (black) are shown. Gaps in S time series represent absence of intraspecific neighbors.

2.4.5 Correlation with oxygen

The linear regressions between segregation index values and dissolved oxygen levels over the year indicated a significant negative trend ($p < 0.05$) only between small and large (i.e., SSL) *Munida* (Fig. 17) and very close to being significant when S was computed between slender sole and large *Munida* (i.e., SFL). A negative non-significant trend was reported in the interspecific S values for large squat lobsters.

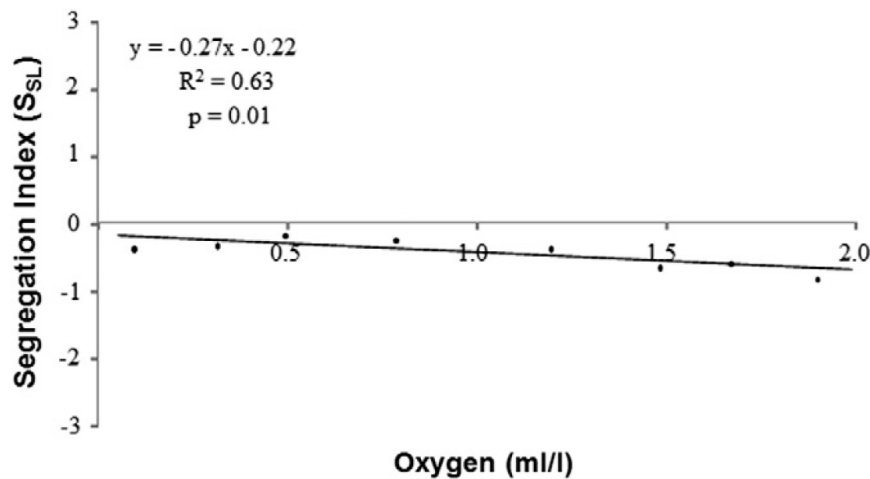


Fig.17. Linear regression depicting the effect of oxygen levels on the monthly S index for the small—large *M. quadrispina* pair at VENUS during the study.

The SFL cross-correlation with oxygen concentration showed a significant and strong negative correlation at lag 0, -1, and -2 meaning that a particular SFL value can be explained by the oxygen concentrations of the same month but also with the oxygen concentrations of the previous 2 months (Fig. 18 A). In contrast, an almost identical response to oxygen concentration was found for the SFF and SSF (Fig. 18B and C, respectively) showing a rising significant positive correlation from lag 0 to lag-2. This means that both S were more affected by oxygen concentration from the previous 2 months than the contemporary one. Cross-correlation analysis between SSL and oxygen concentration is in agreement with the related linear regression results showing a significant and strong negative relationship ($p < 0.05$) at lag 0 with a R^2 of 0.59, meaning that the 59% of a particular SSL value can be explained by the oxygen concentrations of the same month. In addition to that, there was a non-significant correlation between a particular SSL and oxygen of previous months (negative lags) indicating that SSL was only affected by contemporary oxygen concentration (Fig. 18 D). In general, the three groups were associated with their respective conspecifics when the oxygen levels were high, thus presenting a clustering behavior as the oxygen got higher, even though this tendency was not significant (data not shown). The principal outcome of these tests was that the small individuals and the slender sole were dissociated from the larger ones when the oxygen concentrations increased and that only the SSL was exclusively correlated with the contemporary oxygen concentration.

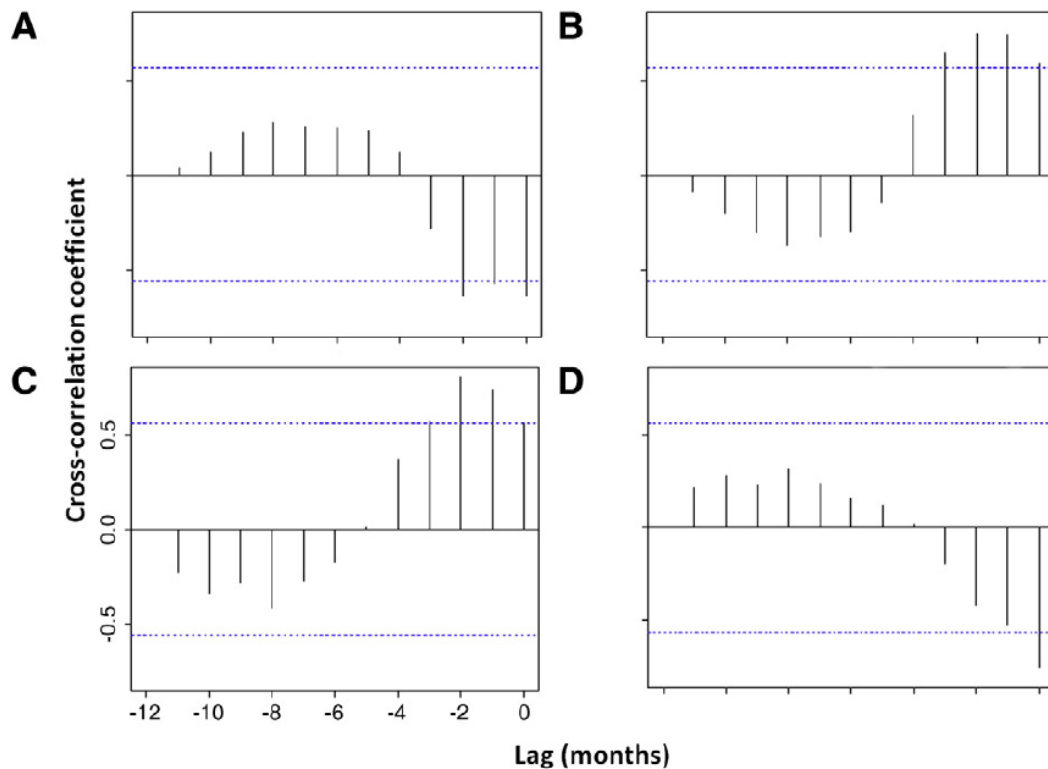


Fig.18. Cross-correlation between: A. SFL; B.SFF; C.SSF; D.SSL and oxygen concentrations. The maximum (or minimum if the signals are negatively correlated) of the cross-correlation function indicates the point in time where the signals are best aligned. The blue dashed line represents the confidence intervals of the cross-correlation.

2.5 Discussion

We observed how benthic *Munida quadrispina* and *Lyopsetta exilis* vary their use of the seafloor with respect to small-scale seabed morphology and their reciprocal presence. These relationships appear to be modified by dissolved oxygen levels, as hypoxia gradually builds up in the Saanich Fjord area along spring and summer. Our results indicated that animals occupy different zones within the VENUS camera field of view, *Munida* in rougher and *Lyopsetta* in flatter parcels. The seasonal fluctuation of the oxygen concentration is caused by two renewal events associated with a combination of neap tides: river discharge, and the spring phytoplankton bloom (Manning et al. 2010). That oceanographic process deeply modified the spatial arrangement of squat lobsters. Size class segregation occurred in *Munida*, with small individuals significantly clustering near the base of seabed structures at normoxic conditions and then atop those structures under severe hypoxia. *Lyopsetta* were mostly displaced by large *Munida* (replaced in the field of view), when a large increase of squat lobsters occurred during early summer (i.e., see June in Figure12). Burd and Brinkhurst (1984) reported a similar aggregation in fall, as shoaling hypoxia forced an upward migration of squat lobsters in Saanich.

However, we do not believe that hypoxia was the cause of the appearance of the aggregation in our case, as we did not see any corresponding decrease in oxygen.

2.5.1 Use of space by *Munida*

Throughout the first 10 days of June, the squat lobster counts showed a sharp increase with densities exceeding 100 individuals/m² (see [Figure 12](#)). This early summer aggregation is noteworthy for its timing.

A similar seasonal phenomenon is recurrent in Saanich although this case occurred in the fall and is related to the oxygen concentration cycle ([Burd and Brinkhurst 1984](#)), which produces a seasonal rise of the OMZ through the depth at which the VENUS node of this study is located ([Macoun et al. 2010](#), [Tunnickliffe et al. 2003](#)). However, the lack of correspondence between the rise in *Munida* abundance and oxygen levels suggests that the origins of the observed aggregation in June are different. In another study 2 years earlier (i.e., in 2010) but 10m deeper, a maximum in squat lobster densities was also noted in June but was not related to oxygen levels ([Matabos 2012](#)). Here, the rise of the hypoxic layer as the cause of the observed peak has been reviewed in view of various aspects of the behavior of the species and with special reference to reproduction, which occurs after molting in some decapod crustaceans ([Raviv et al. 2008](#)).

We detected the presence of shed exoskeletons of squat lobsters (not quantified) throughout the period of increased animal density and afterwards. This observation raises the question whether these fragments were due to aggressive intraspecific behavior or resulted from synchronized molting. The lack of regular spacing among squat lobsters expected in a framework of intraspecific aggressive behavior (see segregation index values SLL in [Figure 16](#)) together with the fact that transiently aggressive behavior in *M. quadrispina* rarely escalates to a real fight ([Antonsen and Paul 1997](#)) suggest that agonistic interactions were not the reason for the presence of shed exoskeletons. Shed exoskeletons were neither related with a hypoxia-induced migration towards shallower depths since hypoxic conditions did not prevail here or deeper in the inlet prior to June in 2012; in contrast, retreat of anoxia to deeper depths allowed the squat lobsters population to expand deeper in the basin between May and September of the following year ([Chu and Tunnickliffe 2015](#)). The latter must be interpreted considering that year-to-year fluctuations in the anoxic and hypoxic water will influence behavior, causing different patterns to emergence. Our data suggest that the aggregation peak could be related to another phenomenon, such as the reproductive cycle.

In areas with seasonal changes in food, reproduction in galatheids is linked to shallower waters ([Sanz-Brau et al. 1998](#)) where the survival of larvae may be higher due to enhanced conditions ([Palma and Arana 1997](#)). According to that, it is plausible that our single peak in squat lobster densities

represents an annual reproductive event and mating might occur outside the range of the camera. That would be in agreement with the fact that we could not detect any copulatory pairs in images.

In this context, the shed exoskeletons found in the field of view in mid to late June could be the result of a synchronous molt before mating, as documented in various crustacean species such as hermit crabs (Wada et al. 2007), squat lobsters (i.e., *Munidopsis polymorpha*; Thiel and Lovrich 2011), and king crabs (Espinoza-Fuenzalida et al. 2012).

Further studies including several years are needed to confirm this annual reproduction hypothesis, but to the best of our knowledge, this is the first report of similar behavior for *M. quadrispina* and represents a clue to understand the population dynamics for this species. In the framework of a global spread of hypoxic conditions, understanding the population dynamics of a hypoxia-tolerant and dominant species is important to model future scenarios.

In our study, the large *M. quadrispina* were generally epibenthic, but they concealed under seabed structures at times. Large squat lobsters primarily occurred in the farthest regions of the field of view (see Figure 10), as observed in the relative density maps (see Figure 14). Accordingly, the results of the spatial autocorrelation analysis indicate the presence of a single wide patch or “zone of influence” (see Figure 15). The preference for rough areas could be related to feeding behavior. Galatheids are carnivores and scavengers (Garm and Høeg 2000), occasionally capturing swimming zooplankton (e.g., *M. quadrispina*; Burd and Brinkhurst 1984), preying on krill or foraging in detritus (Aguzzi and Company 2010).

Little is known about the behavior of the small squat lobsters in relation to seasonally changing oxygen levels. We have observed these individuals progressively concentrating on prominent seabed structures (e.g., the sponges) as the oxygen concentration dropped (see the relative density map analysis for August in Appendix B). The oxygen concentration decrease in August may have been forcing small (thus less tolerant to hypoxia; Burd, 1985) *M. quadrispina* to move up onto seabed projections in an attempt to gain access to the layers of more highly oxygenated water above them. An identical response has also been found in various epibenthic crustacean species (Haselmair et al. 2010, Riedel et al., 2014). Similarly, the burrowing crustacean decapod Norway lobster (*Nephrops norvegicus*) suppresses its retraction behavior, constantly remaining exposed on the more oxygenated seabed when oxygen drops in eutrophic North Sea areas (reviewed by Aguzzi and Sardà 2008). In contrast, when oxygen was not a limiting factor, small *Munida* were observed hiding, primarily under the PVC pipe.

Therefore, one may speculate that the hiding behavior of small individuals under normoxic conditions is the result of predation pressure and of avoidance of intraspecific aggression (by large individuals). That explanation is consistent with the significantly negative linear regression between oxygen levels and the intraspecific segregation index (SSL) and with the strongly significant negative cross-correlation in which the 59% of the variability is explained by the oxygen concentration of the

SSL. In fact, predation pressure affects the small-scale spatial distribution of benthic macrofauna (Serpetti et al. 2013), as the need for protection against predators is a behavioral driver for strong aggregations of epibenthic decapod crustaceans (Corgos et al. 2010). In agreement with the aforementioned distribution of small individuals, we could only detect a very narrow patch or “zone of influence” from the spatial autocorrelation analysis.

In general, despite this oxygen-induced movement, small *Munida* remained aggregated in patches throughout the whole year, as revealed by the constantly positive intraspecific SSS value. However, large *Munida* did not show a similar trend, with the SLL close to 0, indicating a random intraspecific dispersion pattern. The existence of a size-dependent tendency has also been found in three different invertebrate phyla in certain Atlantic fjords, where small species were highly aggregated, in contrast with the larger ones (Kristensen et al. 2013). Findings similar to our results have been obtained in spider crabs. Adult spider crabs do not display a clear spatial structure, whereas small individuals are found in strong aggregations (Corgos et al. 2010).

2.5.2 Use of space by *Lyopsetta*

The biological time series (see Figure 12) highlighted that the slender sole rarely increases in number when the squat lobsters do, and *viceversa*. This opposite trend is confirmed by the interspecific dominance relationships determined by the Pearson test of independence (see Table 1). The absence of spatial overlap among benthic species might be caused by reciprocal avoidance, competition, territoriality, different preferences for food supply or habitat, or physical barriers (Brown and Orians, 1970). It is well known that Pleuronectiformes such as *Lyopsetta* emerge from the sediment in the benthic boundary layer to feed and then re-bury themselves (Holmes and Gibson 1983, Yahel et al. 2008). This lifestyle restricts their presence to flat seabed areas in which their burying behavior is feasible. Therefore, the spatial autocorrelation analysis indicates a narrow distance between zones of high and low concentrations also in agreement with the annual relative density maps outputs (see Figure 6).

The preference for different substrates was not the only reason explaining the absence of overlap with *Munida*. Simultaneously with the seasonal peak in densities of the squat lobsters, we detected a sharp reduction in the counts of the slender sole. Given that *Lyopsetta* is very resistant to hypoxia (i.e., animals are reported to occur down to oxygen levels of 0.1 ml/l, Matabos 2012), the concentrations recorded in the summer of 2012 could not be the reason behind the aforementioned decrease. The negative segregation index SFL values (see Appendix C) indicate that the slender sole rarely occurred close to large *Munida* and suggest the occurrence of strong interspecific competition for space that results in the displacement of the flatfish.

Conversely, large squat lobsters are less affected by the slender sole (see less negative SFL values in Appendix C). The significant and negative cross-correlation between SFL may be interpreted a

clustering behavior of slender sole in relation to large *Munida* when oxygen concentration was high. Although these species are highly resistant to hypoxia, their optimal range of oxygen concentration may entrain this behavior.

Taken together, these results indicate that slender sole aggregates in optimal oxygen conditions and their life habits limit its presence to flat areas (i.e., for burying) but that spatial limitation becomes even stronger during the *Munida* aggregation.

This spatial study at small scale using imaging of high-tolerant to hypoxia species is of importance to understand community dynamics at different levels, including the role of large scale movements. Additionally, probable scenarios in the framework of expanding hypoxia may be inferred from our results on the reciprocally different spatial influence between slender sole and large squat lobsters when oxygen is low (although those results must be carefully interpreted as our study is based in a single location).

2.5.3 Methodology remarks

The presence of the observatory platform could have biasing effects on animal detection (and counting) for a phenomenon of attraction. We assume that these effects were constant throughout the study, so that the observations were related exclusively to external factors ([Aguzzi et al. 2010, 2013](#)).

Another factor that could have been affecting the accuracy in counts was transient turbidity. During periods of low visibility caused by resuspended sediment ([Yahel et al. 2008](#)), smaller squat lobsters located in the distant field of view might have been miscounted. Despite that, the high frequency of sampling (12 images/day every 3 days) minimized the effect of the aforementioned considerations on the results.

2.6 Conclusions

This high-frequency sampling over a large temporal scale, focusing on small-scale dispersion patterns, provides new hints about those mechanisms affecting the distribution of benthic organisms in relation to an essential ocean variable such as oxygen in a global change scenario with expanding hypoxic zones worldwide. Although the drawn inferences are based on a sole location, it is interesting to highlight that Saanich Inlet is a natural laboratory to study the effects of hypoxia on benthic communities. At this site, VENUS imaging reveals the role of behavior (and its environmentally modulated changes), as the ultimate mechanism underlying population space use and dispersion patterns. The spatial relationship between two size classes of the decapod crustacean *Munida quadrispina*, and between the slender sole *Lyopsetta exilis* and the larger class was oxygen dependent. In addition, *Lyopsetta exilis* space use was affected by the morphology of the seafloor and the reproductive behavior (specifically, the reproductive migration of *M. quadrispina*). Conversely, the use of space by the large squat lobsters was not related to changes in oxygen levels but depends on the morphology of the seafloor.

2.7 Acknowledgements

The authors would like to thank the following people who have contributed to this research: C. Curkan and J. Chu (Univ. of Victoria, Canada), N. Bahamon (Centro de Estudios Avanzados de Blanes, Spain). RITFIM project (ref. CTM2010-16274) of the Spanish national RTD program funded this work without any further involvement in the preparation of the article. Jacopo Aguzzi is a Research Fellow of the Ramon y Cajal Program (MINECO).

**Chapter 3. Seasonal monitoring of deep-sea megabenthos in
Barkley Canyon cold seep by Internet Operated Vehicle (IOV)**

3.1 Abstract

Knowledge of the processes shaping deep-sea benthic communities at seasonal scales in cold-seep environments is incomplete. Cold seeps within highly dynamic regions, such as submarine canyons, where variable current regimes may occur, are particularly understudied. Novel Internet Operated Vehicles (IOVs), such as tracked crawlers, provide new techniques for investigating these ecosystems over prolonged periods. In this study a benthic crawler connected to the NEPTUNE cabled infrastructure operated by Ocean Networks Canada was used to monitor community changes across 60 m² of a cold-seep area of the Barkley Canyon, North East Pacific, at ~890 m depth within an Oxygen Minimum Zone (OMZ). Short video-transects were run at 4-h intervals during the first week of successive calendar months, over a 14-month period (February 14th 2013 to April 14th 2014). Within each recorded transect video megafauna abundances were computed and changes in environmental conditions concurrently measured. The responses of fauna to environmental conditions as a proxy of seasonality were assessed through analysis of abundances in a total of 438 video-transects (over 92 h of total footage). 7698 fauna individuals from 6 phyla (Cnidaria, Ctenophora, Arthropoda, Echinodermata, Mollusca, and Chordata) were logged and patterns in abundances of the 7 most abundant taxa (i.e. rockfish Sebastidae, sablefish *Anoplopoma fimbria*, hagfish *Eptatretus stoutii*, buccinids (Buccinoidea), undefined small crabs, ctenophores *Bolinopsis infundibulum*, and Scyphomedusa *Poralia rufescens*) were identified. Patterns in the reproductive behaviour of the grooved tanner crab (*Chionnecetes tanneri*) were also indicated. Temporal variations in biodiversity and abundance in megabenthic fauna was significantly influenced by variabilities in flow velocity flow direction (up or down canyon), dissolved oxygen concentration and month of study. Also reported here for the first time are transient mass aggregations of grooved tanner crabs through these depths of the canyon system, in early spring and likely linked to the crab's reproductive cycle.

Keywords: Crawler; deep-sea benthic communities; coldseep; submarine canyon; seasonality; behavioural rhythms; grooved tanner crab; sablefish; Barkley Canyon; Video-monitoring; buccinids; multivariate statistics

3.2 Introduction

The continental margins are characterized by high temporal variability in key benthic habitat variables, (such as current regimes, sedimentation rates, and light intensity and spectral quality), with variability often related to depth (Aguzzi and Company 2010). In the aphotic deep sea, light intensity is often assumed to be replaced by current regimes (Aguzzi et al. 2010) as the *zeitgeber* (i.e., the environmental synchronizer of biological rhythms) but recent data also suggest that indirect day-night synchronization may occur as a result of the presence or absence of fauna making diel vertical migrations, potentially between different depth strata within the water column (Aguzzi et al. 2011, Aguzzi et al. 2015). In general, behavioural responses of deep-sea benthic and benthopelagic fauna to variations in light, internal tides, and inertial current cycles remain poorly understood, in part because of a lack of continuous monitoring. Continuous monitoring of oceanographic variables and hourly to seasonal turnover of species compositions can permit the identification of environment drivers that shape benthic community composition (Aguzzi et al. 2011, Doya et al. 2014).

This lack of knowledge is particularly pronounced in regions with complex topography, such as marine canyons, where detrital funneling and changing flow regimes may occur (De Leo et al. 2010, Ceramicola et al. 2015). This funneling and variability in flow have been identified as drivers of canyon high productivity and biodiversity (Schlacher et al. 2010, Allen and Hickey 2010, Vetter and Dayton 1997). The enhancement of primary productivity within these geomorphologies (Allen and Hickey 2010), concentrating zooplankton (Genin 2004) and scavengers (Vetter 1995), contribute to an increase food availability for benthos (De Leo et al. 2010) and benthopelagic species (Doya et al. 2014), as well as driving seasonal reproduction patterns of fishes, which may use canyons as breeding area (Baillon et al. 2012). Predicting patterns of megafaunal increase of abundance in submarine canyons is of relevance for ecosystem and fishery management (Vetter 2010). Although canyons may have an increased diversity and abundance in fauna when compared to adjacent continental slopes, oxygen minimum zones (OMZs), can prevent colonization by fauna less tolerant to low oxygen concentrations, hence reducing the benefits of the locally elevated food availability (De Leo et al. 2012). The response of many marine fauna to hypoxia still remains largely uncertain, so the degree to which locally low oxygen concentration bottom waters may impact species abundance and biodiversity is difficult to directly gauge (Chu and Tunnicliffe 2015; Doya et al. 2016). As a dynamic canyon system cutting through a Northeast Pacific OMZ region, Barkley Canyon (off Vancouver Island, Canada), represents an optimal study site for carrying out work aimed at improving our understanding of how deep-sea canyon communities respond to seasonal oxygen variations (Helly and Levin 2004). Our study site in Barkley Canyon corresponded to the core of the North Pacific OMZ between 600-700 m and 900-1100 (Gallo and Levin 2016).

The section of the Barkley Canyon investigated here (850-900 m depth) is also characterized by outcropping methane hydrate deposits that mark the boundary of the temperature-pressure methane hydrate stability field (Chatzievangelou et al. 2016). The susceptibility of these gas hydrates, and their associated faunal communities with their presence to ocean warming is significant. Despite their low

biodiversity, cold seeps are highly productive ecosystems (Armstrong et al. 2012) and are increasingly recognized as providers of ecosystem services (Levin et al 2016). Oxygen depletion (Childress et al. 2011), changes in water-mass circulation (Adams et al. 2011) and temperature increases (Glover 2010) highlighted in future climate change scenarios represent particular threats to cold seep ecosystems in low oxygen environments, because of their potential impact on hydrate stability and worsening of hypoxia. At these cold seeps, chemosynthetic microbial production driven by oxidation of reducing substances (methane and sulphide) in discharging seafloor fluids sustains symbiont-bearing tubeworm and bivalve communities (Tunnicliffe et al. 2003, Le Bris et al. 2016), and free-living bacterial mats (e.g., *Beggiatoa* sp.). These in turn support higher order consumers, including fish, squid, octopii, echinoderms, other molluscs, and crabs.

The recent extension of cabled observatory technologies to the deep sea is finally permitting the continuous imaging and oceanographic monitoring required investigating processes that shape submarine canyons and cold-seep communities (Favali and Beranzoli 2016, Barnes and Tunnicliffe 2008, Ruhl et al. 2011) at hourly to annual time scales. A new generation of tethered mobile Internet Operated Vehicles (IOV), such as benthic crawlers, extends the potential observational footprint from a few square meters around fixed seafloor platforms (Juniper et al. 2013, Aguzzi et al. 2015), to hundreds of square meters (Purser et al. 2103) in areas surrounding seafloor observatory nodes. This substantially extends our ability to document spatial habitat heterogeneity, and provides a larger sample size for detecting temporal variability. The crawler ‘Wally I’ is an advanced example of this mobile technology, and has been deployed in a cold-seep site in Barkley Canyon at ~890 m for several years. In addition to supporting imaging equipment, Wally I also hosts a complex suite of oceanographic sensors (Purser et al. 2103, Thomsen et al. 2012)

In this study, a 14 month temporally structured video-monitoring campaign to investigate the megafaunal communities of a Barkley Canyon cold-seep ecosystem was conducted, in order to test the hypotheses that (i.) abundance, richness, and biodiversity changes within the surveyed area are directly driven by the oceanographic parameters such as oxygen concentration, current velocity, upwelling events and indirectly by seasonal bethopelagic and nektobenthic migrations along the canyon; (ii.) IOV technology can be used as a solid faunistic monitoring tool.

3.3 Materials and Methods

3.3.1 The NEPTUNE network and the Barkley Canyon node

Authorization for installation of the infrastructure supporting this research was provided by the Transport Canada (<http://www.tc.gc.ca>), after Fisheries and Oceans Canada (<http://www.dfo-mpo.gc.ca>) assessed that the cabled installation would not have a negative impact on fish habitat. Field studies did not involve endangered or protected species.

The NEPTUNE cabled observatory network, off Vancouver Island (BC, Canada) operated by Ocean Networks Canada (ONC; <http://www.oceannetworks.ca>; Barnes et al. 2015) supports continuous multiparametric and video observations from coastal to deep-sea habitats, providing power and data connectivity through a 840-km looped fiber-optical cable (Fig. 19).

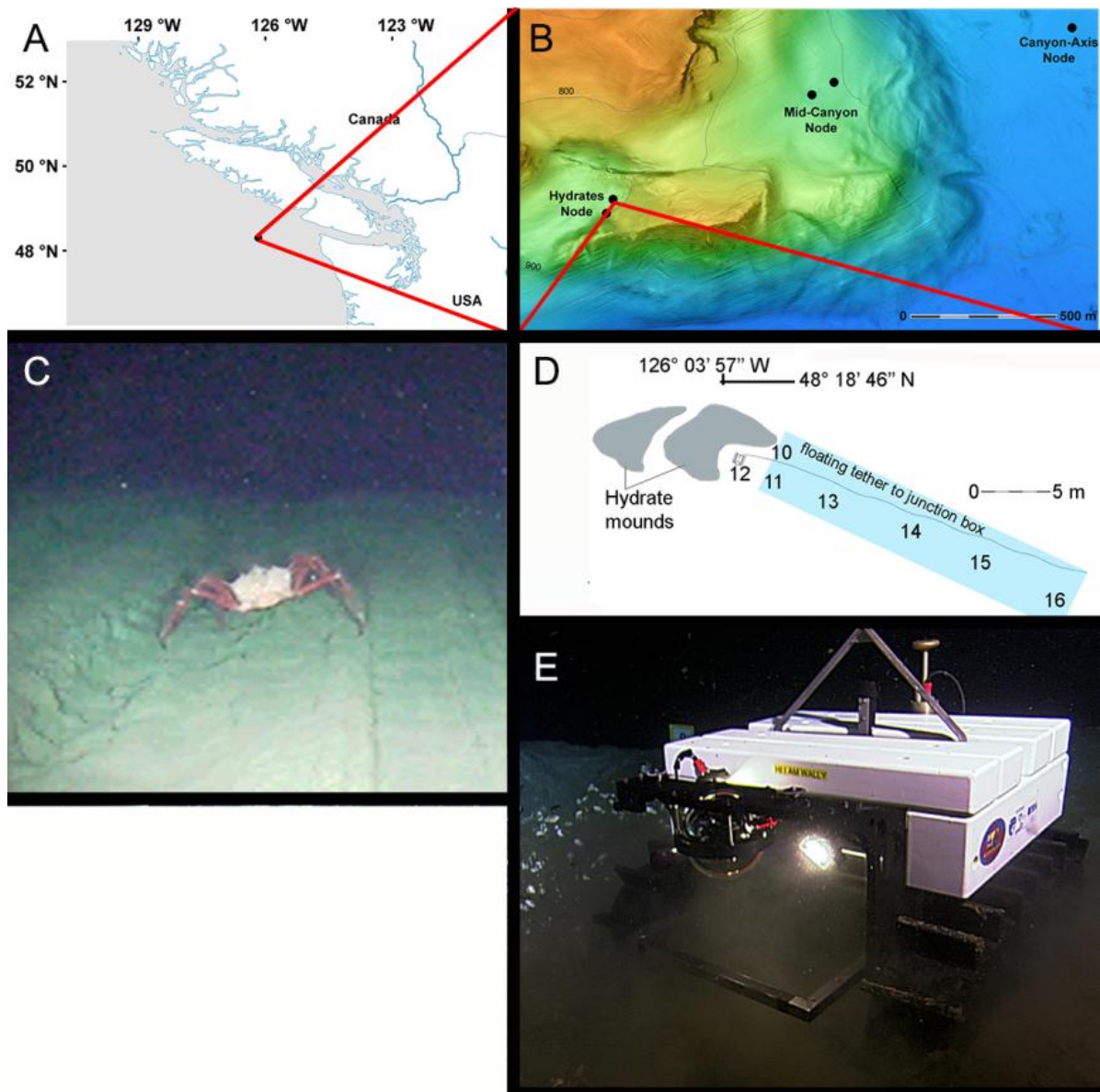


Fig.19. Overview map of the cold-seep site in Barkley Canyon (northeast Pacific, Canada). (A) The cabled observatory network, The Barkley Canyon node, site of Wally I crawler deployment is highlighted by a black dot. (B) High-resolution bathymetric map showing the region of Barkley Canyon investigated in the current study. The black dots within the canyon axis represent the crawler node with the nearby mid-canyon POD4 platform and other deeper nodes. (C) Image demonstrating the crawler Field Of View (FOV) as used to acquire the faunal data. (D) Map showing position of navigation waypoints arranged around the hydrate outcrop, the crawler (near waypoint no. 12 in this schematic) and the route from waypoint no. 10 to 14, representing the survey transect analysis area. The cold seep community was distributed on a soft bottom zone with no apparent emerging rocks. At the end of the transect analysis area, a 5 m depth cliff (dashed grey line) separated our study area from a from the gas-hydrate mound (E) The crawler in operation.

The observatory network is powered by a shore station located in Port Alberni, Vancouver Island (see Figure 19 A). This sophisticated interdisciplinary monitoring infrastructure supports a node in Barkley Canyon at ~890 m depth (Fig. 19 B; 48°18.89' N, 129°03.48' W), a node which has become an

important hub for *in-situ* study of the environmental drivers modulating ecosystem functioning of deep-sea cold-seep communities (Belley et al. 2016, Thomsen et al. 2012). For the duration of the study described herein, the Wally I crawler was in operation on the western flank of the main canyon, connected by an umbilical power and data cable to the node (Fig. 19 B). The node is also within the local Oxygen Minimum Zone (OMZ), and thus a site of further global interest as a location for ongoing monitoring during global environmental change. A full description of the study site (Figs 19 C and 19 D) the images recorded by the crawler (Fig. 19 E) installed in this area (Fig. 19 F) is provided in (Purser et al. 2013).

3.3.2 The ‘Wally I’ crawler deployment, connectivity, operations and sensor systems

For the duration of the current study, the mobile ‘Wally I’ crawler was connected *via* a 70-m fiber-optic tether to the Barkley Canyon node (Purser et al. 2015) with syntactic foam floats arrayed every 3 m along the tether to insure buoyancy and to preclude entanglement with the crawler tracks. Crawler driving control and data acquisition were carried out in real-time *via* a custom web interface, with sensor data and imagery automatically stored to the NEPTUNE archive at the sampling resolution of each device (Purser et al. 2015).

The ‘Wally I’ crawlers’ mobility is provided by a pair of caterpillar tracks, which may be operated together, or independently to drive the vehicle forward, backward or to rotate it on the seafloor. Movement commands are made directly from the home laboratory over an internet connection.

Movement of the caterpillar tracks (and therefore, the vehicle) creates a footprint on the seafloor that could potentially disturb infauna. To prevent these impacts influencing the collected results transects aimed at collecting time series data are usually run over the same track, hence reducing the impacts of the tracks on the ecosystem. Such an operational plan was carried out in the current study (see Figure 19 E).

One of the primary sampling systems on the ‘Wally I’ crawler is the forward looking camera system. Video footage can be acquired using the 470 Line ROS Inspector low-light, colour camera, equipped with an 18X optical zoom whenever suitable illumination is also provided. For the current study, 20 m transects were driven every 4 hours, over the first 5 days of each month, from February 14th 2013 to April 14th 2014, with video data recorded on every occasion. For all transects, the camera was always oriented with a fixed tilt angle of 45° from the horizontal, from a mounting position roughly 1m from the seafloor at the front of the crawler. During operations, the crawler’s motion was kept at a near constant speed (0.02 m/s). Light was provided by two deep-Sea power and light-variable intensity lamps (Purser et al. 2015). Lights were switched on during transect driving and turned off immediately after, in order to minimize photic contamination in the area. The total observed seafloor area recorded within each transect was approximately 60 m².

The ‘Wally I’ crawler can mount a plethora of sensor systems, and for the duration of the current study an upward facing 2-MHz ADCP (Nortek Aquadopp Profiler AQD 9917), measuring water velocity and temperature at 1 mab and a Seapoint Turbidity Meter, measuring at approx. 0.2-0.3 mab the turbidity were equipped. An adjacent observatory (the POD4 NEPTUNE node), situated at a distance of ~500 m from the site of crawler operations, within the mid-canyon at 896 m depth (48°18.8923' N, 126°03.4804'W; see [Figure 19 B](#)) was simultaneously recording pressure, water density data and oxygen, as collected respectively by a CTD (Sea-Bird SeaCAT SBE16plus V2 7027) and an oxygen sensor (Sea-Bird SBE 63 630111). Collected data at 1 min frequency throughout the entire survey period, both at times coinciding to the collection of video transect data as well as during the periods of immobility between crawler transects. These data are freely available online (<http://dmas.uvic.ca/DataSearch>). Additionally, the Bakun Index, as a proxy of upwelling and downwelling processes, was also computed at 48N, 125W from National Oceanic and Atmospheric Administration (NOAA) / National Marine Fisheries Service(NMFS) / Pacific Fisheries Environmental Group (PFEG) data.

3.3.3 Faunal data collection and treatment

Following collection of the transect video data, one user made visual counts of the megafauna individuals present within each transect. The same user analysed all collected videos, identifying individuals to the lowest taxonomic level as possible using the NEPTUNE Canada Fauna Identification Guide ([Gervais et al. 2012](#)). All video recorded were archived and are available online through the Oceans 2.0 portal (<http://dmas.uvic.ca/DataSearch>).

Although a near constant crawler speed and camera angle were maintained throughout the duration of the study, occasional variabilities in field of view recorded did result from small differences in seafloor relief across the transect survey length. To account for this, we analysed only the portions of video data where 75% of the field of view encompassed the seabed, and with sufficient water transparency for animal classification and counting.

Slight variabilities in transect duration also occurred, due to slight differences in seafloor angle, firmness and due to technical driving and internet connectivity issues (e.g. interruption of signal send / return from our working office in Barcelona to the Pacific). Therefore, to make the biological data recorded as comparable as possible over the video transects collected, we standardized visual counts for the each megafaunal taxa and transect to the maximum video duration recorded within the study, which was 23 min.

In order to highlight species count patterns as proxies of seasonality, we plotted time series of average visual counts (\pm SD) for each month, based on all transects recorded during the 5 days of monitoring at the start of each calendar month throughout the 14 month period. In the resulting plots, we superimposed horizontal dashed lines representing the ‘Midline Estimated Statistic of Rhythm

(MESOR; [Aguzzi et al. \(2015\)](#)), computed by re-averaging all monthly values. Their overlaying onto the monthly plot allows the identification of significant seasonal increases or decreases in abundance.

Current velocity component-vectors (i.e. North-South and East-West, xy direction data collected *via* the ADCP system) were transformed to flow magnitude (m/s). All environmental data collected by the crawler and the POD4 node (see 2.2) were averaged into 4 h bins to match the video-sampling frequency. Bakun Index values, the daily-averages of wind-driven cross-shore transport, were computed from Fleet Numerical and Meteorology Oceanographic Centered (FNMOC) 6-hourly surface pressure analyses.

3.3.4 Analysis of the community structure linkage with oceanographic variables

A Kruskal Wallis test was carried out using the R statistical language ([R Development Core Team 2008](#)), to detect significant differences in the number of megafaunal visual counts (of each species or taxa logged) between months, following the methodology presented in ([Zar 2010](#)).

A Kruskal Wallis test was carried out using the R statistical language ([R development core Team, 2008](#)), to detect significant differences in the number of megafaunal visual counts (of each species or taxa logged) between months, following the methodology presented in ([Zar 2010](#)).

A Nonmetric Multidimensional Scaling (NMDS; [Minchin 1987](#)) analysis was performed in the R library *vegan* ([Oksanen et al. 2006](#)) to visualize the level of similarity among species presence and visual counts (i.e. assemblage structure) together with correlated environmental vectors into a Cartesian plane. The Bray-Curtis dissimilarity Index was used to quantify the dissimilarity between megafaunal species based on the time series visual counts, while a Wisconsin double standardization was performed (since this improves the gradient detection ability of dissimilarity indices; [Oksanen et al. \(2015\)](#)). The significance of the estimated determination coefficients (r^2) of the environmental variables fitting onto the species ordination, produced by the NMDS analysis, was estimated using a permutation test. Results of the species ordination using NMDS and the correlation with the environmental variables are shown in a plot, with environmental vectors (arrows) showing significant ($p < 0.05$) maximum correlation with the species ordination. Results are shown only for the environmental variables significantly correlated to the species ordination.

Biodiversity was calculated with two indices presented as mean diversity per month: the Shannon index (H') and the Simpson Index, presented as 1-D. In a similar manner, we presented the species richness (S). The monthly abundance (number of individuals of all species) was normalized to the maximum number of transects per month (i.e. 48). Herein we refer to these means as biodiversity indices, Shannon index, Simpson Index or abundance as appropriate.

3.3.5 Ethological remarks

Behavioural observations were logged for the motile fauna imaged during the crawler surveys. These, though opportunistic, were described in order to increase general information on the ethology of several deep-sea species, and may represent pivotal aspects of the functioning of some ecosystems, particularly in terms of inter- and intraspecific relationships ([Aguzzi et al. 2012](#)), and also to help support the second hypothesis of the current study, that IOV technology has application as a solid faunistic monitoring tool.

3.4 Results

438 video transects, representing a total of 92 h of footage of acceptable quality for analysis was collected during the 14-month monitoring period. No video data was collected during March 2014 due technical problems. 7698 megafauna individuals, belonging to 6 phyla were observed (Appendix E). These included representatives of 26 taxa, 12 of which could be identified to species level, with remaining individuals classified to higher taxonomical levels (S1 Fig).

We detected considerable differences in megafaunal abundances, between species and temporally, throughout the study period (see [Appendix E](#)). The most abundant species within the study period were the sablefish (*Anoplopoma fimbria*) with 2214 visual counts, representing 29% of the total observed megafauna. Buccinids (Buccinoidea) were also abundant with 1318 individuals representing 17% of the total megafauna. The third most abundant taxon was hagfish (*Eptatretus stoutii*; i.e. 852, as 11%). The fourth was abundant was Scyphomedusa (*Poralia rufescens*) with 789 individuals (10%). Next were rockfish (i.e. from the family Sebastidae) with 573 filmed individuals (7%) and small crabs (of undefined taxon) showing a similar abundance (N=535, 7%). The final significantly abundant taxon, with 449 records, was ctenophores (*Bolinopsis infundibulum*), representing 6% of recordings of fauna.

3.4.1 Seasonal patterns

Time series analysis was carried out for the 7 most abundant megafaunal species ([Fig. 20](#), plotted to show the occurrence of any monthly variation as a proxy of seasonal fluctuation). Grooved tanner crab count time series were also plotted to show the particular variabilities in their abundance resulting from their reproduction dynamics. Since no video data was collected during March 2014, we assumed significant values during this month when the concomitant months were significant. An overview of the time series analysis showed species peaking frequently from February to August 2013 and from January to April 2014. A general lack of species occurred during the central months of the study (autumn and December 2013).

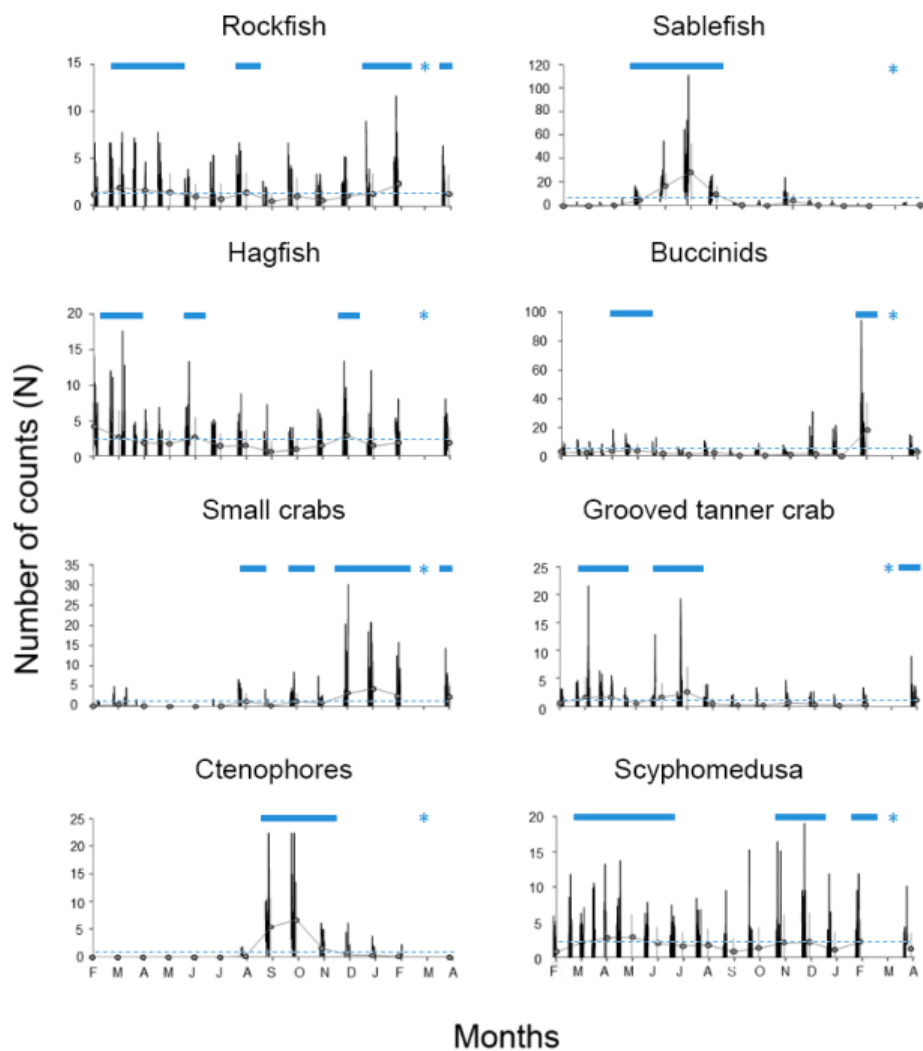


Fig.20. Visual counts time series (i.e. from 14th February 2013 to 14th April 2014) for the 7 most abundant megafaunal species and the particular case of the grooved tanner crab, as reported by crawler video-imaging. Average values (the grey dots) have been reported in order to better highlight the occurrence of seasonal trends. From left to right and from top to bottom taxonomic units are: Rockfish (i.e. Sebastidae); Sablefish (*Anoplopoma fimbria*); Hagfish (*Eptatretus stoutii*); Buccinid (Neptunidae); Small crab; Grooved tanner crab (*Chionnecetes tanneri*); Ctenophore (*Bolinopsis infundibulum*); and finally, Scyphomedusa (*Poralia rufescens*). Horizontal blue dashed lines correspond to the Midline Estimated Statistic of Rhythm (MESOR) and horizontal blue lines identify significant seasonal increases visual counts increases. Blue asterisks correspond to a month with no data due technical problems.

A close-up of Figure 20 showed that rockfish were present in roughly consistent densities throughout the observation period, though significantly higher (i.e. above the MESOR) numbers of them were observed during spring and August 2013 and from January to April 2014. We observed a significant sharp peak in sablefish visual counts during late spring (March) and summer 2013 reaching their maximum abundance in July, with a mean of 29.1 ± 23.8 SD individuals per transect. Hagfish were also

uniformly abundant throughout the study, with a modest but significant count peak in February-March and July 2013, and another one of similar magnitude in January 2014. Buccinids showed low but consistent abundances during much of the survey period with a mean of 3.3 ± 4.46 SD individuals per transect. Though a moderate but significant increase occurred from May to June 2013 and a sharper one occurred in February 2013 (i.e. 18.3 ± 18.9 SD individuals per transect).

Small crabs were rarely present during the study period, although their numbers were reaching significant levels intermittently from August 2013 to April 2014 (i.e. August, October and from December 2013 to April 2014), reaching a maximum in January (i.e. 4.5 ± 6.7 SD individuals per transect). Grooved tanner crabs were present all year-round with visual counts increasing moderately but significantly during March and April 2013 (1.6 ± 3.7 and 1.6 ± 2.1 SD individual per transect, respectively) and again in April 2014, with 1.1 ± 2 SD individuals per transect being observed (coinciding with reproduction; see the Behavioural Remarks Section below). Another significant peak was observed during early and mid-summer 2013 (June and July).

Ctenophore visual counts displayed clear seasonal patterning. A sharp increase in numbers occurred during autumn with a maximum density observed in October 2013 (i.e. mean density of 6.9 ± 6.4 SD individuals per transect). Finally, the Scyphomedusa was significantly present during almost all months of the monitoring period (i.e. from February to June and from November to December 2013 and February 2014) with a moderate count decrease from mid-summer to mid-autumn.

Fig. 21 shows the time series data for the investigated oceanographic parameters, as measured by the crawler on board sensors and the nearby POD4 network node. There were a few occasional gaps in data acquisition produced by sensor malfunctions or data network issues. A patterning in seasonality is evident in water density, temperature and turbidity measurements. Additionally, the Bakun Index and oxygen concentrations measured during the 14 months of the study showed seasonality in the values measured. Velocity was highly related to the diurnal and semi-diurnal tidal cycle. The Bakun Index presented the lower values during February 2013, indicating predominant downwelling processes ongoing during that month. A progressive increase in the Bakun Index led to positive values as sustained pulses (i.e. upwelling events) from mid-April to August 2013. Coinciding with these upwelling events, we detected the greatest recorded variations in turbidity. Elevated turbidity levels were coincident with the first shallow water incursion in the local deep-sea area in August, which brought in warmer and less salty waters. Oxygen levels ranged from 0.24 (October 2013) to 0.29 ml/l (March 2014), with a mean of 0.26 ml/l. Oxygen concentrations gradually decreased in August, reaching their minimum values in September-October. Thereafter, oxygen progressively increased to return to the initial concentrations by the end of the study. This lower oxygen period coincides in time with Bakun Index reaching values close to zero. Water density also showed a weak seasonal trend, with generally warmer and fresher water masses present at the study site from July to October.

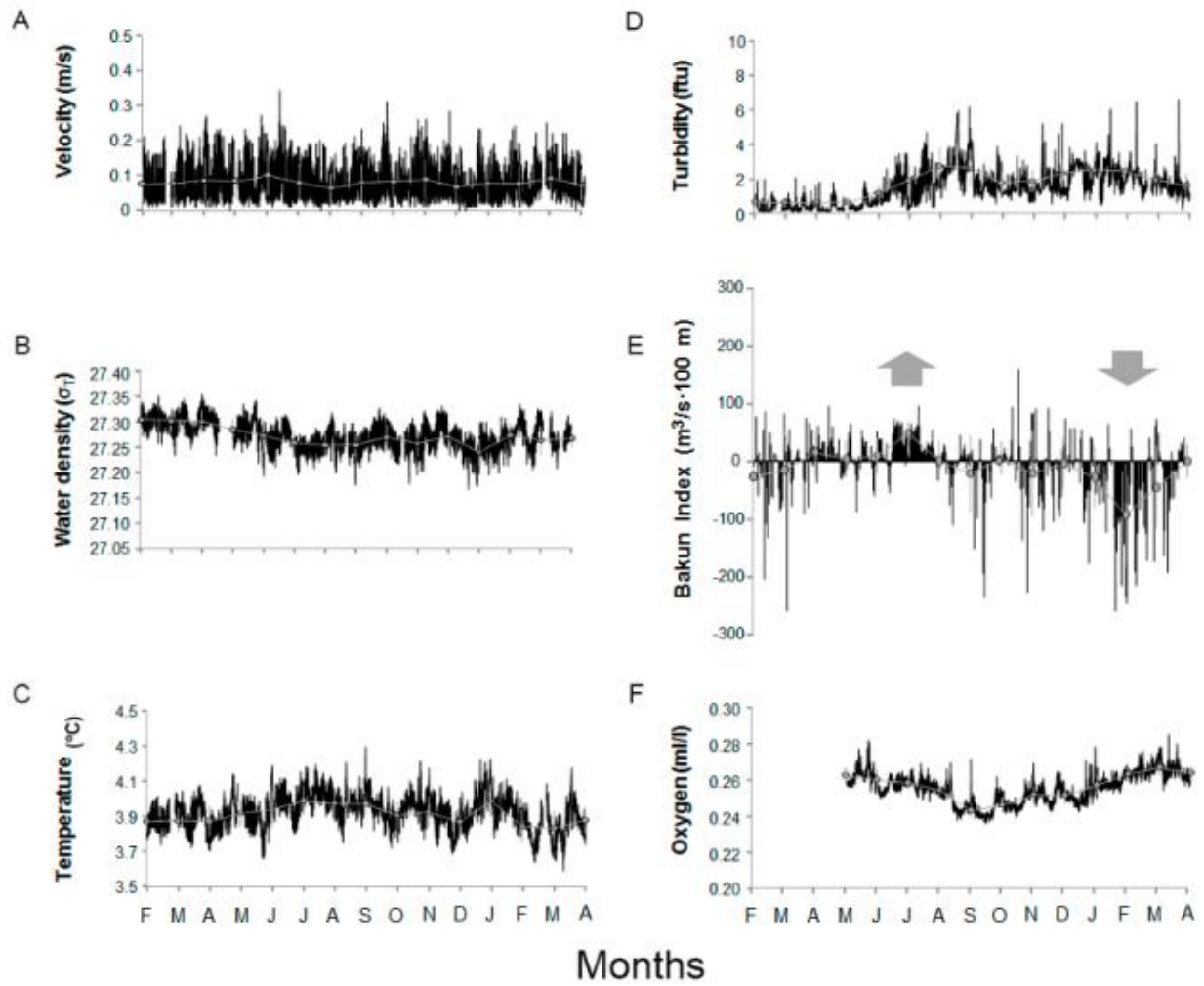


Fig.21. Oceanographic parameters time series (i.e. from 14th February 2013 to 14th April 2014), as recorded by crawler and the nearby POD4 platform within the Barkley Canyon. Average values (the grey dots) have been reported in order to better highlight the occurrence of seasonal trends. Gaps in data acquisition were due to instrument malfunctioning or downtime for the cabled infrastructure. These parameters are: (A) Velocity; (B) Water Density; (C) Temperature; (D) Turbidity; (E) Bakun Index; and finally, (F) Oxygen. We used up-looking and down-looking arrows to highlight upwelling and downwelling periods respectively.

3.4.2 Analysis of the community structure linkage with oceanographic variables

Kruskal-Wallis tests (Table 3) revealed significant differences among months for the most abundant species, with a $p \leq 0.01$.

Table 3: Kruskal-Wallis test among the 14 months of the study for the 8 most abundant species with 13 degrees of freedom

Taxonomical Units	Common name	χ^2	p -value
Sebastidae	Rockfish	29.23	< 0.01
<i>Anoplopoma fimbria</i>	Sablefish	346.8	<0.01e ⁻¹⁵
<i>Eptatretus stoutii</i>	Hagfish	44.39	<0.01e ⁻⁴
Buccinoidea	Buccinids	275.13	<0.01e ⁻¹⁵
	Small crabs	99.5	<0.01e ⁻¹⁵
<i>Chionoecetes tanneri</i>	Grooved tanner crab	46.81	<0.01e ⁻⁴
<i>Bolinopsis infundibulum</i>	Ctenophores	275.13	<0.01e ⁻¹⁵
<i>Poralia rufescens</i>	Scyphomedusa	27.3	<0.01

Environmental parameter fitting onto species ordination as obtained from NMDS analysis is shown in Fig. 22. Current velocity, Bakun Index, dissolved oxygen and months were the ‘environmental’ variables showing significant ($p < 0.05$) maximum correlations with the species ordination, with r^2 values of 0.14, 0.29, 0.29, and 0.47 respectively. Month was included as a proxy for the presence of a seasonal pattern in abundance variations (See Figure 20 and Appendix D for species individual counts). The Bakun Index was negatively correlated with the variable month (see Figure 22) likely resulting from the progressive change from predominantly upwelling to downwelling conditions over the monitoring period (see Figure 21). A weaker negative correlation was also observed between dissolved oxygen concentration and current velocity (see Figure 22). An inverse correlation between rockfish visual counts and Bakun Index values was also indicated (i.e. increases in rockfish abundances were correlated with downwelling), whereas sablefish, correlated with both Bakun Index and low current velocities. As with rockfish, elevated densities of buccinids correlated with periods of sustained downwelling (i.e. negative Bakun Index values), occurring toward the end of the monitoring period. A positive correlation with increasing oxygen was also indicated for the buccinids. The similarities in the abundance curves of buccinids and rockfish is shown in Figure 22. In general, grooved tanner crabs were observed in highest abundances during the first half of the study (from February to August 2013), with these higher abundances correlating with higher oxygen levels and lower current velocities. Small crabs’ abundance was clearly higher during the second third of the study (see Figure 22). In the case of ctenophores, NMDS showed that highest abundances correlated with lower oxygen levels. The abundance of another cnidarian, the

Scyphomedusa, was strongly associated with periods of weak current flow and higher oxygen concentrations.

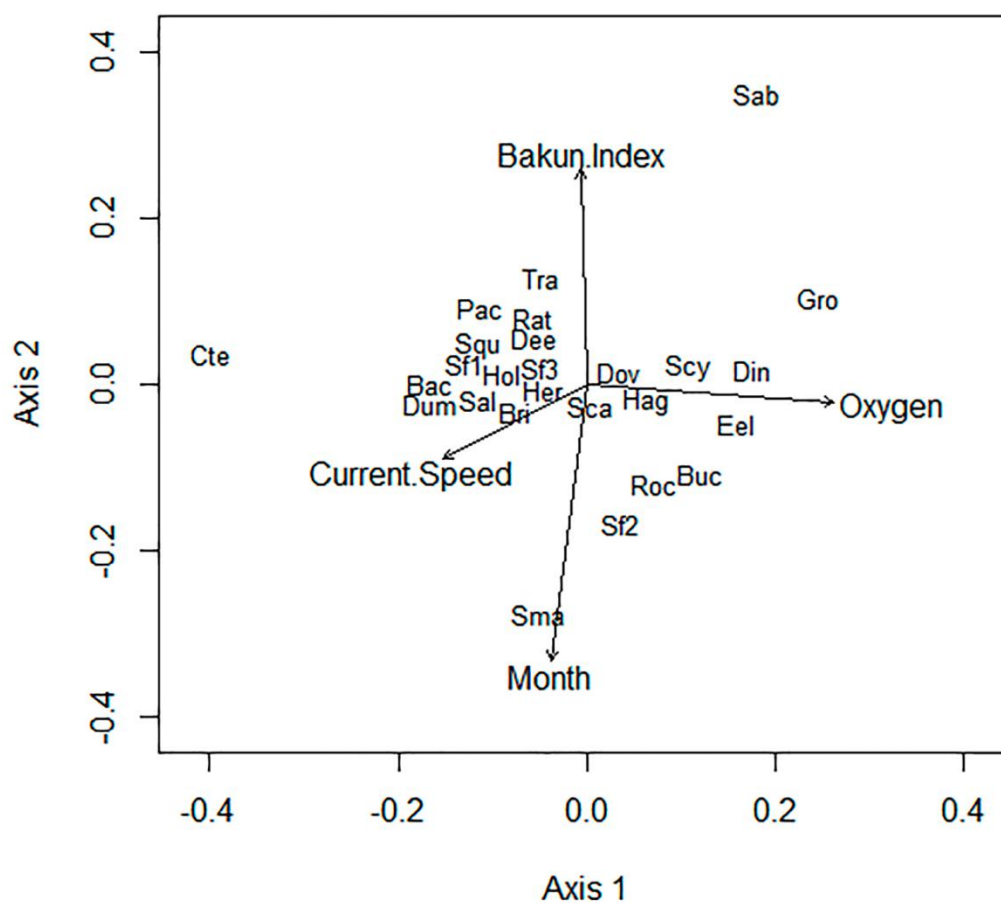


Fig.22. Results of fitting environmental variables onto species ordination. The increasing gradient of the environmental variable is indicated by the vector direction. The vector length is proportional to the correlation between the variable and the ordination pattern of the species. Species abbreviations are (taxonomical order; see S1 Table): Eel (*Eelpout*, *Licenchelys* spp.); Dov (Dover sole, *Microstomus pacificus*); Dee (Deep sea sole, *Embassichthys bathybius*); Pac (Pacific halibut, *Hippoglossus stenolepis*); Rat (Rattail, *Coryphaenoides* spp.); Roc (Rockfish, i.e. Sebastidae); Bac (Blackfin poacher, *Bathyagonus nigripinnis*); Sab (Sablefish, *Anoplopoma fimbria*); Hag (Hagfish *Eptatretus stoutii*); Sal (Salp, Salpidae); Dum (Dumbo octopus, *Grimpoteuthis* sp.); Squ (Squid *Gonapus* sp.); Buc (Buccinids, Neptunidae); Bri (Brittle star, Ophiuroidea); Sf1 (Starfish, *Asteroidea*); Sf2 (Starfish, Zoroasteridae); St3 (*Hippasteria* sp.); Hol (Holoturian, Holoturoidea); Her (Hermit crab, *Diogenidae*); Sca (Scarlet king crab, *Lithodes couesi*); Gro (Grooved tanner crab, *Chionnecetes tanneri*); Sma (Small crabs); Cte (Ctenophore, *Bolinopsis infundibulum*); Scy (Scyphomedusa, *Poralia rufescens*); Din (Dinner plate jelly, *Solmissus* sp.); Tra (Traquimedusa, *Voragonema pedunculata*).

Species richness was almost constant throughout the studied period (14.93 ± 1.82 species/60m²) with two moderate drops, one from March to June 2013 (13 species/60m²) and another one of the same magnitude in October of the same year with similar levels lasting until the end of the study (Fig.23 D). Abundances increased progressively from low levels at the beginning of the study (550.42 individuals/60m² in February 2013) being in March 2013 very close to the significant level (MESOR; 814.05 individuals/60m²). A significant peak occurred from June to August 2013 (maximum 1810.56 individuals/60m² in July) and again in February 2014 (1412.59 individuals/60m²; Fig. 23 B). The two biodiversity indices values (H' and 1-D), respectively Figs 23C and A, followed a very similar pattern. Both were relatively constant (H': 1.83 ± 0.34 ; 1-D: 0.74 ± 0.13) apart from 3 decreases below the significant levels leading to low points. June to July (minimum being in July: 1.00), October 2013 (1.79) for H' and June to July (minimum being in July: 0.40) and September to October 2013 (minimum being in September: 0.71) for 1-D. Both indices experienced a drop in February 2014 (H': 1.36; 1-D: 0.59).

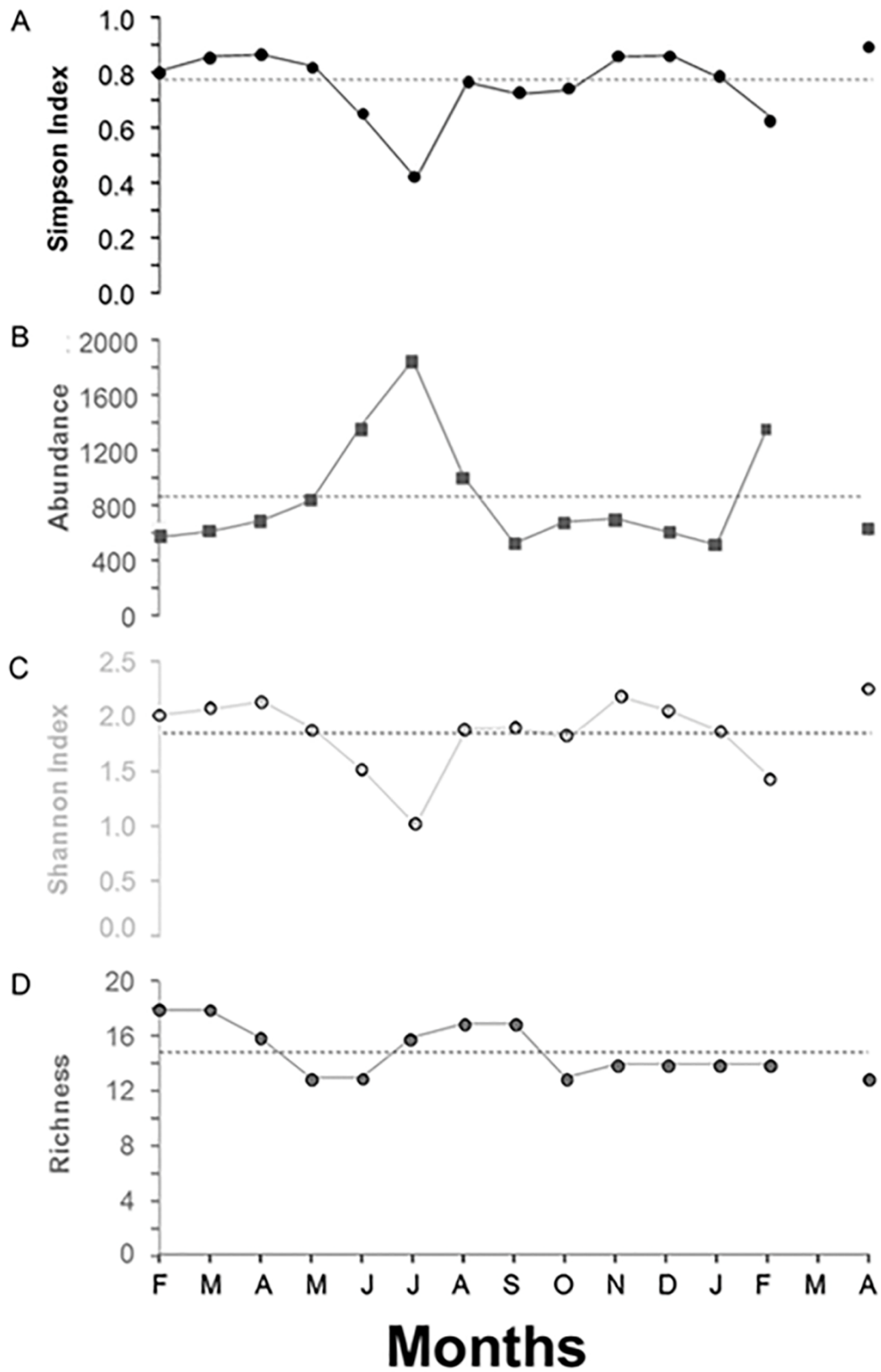


Fig.23. Biodiversity, richness and megafaunal species visual counts (i.e. from 14th February 2013 to 14th April 2014) time series, as reported by crawler video-imaging. Biodiversity have been reported as mean per month Shannon Index (C) and Simpson Index (A). Similarly, we reported the species richness (D). Abundance (B) was normalized for the maximum transects of the study period (i.e. 48). Horizontal dashed lines correspond to the Midline Estimated Statistic of Rhythm (MESOR).

3.4.3 Ethological remarks

Ethological observations were made for a range of different megafaunal species (see [Appendix E](#) for dates and hours, [Appendix F](#) for a reference on their physical appearance and [Appendix D](#) for their total visual counts). Fishes were usually observed lying on the seabed, while ignoring the approaching crawler. Some species (e.g. Dover sole, *Microstomus pacificus*, Deep sea sole, *Embassichthys bathybius*, Pacific halibut, *Hippoglossus stenolepis*, rockfish and hagfish) retreated approximately 2 to 3 m when crawler approached too close if they were lying directly in front of the crawler. Rattails (*Coryphaenoides* spp.) and Blackfin poacher (*Bathyagonus nigripinnis*) did not react at all to the crawler approach.

We observed once the agonistic display of a rockfish toward the crawler, which consisted in it approaching very close to the camera with its mouth open and then escaping ([Appendix DA](#)). Eelpouts were also seen escaping, by touching the seafloor and producing mud puffs, quickly leaving the vicinity of the crawler. Sablefish approached the camera of the crawler and then swam away from the field of view. During one encounter, a sablefish swam close to crawler for approximately 10 m of the transect ([Appendix DB](#)). On most occasions, sablefish appeared actively swimming but in some occasions they were observed lying on the seabed. Hagfish were similarly observed either laying on the seafloor or actively swimming but never drifting.

Dumbo octopii (*Grimpoteuthis* sp.) were observed lying on the seafloor on four occasions, without reacting to the presence of the crawler. In contrast, another cephalopod (the squid *Gonapus* sp.) quickly swam away releasing ink when it encountered the approaching crawler.

Feeding agonistic behaviour between grooved tanner crab and scarlet king crab (*Lithodes couesi*) was observed ([Appendix DC](#)). While a male scarlet king crab was trying to open a *Calypptogena* spp. clam, a grooved tanner crab appeared within the frame and tried to steal its prey (i.e. by advancing its chelipeds toward the clam). This interaction took 8 minutes, during which the scarlet king crab responded by hiding the prey below its body.

Grooved tanner crabs were particularly undisturbed by the presence of the crawler walking very slowly upon encounter. Only one individual displayed an agonistic posture ([Appendix DD](#)). Several observations on tanner crab reproductive behaviour were made in March and April 2013, and again in April 2014. Male and females were observed facing each other, touching their respective maxillipeds whilst the male took both female claws. The couples either ignored the crawler or avoided it. In the latter case, the males (considerably bigger than the female) lifted his partner by one claw above its body and walked away from the crawler, to later restart the mating ([Appendix DE](#)). Finally, we detected on 5 occasions females carrying eggs from March to April 2013 ([Appendix D F](#)).

3.5 Discussion

This study represents the first, high resolution documentation of seasonal patterns in megafaunal abundances and biodiversity at a cold-seep site. Our results of the visual counts of individuals observed across a 60 m² area of seafloor, made throughout a 14-month period, provide some indications of abundance patterns for different species through consecutive months, as a proxy of seasonality in behaviour and recruitment. Year-long monitoring programs have been used successfully in other studies to document seasonality in deep-sea megafaunal abundances (see [Aguzzi et al. 2013](#), [Tecchio 2013](#)). Similar species abundance levels at the beginning and end of our time series may indicate annual patterns. We observed individuals belonging to 6 phyla as being particularly abundant (26 taxa within cnidarians, ctenophores, arthropods, echinoderms, molluscs, and chordates). Our results are comparable with those from two other studies conducted at fixed observatory nodes in nearby non-seep regions of Barkley Canyon (see [Juniper 2013](#), [Matabos et al 2014](#)). Slight differences in visual counts and composition of the megafaunal communities between these sites may be attributed either to the different methodological approaches (i.e., fixed *versus* mobile observations), to differences in topography and oceanographic conditions occurring along the depth gradient ([Juniper et al 2013](#), [Doya et al. 2014](#), [Doya et al. 2016](#)) or with proximity to the canyon walls.

Compared with imaging from a fixed camera platform, running imaging transects with the crawler provided a larger sample of the less abundant, benthic and benthopelagic megafauna that inhabited the seafloor and adjacent benthic boundary layer ([Chatzievangelou et al. 2016](#)). Nevertheless, we underline the necessity of combining video transects (as performed in the current study) with close-up imaging of the seabed for detecting and identifying very small species (e.g., Caridea, Cirripeda or *Heptacarpus* sp.) as well as buccinids and small crab species), that are difficult to image from a mobile platform.

3.5.1 Seasonal patterns and the oceanographic influences

We detected monthly patterns in abundances of 8 benthic megafaunal taxa (rockfish, sablefish, hagfish, buccinids, small crabs, grooved tanner crab, ctenophores and Scyphomedusa) as shown by the time series analysis, the Kruskal-Wallis test and the NMDS analysis. Monthly abundance patterns can be considered a proxy of local seasonal drivers of species abundances ([Aguzzi et al. 2015](#)). Massive seasonal bathymetric displacements of benthic or benthopelagic megafauna on continental slopes can be linked to food availability ([Sardà et al 1994](#), [Moranta 2009](#), [Papiol 2012](#)), growth, and reproduction cycles (e.g. [Aguzzi et al. 2013](#), [Papiol 2012](#)), as well as to changes in predation pressure ([Aguzzi et al. 2009](#)). In high latitude biogeographic regions such as the NE Pacific, which display strong seasonality in primary production ([Brickley et al. 2004](#)), such seasonal displacements may serve as integral energy pulses that support the trophic web ([Csepp et al. 2011](#)).

Conversely, less information exists on deep-sea populations' responses to seasonal oceanographic variations, especially where benthic habitats occur within OMZs (i.e. depth strata with oxygen concentrations < 0.5 ml/l; (Levin et al. 2002). The depth of our study site corresponds to the core of the OMZ in the North Pacific (Juniper et al. 2013). The high-frequency variations in water mass physical properties (i.e., water density, O₂ levels, current velocity and temperature) detected at this cold-seep site were relatively minor in comparison with those measured at shallower depths of the canyon in (Juniper et al. 2013). This suggests that the region surveyed by the crawler in the current study, at ~890 m depth, was below the depths affected by shelf-edge upwelling, as observed at similar depths. Our results in the seasonal patterns in abundances, as well as the NMDS analyses suggest that some of our assessed species are indirectly influenced by upwelling (sablefish) and downwelling (rockfish and buccinids). In Juniper et al. (2013), the authors suggested that an inverse correlation of dissolved oxygen concentration and temperature could be an indication of water mass changes, as seems also to have been the case in the area investigated in the current study. Sablefish day-night nektobenthic migrations in Barkley Canyon are in antiphase with current speed, a possible compromise strategy between search for prey and energy saving due to physiological limitations (Doya et al. 2014, Chatzievangelou et al. 2016). Our data suggest that sablefish could follow a similar strategy also at a seasonal scale with animals avoiding shallower depths affected by upwelling. This would explain the peak in sablefish visual counts, the peak in total megafaunal abundance and the sharp decrease of biodiversity in July. Significant seasonality in sablefish abundance has been previously reported in SE Alaska, with the local population associated with deeper waters during the winter period (Csepp et al. 2011).

Buccinids exhibited a sharp increase in densities during February 2014. These gastropods are both predators and scavengers, known to form aggregations either to exploit prey (Aguzzi et al. 2012, Lapointe 1992) or to mate (Himmelman et al. 1993). They were not affected by currents above the seafloor, yet their maximum abundances coincided with the most pronounced downwelling period of the year. NMDS showed a positive correlation of buccinid abundances with increasing oxygen levels. In contrast, gastropods are known to be particularly resistant to hypoxia (Theede et al. 1973). This suggests an indirect effect of downwelling on the abundance of this species in our location. In agreement with this, (Matabos et al. 2014) found that *B. viridum* migrated from shallower depths to a location ~200 m from our study area, presumably to avoid enhanced currents. Highest rockfish densities also coincided with the strongest downwelling period (from January to April 2014). The NMDS indicated that their abundances were affected by the same environmental factors that influenced buccinid abundances. Although rockfish has often observed to be resident at fixed locations (Marliave et al. 2013, Reynolds et al. 2010, Yoshiyama et al. 1992), our findings suggest that at least some individuals move into this area to avoid enhanced currents in a similar strategy to the buccinids. This hypothesis needs to be confirmed with further studies. Although buccinids and rockfish were also observed outside of the strongest downwelling periods, their numbers were close to the significant threshold and coincided with Bakun Index values close to zero.

Additionally, rockfish are the major contributors to sablefish diet (Liadig et al. 1997). This could explain the decrease in rockfish counts during June and July when sablefish abundances were the highest of the study period.

Hagfish and the Scyphomedusa increased in abundance coinciding with an increase of oxygen concentration following the period of low oxygen concentrations from August 2013 to January 2014. NMDS outputs suggest that these species have their ideal oxygen threshold above the minimum levels observed in our study. Data on small crab abundance suggest a more complicated picture, with both seasonal (month-scale) fluctuations and diel trends negatively correlated with oxygen levels (Chatzievangelou et al. 2016).

A seasonally-related change in the depth zonation of the grooved tanner crab has been reported for the US West coast, with local densities at particular depths varying temporally and as a consequence of their growth and reproductive cycle (Keller et al. 2012). Sexes are also completely segregated by depth during spring and summer, whereas males and females mix in autumn and winter months, when males move into deeper waters (Pereyra et al. 1966). The observed peaks in visual counts of individuals within the current study, during March-April and June-July 2013, together with the subsequent sharp decrease and maintenance of low abundance maintained until the next spring, could be related to a similar seasonal displacement. Here, high visual counts of small crabs were made in December 2013, with abundances remaining high throughout winter. To our knowledge, there have been no previous studies of seasonal recruitment of *Chionoecetes tanneri*, so this potential evidence of a synchronous recruitment event should be considered with caution. According to (Jamieson et al. 1990) female Tanner crabs, which live at deeper water depths than males, move shallower for egg release and mating in March and April. Their higher abundance here in March-April, during higher oxygen levels, could be explained by a requirement of egg-carrying females to reduce the energy investment for oxygenating their eggs, as has been observed for other crustaceans (Fernández et al. 2003). To summarize, abundance trends and ethological observations throughout the study period, suggest that a massive reproductive aggregation of grooved tanner crab occurred during March and April 2013, following a previous migration from shallower waters (males) and deeper waters (females). This may have resulted in an associated peak in recruits observed in from December 2013 to February 2014.

Ctenophores were present during the autumn months of 2013. In Juniper et al. (2013), the authors also detected an increase in ctenophore visual counts in October-December at a nearby mid-canyon site. After occupying shallower depths near the surface ocean in spring and summer, a period coinciding with the maximum surface chlorophyll levels, (Båmstedt et al. 2015) found larger ctenophore individuals overwintering in deep waters, where they prey on copepods. Such vertical displacement of larger zooplankton represents a trade-off between feeding efficiency and predation avoidance (Darnis et al. 2014). Ctenophores are able to perform vertical movements at various temporal scales (i.e., diel, tidal, and seasonal migrations) thanks to their high tolerance of transient hypoxia (Thuesen et al. 2005). Our

time series counts and NMDS outputs support the occurrence of a similar phenomenon at the cold-seep site investigated here. We detected a subsequent increase in the visual counts of the Scyphomedusa, a species previously reported as being associated with OMZs (Osborn et al. 2007). Although little is known about the diet preferences of the species, other Scyphomedusa prey on *Bolinopsis infundibulum*, which could explain the concurrent peaks of these two gelatinous species (Martinussen et al. 1999, Båmstedt et al. 2015). The same occurrence pattern for this jellyfish has been also observed in the mid-Barkley Canyon (Juniper et al. 2013). As previously mentioned, this species was not present in video-data during the periods with the lowest oxygen levels, likely due to physiological limitation.

Although community composition differed throughout the study period, changes in species richness did not reach an order of magnitude, with a similar number of species replacing some of the previously existing ones. This was also reflected in the two biodiversity indices, which maintained a relatively constant level apart from 3 sharp decreases leading to low points (i.e. June-July, September-October 2013 and February 2014). In these particular periods, a single species (i.e. sablefish, ctenophores and buccinids, respectively) was disproportionately abundant, resulting in low biodiversity through low evenness. Taken together, these findings confirm our first hypothesis that abundance, richness, and biodiversity annual changes in relation to oceanographic conditions are directly driven by oxygen, current velocity, and upwelling/downwelling, and indirectly driven by seasonal benthopelagic and nektobenthic migrations along the canyon.

3.5.2 Methodological remarks

Crawler motion produced a transient sediment clouds in the water column behind the vehicle. Since all monitoring and environmental sensors were mounted at the front of the crawler, this is not expected to have affected any of the data values measured by the sensors. Though capable of surveying similar areas of seafloor as ROVs, crawlers (particularly IOVs such as ‘Wally I’) do not need ship assistance to operate, and in this study a crawler was efficiently used to perform a long-duration, spatially extensive study. In addition, ROVs are commonly perceived as “foreign objects” to the local or periodically visiting fauna, whereas permanently deployed, slower moving IOVs are permanent elements of the local benthic panorama rapidly accepted by the resident fauna. Crawlers may therefore be considered a less intrusive ethological monitoring technology (e.g., for monitoring reproduction and making natural situation feeding and agonistic behaviour observations), since they are likely “accepted” by the local fauna.

The disturbance caused by crawler lights on the behaviour of resident animals has not been well investigated. Sablefish have been previously found to be attracted by observatory lights for short periods of time and then to leave the field of view of cameras mounted on the NEPTUNE nodes (Doya et al. 2014). This short-duration light attraction suggests that animals are unlikely follow the crawler during transects and therefore unlikely to be recounted erroneously as successively imaged individuals. The

remainder of the mobile species detected didn't react or showed only minor reactions to crawler presence, avoiding it only when it was in extremely close proximity. In any case, bias generated by the presence of the crawler would have been maintained as constant throughout the study period given the uniform methodology employed in collecting the transect video data, and therefore not prevent the detection of seasonal patterns in megafauna abundance or biodiversity, or the successful collection of ethological observations. Therefore, our second hypothesis, that IOV technology represents a reliable faunal monitoring tool for work in the deep sea is also confirmed.

3.6 Acknowledgements

This work was conducted within the framework of Ocean Networks Canada (ONC) scientific activities, being led by Dr. J. Aguzzi “Science Theme Leader” for “Life in the North-East Pacific”. C. Doya is a PhD Student with a FPI grant by Spanish Industry, Economy, and Competitiveness Ministry (MINECO). The authors would like to thank the shipboard teams and staff scientists of Ocean Networks Canada and OceanLab Bremen. Dr. S. Mihály provided CTD and fluorometer data. The study was supported by ROBEX project of the Helmholtz Society.

**Chapter 4. Faunal activity rhythms influencing
early community succession of an implanted
whale carcass offshore Sagami Bay, Japan**

4.1 Abstract

The fate of large whale carcasses sinking to the deep-sea environments has intrigued scientists in the last three decades. Whale carcasses provide a surplus in food supply to demersal animals from a vast array of life strategies, serving as habitats for a specialized fauna that represents the counterpart of chemosynthetic symbiont-bearing taxa, generally inhabiting hydrothermal vents and hydrocarbon seeps. A distinctive pattern in benthic community succession resulting from animal scavenging activity has been established but previous studies relied on punctual sampling and observations conducted by submersibles and ROVs. The contribution of diel (i.e. 24 hrs. based) activity rhythms within internal tidal scenarios to the dynamism of that community succession has never been evaluated before. Here, we used an autonomous time-lapse video-imaging system mounted on a lander at 2 hrs. frequency, in order to count and identify all benthic and demersal fauna, near an artificially implanted juvenile sperm whale carcass at 500 m depth off Sagami Bay in Japan, over a 2.5-month period. We also acquired concomitant water current speed and temperature data, through an Acoustic Doppler Current Profiler, showing that the local diurnal internal tides are mixed with a dominant semi-diurnal periodicity of currents and water temperatures in the whale deployment area. Notwithstanding, with chronobiologic time-series analysis protocols (i.e. periodogram and waveform analyses), we discovered that visual count patterns of most abundant megafauna mostly followed a 24 hrs. fluctuation pattern (i.e., the snubnosed parasitic eel, *Simenchelys parasiticus*, the Japanese spider crab *Macrocheira kaempferi*, and finally the Japanese gissu *Pterothrissus gissu*). Only one species (the Japanese codling, *Physiculus japonicus*), showed a semi-diurnal rhythmicity. Our results highlighted the early occurrence of scavengers and the later appearance of predators and detritivores. The diel alternation of species at the scavenging site and the temporal succession recorded suggest the occurrence of temporal partitioning in the access to whale carcasses among deep-sea animals as ecological strategy to reduce interspecific competition and predatory-mediated mortality risks.

Keywords: scavenging activity, whale carcass, benthic communities, high-frequency analysis, behavioral rhythms, internal tides.

4.2 Introduction

The fate of large whale carcasses sinking to the seafloor in both shallow and deep-sea environments has intrigued scientists in several research fields spanning from community ecology, evolution, and biogeography for almost three decades (Smith et al. 2015, Sumida et al. 2016). The term ‘whale-fall’, coined after the incidental discovery and observations of a balaenopterid whale skeleton at 1240 m depth in Santa Catalina basin (California, USA), has been since used to generally define these oases-like organic-enriched seafloor environments (Smith et al. 1989, Smith and Baco, 2003). In the extremely poor food-supply environments such as the deep sea, a 40-ton sunken whale approximately provides an enormous input of organic matter ($\sim 2 \times 10^6$ g C), that may be equivalent to over 200 years of particulate organic matter arriving the seafloor *via* vertical and lateral fluxes in the form of marine snow aggregates and phytodetritus (Smith and Baco 2003).

Whale carcasses not only provide a surplus in food supply to benthic and demersal animals belong to a vast array of trophic guilds, but they also serve as habitats for a specialized fauna that represents the counterpart of chemosynthetic symbiont-bearing taxa, inhabiting other reducing environments such as hydrothermal vents and seeps (Smith et al. 1989). For that resemblance, particularly the sharing of at least 20 species with hydrocarbon seeps, whale falls have been hypothesized to act as dispersal stepping stone habitats for vent and seep faunas (Baco et al. 1999, Smith and Baco 2003, Smith et al. 2014, Sumida et al. 2016). At evolutionary time scales, whale carcasses have also been postulated to support the invasion of deep-sea chemosynthetic habitats by shallow water taxa, also in a stepping stone fashion (Baco et al. 1999, Fujiwara et al. 2010, Lorion et al. 2013).

After almost three decades of studies around naturally occurring and artificially implanted whale carcasses on the seafloor, a distinctive pattern in benthic community succession has been established, with four well defined stages (see Smith and Baco 2003, Smith et al. 2015 for details): *i.* a mobile-scavenger stage, lasting months up to 1.5 years, *ii.* an enrichment-opportunistic stage, also lasting months up to 4.5 years, *iii.* a sulphophilic stage, lasting for decades, and finally *iv.* a reef stage, potentially lasting also for several years. Duration of each stage is ultimately dependent upon whale carcass size and seafloor environmental conditions such as depth, currents, temperature and dissolved oxygen.

Cyclic changes in the environmental conditions around whale carrion may deeply influence the succession dynamic, by generating a rhythmic turnover in local species composition. In the aphotic deep sea, changes in water flow speed and temperature (Wagner et al. 2007, Aguzzi et al. 2011), together with seasonal food input from the euphotic zone (Billet et al. 1983, Graf 1989, Fanelli et al. 2011), are the main environmental drivers in temporizing behavioral rhythms of benthos. In fact, rhythmic population displacements into the water column-seabed three-dimensional scenario occurs more typically at a diel (i.e. 12 and 24 hrs.) base into the water column (as Diel Vertical Migrations or DVMs), horizontal

displacements along the seabed (as nektonic movements across shelves and slopes), or in and out from the sediment (as endobenthic) (Aguzzi and Company 2010). The role of those population displacement rhythms on whale scavenging dynamic in relation to overt environmental cycles has been poorly investigated to date. The behavioral activity of scavenging species and their access to the whale carrion could be temporally regulated upon internal tidal motions, as well as upon the rhythmic presence of benthopelagic predators into the local benthic boundary layer (Aguzzi et al. 2015). Other factors regulating species turnover could be related to intraspecific competition pressure which may provoke a partitioning of time of access to the same food resource by species with overlapping trophic niches (Kronfeld-Schor and Dayan 2003), namely the carrion in the case of facultative *versus* obligated scavengers.

Previous studies on whale fall communities have relied on punctual sampling and observations conducted by submersibles and remote operated vehicles (ROVs) (Smith et al., 1989; Lundsten et al., 2010a, b; Smith et al., 2014). More long-term and high-frequency *in-situ* observations and sampling are currently lacking due to logistical constraints, mostly associated with high operational costs in accessing remote deep-sea environments and/or difficulty in whale availability and sampling. However, multiparametric benthic platforms such as landers can be efficiently used to study the contribution of species activity rhythms in the scavenging dynamics, the time scales of the transitions between successional stages, as well as the role of interspecific relationships among species competing for carrion resources, including predator-prey interactions (De Leo et al., 2016). These autonomous platforms enable high-frequency, continuous and prolonged time-lapse imaging of benthic communities protracted over consecutive months along with concomitant oceanographic monitoring to assess the environmental control on behavior (Aguzzi et al. 2012a, 2015a; De Leo et al., 2016).

The present contribution offers insights on how multiparametric landers time-lapse video-imaging can be used to gather data about whale fall species turnover, resulting scavenging dynamic, and the environmental control, by applying time series analyses fitting chronobiology standards and multivariate analysis.

4.3 Materials and Methods

4.3.1 The study site and the experimental setting

A juvenile male sperm whale (*Physeter macrocephalus*, Linnaeus 1758), 464 cm in total length and 1.2 tons of body weight, was collected whole as it beach-stranded at Mihama-cho, Aichi, Japan on April 24th, 2008. The carcass was immediately preserved in a freezing container at -30 °C till June 5th, 2012. The whale was then transported to the Atami Port and stored on a barge that was used for the carcass deployment under natural conditions. The free-fall deployment of the carcass was then conducted at a depth of 492 m at the halfway point between Hatsushima Island and the tip of the Manazuru Peninsula in Sagami Bay (35°05.576'N, 139°10.271'E) on June 8th, 2012 (Fig. 24A). The deployment site was about 12 km NW of the local cabled seafloor video-observatory located in Sagami Bay lower slope, at 1100 m depth (Aguzzi et al. 2010).

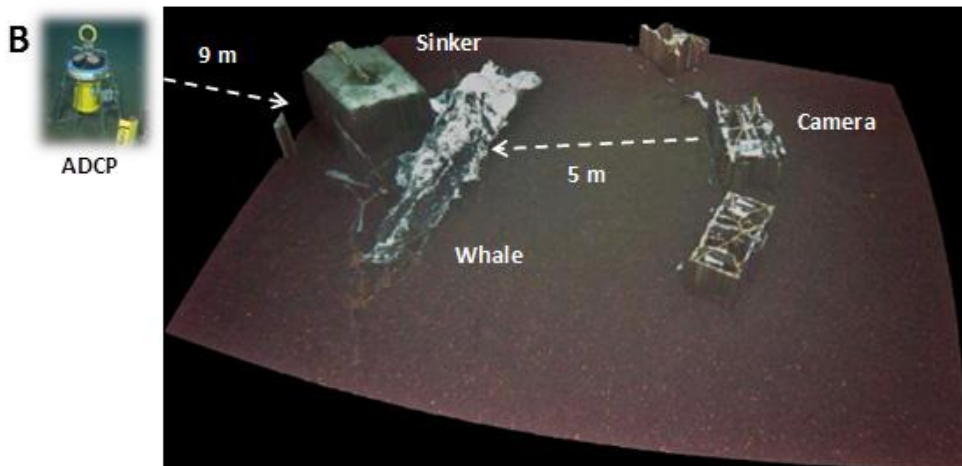
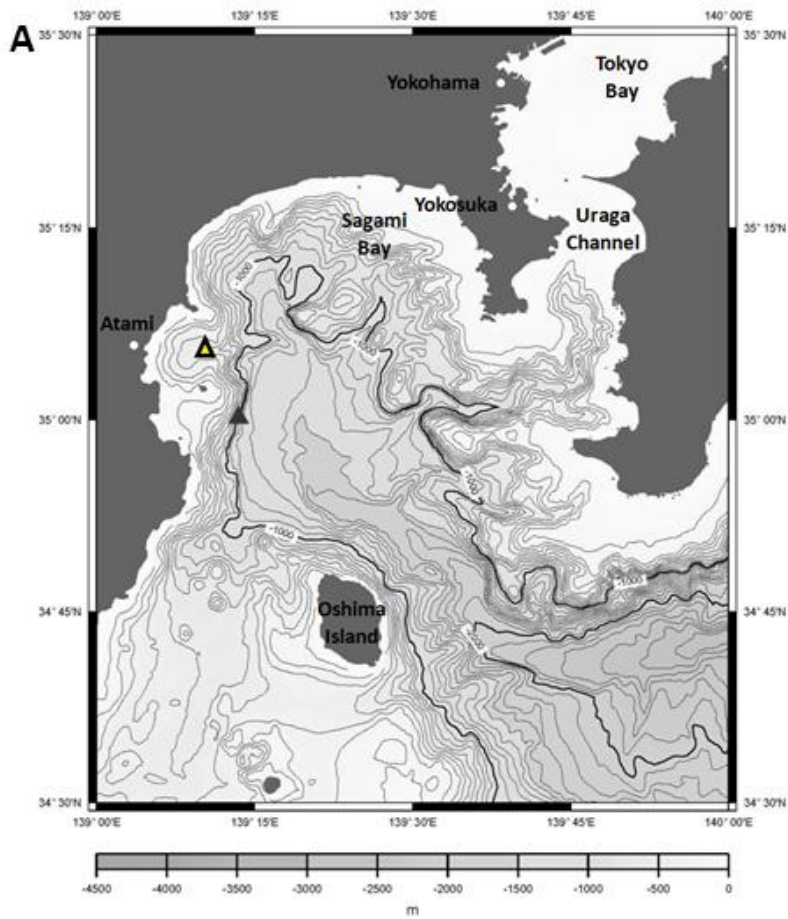


Fig.24. Map showing the deployment site of the juvenile sperm whale SW off Sagami Bay (empty triangle) at 500 m depth and in relation to the seafloor cabled video observatory (filled triangle) at 1100 m depth (Aguzzi et al. 2010). The deployment site was about. B. 3D laser scan image of the deployment site shows the whale carcass relative to the ballast used to sink it, the camera and ADCP instrumented landers (courtesy of B. Thorton and A. Bodemann).

Two concrete blocks (1 m³ each) were tied to the base of the whale tail as sinkers with negative-buoyant ropes (45 mm in diameter) under the instruction shown by the Japanese Fisheries Agency (http://www.jfa.maff.go.jp/j/whale/w_faq/pdf/manual.pdf). The deployment took place within the documentary filming activities of NHK (Japan Broadcasting Corporation) and Discovery Channel (http://www.godac.jamstec.go.jp/catalog/data/doc_catalog/media/NT12-15_all.pdf).

A lander bearing a camera was used to carry out image acquisition. The time-lapse still camera system (Goto Aquatics Inc., Japan), consisting of a digital camera Pen Lite E-PL2 (Olympus, Japan), a Zuiko Digital ED 8 mm F3.5 Fisheye lens (Olympus), and two flashlights FL-50R (Olympus) installed on both sides of the camera. Owing to this fisheye lens and dome port, this camera system was capable of commanding very wide view. The exposure of the camera was manually set to 1/125 sec for the shutter speed and to f. 16.0 for the aperture. The white balance was set to 5500 K and the focal distance was set to 120 cm. The flashlights fully radiated using diffuser (GN28, ISO200).

The camera was installed horizontally and the height of the center of the lens was 42 cm from the seafloor. The camera system was deployed at approximately 280 cm away from the carcass (Fig. 24B). With those imaging settings, we approximately could video survey an area of 10 m², encompassing the whole whale body. Photographs were acquired at a 2 hrs. interval for a period of 72 days starting on June 14th (6 days after carcass implantation) at 16:30 and ending on August 24th at 10:30 (Japan Standard Time, JST). A total of 850 photographs were used for counting and identifying organisms.

Image acquisition was supplemented by the monitoring of the oceanographic conditions around the carcass (see Figure 24B). Current and temperature profiles at the seafloor were measured, since their fluctuation may drive the distribution and dispersion of organisms. Furthermore, odor plumes coming from the carcass attract scavengers (Stockton and DeLaca 1982), and activity rhythms of ectotherms may be thermally dependent (Natarajan 1989, Bale et al. 2016; Audrey et al. 2017). A 300 kHz Workhorse Sentinel Acoustic Doppler Current Profiler (ADCP; Teledyne RD Instruments) was installed upward-looking in the southwestern side of the whale carcass (see Figure 24B), providing current velocity (horizontal and vertical components), temperature, and hydrostatic pressure (water column height, as proxy of depth) data. It was set at a 20-minutes sampling interval and the cell size and number of cells were 3 m and 50, respectively. Current flow velocities were analysed for the North-South, East-West and vertical components. Both, bottom current and temperature data were reported into 2 hrs. intervals to match the frequency of image acquisition.

4.3.2 Data analysis

Fluctuations in megafaunal visual counts at a still imaging site can be considered as a proxy of local population rhythm, resulting from synchronic displacement among individuals (Aguzzi et al. 2012,2015). For each image, we classified animals to the lowest taxonomic level as possible and then, we reported their number per each taxonomic unit. We could only identify animals that were approximately within 4-5 m² of the seafloor right in front of the camera, with a few exceptions, represented by large-size species.

The occurrence of significant diel periodicities in visual counts fluctuations for the different species (i.e. day-night or internal tides-associated) was studied using the Lomb-Scargle Periodogram with El Temps (<http://www.el-temps.com>). Periodicities were screened within the interval 600-1620 min, equivalent to 10 and 27 hrs., respectively, to cover a wide range of diel cycles (i.e. inertial, tidal, and day-night patterning at the latitude and depth of the study area; Aguzzi et al. 2010). In the periodogram output plots, the highest peak exceeding the significant threshold ($p < 0.05$) represents the maximum percentage of total data variance explained by the inherent dominant periodicity.

A rhythm is the temporal succession of peaks and troughs while the phase represents the timing of that average peaking in relation to an external controlling cycle (Refinetti 2006). Waveform analysis serves to identify the rhythms' phases and we carried out such an analysis on visual count data sets for those species showing significant diel periodicities in previous periodogram analysis, according to Chiesa et al. (2010). Each time series was partitioned into 24 hrs. segments (i.e. 12 values length per segment, given the 2 hrs. sampling frequency). Values at corresponding timings were then averaged within all segments, thus obtaining a mean fluctuation plot (i.e. the waveform). Phase timing and duration were statistically assessed using the Midline Estimating Statistic Of Rhythm (MESOR) (Aguzzi et al. 2006). MESOR was estimated by re-averaging all waveform values and representing the resulting mean as a horizontal threshold line on the waveform plots. This diel threshold is used to discern waveform values above it as a significant increment representative of the phase (Refinetti 2006).

For those species showing significant visual count patterns of tidal periodicity, waveform analysis was repeated as above, but at an approximated 12 hrs. length (i.e. by subdividing the whole data set in sub-segments, each of 6 values), to evidence the role of that water flow patterning on species behavior. That analysis, together with an FFT approach, was also repeated in a similar manner for ADCP data of the first layer (i.e. 5 m) to target the hydrodynamic variations in the benthic boundary layer environment, indicating tidal motions and comparable results between the two approaches, as shown in Appendix M. The 24 hours Fourier component of East-West current was also integrated in time to evaluate the periodic displacements along this direction induced by diel tidal current. Thus, the East-West component was selected as representative of the horizontal flow, being oriented approximately towards the main direction of the bottom topography.

Time series analysis (i.e. periodogram plus waveform) were repeated by subdividing species according to their trophic habits: scavengers (which can also be facultative predators), detritivores and predators. According to that, visual counts for species within the groups were summed at 2 hrs. intervals, and time series analyses were repeated and results compared.

Multivariate analyses were carried to define the temporal succession in species occurrence. First, a cluster analysis with a SIMPROF test (Clarke et al. 2008) was carried out on the week-averaged 4th root transformed biological data in order to highlight separation in species occurrence within the observation periods. Then, nMDS was performed on the same matrix and graphical bubble plots were used to highlight those species which most contributed to the observed ordination. A PERMANOVA test (Anderson et al. 2008) was finally carried out on the groups found to be significantly separated by SIMPROF test and a SIMPER analysis was run to identify those species which most typify each week and the average similarity within each period (week). All these analyses were carried out with the software PRIMER6&PERMANOVA+ (Clarke and Gorley, 2008, Anderson et al., 2008).

Further, in order to weight the contribution of each oceanographic parameter on species temporal patterning and the occurrence of certain recurrent species associations, a Canonical Covariate Analysis (CANOCO; Legendre and Legendre 1998) and a 2-block Partial Least Squares analysis (2B-PLS) were carried out. A matrix composed by the time series (822 observations) and 2 series of variables (i.e. “block” hereafter) were considered. Block 1 was composed by 5 variables: Date (numerically transformed in Excel), Time (also numerically transformed in Excel and shifted starting from 4:30 a.m. as “dawn”, to obtain lower values in the photophase and high values at night), and finally temperature, depth, and current velocity (horizontal East-West and vertical current components). The East-West component was selected as representative of the horizontal flow, as approximately follows the main direction of the bottom topography. Block 2 was composed by variables as species visual counts and block 3 encompassed trophic-behavior variables of scavengers (and facultative predators), detritivores, and predators. Being an ordination technique, CANOCO was then applied to observe in a same space the contribution of both environmental and species abundances matrices. The ordination axes are linear combinations of the environmental variables. CCA analysis was run under the free software PAST 3.14 (<http://folk.uio.no/ohammer/past/>).

4.4 Results

4.4.1 Benthic and scavenger community composition

16 species of vertebrates and invertebrates from four different phyla (Mollusca, Arthropoda, Echinodermata and Chordata) could be distinguished (Fig. 25) and their putative abundances resulted markedly different (Appendix G).

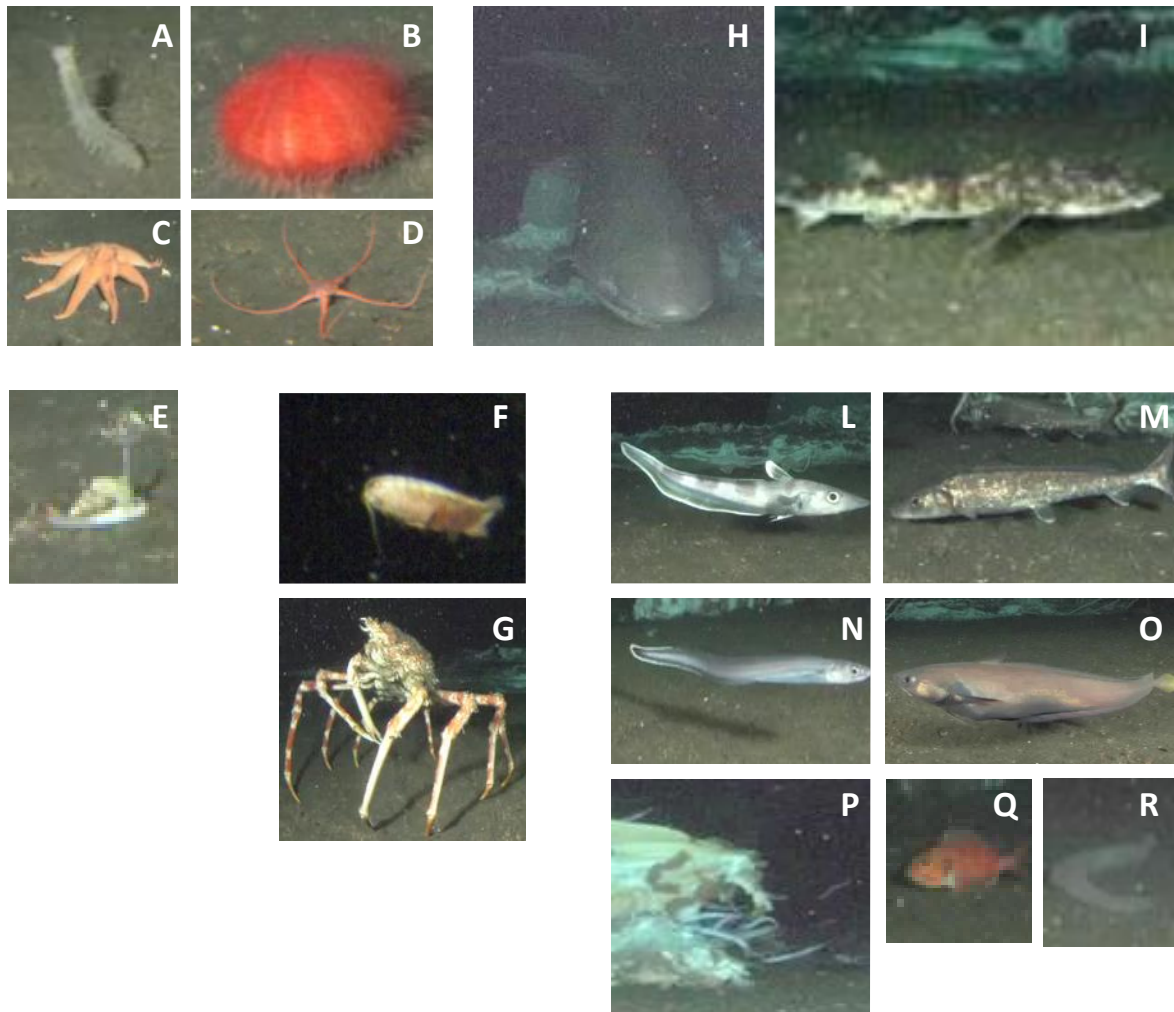


Fig. 25. Images of the taxonomical units as components of the local megafaunal assemblage detected at whale carcass positioning by time-lapse camera imaging (see also Appendix G): A. *Pannychia moseleyi*; B. *Echinothurioida*; C. *Solaster paxillatus*; D. *Ophiurida*; E. *Buccinum yoroianum*; F. *Bathynomus doederleini*; G. *Macrocheira kaempferi*; H. *Hexanchus griseus*; I. *Cephaloscyllium umbratile*; L. *Coelorinchus* sp.; M. *Pterothrissus gissu*; N. *Zoarcidae*; O. *Physiculus japonicus*; P. *Simenchelys parasiticus*; Q. *Helicolenus hilgendorffii*; and finally, R. *Eptatretus deani*.

The snubnosed parasitic eel, *Simenchelys parasiticus*, was the most abundant species, representing more than half of total observations (56.5 %, 4052 individuals) (see Appendix G). The Japanese spider crab, *Macrocheira kaempferi*, was the second most abundant species, present in 14.0 % of the observations and with 1002 individuals, followed by another bony fish, *Pterothrissus gissu* with 5.4% in frequency of occurrence and 390 individuals (see Appendix G). Finally, the isopod *Bathynomus doederleinii* was the fourth most abundant species with 4.9% (N=349) of occurrence.

The detection at the beginning of the time-lapse sequence of a large individual of the bluntnose six-gill shark, *Hexanchus griseus*, feeding on the whale carcass (see Figure 25 H) was noteworthy. Also, the whole whale carcass slightly shifted its position at the beginning of the survey (i.e. 6:30 a.m., on June 15th). Then, it suffered other 3 major shifts during the experiment, at 8:30 a.m. on July 15th, 4:30 a.m. on July 26th, and finally at 2:39 a.m. of the on August 7th (Fig. 26) with no apparent co-detection of other shark individuals.

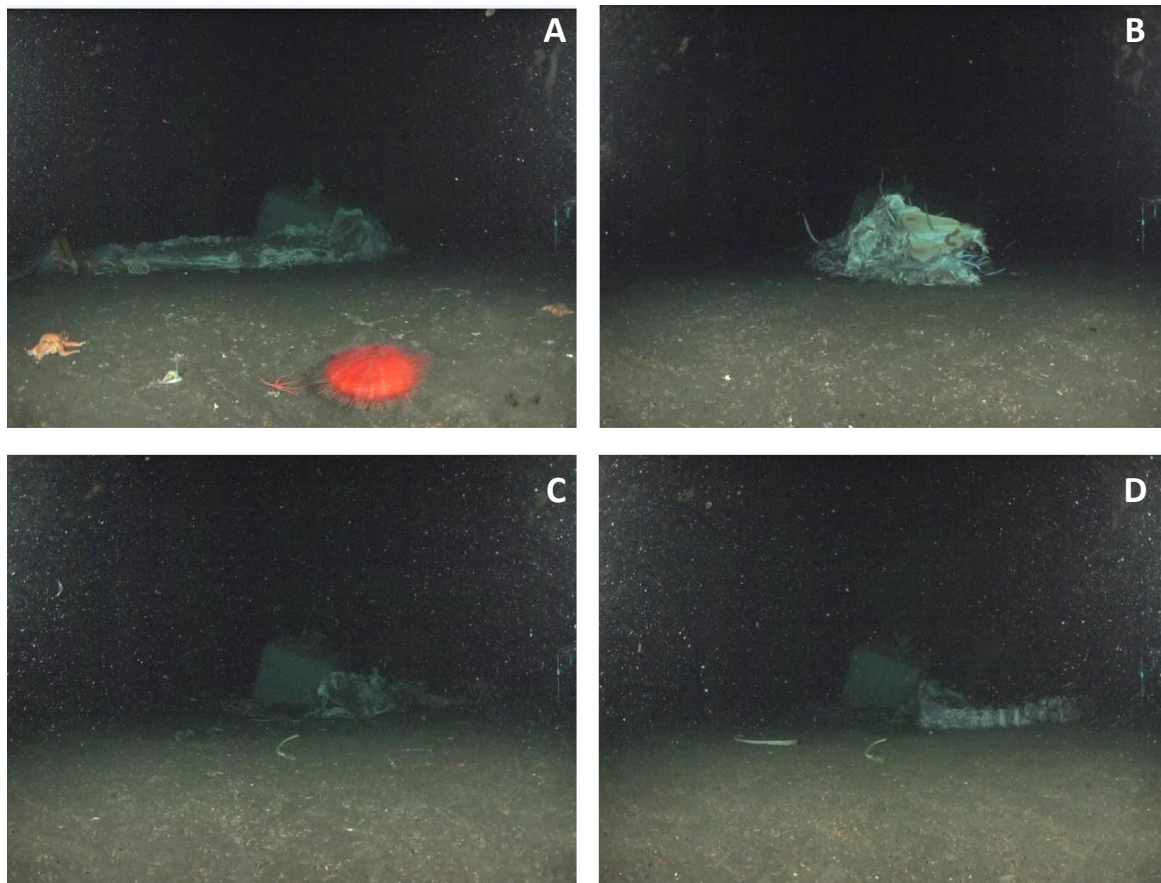


Fig.26. Temporal changes in the whale carcass positioning with respect to the camera field of view as detected by time-lapse imaging. A. 06.15.2012 to 07.15.2012; B. 07.15.2012 to 07.26.2012; C. 07.26.2012 to 08.07.2012; and finally, D. 08.07.2102 to 08.24.2012. In A, two individuals of *Solaster paxillatus*, and single individuals of Echinothurioidea, Ophiuridea, and *Buccinum yoroianum* are visible. In C and D, two ribs appear on the seafloor.

In terms of the biological data, the visual counts time series for all species indicate different patterns of occurrence near the carcass ([Appendix H](#)) depicting a noticeable change in community composition particularly marked by the slow replacement of the crab *M. kaempferi* by the fish *P. gissu* around the 34th day of the experiment (between the 4th and the 5th week). While some species occurred during the entire period of observations (e.g. *S. parasiticus*), others peaked toward the middle (e.g. the isopod *B. doederleini*) or the end (e.g. ophiuroids and the sea cucumber *Pannychia moseley*) of observations.

4.4.2 Time series analysis outputs

Oceanographic time series of water temperature, pressure, and current flow speed (East-West and vertical components) at sea bottom, re-sampled at 2 hrs. intervals, are presented in [Figure 27](#). A mixed diurnal-semidiurnal tidal cycle occurred in the area, as indicated by the FFT analysis. In all these series, the semi-diurnal cycle is dominant with lower cycles present at 6 and 24 hrs. periods. Average (\pm SD), maximum and minimum values for the measured oceanographic variables were: temperature ($^{\circ}$ C) = 5.73 ± 0.44 , max. = 7.00, min. = 4.23; pressure (dBar) = 493 ± 0.49 , max. = 493.68, min. = 491.31; vertical velocity component (cm/s) = -1.89 ± 1.2 , max. = 3.7, min. = -5.6; east-west velocity component (cm/s) = 1.47 ± 13.5 , max. = 51.2, min. = -30.3.

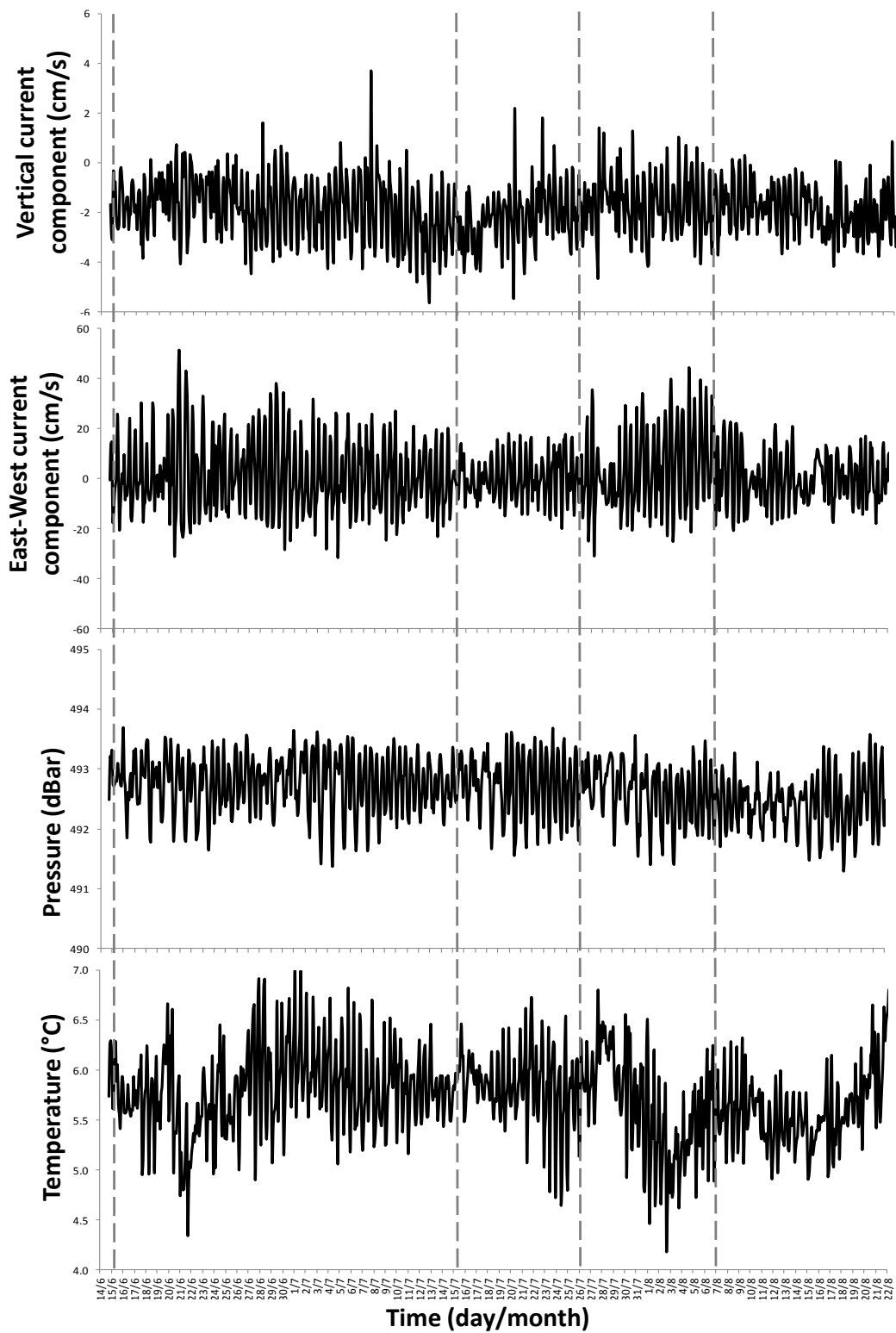


Fig.27. Temperature at sea bottom, water pressure, vertical and East-West current component as recorded over 72 days by ADCP close to the whale carcass deployment. Whale carcass position changes (see Figure 25) are indicated by vertical light grey dotted lines.

Using the FFT diel component of East-West current it is possible to evaluate the water displacement associated to this tidal motion: by integrating in time the current we obtain exactly this displacement. This allows estimating both the distance reached in this movement (ranging between 0 to 440 m) and the time phase of this process.

Time series and stick diagrams of daily mean horizontal currents (shown in [Appendix I-J](#)) allowed describing their temporal and spatial evolution during the period of observation. The currents were not vertically homogeneous: southeastward flow was dominant up to the 10th ADCP level (i.e. about 32 m above sea bottom), whereas northwestward flow was characteristic from 30 to 60 m above the bottom, indicating different transportation processes and water mass origin for the two layers. This difference in the pattern was also consistent with the results of the complex correlation analysis which reports lower value coefficients moving from lower to upper layers.

In relation to the vertical components analysis, data show that a downward flow was prominent across the investigated water column, being stronger near the bottom and basically following the semi-diurnal period, as shown by the pressure time series and in [Appendix K](#) (i.e. weak downward flows correspond to neap tides, represented by the lowest pressure excursion).

To detect the occurrence of tidal motions and to analyze their temporal evolution, time-dependent complex frequency analysis was performed on the horizontal and vertical components time series (shown in [Appendix L](#)). The predominance period of the spectrum was observed for 24, 12 (the highest peak), and 6 hrs., confirming tidal (diurnal and semidiurnal) periodicity for the flow around the sea bottom. Same results have been obtained for water temperature data (but with a less evident peak in correspondence of the 24 hrs. period).

Periodogram analysis identified the occurrence of significant day-night related (i.e. 24 hrs.) visual count fluctuation patterns for 3 species (see [Appendix G](#)): *S. parasiticus* (swimmer; P=24.0 hrs.; Var.=15.79%), *P. gissu* (swimmer; P=24.0 hrs.; Var.=22.64%), and finally *M. kaempferi* (walker; P=23.8 h; Var.=7.76%). A single species showed a tidal-related periodicity, the fish *Physiculus japonicus* (swimmer; P=12.3 hrs.; Var.= 7.78%; see [Appendix G](#)). Interestingly, no other significant tidal periodicity was revealed for the remaining species, and only *Coelorinchus* sp. showed a different periodicity related to inertial currents (P=19.5 hrs.; Var. =8.56%).

The waveform analysis conducted for *S. parasiticus*, *M. kaempferi* and finally *P. gissu*, as species showing significant 24 hrs. ([Fig. 28 A, B, C](#) respectively), from count patterns in previous periodogram analysis (see [Appendix G](#)), indicated the occurrence of temporally coherent phases (i.e. a continuous series of values above the MESOR). The phase timing comparison through species indicates the occurrence of a progressive phase shift from night (*S. parasiticus*) to daytime (*P. gissu*). The correspondent integrated diurnal displacements along the East-West axis, computed from the FFT results,

are superimposed with a 2 hrs. delay to match the *S. parasiticus* periodicity, while for the *M. kaempferi* the delay is of about 8 hours.

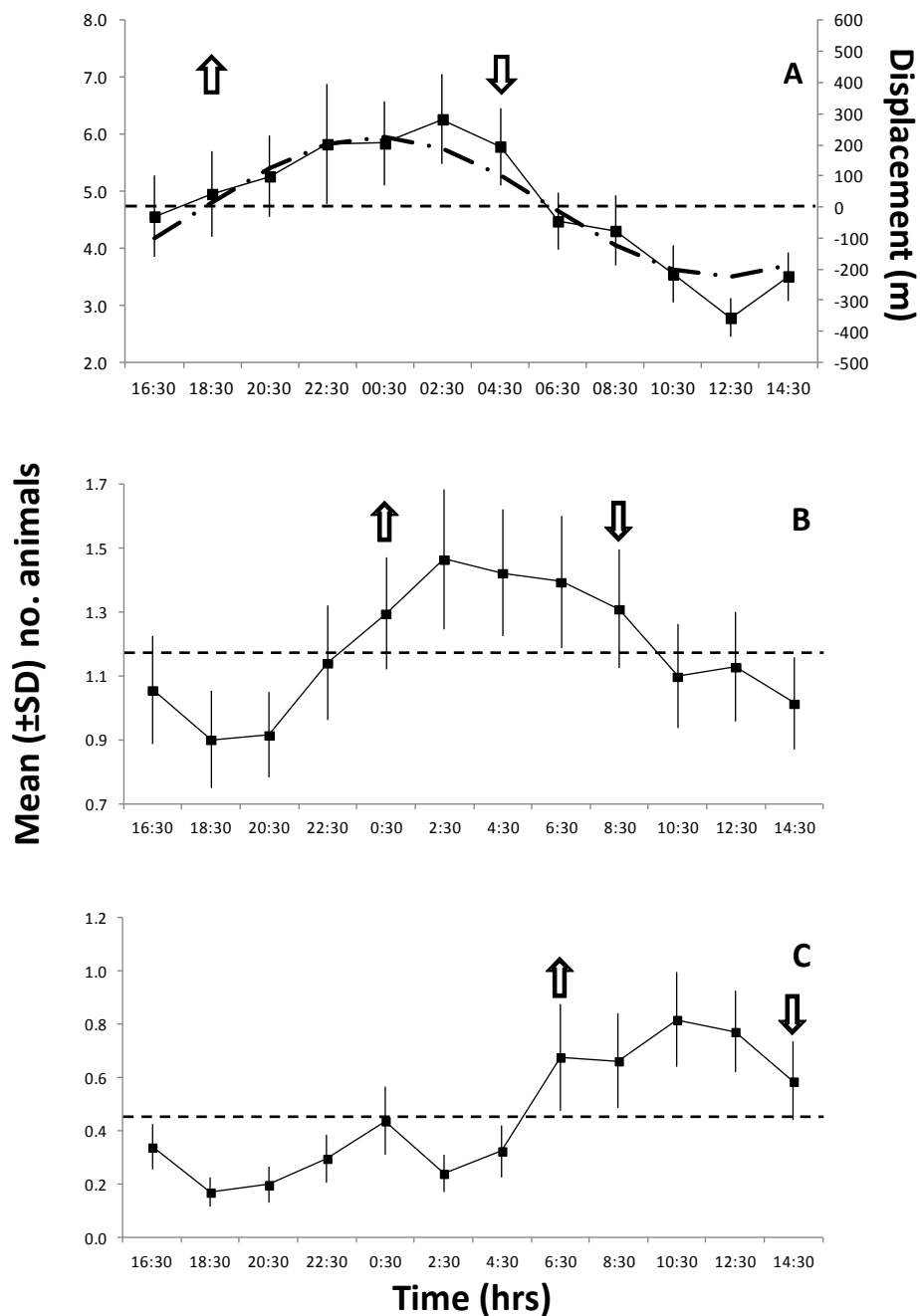


Fig.28. Waveform analysis outputs for the visual count time series of those species showing significant 24 hrs. periodicity patterns in the periodogram analysis (see Appendix G for A. *S. parasiticus*, B. *M. kaempferi*, and C. *P.gissu*). Note the varying Y-axis abundance scales. Up and down arrows indicate onset and offset of significant increments in abundance peaks, respectively. They also indicate the first and last calculated mean abundance values above the Midline Estimated Statistic Of Rhythm (MESOR as dashed horizontal lines) line as re-average of all waveform data. MESORs are: A, 4.76; B, 1.18; C, 0.46. The correspondent integrated diurnal displacements (m) along the E-W axis, computed from the FFT results, are superimposed, showing a 2 hrs. delay in the animal periodicity.

Waveform analysis was repeated for the vertical and the East-West current components (Appendix M), partitioned once in 12 hours and then in 24 hrs. segments, to show both diurnal and semidiurnal tides. Vertical current speed values were in average negative (i.e. downward) and its tidal components (diurnal and semidiurnal) were in phase with the East-West components. Hence both components produced oscillations along the local topography. The correspondent diurnal and semidiurnal Fourier component curves (the dash-dotted lines superimposed in Appendix M), confirmed the same trends. Both the vertical and East-West current components showed an evident bimodal fluctuation, typical of mixed diurnal and semidiurnal regime, even if the semidiurnal cycle was clearly dominant (about tenfold the diurnal cycle).

The waveform analysis conducted separately for scavengers, detritivores and predators, indicated the presence of a temporal segregation of species according to their food preferences (Appendix N). Values above the MESOR indicate significant nocturnal and diurnal increases, respectively for scavengers (and facultative predators) and predators. Conversely, no clear phase is reported for detritivores, likely due to a scarcity of visual counts. These results were sustained by periodogram analysis outputs (see Appendix G), which identified a 24 h significant rhythmicity in respective data sets, with arrhythmia for detritivores.

4.4.3 Multivariate analysis outputs

Multivariate analyses partially confirmed and added information to previous results: two main phases were identified by cluster analysis, with weeks 1-6 significantly separated by weeks 7-11 (accordingly to SIMPROF test at $p < 0.05$, black lines in Figure 29A), at 60% of resemblance level. This separation (weeks 1-6 vs. 7-11) resulted highly significant also according to PERMANOVA test ($F_{1,10} = 11.34$, $p < 0.001$). Consistently, SIMPER analysis evidenced those species which mostly typified each phase (Table 4), with *S. parasiticus* abundant in both phases and *M. kaempferi* and ophiuroids being the taxa that most typifying phase 1 (weeks 1-6) and phase 2 (weeks 7-11), respectively. The 2-D bubble nMDS (Fig. 29B) showed the abundance of these latter taxa in the two different phases: the overlaid clusters at 60% of similarity mostly divided weeks 1-6 from 7-11.

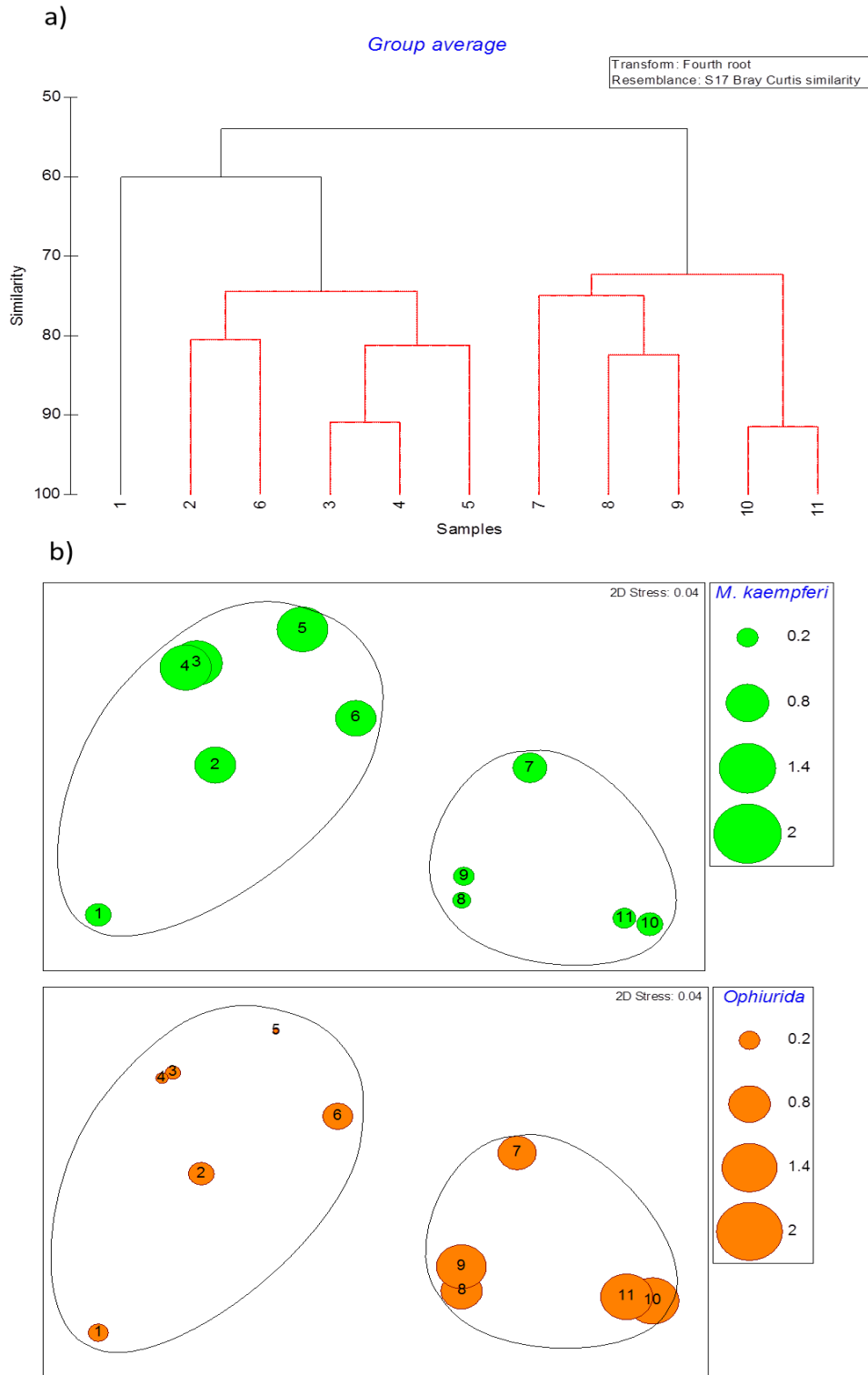


Fig.29. Cluster analysis of the mean abundance values by day of species recorded at the whale fall for factor “week”. Black lines indicate significant separation at $p < 0.05$ according to SIMPROF test; B. Bubble nMDS plots with over imposed cluster analysis results (at 60% of resemblance level) of two of the dominant taxa of each phase (weeks 1-6 vs. 7-11): *Macrocheira kaempferi* and ophiuroids.

Table 4 Results of the SIMPER analysis carried out on the two periods (weeks 1-6 vs. 7-11) evidenced by multivariate analysis

Weeks 1-6		Average similarity: 72.08		
Species	Av. Abund.	Av. Sim	Contrib. (%)	Cum. (%)
<i>S. parasiticus</i>	1.37	36.87	51.16	51.16
<i>M. kaempferi</i>	0.86	19.11	26.51	77.67
<i>P. japonicus</i>	0.25	5.37	7.45	85.11
<i>B. doederleini</i>	0.27	3.91	5.43	90.55
Weeks 7-11		Average similarity: 75.77		
Species	Av. Abund.	Av. Sim	Contrib. (%)	Cum. (%)
Ophiurida	1.03	26.33	34.75	34.75
<i>S. parasiticus</i>	0.92	23.74	31.33	66.08
<i>P. japonicus</i>	0.23	6.16	8.12	74.2
Zoarcidae	0.25	5.95	7.85	82.06
<i>M. kaempferi</i>	0.28	5.87	7.74	89.8
<i>P. gissu</i>	0.3	5.58	7.37	97.17

The ordination on the first two axes of the CANOCO (Fig. 30 A) showed the association of species (represented by point, block 2) with the environmental variables (represented as vectors, block 1). The first (horizontal) axis represents consistent patterning in species ordination, from positive (right) to negative (left) side with a variable time of appearance according to the “Date” variable (see Figure 30 A). From right to left that ordering is made by scavengers then predators, and finally detritivores. 2-block PLS (Fig. 30 B) showed how the most important variables on the first axis of the block 1 (88.5% Covariance) were mainly Date and then, the Horizontal Component V; variables on the first axis of the second block for this reason, are associated with species succession from the earlier (positive side) to the later (negative side).

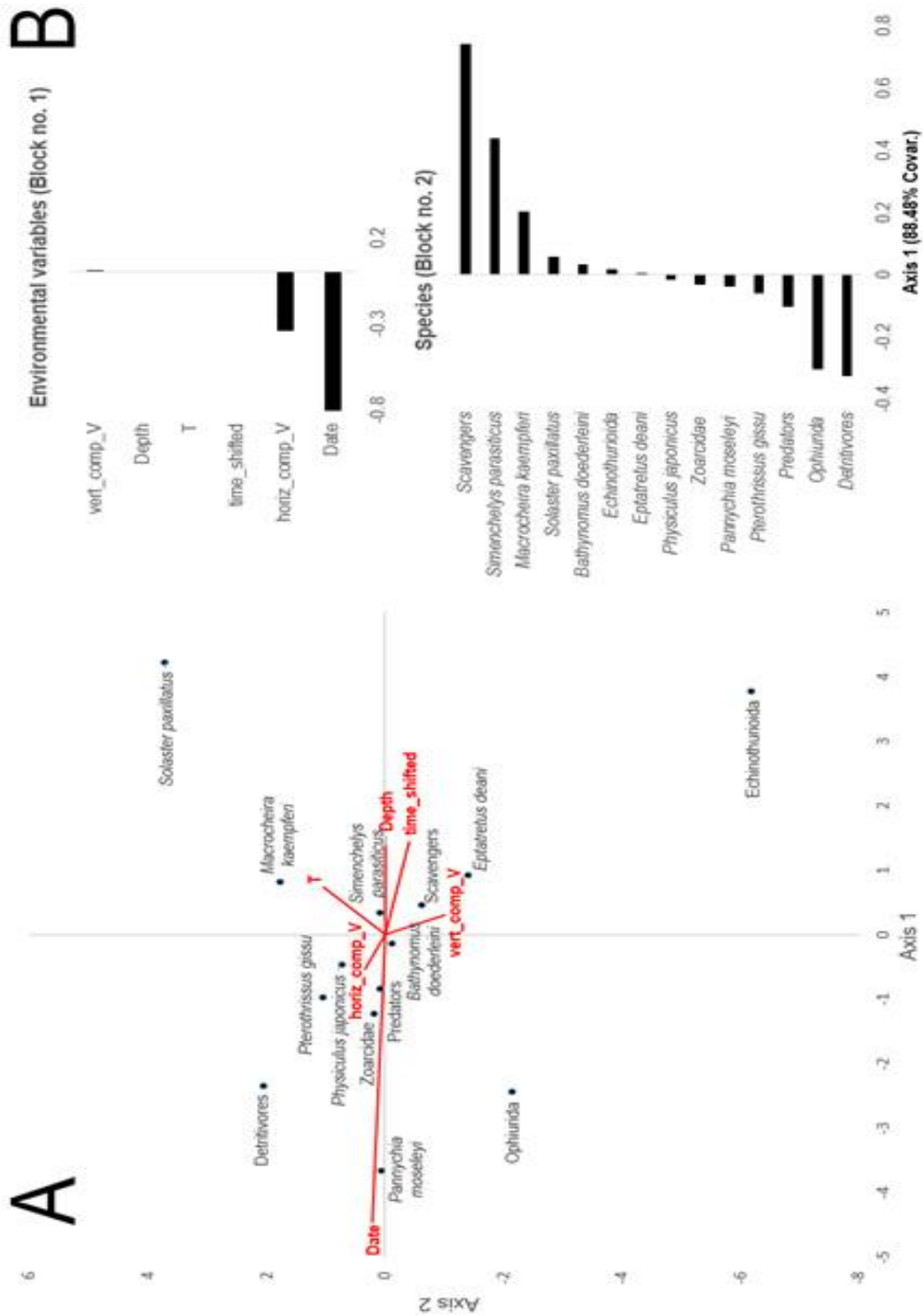


Fig.30. Scatter plot of the first two axes of the CANOCO. Species and trophic categories (i.e. scavengers, predators, and detritivores) were represented by black points and environmental variables were represented by red vectors. Environmental variables considered are: Date of the observation as “Date”, spatial components of current velocity as “EW_Comp_V” and “Vert_Comp_V”, as well as Depth, Temperature and the time shifted. B, Bar chart of the loadings relative to the first latent vector (explained variance = 77.44%) for both environmental and species blocks (no. 1 and 2, respectively).

4.5 Discussion

We reported for the first time to our best knowledge, the occurrence of a diel turnover in species appearance at a slope whale fall site (i.e. about 500 m depth), which accounts for the importance of behavioral rhythms in regulating processes in deep-sea environments. Interestingly, despite the local internal-tidal diurnal mixed with a dominant semi diurnal regime of currents, visual counts fluctuations of most abundant macro- and megafauna (as a proxy of population rhythms; [Aguzzi et al. 2010](#)) followed a day-night like patterning. No information on the light intensity at slope depths exists for this area. Notwithstanding, our behavioral data indicate that light temporal axis, together with a weak, but not negligible, diurnal tidal cycle, may still indirectly exert a role in regulating slope benthic communities' temporal turnover based on species rhythmic behavior in the dark deep-sea environment.

Currents FFT analysis shows peaks with periods of 24, 12 and 6 hours (shown in [Appendix L](#)) and, coherently, the correspondent integrated displacements along the E-W axis in each semi-period are: 440, 940, and 140 m, respectively. These lengths may be considered as the average distances reached by each cyclic movement.

The presence of that diurnal tidal cycle, even if not dominant, may explain, together with a still possible day-night effect, the evidence of the 24 hrs. based local community turnover in most video-abundant species (i.e. *Simenchelys parasiticus*, *Macrocheira kaempferi*, and *Pterothrissus gissu*), despite their progressive trends in overall detection over the 72-days monitoring period (see [Appendix H](#)), in agreement with successional stages at whale scavenging sites ([Smith and Baco 2003](#)).

This alternation of species may be temporally sustained at aphotic deep-sea depths by species undertaking massive displacements along bathymetric gradients involving photic and aphotic strata at their extremes ([Bird and Au 2012](#)). Animals swarming as isolated or into schools within the Benthic Boundary Layer or BBL (nektobenthic mode) or, vertically into the water column (benthopelagic mode) may be rhythmically present in the local BBL despite the overt tidal flows drift ([Aguzzi et al. 2010, 2011](#)). That movement may convey day-night timing information ruling communities' turnover into aphotic benthic zones in an indirect manner, adding another layer of temporal complexity to deep-sea ecosystems ([Aguzzi et al. 2010](#)).

Our observations agree with day-night changes in deep-sea species demersal assemblages at 500 m depth in central Japan, as reported through temporally-scheduled trawling and are consistent with the idea of benthopelagic and nektobenthic displacements ([Suetsugu and Ohta 2005](#)). Specific examples can be given by interpreting our results for some of the species here analyzed, in the light of different rhythmic behavior according to their life traits (i.e., locomotor and/or feeding behaviors see [Appendix G](#)). For example, diel current appears in phase with the walking Japanese spider crab *M. kaempferi* (see [Fig. 28B](#)): its abundance increases when the East-West flux reaches its minimum values ([Appendix M part B](#)) and about 8 hours after the maximum correspondent displacement (i.e. possibly, the time to the odor

plume reaching its maximum spread). Rhythmic flow variations may result in crab presence patterning at the whale corpse, when swarming across different slope depth strata. Animals may perform not yet fully characterized depth-oriented migrations within the BBL horizon. In the case of the swimming fishes *P. gissu*, *S. parasiticus*, and the giant isopod *Bathynomus doederleinii* similar nektobenthic rhythms may also occur, but animals may likely disperse into schools.

Interestingly, internal tides seem to have only a weak effect in ruling the timing of access of most of the demersal species to the carrion site, with only few species showing semidiurnal rhythms (see [Appendix G](#)). Water flow regimes affect the behavior of swimming and walking benthos in deeper middle slope strata (i.e. 1100 m), but not in shallower ones of the Sagami Bay area ([Aguzzi et al. 2010](#)). Other species abundant in still imaging video-surveys of deeper strata of the same area such as zoarcid fishes, did not present any tidal-driven significant periodicity while in deeper slope such a hydrodynamic related pattern is evident. Possibly, this negative result may be provoked by the scarcity of visual detections for this taxonomic group at our study site. The presence of the sole species showing a semidiurnal tidal-driven visual count patterns, the Japanese codling *Physiculus japonicus* (see [Appendix G](#)), may be favored by the hydrodynamic horizontal increase, since, according to the current data analysis, the materials and odors around the body of the whale were transported offshore, towards the bottom direction of the Sagami Bay, moving from the interior part of the Gulf. Coherently the snubnosed eel *Simenchelys parasiticus*, typically living at depths from 500 m to 1800 m, was the most abundant recorded species. Its rhythm appears to occur two hours later with respect to the diel water displacement along the canyon (see [Appendix M](#)), probably following the odor transport from the whale carcass. Consistently one of the greatest explanatory variables of species ordination according to 2D-PLS analysis seemed to be the horizontal component of current velocity.

Olfactory information plays a key role in the life of bottom-living fishes, such as morids or macrourids and a great number of olfactory fibers were generally observed in these species ([Hara 1993, 1994](#)). In this way, they can easily follow the downstream odor plume from the whale fall, according to the southeastward horizontal and downward vertical directions highlighted by current measurements for the bottom layer. Further, this species has a low swimming capability, as other morids ([Bailey et al. 2005](#)) and individuals may use the water flow to enhance the efficiency of a low-energy budget displacement, performed to detect food sources, resulting, in the present case, with the encounter of the whale corpse. Few studies to date relate the behavior *in situ* of marine species according to tidal changes in flow velocity, but fishes can use those cyclic flows to favor low-energy wide-range dispersal ([Sbragaglia et al. 2015](#)).

Mechanisms by which species detect the presence of a scavenging site and reach it are intriguing. In fact, species were rhythmically and not constantly present at the food source. Animal chemoreception could be constrained (being its sensibility enhanced) within specific temporal windows matching biological clock control and consequent behavioral activation. According to our behavioral data

such a gating corresponds to the time windows at which a certain species can accede to the whale carcass. The biological clock-mediated behavioral activation as well as the orientation capability into “chemical-odor panoramas” may represent temporally modulating important elements. Here, we showed that whale presence itself is not sufficient to justify the continuous presence of species at this site, suggesting this capability of access somehow temporally constrained and not continuous, but rhythmic and gated into specific phases over the 24 hrs. Biological clocks control the expression of behavioral rhythms relegating activity within specific temporal windows (Refinetti 2006). Temporal restrictions in behavioral activation by locomotor activation and suppression, generates specific temporal gates for the expression of feeding activities, which in turn conditions all inter- and interspecific relationships (Naylor 2005).

The species succession we observed in this study fully fitted with previous observations (Smith et al. 1998). At a weekly time scale we found a segregation of species occurring in the first phase (weeks 1-6) from the whale deployment from species appearing later (weeks 7-11) with some species being abundant throughout the sampling period, such as *S. parasiticus* and *P. japonicus*. Conversely *M. kaempferi* was one of the dominant species of the first phase, according to its scavenger behavior (Park, 1988, Okamoto 2001). Indeed, during the first phase mostly mobile scavenger species appeared at the whale site (Smith and Baco, 2003). This phase was essentially driven by chemoreception which allows large, active necrophages to track carrion odors into currents (Stockton and DeLaca, 1982). As detailed above, such mechanism is also enhanced by periodical bottom current movements. The second phase (weeks 7-11) was still characterized by scavengers, as the mobile-scavenger stage lasts on average up to 4-5 months (Smith and Baco, 2003), but detritivores also appeared, such as ophiuroids, echinothurioids and the elaspod holothurian *Pannychia moseleyi*. These taxa colonized the organically-enriched sediments surrounding the skeleton. Further, the multivariate correlations of species composition with available environmental variables showed a strong relationship of detritivores to “date”, which agreed with their late appearance at the whale fall.

The occurrence of a temporal lag in significant increases of visual counts for the three trophic groups (scavengers, detritivores, and predators) and the most abundant species (i.e. *S. parasiticus*, *P. gissu*, and finally *M. kaempferi*; see Appendix M), seems to indicate the occurrence of some level of interspecific competition among species, acceding to the site resource. In macrourids, individuals do not remain in the proximity of a bait for long, apparently moving off to feed further afield as the inter- and intraspecific competition at the bait (the whale in this case) increases from later arrivals and the chance of a net energy gain decreases quickly (Bailey et al., 2007). This observation is also in agreement with the temporal character of animal ecological niches. Biological clocks evolved to adapt behavioral activity of animals within the temporal framework of prey and predator interactions (Kronfeld-Schor and Dayan 2003). Temporal partitioning mechanisms in the exploitation of ecosystem resources are usually found when species competing for the same resource avoid entering near each other, to reduce aggressive interactions (Jamieson et al., 2006).

Interestingly, we documented the incursion of larger predatory fauna which actively intervened within the scavenging dynamic. In fact, we identified the presence of *H. griseus*, feeding at the carcass (see [Figure 26H](#)). Noteworthy, the multiple changes in carcass position not associated to increases in bottom vertical velocity component are possibly the result of the feeding activity of other large sharks. Shark feeding incursions could particularly be the cause of carcass position shifts on August 8th, when at a later decomposition stage, when it was much lighter. That feeding action could not be fully evidenced in our time-lapse imaging survey due to its frequency rate, resulting in 2 hrs. blindness intervals between consecutive observations. Interestingly, the movements of the whale were always in correspondence of absolute tidal/pressure minima (see [Figure 27](#)), possibly due to increase feeding activity of *H. griseus* at those periods.

We observed different invertebrate and vertebrate species that can be classified into different trophic guilds in relation and with a different mode of displacement (see [Appendix G](#)). Scavengers were video-sampled along with others species of more active predatory habit, showing how the middle slope community composition is fully represented around the whale carcass. Fall sites are therefore fully representative in terms of sampled fauna, as any other muddy bottom area at an equivalent depth range. Notwithstanding, important differences are reported in the scavenging dynamic comparing the upper vs. the middle slope community. The gastropod *Buccinum yoroianum* played a minimal role in the portrayed scavenging dynamic (being observed only during the first week), while it seems to dominate that process in the local deeper slope ([Aguzzi et al. 2012](#)). Other differences were accounted by behavioral activities of scavengers. Imaging surveys by Fujita and Otha (1990) and Naganuma et al. (1996) at a whale fall site report respectively a detritivore or a scavenging activity for Ophiuroidea. We did observe the presence of only few of these individuals, especially toward the final phase of image sampling, with no evidences of active feeding activity. However, ophiuroids are generalist feeders and they are usually found in dense aggregations at whale falls, with other generalist taxa such as sea urchins and sea cucumbers, which exploit the intense organic enrichment of adjacent sediments associated with whale falls ([Goffredi et al. 2004](#)). Echinoderms are mostly suspension and deposit feeders in the deep sea and probably utilize fresh organic carbon material resulting from the breakdown of a whale carcass ([Lauerman and Kaufmann, 1998](#)).

4.6 Acknowledgements

This project is under collaboration with NHK and Discovery Channel for broadcasting. Special thank is devoted to B. Thorton and A. Bodemann form the Ura L. (University of Tokyo, Japan), which carried out the accurate high-resolution 3-D mapping of the whale deployment site. The authors also wish to thank Dr. F. de Leo (ONC and Univ. Victoria, BC Canada) for the helpful suggestions provided during the preparation of the manuscript.

The general objective of this Thesis was to understand how activity rhythms of benthic species within deep-water and deep-sea communities modulate overall richness and evenness, hence biasing biodiversity measured in our seabed sampling windows, through the use of novel remote, multiparametric and continuous observational multiparametric video-technology, highlighting at the same time, methodological sampling problems associated to the different fixed or mobile character of platforms. My major goal was to scale observed changes in community composition down to the behaviour of individuals which show temporal expression in response to cyclic environmental changes.

In large-scale studies, different locations are usually sampled at different times of the day and/or different days throughout a sampling trawling or ROV cruise (e.g. [Young et al. 1986](#), [Olivar 1990](#), [Sabatés 1990, 1990](#), [Gray, 1993](#)). Consequently, any reported difference among sites or studies may potentially be confounded with species behaviourally time-induced variations (e.g. [Morrisey et al, 1992](#), [Trush et al. 1994](#)). There is particularly scant information in case of deep-water and deep-sea areas, where behavioural rhythms of residing species and their nekto-benthic or benthopelagic mode of displacement are still largely undescribed. This is due to the difficulties of performing direct and long-lasting observations in such extreme and distant locations at frequencies disclosing abundance changes and resulting community dynamics. Nevertheless, a scientific approach considering this time-dependent constrains, is of paramount importance, since the biodiversity we can perceive in our limited sampling windows is directly related upon the movement of populations within a three-dimensional water column-seabed environment ([Aguzzi and Company, et al. 2011](#)). Therefore, the first aim of this Ph.D. thesis was to move a step forward, shedding new light on the regulation that environmental cycles exerts to animals' rhythmic behavior within three iconic deep-water and deep-sea ecosystems: a large canyon, a cold-seep, a temporal hypoxic fjord (as a proxy of a temporal hypoxic deep-sea area) and finally, an ephemeral whale fall site.

In this context, the second specific objective of this Ph.D. dissertation was to provide information about faunal composition, richness, species abundances and evenness, and other valuable ecological information in other to date still unknown species life traits within the abovementioned three deep-water and deep-sea ecosystems.

The difficulties to perform high-frequency and long-lasting studies at those sampling frequencies matching the expression of rhythmic displacements of populations are inherent to the present limitations of marine observational technology. Fortunately, enhanced and novel subsea monitoring platform engineering occurred in the last 30 years, nowadays allowing us to fill gaps of ecological knowledge impossible to achieve in earlier in time. Accordingly, the third specific and last specific objective of this Ph.D. thesis was to establish a methodology to solve operational difficulties in sampling and data analysis due to the peculiar and different fixed and motile nature of the used platforms.

1. Internal and external validity of the thesis

1.1 First objective: time as ruler of deep-sea community changes

To date, the use of chronobiology approaches and data analysis practices only received poor attention in deep-sea ecology. While most of data have been derived by direct trawl sampling, and some with by ROV or AUV technologies, only few of them could achieve a temporally structured sampling. Additionally, only few studies addressed the behavioural activity and admit regulation upon habitat variations (e.g., fishes and internal tides by ROV). In the present work, I applied concepts and data treatment methodologies from the chronobiology field to time series of biological and environmental data acquired with new observational technologies, hence highlighting species abundance variations as a putative product of populational rhythmic displacement in and out from the sampled seabed window.

In Chapters 1 and 4, I used periodogram and waveform analyses to characterize behavioural rhythms in deep-sea twilight zone ranges and determine the influence of different environmental factors. By using these methods, I succeeded in the determination of significant day-night and tidal rhythms of sablefish by cabled video-stations, but I couldn't find any significant rhythm in hagfish and crabs presumably due to the scarcity of their counts. My results were recently confirmed by [Chatzievangelou et al \(2016\)](#) who also found those behavioral rhythms with the use of mobile crawler. Different rhythms were heightened in shallower but still disphotic zones of the Japanese continental margin. Most abundant whale-fall-ecosystem associated macrofaunal species (the snubnosed parasitic eel, *Simenchelys parasiticus*, the Japanese spider crab *Macrocheira kaempferi*, and finally the Japanese gissu *Pterothrissus gissu*) followed a 24-h day-night oriented rhythmicity while only one species, the Japanese codling (*Physiculus japonicus*) followed a semi-diurnal (tidal) rhythmicity (see Chapter 4). Both day-night oriented and tidal rhythms seem to be a widespread phenomenon occurring in the deep-sea waters of all oceans, showing the pervasive character of photic and hydrodynamic cycles in shaping ecosystem functioning in oceans worldwide. Apparently, species performing vertically extensive diel benthopelagic vertical migrations reaching shallower photic strata may convey temporizing information to benthic deep-sea communities into disphotic and aphotic zones when touching the seabed.

Ocean tides are recognized to be one of the main factors controlling intertidal communities ([Connell, 1972](#)) but their temporizing action in deep-sea environments is still very unclear. The determination of tidal rhythms at nearly 1 km depth (Chapter 1) demonstrated how important can be this factor all over the continental margin extensions. Recently, [Lelièvre et al. \(2017\)](#) confirmed the influence of tides at 2 km depth in animal's behavioral rhythms therefore, supporting my results. In addition to ocean tides, wind-generated forcing such as that brought by storms can have a strong influence on bottom-currents ocean dynamics ([Lelièvre et al. 2017](#)) by generating downward-propagating inertial waves and low-frequency currents by pressure fluctuations ([Thomson et al., 1990](#); [D'Asaro et al. 1995](#)).

In contrast, in Chapters 1 and 4, periodogram analysis screening periods within the circa-tidal and day-night range could not find a single species showing a significant periodicity related to the inertial motion cycle. This indicates that inertial-currents might not be an important environmental synchronizer of deep-sea animals since blurred by stronger tidal bulges. In fact, in the Mediterranean where these latter are weak and the former are hence much appreciable in current seed data sets, abyssopelagic species show more often inertial-oriented periodicities. This is the case of bioluminescence time series of data as recorded by the Italian neutrino deep-sea telescope highlighting 20-h periodicity in biogenic light peaking due to the clashing of descending deep-scattering layers of organisms against the infrastructure (Aguzzi et al., 2017 Sci Rept. Km3 NET bioluminescence). Nevertheless, behavioral rhythms of particular deep-sea communities such as hydrothermal vents can substantially disrupted by local hydrodynamics that substantially change local chemical conditions (Lelièvre et al. 2017). In these communities, behavioral rhythms are more influenced by tides and inertial-waves than for day-night cycle, though this seems to be an exception to the general rule.

Three years of monitoring would ensure the discernment of seasonal cycles though, most of the seasonal studies are based on scattered sampling along few years being their results subject to a lack of redundancy. In this sense, our high-frequency studies can partially counteract the lack interannuality. The utility of long-term observatories in the detection of deep-sea reproductive biology such as the detected in the present work (Chapters 2 and 3 reproductive migration of squat lobsters and grooved tanner crab, respectively) is corroborated by other studies such as the one of Fujiwara et al. (2007), that could find short-term and rare synchronized gamete emission by *Calypptogena* spp. thanks to the high-frequency sampling of a long-term *in situ* observatory. Reproductive patterns were also detected for deep-sea fish communities in more physiological studies at seasonal base for other Galatehids in the NW Mediterranean continental margin (Aguzzi et al., 2013) as well as for fishes (Fernandez-Arcaya et al., 2012, 2013) being also some reproductive rhythm phased the upon lunar motion (Mercier et al. 2011).

For all that, the assessment of biological rhythms and the broad ecological monitoring represent a fast-growing motivation in the development of the “cabled observatory science” (*sensu* Favali and Beranzoli 2006, Danovaro et al. 2017). In this framework, present results on biological rhythms represent a small but important fraction of what is needed to generalize the observed temporal dynamics to other deep-sea environments.

As conclusion of this sub-section I determined that the main environmental cycles entraining behavioral rhythms are day-night, tidal and seasonal cycles. Inertial-currents might not be as important as environmental synchronizer for biological rhythms in deep-waters in comparison with the tides. This is true with some exemptions such as hydrothermal vents in which inertial currents can deeply modify the local chemical environment (Lelièvre et al. 2017). The detection of biological rhythms can reveal the existence of deep-sea mesoscale features and their variability. Migrations along the water column in deep-sea areas stress how complex populational rhythms can be thus highlight that the sampling methodologies

that produce too scattered results might have a deep bias. Therefore, long-term in situ observatories represent an ideal tool for seasonal studies permitting an otherwise impossible temporal resolution.

1.2 The Second objective: community composition, dynamics and behavior of species in deep-sea environments

The response of species to environmental changes may directly affect intra- and interspecific relationships, overall diversity and being hence of relevance for the evaluation of important ecosystem services such as fisheries (Danovaro et al. 2017). In Chapter 2, I demonstrated that an Essential Ocean Variable, EOVI (i.e. oxygen) may force the local spatial arrangement of different benthic species exposing them to predating pressure and competition for the substrate. Good evidence of this was seen in the squat lobster *Munida quadrispina* and the slender sole *Lyopsetta exilis*, the number of which (as a proxy of local population density) showed important seasonal modifications according to increasing hypoxia. My results contribute to the understanding of the modulation of substrate use by benthic species in the framework of a global expansion of hypoxia in coastal and ocean areas named as Oxygen Minimum Zones.

Chapter 2 species spatial arrangement was also conditioned by the small-scale seabed morphology, which might also be the reason behind the differences of sablefish counts between POD 3 and 4 (see Chapter 1). In fact, recently Lelièvre et al. (2017) highlighted the importance of local favourable conditions in the small-scale distribution of animals supporting our research results of Chapter 2 supporting my findings.

Also in Chapter 4, I found a temporal lag in diel increases of visual counts for the 3 most abundant species (i.e. the snubnosed eel *Simenichelys parasiticus*, the Japanese spider crab *Macrocheira kaempferi*, and finally the Japanese gissu *Pterothrissus gissu*), which I interpreted as the occurrence of interspecific competition among species acceding to the feeding resource at the study site.

The use of observational technologies allows documenting punctual events impossible to report otherwise. This is the case of the reproductive behavior of the grooved tanner crab videoed for the first time in Chapter 3. In this footage I could observe individuals engaged in a particular moment of their mating, in which a large male holds a smaller female above the ground with its left claw. These technologies can potentially witness also other behavioural activities in relation to interactions among species, as for example in the case of crabs feeding on a clam or the seal feeding on a hagfish at Pod 4 camera in Barkley Canyon (depth: 894 m) in January 2013. This latter event was detected within the framework of the [Digital Fishers](#) citizen science project (Matabos et al. 2017). In relation to that, the other punctual but important observations refer to the activity of large predators as in the case of the six-gill shark (see Chapter 4) heating chunks of a sperm whale carcass. Also in chapter 3, we demonstrated the

existence of monthly fluctuations of abundance, biodiversity and richness of megafauna with the mobile platform Wally I.

As a conclusion of this section, I determined that the factors affecting the spatial but also temporal distribution of deep-sea species and their populations are driven by the competition for the substrate and feeding as key ecological resources within the framework of intra- and interspecific relationships (e.g. reproduction behavior and predation) as well as in response to the variation of environmental key drivers such as the dissolved oxygen. Additionally, increasing our knowledge of animal's behavior within a changing deep-sea environment through the non-invasive monitoring has also socio-economic implications and I determined here that observational technologies represent an appropriate tool to reach this goal. Nevertheless, physical collection is irreplaceable for robust record of species ecological traits requiring the taxonomical determination of the species beyond the resolution capacity of imagery, as required to monitor changes on species level. The novelty of the present ecological research lies in how the information mainstreaming obtained by means of new underwater observational technologies applies in an integrative manner to form an idea of a specific niche within a community for an specific species. An approach that is hardly achievable with laboratory studies.

1.3 Third objective: methodology remarks

Some ecosystems are difficult to study with the traditional physical sampling strategies (e.g. rough bottom ecosystems with demersal trawls or dredges; [Beisiegel 2017](#)). Besides the fact of being intrinsically destructive and disruptive, these tools do not allow a high frequency in sampling repetition for evident technological difficulties and also drive to ulterior misleading samplings outcomes in the case of repetition in a certain area, since this has been previously impacted. Actually, one should assume that, some parts of the ecosystems are also difficult to investigate with the novel observational technologies presented in this Thesis. Notwithstanding, one should bear in mind that for an evident reduction of observed seabed area, a dramatic increase in time coverage can be achieved.

One limitation of the observational technologies proposed here is that the resolution of the used camera will prevent the observation of the entire community. In Chapter 3, I proposed a methodology that will notably reduce this flaw (see "recommendations and future researches" in the Section below). Together with that, it's a fact that the scientific community only sampled a tiny fraction of the deep sea (5%; [Ramirez-Llodra et al. 2010](#)), hence, regardless of the used technology and methodology we are still far from being able to reach a complete description of deep-water and deep-sea ecosystems' structures and dynamics. The continuous discovering of new habitats is far to be completed ([Danovaro et al. 2017](#)), with a number of species being continuously described and leaving accumulation curves unsaturated ([Roberto Danovaro et al. 2010](#)). In this context, the scientific community should not despise the considerable information that can be extracted from the use of observational technologies in terms of

perceived richness and evenness and how these respond upon the environmental modulation, if we formulate the specific questions in a correct manner.

Although multiparametric fixed video-stations may lack of sufficient spatial coverage, their detailed imaging may represent a true advantage. For instance, these may help to understand community dynamics in relation with key changing habitat factors, elucidating new aspects of species ecological niches in continental margins. In Chapter 2, I focussed on small scale seabed surface use in moments of environmental crisis such as transient hypoxia and I could determine that the massive aggregation of squat lobster was not due to shoaling hypoxia forcing an upward migration only with a single small-scale fixed observatory platform and the support of bibliography although in other occasions this species has been reported to migrates due to shoaling hypoxia (Burd and Brinkhurst 1984, Chu and Tunnicliffe, 2015). I highlighted the value of observational technologies in contraposition with other sampling methodologies, such as trawling which, although presenting much larger space coverage (therefore with apparently less limited ecological representativeness), are non-useful to describe phenomena such as massive aggregations for depth oriented migrations of benthic fauna in response to shoaling hypoxia. The species intra- and interspecific competition for space use at small-scale was described during the upward migration thanks to spatially calibrated methods for counting (i.e. with metric bars within a fixed and constant field of view, as deployed by ROV). I also succeeded in describing the dominance hierarchy in the spatial occupancy between two species and in relation to decreasing dissolved oxygen. Such a methodology could be extended to other key habitats in Pacific continental margins (e.g. Oxygen Minimum Zones) and considering other essential ocean variables (EOV; Grimes 2014) for which data on a biodiversity crisis driven by upward benthos migrations are still scant.

In Chapter 1 I stresses how to overcome the limited representational power of ecological data from fixed observational nodes by integrating them into monitoring-coordinated spatial networks. This can be of utility to detect and follow benthopelagic and nektobenthic migrations. Good evidence of this could be find in the phase delay in the 24-h averaged number of counts of sablefish (*Anoplopoma fimbria*) between cameras at different depths along the canyon axis, as a putative product of a nektobenthic migration. Sablefish migrations along the canyon have been corroborated by adding another observing station (i.e. the crawler) in a shallower canyon head position by Chatzievangelou et al. (2016).

Here, I also demonstrated the potential applicability of observational technologies to extract demographic indices for benthic species, by disentangling the population structure of sablefish by using coordinated, video-based, class-sizing of individuals appearing as parallel within the field of view. This methodology potentially has high socio-economic implications if the target species are directly studied that way to improve fishery management. Networks could be implemented by adding moving platforms such as crawlers, conferring an adaptive character to the network geometry itself.

The heterogeneity of physical and chemical conditions may lead to a small-scale spatial distribution of species that is an indicator of animal's physiological tolerance to abiotic factors, resource availability and biotic factors (Lelièvre et al., 2017). Therefore, there is a need of a technology and methodology that is able to achieve enough spatial coverage without rescind from long-term temporal resolution. In Chapter 3, the rover used corresponds to a new generation of semi mobile multiparametric video-platforms (i.e. Internet Operated Vehicles, IOVs) as hydrides in between epibenthic moving ROVs and fully benthic and fixed cabled observatories or landers. IOVs could provide "higher-spatial" (60 m²) coverage compared to observatories, still with at high-temporal resolution (i.e. hourly data by 14 months). One difficulty was related to the lack of automation in crawler nested routines, which obliged the operator to drive it by certain time intervals, hence liming the frequency for data acquisition to central data within each week. In the future, the elimination of the tether (platform recharge and data transference will occur in an inductive fashion) and the automation in driving, will surely increase the spatiotemporal representation power of acquired data. Further, I acquire highly valuable ecological data that endorse this technology and methodology for ecological studies in problematic areas associated with deep sea environments, in this particular case, in a deep-sea and cold seep environment. A detailed explanation of the achieved ecological goal achieved is provided under the sub-section 1.2.

Another technical limitation of the used monitoring technologies is that imaging still requires lighting, which may have an impact on the number of counts (Aguzzi et al. 2015; Doya et al. 2014). I observed a light-biasing effect on sablefish counts in Chapter 1 although globally, both attraction and subsequent retreat seem to occur over a temporal scale of few tens of seconds and hence likely compensate each other, so an overall biasing may be absent in our video samples (i.e. footages lasted 30 s). Additionally, this was a constant input along the study, thus, I assumed that any observed variations in the number of counts would be attributable to external factors and not to an environmental memory (i.e. blurred by the 30 min time-lapse acquisition procedure implying light on only at moment of filming). In any case, lighting on did not disrupt the occurrence of populational rhythms as we could appreciate in all the Chapters of this Thesis, being able to detect several behavioral temporal patterns (see sub-section 2.3.). In Chapter 3, we noticed a similar behavior of sablefish with the rover, thus we limited the light contamination by switching off the lights when the rover was not moving and performed similar lighting effect analysis of those performed in Chapter 1 (data not shown).

An important methodological limitation was related with the scarcity of animals within the field of view which could limiting the quality of time series for the disclosure of behavioral rhythms. When counts for a species were scant, behavioral rhythms analysis could be anyway performed by joining counts into larger time-spans (i.e. averaging or summing) per day. Since each species has its own behavioural rhythm, it is difficult to determine a minimum number of counts needed to ensure a successful analysis with periodogram and waveform. Anyway, some species concentrate their counts in a certain phase of the day, being the time-series analysis efficient in discriminating "squared" datasets with

clear peaks from troughs. Nevertheless, the data processing using in a combined fashion different methodologies inspired from chronobiology (see chapter 1) can make hint on activity rhythms, when there is a scarce number of counts for a species. It was the case of the undetermined crabs (see chapter 1), with which the waveform analysis could detect a nocturnal activity that was not detected in the periodogram analysis virtually due to their reduced counts.

A problem of small scale imaging analyses is the distortion of the field of view depth due to the angle of cameras which is oblique (around 45°). I focussed on that aspect in Chapter 2. I solved the perspective issue by creating a digital grid from a real grid temporarily placed on site and obtaining a correction factor for the vertical component since in this particular case, the horizontal component of the image was considered minimal. This methodology is appropriate as long as the camera either doesn't change its orientation or perform a predefined path.

Finally, another factor that could be affecting the accuracy in counts was transient turbidity. I solved that in two ways, either increasing the number of sampled images in a first screening of the images (in the case of Chapter 2) or eliminating fractions of the videoed samples (like in Chapter 3).

As a conclusion of the aforementioned sub-section (1) with minimal habitat disturbance imagery provides valuable cost-efficient assessment of general ecosystem functioning at large temporal scales (2) observational technologies improve their spatial resolution by an appropriate coordination with each other into a network and (3) despite poor taxonomic resolution of image-derived data the sampling methodology is sufficient to infer aunal composition, richness, species abundances and evenness, and other valuable ecological information of mobile megafauna (although there are no captured specimens concomitantly, comparisons with guides and previous sampling surveys can be done). In this sense, present findings represent a step forward to settle and systematize an adequate methodology to monitor biological rhythms in the deep sea highlighting the problems and advantages of such methodologies to solve how important is to consider temporal dependent universal phenomena in marine ecosystem. Finally, automatization of data processing using the methodology inspired by chronobiology here exposed (i.e. periodogram, waveform and phase integrated chart analyses...) is of relevance for the real-time and continuous monitoring of deep-sea diel and seasonal dynamics.

2. Recommendations and future researches

Although it would be desirable to perform behavioral, physiologic, and chronobiologic studies in laboratory conditions, the reality is that is not possible to maintain in captivity most of marine species. In addition, laboratory studies are reductionist and lacking of a functional vision, with very few testing rhythms responses with few environmental conditions. Also in the case of modelling only certain conditions are tested, though in essence, animals are not found in laboratories or in mathematical approximations but in the field which is a much complex scenario. Big ecological data approach with the

use of new transversal subsea observatories will not replace other disciplines and methodologies used nowadays but will be an important complement to later deepen our knowledge with more focused laboratory approaches.

Taking into account the enormous benefices of observational technologies mentioned in the present work, and the difficulties of getting permanent funding for the stablishing long-standing monitoring programs, I adhere to the discovery and monitoring strategy protocol proposed by [Juniper and Tunnicliffe \(1997\)](#) made by consecutive phases: determining the composition and richness of the system, determining its communities structure and finally the dynamics of the system. In that sense, I would add that being marine ecological monitoring a matter of economic resources, the selection of surveyed ecosystems must be carefully agreed with relevant end-users such as the industry, which will provide those deployment and technological assets allowing scientists to extend their observation capability from the continental margins to the abyssal plains ([Danovaro et al. 2017](#)). In order to pursue this approach, testing of methodologies and technologies is needed and results must be shared in an inverse pyramid from research centres and universities to national and international organizations that will envisage the creation of protocols for environmental evaluation of impact, supervising their application at the development on maritime activities.

The major impediment for that is the high economic effort to be done in the construction and maintenance of observational technologies. Nowadays, fishing, mining, oil and gas industries are the main source of income for this purpose being ecological research considered as subservient to overall economic interest. Besides these difficulties, we are facing highly performant technology not only concerning the purely scientific and industry interests but also a virtually endless source of didactic and citizen awareness. In this context, an aware society (1) puts pressure on industry and governments to prevent the indiscriminate exploitation of marine services (2) is much more prone to invest in research and conservation purpose than an unconscious population.

Because of that, and ideally considering the independence of research from particular economic interest as a priority of general interest, future researches would need to concomitantly achieve scientific goals and promote the general public's awareness. A prove of the remarkable power "power of the image" can be seen in the use of images of Chapter 4, the imaging material of which has been obtained for a Discovery Channel science documentary. Additionally, this same whale has been monitored using 3D technology to perform high-spatial resolution, long term ecological studies. My recommendation is to use this kind of images for virtual reality combined with long-term time-lapses in science disclosure within the context of an increasing naturalization of technologies in our societies.

Regarding the scientific goals for future research, main efforts must be directed towards solving the problems of photic contamination at filming and spatial underrepresentation, depending from used observational technologies. The researcher must pay special attention to each species reaction to different

platforms and a previous test must be done before further deployments and network expansions are undertaken, in order to ensure that lighting and platform structures themselves do not affect species behaviour and hence counts. Further, future research must include an optoacoustic approach (species monitoring with acoustic cameras, hydrophones) in order to reduce the impact of lights.

Networks of fixed cabled observatories combined with stepping-stone movable landers and highly displaceable crawls endowed with combined video and acoustic imaging technologies would be then a key element to obtain reliable biological indicators for species and their ecosystems. Animals' abundance could be derived over larger and ecologically more meaningful spatial scale, being faunal composition, richness, species abundances and evenness results compared with those proceeding from other sources, e.g. historic data from ROV imaging as well as from nearby trawl commercial data. Long-standing monitoring programs may provide unique opportunities to investigate changes of impacts that physical processes have on estimates of population abundances and structure (e.g. class-size and sex ratio). Such an understanding may prove to be essential if researchers pretend to effectively couple biophysical models to elucidate future or past scenarios of sufficient accuracy and precision to infer the impacts of environmental changes on sea populations (Hanna 2007, Miller 2007, Pepin and Helbig 2012).

In order to improve spatial resolution of new technological applications such as the rover of Chapter 3, research is already envisaging the docking of AUVs and pelagic gliders which would be then autonomously operating *in situ* with no (or very limited) need of vessel assistance (Bellingham et al. 2016). The main axes for that future development would be autonomy (with a pre-programmed mission) in rover mobility and docking, as well as the development/addition of more utility parts. Depending on the substrate and specific habitat characteristics, a combined user-based and autonomous approach might be needed in order to minimize the disturbance on the epi- and endobenthic community. Regarding utilities, the addition of a robotic manipulator/arm could be discussed depending on the requirements of the project. In Chapter 3 I recommend to alternate closer views with general views together with moving cameras such as those of Wally I in order to maximize the detection of small benthic and also benthopelagic animals. Finally, in the particular case of behavioral rhythms, future research should address the question of why some animals did not seem to have any apparent rhythmic behavior.

-
- The factors affecting the spatial but also temporal distribution of deep-sea species and their populations are driven by the competition for the substrate and feeding as key ecological resources within the framework of intra- and interspecific relationships (e.g. reproduction behavior and predation) as well as in response to the variation of environmental key drivers such as the dissolved oxygen.
 - Increasing our knowledge of animal's behavior within a changing deep-sea environment through the non-invasive monitoring has also socio-economic implications. In this context, observational technologies represent an appropriate tool to reach this goal. Nevertheless physical collection is irreplaceable for robust record of species ecological traits requiring the taxonomical determination of the species beyond the resolution capacity of imagery, as required to monitor changes on species level.
 - Information mainstreaming obtained by means of new underwater observational technologies applies in an integrative manner to form an idea of a specific niche within a community for a specific species in the context of a community being this approach not achievable with laboratory studies.
 - With minimal habitat disturbance imagery provides valuable cost-efficient assessment of general ecosystem functioning at large temporal scales
 - Observational technologies improve their spatial resolution by an appropriate coordination with each other into a network
 - Despite poor taxonomic resolution of image-derived data the sampling methodology is sufficient to infer faunal composition, richness, species abundances and evenness of mobile megafauna (although there are no captured specimens concomitantly, comparisons with guides and previous sampling surveys can be done).
 - Data processing using the methodology inspired by chronobiology such as periodogram, waveform and phase integrated chart analysis of relevance for the real-time and continuous monitoring of deep-sea diel and seasonal dynamics.

- The main environmental cycles entraining behavioral rhythms are day-night, tidal and seasonal cycles. In comparison, inertial-currents might not be as important as environmental synchronizer for biological rhythms in deep-waters.
- The detection of biological rhythms can reveal the existence of deep-sea mesoscale features and their variability. Migrations along the water column in deep-sea areas stress how complex populational rhythms can be thus highlight that the sampling methodologies that produce too scattered results might have a deep biased. Therefore, long-term in situ observatories represent an ideal tool for seasonal studies permitting an otherwise impossible temporal resolution.

References

- Adams, D.K., D.J. Mc.Gillicuddy, L. Zamudio, A.M. Thurnherr, X. Liang, O. Rouxel, C. German, and L.S. Mullineaux. 2011. Surface-generated mesoscale eddies transport deep-sea products from hydrothermal vents. *Science*. **332**: 580-583.
- Adlerstein, S., and S. Ehrlic. 2003. Patterns in diel variation of cod catches in North Sea bottom trawl surveys. *Fish. Res.* **63**: 169-178.
- Aguzzi, J., Company, J.B. Sardà F. 2004. The feeding activity rhythm of *Nephrops norvegicus*(L.) of the western Mediterranean shelf and slope grounds. *Marine Biology*, **144**: 463-472.
- Aguzzi, J., N.M. Bulloc, and G. Tosini, 2006. Spontaneous internal desynchronization of locomotor activity and body temperature rhythms from plasma melatonin rhythm in rats exposed to constant dim light. *J. Circadian. Rhythms* **4** 6.
- Aguzzi, J., J.B. Company and J.A. García. 2008a. Ontogenetic and gender modulated behavioural rhythms in the deep water Decapods *Liocarcinus depurator* (Brachyura: Portunidae), *Munida tenuimana* and *M. intermedia* (Anomura: Galatheidae). *Mar. Ecol.* **30**: 93–105.
- Aguzzi, J., and F. Sardà, 2008b. A history of recent advancements on *Nephrops norvegicus* behavioral and physiological rhythms. *Rev. Fish Biol. Fish.* **18**: 235–248.
- Aguzzi, J., J. B. Company, P. Abelló, and J.A. García. 2008c. Rhythmic diel movements of some Pandalid shrimps (Decapoda: Caridea) in the Western Mediterranean continental shelf and upper slope. *J. Zool.* **273**: 340–349.
- Aguzzi, J., J.B. Company and J.A. García. 2009. Ontogenetic and gender-modulated behavioural rhythms in the deep-water decapods *Liocarcinus depurator* (Brachyura: Portunidae), *Munida tenuimana* and *Munida intermedia* (Anomura: Galatheidae). *Mar Ecol.*; **30**:93-105.
- Aguzzi, J., P. Puig, and J. B. Company. 2009. Hydrodynamic, Non-Photic Modulation of Biorhythms in the Norway Lobster, *Nephrops Norvegicus* (L.). *Deep-Sea Research Part I: Oceanographic Research Papers* **56**:366–73. doi:10.1016/j.dsr.2008.10.001.
- Aguzzi, J, and J.B. Company. 2010. Chronobiology of Deep-Water Decapod Crustaceans on Continental Margins. *Advances in Marine Biology* **58**. Elsevier Ltd.: 155–225. doi:10.1016/B978-0-12-381015-1.00003-4.
- Aguzzi, J., C. Costa, Y. Furushima, J. J. Chiesa, J. B. Company, P. Menesatti, R. Iwase, and Y. Fujiwara. 2010. Behavioral rhythms of hydrocarbon seep fauna in relation to internal tides. *Marine Ecology Progress Series*, **418**, 47-50.

- Aguzzi, J., Company J.B., Costa C., Menesatti P., Garcia J.A., Bahamon N., Puig P., Sardà F. 2011. Activity rhythms in the deep-sea: a chronobiological approach. *Frontiers in Bioscience-Landmark* **16**:131-150
- Aguzzi, J., C. Costa, K. Robert, M. Matabos, F. Antonucci, S. Kim Juniper, and P. Menesatti. 2011. Automated Image Analysis for the Detection of Benthic Crustaceans and Bacterial Mat Coverage Using the VENUS Undersea Cabled Network. *Sensors* **11** 10534–56. doi:10.3390/s111110534.
- Aguzzi, J., J.B. Company, C. Costa., M. Matabos, E. Azzurro, A. Mànuel, P. Menesatti, F. Sardà., M. Canals, E. Delory., D. Cline, P. Favali, S.K. Juniper, Y. Furushima., Y. Fujiwara., J.J. Chiesa., L. Marotta., and I.M. Priede. 2012a. Challenges to assessment of benthic populations and biodiversity as a result of rhythmic behaviour: video solutions from cabled observatories. *Oceanography and Marine Biology: An Annual Review (OMBAR)* **50**: 235-286.
- Aguzzi, J., A. J. Jamieson, T. Fujii, V. Sbragaglia, C. Costa, P. Menesatti, and Y. Fujiwara. 2012. Shifting Feeding Behaviour of Deep-Sea Buccinid Gastropods at Natural and Simulated Food Falls. *Marine Ecology Progress Series***458**:247–53. doi:10.3354/meps09758.
- Aguzzi, J., J.B. Company, N. Bahamon, M.M. Flexas, S. Tecchio, U. Fernandez-Arcaya, J.A. García, A. Mechó, and S. Koenig, 2013. Canals M. Seasonal bathymetric migrations of deep-sea fishes and decapod crustaceans in the NW Mediterranean Sea. *Prog Oceanogr.***18**: 210-221.
- Aguzzi, J., V. Sbragaglia, G. Santamaría, J. del Río, F. Sardà, M. Noguerras, and A. Manuel, 2013a. Daily activity rhythms in temperate coastal fishes: insights from cabled observatory video monitoring. *Mar. Ecol. Prog. Ser.* **486**: 223–236.
- Aguzzi, J., C. Costa, V. Ketmaier, C. Angelini, , F. Antonucci., P. Menesatti, and J.B. Company, 2013b. Light-dependent genetic and phenotypic differences in the squat lobster *Munida tenuimana* (Crustacea: Decapoda) along deep continental margins. *Prog.Oceanogr.* **118**: 199–209
- Aguzzi, J., C. Doya, S. Tecchio, F.C. De Leo, E. Azzurro, C. Costa, et al. 2015a. Coastal observatories for monitoring of fish behaviour and their responses to environmental changes. *Rev Fish Biol Fisher.***25**: 463-483.
- Aguzzi, J., V. Sbragaglia, S. Tecchio, J. Navarro, J.B. 2015b. Company.Rhythmic behaviour of marine benthopelagic species and the synchronous dynamics of benthic communities. *Deep-Sea Res I.***95**:1-11.
- Allen, S.E., and B.M.Hickey.2010. Dynamics of advection-driven upwelling over a shelf break submarine canyon. *J Geophys Res.***115**: C08018.

- Aiken, C.M., and S.A. Navarrete, 2014. Coexistence of competitors in marine metacommunities: environmental variability, edge effects, and the dispersal niche. *Ecology* **95**: 2289–2302.
- Anderson, J. J., and A.H. Devol, 1973. Deep water renewal in Saanich Inlet, an intermittently anoxic basin. *Estuar. Coast. Mar. Sci.* **1**, 1–10.
- Antonsen, B.L., Paul, D.H., 1997. Serotonin and octopamine elicit stereotypical agonistic behaviors in the squat lobster *Munida quadrispina* (Anomura, Galatheidae). *J. Comp. Physiol.* **181**: 501–510.
- Andersen, V., and J. Sardou, 1992. The diel migrations and the vertical distributions of zooplankton and micronekton in the Northwestern Mediterranean Sea. 1. Euphausiids, mysids decapods and fishes. *J. Plankton Res.* **14**: 1129–1154.
- Anderson, M.E. 2005. Food habits of some deep-sea fish off South Africa's west coast. 2. Eels and spiny eels (Anguilliformes and Notacanthiformes). *African Journal of Marine Science*, **27**:557-566.
- Andrews, K.S., D.W. Greg, F. Debbie, N. Tolimieri., C.J. Harvey., G. Bergman, and P.S. Levin. 2009. Diel activity patterns of six-gill sharks, *Hexanchus griseus*: The ups and downs of an apex predator. *Anim. Behav.* **78**:525–536
- Armstrong, C.W., N.S. Foley, R. Tinch, S. van den Hove. 2012. Services from the deep: Steps towards valuation of deep sea goods and services. *Ecosyst Serv.* **2**: 2-13.
- Assis, J., B. A. Claro, J. Ramos, J. Boavida, and E. A. Serrão. 2013. Performing Fish Counts with a Wide-Angle Camera, a Promising Approach Reducing Divers' Limitations." *Journal of Experimental Marine Biology and Ecology* **445**: 93–98. doi:<http://dx.doi.org/10.1016/j.jembe.2013.04.007>.
- Audrey, M.M., G.P. Dunster, V. Sbragaglia, and J. Aguzzi, H.O. de la Iglesia. 2016. Influence of temperature on circadian locomotor activity in the crab *Uca pugilator*. *PloS ONE*.e0175403.
- Babanin, A. V., A., Ganopolski, W. R., Phillips, 2009. Wave-induced upper-ocean mixing in a climate model of intermediate complexity. *Ocean Modelling*, **29**:189-197.
- Baco, A. R., C. R. Smith, A. S. Peek, G. K. Roderick, and Vrijenhoek, R. C. 1999. The phylogenetic relationships of whale-fall vesicomyid clams based on mitochondrial COI DNA sequences. *Marine Ecology. Progress Series*, **182**:137–147.
- Bahamon, N. A., Z. Cruzado, R. Velasquez, D. Bernardello, Donis, Keywords Time Series, and Wind Font. 2010. Patterns of phytoplankton chlorophyll variability in the mediterranean and black seas 1 Centre D 'Estudis Avançats de Blanes (CSIC) - Bahamon@ceab.csic.es 2 Oceans Catalonia International SL Abstract Time Series Decomposition of Remote Sensing Observat. 2010.

- Baillon, S., J.F. Hamel, V.E. Wareham, and A. Mercier. 2012. Deep cold-water corals as nurseries for fish larvae. *Front Ecol Env.* **10**: 351-356.
- Balanov A.A., M. Moku., K. Kawaguchi., and G. Shinohara. 2009. Fish collected by commercial size midwater trawls from the Pacific Coast off Northern Japan. *Nat. Mus. Nature Sci. Monogr.* **39**: 655-681.
- Bale, A.D., D. Whitmore, and D. Moran., 2016. Life in a dark biosphere: a review of circadian physiology in “arrhythmic” environments. *J. Comp. Physiol. B.* In Press.
- Båmstedt, U., and M.B. Martinussen. 2015. Ecology and behavior of *Bolinopsis infundibulum* (Ctenophora; Lobata) in the Northeast Atlantic. *Hydrobiol.* **759**: 3-14.
- Barnes, C.R., and V. Tunnicliffe. 2008. Building the world's first multi-node cabled ocean observatories (NEPTUNE-Canada and VENUS, Canada): science, realities, challenges and opportunities. *OCEANS 2008 — MTS/IEEE Kobe Techno-Ocean* 1–8.
- Barnes, C.R., M.M.R. Best., L. Paudet., and B. Pirenne., 2011. Understanding Earth–ocean processes using real-time data from NEPTUNE Canada's widely distributed sensor networks, north-east Pacific. *Geosci. Can.* **38**:21–30.
- Barnes, C. R., M. M., Best, F. R., Johnson, L. Pautet, B. Pirenne. 2013. Challenges, benefits, and opportunities in installing and operating cabled ocean observatories: Perspectives from NEPTUNE Canada. *IEEE Journal of Oceanic Engineering*, **38**: 144-157.
- Barnes C.R., M.M.R. Best, F.R. Johnson, and B. Pirenne. 2015. NEPTUNE Canada: Installation and initial operation of the world’s first regional cabled ocean observatory. *Seafloor observatories in four dimensions*. In: *Seafloor Observatories*. Springer Berlin Heidelberg., 415-438.
- Beamish, F.W.H., 1966. Vertical migration by demersal fish in the Northwest Atlantic. *J. Fish. Res. Board Can.* **23**:109–139.
- Beamish, R.J., and G.A. McFarlane, 1988. Resident and dispersal behavior of adult sablefish (*Anoplopoma fimbria*) in the slope waters off Canada's west coast. *Can. J. Fish. Aquat. Sci.* **45**:152–164.
- Beauxis-aussalet, E., S. Palazzo, L. Hardman, and Elvira Arslanova. 2013. A Video Processing and Data Retrieval Framework for Fish Population Monitoring Categories and Subject Descriptors. In: *Proceedings of the 2nd ACM International Workshop on Multimedia Analysis for Ecological Data*, 15–20. Barcelona: ACM Publications. doi:10.1145/2509896.2509906.
- Belley.R., P.V. Snelgrove, P. Archambault, and S.K. Juniper. 2016. Environmental drivers of benthic flux variation and ecosystem functioning in Salish Sea and Northeast Pacific sediments. *PloS One.*; **11**: e0151110.

- Benedetti-Cecchi, L. 2001. Variability in abundance of algae and invertebrates at different spatial scales on rocky sea shores. *Mar. Ecol. Prog. Ser.* **215**: 79–92.
- Benoit-Bird, K. J., and W. W. Au. 2006. Extreme diel horizontal migrations by a tropical nearshore resident micronekton community. *Marine Ecology Progress Series* **319**:1-14.
- Bergstad, A.O., A.D. Wik, O.Hildre, 2003. Predator–prey relationships and food source of the Skagerrak deep-water fish assemblage. *J. Northwest Atl. Fish. Sci.* **31**, 165–180.
- Bertrand, J., L. Gil de Sola, C. Papaconstantinou, G. Relini, and A. Souplet. 1997. An International Bottom Trawl Survey in the Mediterranean: The MEDITS Programme. In ICES Annual Science Conference, 76–96. 1997 ICES Annual Science Conference. http://www.sibm.it/MEDITS_2011/Medits_history.htm
- Bertrand, J., L., Gil de Sola, P., Papacostantinou, G., Relini, A., Souplet. 2002. The general specifications of the MEDITS survey. *Sci. Mar.* **66**: 9–17.
- Best, M., P. Favali, L. Beranzoli, M. Cannat, N. Cagatay, J. J. Dañobeitia, E. Delory, H. de Stigter, B. Ferré, M. Gillooly, F. Grant, P.O.J. Hall, V. Lykousis, J. Mienert, J.M.A. de Miranda, G. Oaie, V. Radulescu, J.-F. Rolin, H. Ruhl, and C. Waldmann. 2014. EMSO: A distributed infrastructure for addressing geohazards and global ocean change. *Oceanography* **27**:167–169.
- Blanchard, A.L., and H.M. Heder, 2014. Interactions of habitat complexity and environmental characteristics with macrobenthic community structure at multiple spatial scales in the northeastern Chukchi Sea. *Deep Sea Res. II* **102**: 132–143.
- Board, O. S. 2000. Illuminating the hidden planet: the future of seafloor observatory science. National Academies Press.
- Bookstein, FL, P. Gunz, and H. Ingeborg. 2003. Cranial integration in Homo: Singular warps analysis of the midsagittal plane in ontogeny and evolution. *J Hum Evol* **44**:167–187.
- Bozzano, A., F. Sardà, J. Ríos, 2005. Vertical distribution and feeding patterns of the juvenile European hake, *Merluccius merluccius* in the NW Mediterranean. *Fish. Res.* **73**, 29–36.
- Breitburg, D., 2002. Effects of hypoxia, and the balance between hypoxia and enrichment, on coastal fishes and fisheries. *Estuaries* **25**, 767–781.
- Brickley, P.J., and A.C. Thomas. 2004. Satellite-measured seasonal and inter-annual chlorophyll variability in the Northeast Pacific and Coastal Gulf of Alaska. *Deep Sea Research Part II: Topical Studies in Oceanography.* **51**, 229-245.
- Brown, J.L., and G.H. Orians, 1970. Spacing patterns immobile animals. *Annu. Rev. Ecol. Syst.* **1**, 239–262.

- Burd, B.J., 1985. Respiration of a low oxygen tolerant galatheid crab, *Munida quadrispina* (Benedict, 1902). *Can. J. Zool.* **63**, 2538–2542.
- Burd, B.J., R.O. Brinkhurst, 1984. The distribution of the galatheid crab *Munida quadrispina* (Benedict 1902) in relation to oxygen concentrations in British Columbia fjords. *J. Exp. Mar. Biol. Ecol.* **81**, 1–20.
- Ceramicola, S., T. Amaro, D. Amblas, N. Çağatay, S. Carniel, F.L. Chiocci. 2015. Submarine canyon dynamics - Executive Summary. In: CIESM Monograph 47 (Briand F. Ed.) Submarine canyon dynamics in the Mediterranean and tributary seas: An integrated geological, oceanographic and biological perspective. 7-20.
- Chatzievangelou, D., C. Doya, L. Thomsen, A. Purser, and J. Aguzzi. 2016. High-frequency patterns in the abundance of benthic species near a cold-seep: An Internet Operated Vehicle application.. *PloS One*.11; e0163808.
- Chabanet, P., N. Loiseau, J. L. Join, and D. Ponton. 2012. “VideoSolo, an Autonomous Video System for High-Frequency Monitoring of Aquatic Biota, Applied to Coral Reef Fishes in the Glorioso Islands (SWIO).” *Journal of Experimental Marine Biology and Ecology***430–431**: 10–16. doi:10.1016/j.jembe.2012.06.024.
- Chiesa, J.J., J. Aguzzi, J.A. García, and F Sardà de la Iglesia, H., 2010. Light intensity determines temporal niche switching of behavioral activity in deep water *Nephrops norvegicus* (Crustacea: Decapoda). *J. Biol. Rhythms* **25**, 277–287.
- Childress, J.J., and P.R. Girguis. 2011. The metabolic demands of endosymbiotic chemoautotrophic metabolism on host physiological capacities. *J Exp Biol.*; **214**: 321-325.
- Cnudde, C., T. Moens, and A. Willems, De Troch, M., 2013. Substrate-dependent bacterivory by intertidal benthic copepods. *Mar. Biol.* **160**: 327–341.
- Cohen, D.M., T. Inada, T. Iwamoto and N. Scialabba, 1990. FAO species catalogue. Vol. 10. Gadiform fishes of the world (Order Gadiformes). An annotated and illustrated catalogue of cods, hakes, grenadiers and other gadiform fishes known to date FAO Fish.Synop. **125**. Rome: FAO. 442.
- Chu, Jackson W F, and V. Tunnicliffe. 2015. “Oxygen Limitations on Marine Animal Distributions and the Collapse of Epibenthic Community Structure during Shoaling Hypoxia.” *Global Change Biology***21** (8): 2989–3004. doi:10.1111/gcb.12898.
- Condal, F., J., Aguzzi, F., Sarda, M., Nogueras, J., Cadena, C., Costa, A., Manuel. 2012. Seasonal rhythm in a Mediterranean coastal fish community as monitored by a cabled observatory. *Marine biology*, **159**:2809-2817.

- Corgos, A., N. Sánchez, and J. Freire, , 2010. Dynamics of the small-scale spatial structure of the population of the spider crab *Maja brachydactyla* (Decapoda: Majidae). *J. Shellfish Res.* **29**, 25–36.
- Costa, C., M. Scardi, V. Vitalini, and S. Cataudella. 2009. A Dual Camera System for Counting and Sizing Northern Bluefin Tuna (*Thunnus Thynnus*; Linnaeus, 1758) Stock, during Transfer to Aquaculture Cages, with a Semi Automatic Artificial Neural Network Tool. *Aquaculture***291**(3–4). Elsevier B.V.: 161–67. doi:10.1016/j.aquaculture.2009.02.013.
- Costa C., F., Antonucci, F., Pallottino, J., Aguzzi, D. W., Sun, P., Menesatti. 2011. Shape analysis of agricultural products: a review of recent research advances and potential application to computer vision. *Food Bioproc. Technol.* **4**:673-692.
- Costa, C., F. Antonucci, C. Boglione, P. Menesatti, M. Vandeputte, and B. Chatain. 2013. Automated sorting for size, sex and skeletal anomalies of cultured seabass using external shape analysis. *Aquacultural Engineering* **52**:58-64.
- Cuvelier, D., P. Legendre, A. Laes, P.M. Sarradin, and J. Sarrazin, 2014. Rhythms and community dynamics of a hydrothermal tubeworm assemblage at Main Endeavour Field – A multidisciplinary deep-sea observatory approach. *PLoS ONE* 9, e96924.
- Cummings, S.M., and E. Morgan, 2001. Time-keeping system of the eelpout, *Zoarces viviparus*. *Chronobiol. Int.* **18**, 27–46.
- Craig, J.K., and L.B. Crowder, 2005. Hypoxia-induced habitat shifts and energetic consequences in Atlantic croaker and brown shrimp on the Gulf of Mexico shelf. *Mar. Ecol. Prog. Ser.* **294**, 79–94.
- Daan, S., and J. Aschoff. 2001. The Entrainment of Circadian Systems. *Circadian Clocks*. doi:10.1007/978-1-4615-1201-1_2.
- Csepp, D.J., J.J. Vollenweider, and M.F. Sigler. 2011. Seasonal abundance and distribution of pelagic and demersal fishes in southeastern Alaska. *Fisheries research.* **108**, 307-320.
- Danovaro, R., J. B. Company, C. Corinaldesi, G. D’Onghia, B. Galil, C. Gambi, A. J. Gooday, et al. 2010. Deep-Sea Biodiversity in the Mediterranean Sea: The Known, the Unknown, and the Unknowable. *PLoS ONE* 5 (8). doi:10.1371/journal.pone.0011832.
- Danovaro, R., P. V Snelgrove and P. Tyler. 2014. Challenging the paradigms of deep-sea ecology. *Trends in ecology & evolution*, **29**: 465-475.
- Danovaro, R., J. Aguzzi, E. Fanelli, D. Billett, K. Gjerde, A. Jamieson, E. Ramirez-Llodra, et al. 2017. An Ecosystem-Based Deep-Ocean Strategy. *Science***355** (6324): 452–54. doi:10.1126/science.aah7178.

- Darnis, G. L., Fortier. 2014. Temperature, food and the seasonal vertical migration of key arctic copepods in the thermally stratified Amundsen Gulf (Beaufort Sea, Arctic Ocean). *J Plank Res.* **36**: 1092-1108.
- D'Asaro, E. A. 2014. Turbulence in the upper-ocean mixed layer. *Annual review of marine science*, **6**: 101-115.
- Davies, S., A. Griffiths, and T. Reimchen, 2006. Pacific hagfish, *Eptatretus stoutii*, Spotted Ratfish, *Hydrolagus colliei*, and scavenger activity on tethered carrion in subtidal benthic communities off Western Vancouver Island. *Can. Field Nat.* **120**, 363–366.
- De Leo, F., C.R. Smith, A.A. Rowden, D.A. Bowden, M.R. Clark. 2010. Submarine canyons: Hotspots of benthic biomass and productivity in the deep sea. *Proc R Soc B.* **277**: 2783-2792.
- De Leo, F.C., J.C. Drazen, E.W. Vetter, A.A. Rowden, and C.R. Smith. 2012. The effects of submarine canyons and the oxygen minimum zone on deep-sea fish assemblages off Hawaii. *Deep Sea Res I*; **64**: 54-70.
- De Leo, F.C., A. Fleury, C.R. Smith, L. A. Levin, and J. Aguzzi. 2016. Early benthic successional processes at implanted substrates in Barkley Submarine Canyon affected by a permanent oxygen minimum zone. AGU Ocean Sciences Meeting, New Orleans, abstract **92**:1-12.
- Del Rio, J., J. Aguzzi, A. Hidalgo, I. Bghieli, A. Manuel, V. Sbragaglia, and F. Sarda. 2013. “Citizen Science and Marine Community Monitoring by Video-Cabled Observatories: The OBSEA Citizen Science Project.” In 2013 IEEE International Underwater Technology Symposium, UT 2013, 1–3. doi:10.1109/UT.2013.6519842.
- Díaz, R.J., and R. Rosenberg, 1995. Marine benthic hypoxia: a review of its ecological effects and the behavioural responses of benthic macrofauna. *Oceanogr. Mar. Biol. Annu. Rev.* **33**, 245–303.
- DFO, 2009. Evaluation of interim harvest strategies for sablefish (*Anoplopoma fimbria*) in British Columbia, Canada for 2008/09.
- Díaz, R.J., and R. Rosenberg, 2008. Spreading dead zones and consequences for marine ecosystems. *Science* **321**, 926–929.
- Dickinson, J. L., B. Zuckerberg, and D. N. Bonter. 2010. “Citizen Science as an Ecological Research Tool: Challenges and Benefits.” *Annual Review of Ecology, Evolution, and Systematics* **41** (1): 149–72. doi:10.1146/annurev-ecolsys-102209-144636.
- Dinning, K.M., and A. Metaxas. 2013. Patterns in the abundance of hyperbenthic zooplankton and colonization of marine benthic invertebrates on the seafloor of Saanich Inlet, a seasonally hypoxic fjord. *Mar. Ecol.* **34**, 2–13.

- Dixon, P.M., 2002. Nearest-neighbor contingency table analysis of spatial segregation for several species. *Ecoscience* **9**, 142–151.
- DFO Can. Sci. Adv. Sec. Sci. Advis. Rep. 2009/060.
- Doya, C., J. Aguzzi, M. Pardo, M. Matabos J.B. Company, C. Costa, S. Milhaly. 2014. Diel behavioral rhythms in the sablefish (*Anoplopoma fimbria*) and other benthic species, as recorded by deep-sea cabled observatories in Barkley canyon (NEPTUNE-Canada). *Journal of Marine Systems* **130**: 69-78
- Doya, C., J. Aguzzi, D. Chatzievangelou, C. Costa, J.B., V. Company Tunnicliffe. 2016. The seasonal use of small-scale space by benthic species in a transiently hypoxic area. *J Mar Syst.* **154**: 280-290.
- Ehrlén, J., and W. F. Morris. 2015. “Predicting Changes in the Distribution and Abundance of Species under Environmental Change.” *Ecology Letters* **18** (3): 303–14. doi:10.1111/ele.12410.
- Eschmeyer, W.N., and E.S. Herald, Hammann, H., 1983. *A Field Guide to Pacific Coast Fishes of North America*. Houghton Mifflin Company, Boston.
- Espinoza-Fuenzalida, N.L., E. Acuña, I.A. Hinojosa, and Thiel, M., 2012. Reproductive biology of two species of squat lobsters—female receptivity and interbrood intervals. *J. Crustac. Biol.* **32**, 565–574.
- Farnsworth, K.D., U.H. Thygesen, S. Ditlevsen, and N.J. King, 2007. How to estimate scavenger fish abundance using baited camera data. *Mar. Ecol. Prog. Ser.* **350**, 223–234.
- Favali, P., and L. Beranzoli. 2006. Seafloor observatory science: A review. *Ann Geoph.* **49**: 2-3.
- Favali, P., R. Person, C. R. Barnes, Y. Kaneda, J. R. Delaney and S. K. Hsu. 2010. Seafloor observatory science. *Proceedings of the OceanObs* **9**, 21-25.
- Favali, P., L. Beranzoli, and A. De Santis. 2015. *Seafloor Observatories: A New Vision of the Earth from the Abyss*. Edited by Paolo Favali, Laura Beranzoli, Angelo De Santis, and Philippe Blondel. *Seafloor Observatories: A New Vision of the Earth from the Abyss*. Springer-Praxis Publishing. doi:10.1007/978-3-642-11374-1.
- Fernholm, B., 1974. Diurnal variation in the behavior of the hagfish *Eptatretus burgeri*. *Mar. Biol.* **27**, 351–356.
- Fernández, M, N., Ruiz-Tagle, S. Cifuentes, H.O. Pörtner, and W. Arntz. 2003. Oxygen-dependent asynchrony of embryonic development in embryo masses of brachyuran crabs. *Marine Biology*. **142**: 559-565.
- Fernandez-Arcaya. U., G. Rotllant, E. Ramirez-Llodra, L. Recasens, J. Aguzzi, M.D.M. Flexas, A. Sanchez-Vidal, P. López-Fernández, J.A. García, and J.B. Company. 2013. Reproductive

- biology and recruitment of the deep-sea fish community from the NW Mediterranean continental margin. *Prog Oceanogr.* **118**: 222-234.
- Francour, P. 1997. Predation on Holothurians: A literature review. *Inv. Biol.* **116**: 52-60.
- Fujita T., D. Kitagawa Y. Okuyama, Y. Ishito, T. Inada, and Y. Jin. 1995. Diets of the demersal fishes on the shelf off Iwate, North Japan. *Mar. Biol.* **123**: 219-233.
- Fujiwara, Y., J. Tsukahara, J., Hashimoto, K., Fujikura. 1998. In situ spawning of a deep-sea vesicomid clam: evidence for an environmental cue. *Deep Sea Research Part I: Oceanographic Research Papers* **45**:1881-1889.
- Fujiwara, Y., J. Tsukahara, J. Hashimoto, and K. Fujikura. 1998. "In Situ Spawning of a Deep-Sea Vesicomid Clam: Evidence for an Environmental Cue." *Deep-Sea Research Part I: Oceanographic Research Papers* **45** (11): 1881–89. doi:10.1016/S0967-0637(98)00033-8.
- Fujiwara, Y., M. Kawato., T. Yamamoto, T. Yamanka., W. Sato-Okoshi, C. Noda, T. Tsuchida, S.S. Cubeli., T. Sasaki, C. Jacobsen, K. Kubokawa., K. Fujikura, T. Maruyama., Y. Furushima., K. H. Okoshi Miyake, M. Miyazaki, Y. Nogi, A. Yatabe, and T. Okutani. 2007. Three-year investigations into sperm whale-fall ecosystems in Japan. *Mar. Ecol.* **28**: 219-232.
- Gage, J.D., 2003. *Ecosystems of the world*, 28. Tyler P. (ed.). Elsevier, Amsterdam.
- Gallo, N.D. and L.A. Levin. 2016. Ecology and Evolution in the World's Oxygen Minimum Zones and Implications of Ocean Deoxygenation. *Adv Mar Biol.* **74**:117-98.
- Garm, A., and J.T.Høeg, 2000. Functional mouthpart morphology of the squat lobster *Munida sarsi*, with comparison to other anomurans. *Mar. Biol.* **137**, 123–138.
- Garrett, C. 2003. Internal tides and ocean mixing. *Science*, **301**:1858-1859.
- Gilbert, D., N.N. Rabalais, R.J. Díaz, and J. Zhang, 2010. Evidence for greater oxygen decline rates in the coastal ocean than in the open ocean. *Biogeosciences* **7**, 2283–2296.
- Giske, J., D.L. Aksens, B. M. Baliño, S. Kaartvedt, U. Lie, J.T. Nordeide, A. Gro Vea Salvanes, S.M. Wakili., and A. Aadnesen, 1990. Vertical distribution and trophic interactions of zooplankton and fish in Masfjorden, Norway. *Sarsia* **75**, 65–81.
- Genin, A. Bio-physical coupling in the formation of zooplankton and fish aggregations over abrupt topographies. *J Mar Syst.* 2004; 50: 3-20.
- Gervais, F., S.K. Juniper, M. Matabos, and A. Spicer. 2012. *Marine Life Field Guide*. First Edition. NEPTUNE-Canada Publications.
- Global Risk Report .2016. <http://reports.weforum.org/global-risks-2016/>

- Glover, A. G., A. J. Gooday, D. M. Bailey, D. S M Billett, P. Chevaldonné, A. Colaço, J. Copley, et al. 2010. "Temporal Change in Deep-Sea Benthic Ecosystems. A Review of the Evidence From Recent Time-Series Studies." *Advances in Marine Biology* **58** (C): 1–95. doi:10.1016/B978-0-12-381015-1.00001-0.
- Grange, Laura J., and Craig R. Smith. 2013. "Megafaunal Communities in Rapidly Warming Fjords along the West Antarctic Peninsula: Hotspots of Abundance and Beta Diversity." *PLoS ONE* **8** (12). doi:10.1371/journal.pone.0077917.
- Grimes, S., 2014. Report on the Essential Ocean Ecosystem Variables and on the Adequacy of Existing Observing System Elements to Monitor Them. First Technical Workshop of the GOOS Biogeochemistry Panel: Defining EOVS for Biogeochemistry 2007 (Australia, Townsville).
- Hammer, Ø., D.A.T. Harper, and P.D. Ryan, 2001. PAST: Paleontological statistics software package for education and data analysis. *Palaeontologia Electronica* **4**(1): 9pp. (Ver. 2.17c)
- Hart, T., 2005. Diel activity patterns in demersal fishes on Heceta Bank, Oregon. Master of Science (M.S.) in Fisheries Science. Oregon State University (Ph.D. Thesis Dissertation).
- Harvey, E. S., J. J. Butler, D. L. McLean, and J. Shand. 2012. Contrasting Habitat Use of Diurnal and Nocturnal Fish Assemblages in Temperate Western Australia. *Journal of Experimental Marine Biology and Ecology* **426–427**. 1-110, Elsevier B.V.: 78–86. doi:10.1016/j.jembe.2012.05.019.
- Harvey, E. S., S. J. Newman, D. L. McLean, M. Cappo, J. J. Meeuwig, and C. L. Skepper. 2012. Comparison of the Relative Efficiencies of Stereo-BRUVs and Traps for Sampling Tropical Continental Shelf Demersal Fishes. *Fisheries Research* **125–126**. Elsevier B.V.: 108–20. doi:10.1016/j.fishres.2012.01.026.
- Haselmair, A., A. Stachowitsch, M. Zuschin, and B. Riedel, 2010. Behaviour and mortality of benthic crustaceans in response to experimentally induced hypoxia and anoxia in situ. *Mar. Ecol. Prog. Ser.* **414**, 195–208. Herlinveaux, R.H., 1962.
- Hays., G. C. 2003. A review of the adaptive significance and ecosystem consequences of zooplankton diel vertical migrations. In: *Migrations and Dispersal of Marine Organisms*. Springer Netherlands. pp. 163-17.
- Helly., J.J., and L.A. 2004. Levin. Global distribution of naturally occurring marine hypoxia on continental margins. *Deep-Sea Res I.* **51**: 1159-1168.
- Herliveaux, R. H., Oceanography of Saanich Inlet in Vancouver Island, British Columbia. *Fish. Res. Board Can.* **19**: 1–37.
- Herring, P. J. 2002. *The Biology of the Deep-Sea*. New York: Oxford University Press.

- Himmelman, J.H., and J.R. Hamel. 1993. Diet, behaviour and reproduction of the whelk *Buccinum undatum* in the northern Gulf of St. Lawrence, eastern Canada. *Mar Biol.* **16**: 423-430.
- Holmes, R.A., and R.N. Gibson. 1983. A comparison of predatory behavior in flatfish. *Anim. Behav.* **31**: 1244-1255.
- Holyoak, M., R. Casagrandi, R. Nathan, E. Revilla, and O. Spiegel. 2008. Trends and Missing Parts in the Study of Movement Ecology. *Proceedings of the National Academy of Sciences* **105** (49): 19060–65. doi:10.1073/pnas.0800483105.
- Infantino, A., G. Aureli, C. Costa, C. Taiti, F. Antonucci, P. Menesatti, F. Pallottino, S. De Felice, M.G. D'Egidio, and S. Mancuso. 2015. Potential application of PTR-TOFMS for the detection of deoxynivalenol DON in durum wheat. *Food control* **57**: 96-104.
- Jamieson, G.S., G. Heritage, and N. Noakes. 1990. Life history characteristics of *Chionoecetes tanneri* off British Columbia. In: *Proceedings of the International Symposium on King and Tanner Crabs*. Alaska Sea Grant College Program, University of Alaska Fairbanks 153-162.
- Jamieson, Alan J., T. Fujii, D. J. Mayor, M. Solan, and I. G. Priede. 2010. Hadal Trenches: The Ecology of the Deepest Places on Earth. *Trends in Ecology and Evolution* **25** (3): 190–97. doi:10.1016/j.tree.2009.09.009.
- Jumars, P.E., D. Thistle, and M.L. Jones, 1977. Detecting two-dimensional spatial structure in biological data. *Oecologia* **28**: 109-123.
- Jumars, P.E., and J.E. Eckman, 1983. Spatial structure within deep-sea benthic communities. In: Rowe, G.T. (Ed.), *The Sea Deep-Sea Biology* vol. 8. Wiley, New York. 399-452.
- Juniper, S.K., M. Matabos, S. Mihály, R.S. Ajayamohan, F. Gervais, and A.O. Bui. 2013. A year in Barkley Canyon: A time-series observatory study of mid-slope benthos and habitat dynamics using the NEPTUNE Canada network. *Deep Sea Res II* **92**: 114-123.
- Keister, J.A., and L.B. Tuttle, 2013. Effects of bottom-layer hypoxia on spatial distributions and community structure of mesozooplankton in a sub-estuary of Puget Sound, Washington, USA. *Limnol. Oceanogr.* **58**: 667-680.
- Keller, A.A., V. Simon, F. Chan, W.W. Wakefield, M.E. Clarke, J.A. Barth, and D. Kamikawa, E.L. Fruh. 2010. Demersal fish and invertebrate biomass in relation to an offshore hypoxic zone along the US West Coast. *Fish. Oceanogr.* **19**: 76-97.
- Keller, A.A., J.H. Harms, and J.C. Buchanan. 2012. Distribution, biomass and size of grooved Tanner crabs (*Chionoecetes tanneri*) from annual bottom trawl surveys (2003–2010) along the US west coast (Washington to California). *Deep-Sea Res I.* **67**: 44-54.

- King, J.R., G.A. McFarlane, R.J. Beamish. 2001. Incorporating the dynamics of marine systems into the stock assessment and management of sablefish. *Prog. Oceanogr.* **49**, 619–639.
- Kim, S. K., and J. Venkatesan. 2015. Introduction to Marine Biotechnology. In: *Springer Handbook of Marine Biotechnology*. Springer Berlin Heidelberg, **9**:1-8
- Kodama, K., M. Oyama, G. Kume, S. Serizawa, H. Shiraishi, Y. Shibata, M. Shimizu, T. Horiguchi, 2010. Impaired megabenthic community structure caused by summer hypoxia in a eutrophic coastal bay. *Ecotoxicology* **19**:479-492.
- Kraan, C., G. Aarts, T. Piersma, C.F. Dormann, 2013. Temporal variability of ecological niches: a study on intertidal macrobenthic fauna. *Oikos* **122**:754-763.
- Krieger, K.J., 1997. Sablefish, *Anoplopoma fimbria*, observed from a manned submersible. Biology and management of sablefish, *Anoplopoma fimbria*: NOAA Tech. Rep. NMFS, **130**:39–43
- Kristensen, E., M. Delefosse, C.O. Quintana, G.T. Banta, H.C. Petersen, and B. Jørgensen, 2013. Distribution pattern of benthic invertebrates in Danish estuaries: the use of Taylor's power law as a species-specific indicator of dispersion and behavior. *J. Sea Res.* **77**:70-78.
- Kronfeld-Schor, N., and Tamar Dayan. 2003. "Partitioning of Time as an Ecological Resource." *Annual Review of Ecology, Evolution, and Systematics* **34** (1): 153–81. doi:10.1146/annurev.ecolsys.34.011802.132435.
- Kross, S. M., and X. J. Nelson. 2011. A portable low-cost remote videography system for monitoring wildlife. *Methods in Ecology and Evolution*, **2**:191-196.
- Laidig, T.E., P.B. Adams, and W.M. Samiere, 1997. Feeding habits of sablefish, *Anoplopoma fimbria*, off the coast of Oregon and California. NOAA Tech. Rep. NMFS, **130**: 65–79.
- Lampitt, R.S., P. Favali, C.R. Barnes, M.J. Church, M.F. Cronin, K.L. Hill, Y. Kaneda, et al. 2010. In Situ Sustained Eulerian Observatories. In *Proceedings of the OceanObs'09*, edited by J. Hall, D.E. Harrison, and D. Strammer, **1**:395–404. Europe Space Agency. <http://www.oceanobs09.net/> (ESA WPP-306).
- Lapointe, V., and B. Sainte-Marie. 1992. Currents, predators, and the aggregation of the gastropod *Buccinum undatum* around bait. *Mar Ecol Prog Ser.* **85**: 245-257.
- Langlois, T. J., E. S. Harvey, B. Fitzpatrick, and J. J. Meeuwig, G. Shedrawi, and D. L. Watson. 2010. "Cost-Efficient Sampling of Fish Assemblages: Comparison of Baited Video Stations and Diver Video Transects." *Aquatic Biology* **9**: 155–68. doi:10.3354/ab00235.
- Le Bris, N., S. Arnaud-Haond, S. Beaulieu, E. Cordes, A. Hilario, A. Rogers, S. van de Gaever, and H. Watanabe. 2016. Hydrothermal Vents and Cold Seeps. In: (UN Ed.) *First Global Integrated Marine Assessment.*; 18.

- Leo, F. C. De., C. R. Smith, A. A. Rowden, D. A. Bowden, and M. R. Clark. 2010. "Submarine Canyons: Hotspots of Benthic Biomass and Productivity in the Deep Sea." *Proceedings of the Royal Society B: Biological Sciences* **277** (1695): 2783–92. doi:10.1098/rspb.2010.0462.
- Leo, F. C. De., J. C. Drazen, E. W. Vetter, A. A. Rowden, and C. R. Smith. 2012. "The Effects of Submarine Canyons and the Oxygen Minimum Zone on Deep-Sea Fish Assemblages off Hawai'i." *Deep-Sea Research Part I: Oceanographic Research Papers* **64**: 54–70. doi:10.1016/j.dsr.2012.01.014.
- Lelièvre, Y., P. Legendre, M. Matabos, S. Mihály, R. W. Lee, P-M Sarradin, Cl.- P. Arango, and J. Sarrazin. 2017. "Astronomical and Atmospheric Impacts on Deep-Sea Hydrothermal Vent Invertebrates." *Proceedings of the Royal Society B: Biological Sciences* **284** (1852): 20162123. doi:10.1098/rspb.2016.2123.
- Lee Van Dover, C.. 2011. Tighten Regulations on Deep-Sea Mining. *Nature* **470** (7332): 31–33. doi:10.1038/470031a.
- Legendre, P., and L. Legendre. 1998. *Numerical Ecology*, 2nd English ed. Elsevier pp. 853.
- Legendre, P., and L.F Legendre, 2012. *Numerical Ecology*. Third English Edition. Elsevier science, Amsterdam, pp. 712–717.
- Levin, L.A., Ekau, W., Gooday, A.J., Jorissen, F., Middelburg, J.J., Naqvi, S.W.A., Neira, C., Rabalais, N.N., Zhang, J., 2009. Effects of natural and human-induced hypoxia on coastal benthos. *Biogeosciences* **6**: 2063-2098.
- Levin, L, D. Gutiérrez, A. Rathburn, C. Neira, J. Sellanes, P. Munoz, and M. Salamanca. 2002. Benthic processes on the Peru margin: A transect across the oxygen minimum zone during the 1997–98 El Niño. *Prog Oceanogr.* **53**: 1-27.
- Levin, LA, A.R. Baco, D.A. Bowden, A. Colaco, E.E. Cordes, M.R. Cunha, and A. Metaxas. 2016. Hydrothermal vents and methane seeps: Rethinking the sphere of influence. *Front Mar Sci.* **3**: 72.
- Levine, J.D., P. Funes, H.B. Dowse, and Hall, J.C. 2002. Signal analysis of behavioral and molecular cycles. *BMC Neurosci.* **3**, 1.
- Longcore, T., and C. Rich. 2004. "Ecological Light Pollution." *Frontiers in Ecology and the Environment* **2** (4): 191–98. doi:10.1890/1540-9295(2004)002[0191:ELP]2.0.CO;2.
- Lorance, P., and V.M. Trenkel , 2006. Variability in natural behaviour, and observed reactions to an ROV, by mid-slope fish species. *J. Exp. Mar. Biol. Ecol.* **332**, 106–119.
- Lundsten, L., C. K.. Paull, K. L. Schlining, M. McGann, and W. Ussler, 2010a .Biological characterization of a whale-fall near Vancouver Island, British Columbia, Canada. *Deep Sea Research Part I: Oceanographic Research Papers*, **57**:918–922.

- Lundsten, L., K. L., Schlining, K., Frasier, S. B., Johnson, L. A., Kuhnz, J. B., J. Harvey, and R. C. Vrijenhoek. 2010. Time-series analysis of six whale-fall communities in Monterey Canyon, California, USA. *Deep Sea Research Part I: Oceanographic Research Papers*, **57**: 1573-1584.
- Macoun, P., R., Dewey, A. Round, 2010. VENUS - a bottom up approach to building an ocean observing system. *OCEANS 2010 IEEE – Sydney* pp.1–9. Manning, C.C., Hamme, R.C., Bourbonnais, A., 2010. Impact of deep-water renewal events on fixed nitrogen loss from seasonally-anoxic Saanich Inlet. *Mar. Chem.* **122**: 1-10.
- Mallet, D., L. Wantiez, S. Lemouellic, L. Vigliola, and D. Pelletier. 2014. “Complementarity of Rotating Video and Underwater Visual Census for Assessing Species Richness, Frequency and Density of Reef Fish on Coral Reef Slopes.” *PLoS ONE* 9 (1). doi:10.1371/journal.pone.0084344.
- Maloney, N.E., and M.F. Sigler, 2008. Age specific movement patterns of sablefish (*Anoplopoma fimbria*) in Alaska. *Fish. Bull.* **106**, 305–316.
- Marliave, J., A. Frid, D.W. Welch, and A.D. Porter. 2013. Home site fidelity in Black Rockfish, *Sebastes melanops*, reintroduced into a fjord environment. *The Canadian Field-Naturalist*. **127**: 255-261.
- Martinussen, M.B., and U. Båmstedt. 1999. Nutritional ecology of gelatinous planktonic predators: Digestion rate in relation to type and amount of prey. *J Exp Mar Biol Ecol.*; **232**: 61-84.
- Matabos, M., J., Aguzzi, K., Robert, C., Costa, P., Menesatti, J.B., Company and S. K., Juniper, .2011. Multi-parametric study of behavioural modulation in demersal decapods at the VENUS cabled observatory in Saanich Inlet, British Columbia, Canada. *Journal of Experimental Marine Biology and Ecology*, **401**: 89-96
- Matabos, M. 2012. “Seafloor Observatories.” In *Biological Sampling in the Deep Sea*, edited by M. R. Clark, Mireille Consaley, and A.A. Rowden, Wiley, J &, 306–37. Wellington.
- Matabos, M., A.O. Bui, S. Mihály, J. Aguzzi, S.K. Juniper, and R.S. Ajayamohan. 2014. High-frequency study of epibenthic megafaunal community dynamics in Barkley Canyon: A multi-disciplinary approach using the NEPTUNE Canada network. *J Mar Syst.* **30**: 56-68.
- Matabos, M., M. Best, J. Blandin, M. Hoeberechts, S. K., Juniper, B. Pirenne and M. Vardaro. 2016. Seafloor observatories. *Biological Sampling in the deep sea*, 306-337.
- Matabos, M., M. Hoeberechts, C. Doya, J. Aguzzi, J. Nephin, Th. E. Reimchen, S. Leaver, et al. 2017. “Expert, Crowd, Students or Algorithm: Who Holds the Key to Deep-Sea Imagery ‘Big Data’ Processing?” *Methods in Ecology and Evolution*. doi:10.1111/2041-210X.12746.
- Matsui, T., and T. Moriyama, and R. Kato 2011. Burrow plasticity in the deep-sea Isopod *Bathynomus doederleini* (Crustacea: Isopoda: Cirolanidae). *Zoolog Sci.* 2011 **28**: 863-868

- Mauchline, J., and D.M. Gordon, 1991. Oceanic pelagic prey of benthopelagic fish in the benthic boundary layer of marginal oceanic region. *Mar. Ecol. Prog. Ser.* **74**, 109–115.
- Mathias, D., A.M. Thode, J. Straley, J. Calambokidis, G.S. Schorr, and K. Folkert, 2012. Acoustic and diving behavior of sperm whales (*Physeter macrocephalus*) during natural and depredation foraging in the Gulf of Alaska. *J. Acoust. Soc. Am.* **132**, 518–532.
- Mazzei, L., S. Marini, J. Craig, J. Aguzzi, E. Fanelli, and Imants G. Priede. 2014. “Automated Video Imaging System for Counting Deep-Sea Bioluminescence Organisms Events.” In *Proceedings - 2014 ICPR Workshop on Computer Vision for Analysis of Underwater Imagery, CVAUI 2014*, edited by Juan E. Guerrero, 57–64. Stockholm: Conference Publishing Services (CPS). doi:10.1109/CVAUI.2014.15.
- McQuinn, I.H., Y. Simard, T.W.F. Stroud, J.-L. Beaulieu, and S.J. Walsh, 2005. An adaptive, integrated “acoustic-trawl” survey design for Atlantic cod (*Gadus morhua*) with estimation of the acoustic and trawl dead zones. *ICES J. Mar. Sci.* **62**, 93–106.
- Menge, Bruce A., F. Chan, S. Dudas, D. Eerkes-Medrano, K. Grorud-Colvert, K. Heiman, M. Hession-Lewis, et al. 2009. “Terrestrial Ecologists Ignore Aquatic Literature: Asymmetry in Citation Breadth in Ecological Publications and Implications for Generality and Progress in Ecology.” *Journal of Experimental Marine Biology and Ecology* **377** (2): 93–100. doi:10.1016/j.jembe.2009.06.024.
- Mercier, A., Z. Sun, S. Baillon, and J-F Hamel. 2011. “Lunar Rhythms in the Deep Sea: Evidence from the Reproductive Periodicity of Several Marine Invertebrates.” *Journal of Biological Rhythms* **26** (1): 82–86. doi:10.1177/0748730410391948.
- Minchin, P.R. 1987. An evaluation of the relative robustness of techniques for ecological ordination. In: *Theory and models in vegetation science*. Springer (Netherlands).; 89-107.
- Mora, C., D. P., Tittensor, S., Adl, A.G.B. Simpson, B. Worm. 2011. How many species are there on Earth and in the ocean? *Plos Biology* e1001127
- Moranta, J., A. Quetglas, E. Massutí, B. Guijarro, M. Hidalgo, and P. Diaz. 2008. Spatio-temporal variations in deep-sea demersal communities off the Balearic Islands (western Mediterranean). *J Mar Syst.*; **71**: 346-366.
- Mortensen, T. 1938. On the vegetarian diet of some deep-sea echinoids. *Annot. Zool. Japo.* **17**: 225-228.
- Naganuma, T., H. Wada, and K. Fujioka. 1996. Biological community and sediment fatty acids associated with the deep-sea whale skeleton at the Torishima Seamount. *Oceanography*, **52**: 1-15.

- Natarajan, P., 1989. External synchroniser of tidal activity rhythms in the prawns *Panaeus indicus* and *Paeneus monodon*. *Mar. Biol.*, **101**: 347 - 354.
- Naylor, R. L., R. J. Goldberg, J. H. Primavera, N. Kautsky, M. C. Beveridge, J. Clay and M. Troell. 2000. Effect of aquaculture on world fish supplies. *Nature*, **405**:1017-1024.
- Naylor, E. 2005. "Chronobiology: Implications for Marine Resource Exploitation and Management." *Scientia Marina* **69** (S1): 157–67. doi:10.3989/scimar.2005.69s1157.
- Naylor, E., 2010. *Chronobiology of Marine Organisms*. Cambridge University Press, Cambridge.
- Okamoto M., N. Sato, T. Asahida, and Y. Watanabe., 2007. Pelagic Juveniles of Two Morids (Teleostei: Gadiformes: Moridae), *Antimora microlepis* and *Physiculus japonicus*, from the Western North Pacific. *Species Diversity* **12**: 17-27.
- Oksanen, J., F.G. Blanchet, R. Kindt, P. Legendre, P.R. Minchin, R.B. O'Hara et al. 2006. *Vegan: Community ecology package*. <http://CRAN.R-project.org/package=vegan>.
- Oksanen, J., F.G. Blanchet, R. Kindt, P. Legendre, P.R. Minchin, R.B. O'Hara et al. 2015. *Vegan: Community Ecology Package*. <http://CRAN.R-project.org/package=vegan>.
- Ooka-Souda, S., H. Kabasawa, S. Kinoshita, , 1985. Circadian rhythms in locomotor activity in the hagfish, *Eptatretus burgeri*, and the effect of reversal of light–dark cycle. *Zool. Sci.* **2**, 749–754.
- Osborn, DA, M.W. Silver, C.G. Castro, S.M. Bros, and F.P. Chavez.2007. The habitat of mesopelagic scyphomedusae in Monterey Bay, California. *Deep-Sea Res I.* **54**:1241-1255.
- Papiol, V., J.E. Cartes, E. Fanelli, and F. Maynou.2012. Influence of environmental variables on the spatio-temporal dynamics of benthic-pelagic assemblages in the middle slope of the Balearic Basin (NW Mediterranean). *Deep-Sea Res I.* **61**: 84-99.
- Park, E., 1988. Around the mall and beyond: Japanese spider crabs at the invertebrate exhibit at the national zoo. *Smithsonian*, **19**: 18.
- Parmesan, C. 2006. Ecological and Evolutionary Responses to Recent Climate Change. *Annual Review of Ecology, Evolution, and Systematics* **37** (1): 637–69. doi:10.1146/annurev.ecolsys.37.091305.110100.
- Parmesan, C, and G. Yohe. 2003. A Globally Coherent Fingerprint of Climate Change Impacts across Natural Systems. *Nature* **421**: 37–42. doi:10.1038/nature01286.
- Patel, Vishal R., N. Ceglia, M. Zeller, K. Eckel-Mahan, P. Sassone-Corsi, and P. Baldi. 2015. The Pervasiveness and Plasticity of Circadian Oscillations: The Coupled Circadian-Oscillators Framework. *Bioinformatics* **31** (19): 3181–88. doi:10.1093/bioinformatics/btv353.

- Peer, A. C., and T. J. Miller. 2014. Climate Change, Migration Phenology, and Fisheries Management Interact with Unanticipated Consequences. *North American Journal of Fisheries Management* **34** (1): 94–110. doi:10.1080/02755947.2013.847877.
- Pelletier, D., K., Leleu, D., Mallet, G., Mou-Tham, G., Hervé, M., Boureau, N , Guilpart. 2012. Remote high-definition rotating video enables fast spatial survey of marine underwater macrofauna and habitats. *Plos One*, **7**: e30536.
- Pereyra, W.T., 1966. The bathymetric and seasonal distribution, and reproduction of adult tanner crabs, *Chionoecetes tanneri* rathbun (Brachyura: majidae), off the northern Oregon coast. In: *Deep-Sea Res Ocean Abs*. Elsevier. pp. 1185-1205.
- Puig, P., M., Canals, J. B. Company, J. Martín, D. Amblas, G. Lastras and A. M Calafat. 2012. Ploughing the deep sea floor. *Nature*, **489**:286-289.
- Purser, A., A. R. Denny, and T. Schoening. 2015. “Integrative Habitat Mapping Technologies for Identification of Different Deep-Sea Habitats and Their Spatial Coverage.” https://www.eu-midas.net/sites/default/files/deliverables/MIDAS_D10.2_Final.pdf.
- Purser, A, L., Thomsen, M. Hofbauer, M. Menzel, H. Wagner, R. Chapman, C. Barnes, M. Best. 2013. Temporal and spatial benthic data collection via Internet operated Deep Sea Crawler. *Met Oceanogr.*; **5**: 1-18.
- Priede, M., P.M. Bagley, K.L. and Smith Jr., 1994. Seasonal change in activity of abyssal demersal Scavenging Grenadiers *Coryphaenoides* (Nematonurus) *armatus* in the Eastern North Pacific Ocean. *Limnol. Oceanogr.* **39**, 279–285.
- Priede, M., A.R Deary, D.M. Bailey, and Smith Jr., K.L., 2003. Low activity and seasonal change in population size structure of grenadiers in the oligotrophic abyssal central North Pacific Ocean. *J. Fish Biol.* **63**, 187–196.
- Priede, M., and M., Solan. 2003. ESONET—European Sea Floor Observatory Network. Final Report EVK3-CT-2002-80008.
- R Development Core Team. 2011. *R: A Language and Environment for Statistical Computing*, Vienna, Austria : the R Foundation for Statistical Computing. ISBN: 3-900051-07-0.
- Raffaelli, D., E. Bell, G. Weithoff, A. Matsumoto, J. J. Cruz-Motta, Pete Kershaw, R. Parker, D. Parry, and M. Jones. 2003. “The Ups and Downs of Benthic Ecology: Considerations of Scale, Heterogeneity and Surveillance for Benthic-Pelagic Coupling.” *Journal of Experimental Marine Biology and Ecology* **285–286** (2003): 191–203. doi:10.1016/S0022-0981(02)00527-0.
- Ramirez-Llodra, E., A. Brandt, R. Danovaro, B. De Mol, E. Escobar, C. R. German, L. A. Levin, et al. 2010. “Deep, Diverse and Definitely Different: Unique Attributes of the World’s Largest

- Ecosystem.” *Biogeosciences* **7** (9): 2851–99. doi:10.5194/bg-7-2851-2010.
- Refinetti, R., 1992. Laboratory instrumentation and computing: comparison of six methods for the determination of the period of circadian rhythms. *Physiol. Behav.* **54**, 869–875.
- Refinetti, R., 2006. *Circadian Physiology*. Francis and Taylor, New York.
- Roe, H.S.J., Badcock, J., 1984. The diel migrations and distributions within a mesopelagic community in the north east Atlantic. 5. Vertical migrations and feeding of fish. *Prog. Oceanogr.* **13**, 389–424.
- Reynolds, B.F., S.P. Powers, and M.A. Bishop. 2010. Application of acoustic telemetry to assess residency and movements of rockfish and lingcod at created and natural habitats in Prince William Sound. *PLoS One.*; **5**: e12130.
- Roberts D., A. Gebruk, V. Levin, and B.A.D. Manship. 2000. Feeding and digestive strategies in deposit-feeding holothurians. *Ocean. Mar. Biol. Ann Rev.* **38**: 257-310.
- Rohlf, F.J., M. Corti. 2000. Use of two-block partial least squares to study covariation in shape. *Syst Biol* **49**:740–753.
- Ruhl, H.A., M. André, L. Beranzoli, M.N. Çağatay, A. Colaço, M. Cannat, J.J. Dañobeitia, P. Favali, L. Géli, M. Gillooly, J. Greinert, P.O.J. Hall, R. Huber, J. Karstensen, R.S. Lampitt, K.E. Larkin, V. Lykousis, J. Mienert, J.M. Miranda, R. Person, I.G. Priede., I. Puillat, L. Thomsen, and C. Waldmann. 2011. Societal need for improved understanding of climate change, anthropogenic impacts, and geo-hazard warning drive development of ocean observatories in European Seas. *Prog Oceanogr.* **91**: 1-33.
- Ryer, C.H., 2004. Laboratory evidence for behavioural impairment of fish escaping trawls: a review. *ICES J. Mar. Sci.* **61**, 1157–1164.
- Sardà, F., J.E. Cartes, and J.B. Company. 1994. Spatio-temporal variations in megabenthos abundance in three different habitats of the Catalan deep-sea (Western Mediterranean). *Mar Biol.*; **120**: 211-219.
- Sardà, F., A. Calafat, M^a M. Flexas, A. Tselepides, M. Canals, M. Espino, and A. Tursi. 2004. “An Introduction to Mediterranean Deep-Sea Biology.” *Scientia Marina* **68** (3): 7–38. doi:10.3989/scimar.2004.68s37.
- Saunders, M.W., B.M. Leaman, and G.A. McFarlane. 1997. Influence of ontogeny and fishing mortality on the interpretation of sablefish, *Anoplopoma fimbria*, life history. Proceedings of the International Symposium on the Biology and Management of Sablefish, *Anoplopoma fimbria*: NOAA Tech. Rep. NMFS, **130**: 81–92.

- Sbragaglia V, J.A., García, J.J. Chiesa, and J. Aguzzi. 2015. The effect of simulated tidal currents on burrow emergence rhythms of the Norway lobster (*Nephrops norvegicus*, L.). *Marine Biology*, **162**: 2007-2016.
- Sbragaglia, Va., 2015 Biological rhythms in the Norway lobster (*Nephrops Norvegicus* L.): Ecological modulation and genetic basis = Ritmos biológicos en la cigala (*Nephrops norvegicus* L.): modulación ecológica y bases genéticas. <http://hdl.handle.net/2117/95788>
- Schlacher, T.A., A. Williams, F. Althaus, and M.A. Schlacher-Hoenlinger. 2010. High-resolution seabed imagery as a tool for biodiversity conservation planning on continental margins. *Mar Ecol*. **31**: 200-221.
- Serge, D., and J. Aschoff. 2001. The entrainment of circadian systems. *Circadian Clocks*. Springer US, pp. 7-43.
- Shaw, W., G.A. McFarlane, 1997. Development of sablefish, *Anoplopoma fimbria* larvae off the West Coast of British Columbia and transformation in the juvenile stage. *Biology and Management of Sablefish, Anoplopoma fimbria*: NOAA Tech. Rep. NMFS, **130**: 3–12.
- Sherman, A. D., and K. L. Smith, .2009. Deep-sea benthic boundary layer communities and food supply: A long-term monitoring strategy. *Deep Sea Research Part II: Topical Studies in Oceanography*, **56**: 1754-1762.
- Silvertown, J. 2009. “A New Dawn for Citizen Science.” *Trends in Ecology and Evolution* **24** (9): 467–71. doi:10.1016/j.tree.2009.03.017.
- Smith, C.R. 1985. Food for the deep sea: utilization, dispersal and flux of nekton falls at the Santa Catalina Basin floor. *Deep-Sea Research* **32**: 417–442.
- Smith, C.R. 1986. Nekton falls, low-intensity disturbance and community structure of infaunal benthos in the deep-sea. *Journal of Marine Research* **44**:567-600.
- Smith, C. R., H. Kukert, R.A. Wheatcroft, P. A. Jumars, and Deming, J. W. 1989. Vent fauna on whale remains. *Nature* **341**: 27–28. doi:10.1038/341027a0
- Smith,, C. R., and A. Baco. 2003. Ecology of whale falls at the Deep-sea floor. *Marine Ecology: An Annual Review* **41**: 311–354.
- Smith, C.R., and A. Demopoulos. 2003. The Deep Pacific Ocean. In *Ecosystems of the Deep Oceans*, 179–218. Elsevier.
- Smith, K. L., R. S. Kaufmann, and W. W. Wakefield. 1993. “Mobile Megafaunal Activity Monitored with a Time-Lapse Camera in the Abyssal North Pacific.” *Deep-Sea Research Part I* **40** (11–12): 2307–24. doi:10.1016/0967-0637(93)90106-D.

- Smith, C. R., A.F., Bernardino, A. Baco, A. Hannides, I. and Altamira. 2014. Seven-year enrichment: macrofaunal succession in deep-sea sediments around a 30 tons whale fall in the Northeast Pacific. *Marine Ecology Progress Series*, **515**, 133.
- Sogard, S.L., and B.L. Olla, 1998. Behavior of juvenile sablefish, *Anoplopoma fimbria* (Pallas), in a thermal gradient: balancing food and temperature requirements. *J. Exp. Mar. Biol. Ecol.* **222**, 43–58
- Sokolove, P.G., and W.N. Bushell, 1978. The chi square periodogram: its utility for analysis of circadian rhythms. *J. Theor. Biol.* **72**, 131–160.
- Stachura, M.M., C.R. Lunsford, C.J. Rodgveller, J. Heifetz. 2012. Estimation of discard mortality of sablefish (*Anoplopoma fimbria*) in Alaska longline fisheries. *Fish. Bull.* **110**, 271–279.
- Steffen, W., K. Richardson, J. Rockström, S. E. Cornell, I. Fetzer, E. M. Bennett, S. R. Carpenter, W. de Vries, C. A. de Wit, C. Folke, D. Gerten, J. Heinke, G. M. Mace, L. M. Persson, V. Ramanathan, B. Reyers, S. Sörlin .2015.. Planetary boundaries: Guiding human development on a changing planet. *Science*, **347**:6223, 1259855.
- Stockton, W.L., and T.E De Laca,. 1982. Food falls in the deep sea: occurrence, quality, and significance. *Deep-Sea Research I* **29**:157–169.
- Stoner, A.W., C.H. Ryer, S.J. Parker, P.J. Auster, and W.W. Wakefield. 2008. Evaluating the role of fish behavior in surveys conducted with underwater vehicles. *Can. J. Fish. Aquat. Sci.* **65**, 1230–1243.
- Stramma, L., S. Schmidtko, L.A. Levin, G.C. Johnson. 2010. Ocean oxygen minima expansions and their biological impacts. *Deep-Sea Res I.* **57**: 587–95.
- Suetsugu, K., and S. Ohta 2005. Day-night changes in species composition of deep-sea demersal fishes. *J. Oceanog.* **61**: 187-196.
- Sumida, P. Y. G., J. M. Alfaro-Lucas, M. Shimabukuro, H. Kitazato, J. A. A. Perez, A. Soares-Gomes, and Y. Fujiwara. 2016. Deep-sea whale fall fauna from the Atlantic resembles that of the Pacific Ocean. *Scientific Reports*, **6**:22139.
- Taniuchi, T. 1988. Aspects of reproduction and food habits of the Japanese Swell shark *Cephaloscyllium umbratile* from Choshi, Japan. *Nipp. Suisan Gakkashi* **54**: 627-633.
- Tecchio, S., E. Ramírez-Llodra, J. Aguzzi, A. Sanchez-Vidal, M.M. Flexas, F. Sardà, and J.B. Company. 2013. Seasonal fluctuations of deep megabenthos: Finding evidence of standing stock accumulation in a flux-rich continental slope. *Prog in Oceanogr.* **118**, 188-198.
- Theede, H., 1973. Comparative studies on the influence of oxygen deficiency and hydrogen sulphide on marine bottom invertebrates. *Netherlands Journal of Sea Research.* **7**: 244–252.

- Thomsen, L., C. Barnes, M. Best, R. Chapman, B. Pirenne, R. Thomson, and J. .Vogt. 2012. Ocean circulation promotes methane release from gas hydrate outcrops at the NEPTUNE Canada Barkley Canyon node. *Geophys. Res. Lett.* **39**, 1–6. [doi:10.1029/2011GL015811](https://doi.org/10.1029/2011GL015811).
- Thomsen, L., Purser, A., Schwendner, J., Duda, A., Flögen, S., Kwasnitschka, T., Rosta, R. 2015. Temporal and spatial benthic data collection via mobile robots: Present and future applications. In: *OCEANS 2015-Genova IEEE*. pp. 1-5.
- Thuesen, E.V., L.D. Rutherford, and P.L. Brommer.2005. The role of aerobic metabolism and intragel oxygen in hypoxia tolerance of three ctenophores: *Pleurobrachia bachei*, *Bolinopsis infundibulum* and *Mnemiopsis leidyi*. *J Mar Biol Ass UK*. **85**: 627-633.
- Thurber, A. R., A. K. Sweetman, B. E. Narayanaswamy, D. O. B. Jones, J. Ingels, and R. L. Hansman, 2014. Ecosystem function and services provided by the deep sea. *Biogeosciences*, **11**: 3941-3963.
- Trenkel, V.M., P. Lorange, and S. Mahévas. 2004a. Do visual transects provide true population density estimates for deepwater fish? *ICES J. Mar. Sci.* **61**, 1050–1056.
- Trenkel, V.M., R.I.C. Chris Francis, P. Lorange, S. Mahéva, M. Rochet, and D. Tracey. 2004b. Availability of deep-water fish to trawling and visual observation from a remotely operated vehicle (ROV). *Mar. Ecol. Prog. Ser.* **284**, 293–303.
- Trenkel, V. M., and P. Lorange. 2011. Estimating *Synaphobranchus kaupii* densities: contribution of fish behaviour to differences between bait experiments and visual strip transects. *Deep Sea Research Part I: Oceanographic Research Papers*, **58**, 63-71.
- Tunnicliffe, V, S.K. Juniper, and M. Sibuet. 2003. Reducing environments of the deep-sea floor. In: Tyler PA (Eds.), *Ecosystems of the World*; 81-110.
- Tunnicliffe, V., C. R., Barnes, R., Dewey, 2008. Major advances in cabled ocean observatories (VENUS and NEPTUNE Canada) in coastal and deep sea settings. In 2008 IEEE/OES US/EU-Baltic International Symposium IEEE pp. 1-7.
- Underwood, A.J. 2005. Intertidal Ecologists Work in the ‘gap’ between Marine and Terrestrial Ecology. *Marine Ecology Progress Series* **304** (2): 297–302. [doi:10.3354/meps304271](https://doi.org/10.3354/meps304271).
- Uiblein, F., P. Lorange, D. Latrouite, 2002. Variation in locomotion behaviour in northern cutthroat eel (*Synaphobranchus kaupii*) on the Bay of Biscay continental slope. *Deep-Sea Res. I* **49**, 1689–1703.
- Vardaro, M. F., P. M. Bagley, D. M. Bailey, B. J. Bett, D. O. B. Jones, R. J. Milligan, I. G. Priede, et al. 2013. “A Southeast Atlantic Deep-Ocean Observatory: First Experiences and Results.” *Limnology and Oceanography: Methods* **11** (6): 304–15. [doi:10.4319/lom.2013.11.304](https://doi.org/10.4319/lom.2013.11.304).

- Vetter, E. W., and P.K. Dayton. 1997. Macrofaunal Communities within and Adjacent to a Detritus-Rich Submarine Canyon System. *Deep-Sea Research Part II* **45**: 25–54. doi:10.1016/S0967-0645(97)00048-9.
- Van Dover, C. L. 2011. Tighten regulations on deep-sea mining. *Nature*,470: 31-33.
- Vetter, E.W., and P.K. Dayton. 1998. Macrofaunal communities within and adjacent to a detritus-rich submarine canyon system.*Deep-Sea Res II*. **45**: 25-54.
- Vetter, E.W. 1995. Detritus-based patches of high secondary production in the nearshore benthos.*Mar Ecol Prog Ser*.**120**: 251-262.
- Vetter, E W, C. R. Smith, and F.C. De Leo. 2010. Hawaiian hotspots: Enhanced megafaunal abundance and diversity in submarine canyons on the oceanic islands of Hawaii. *Mar Ecol*. **31**: 183-199.
- Wagner, H. J., K., Kemp, U., Mattheus, I. G. Priede, 2007. Rhythms at the bottom of the deep sea: cyclic current flow changes and melatonin patterns in two species of demersal fish. *Deep Sea Research Part I: Oceanographic Research Papers*, **54**:1944-1956.
- Watling, L. 2014. Trawling exerts big impacts on small beasts. *Proceedings of the National Academy of Sciences*, **111**:8704-8705.
- Watson, D. L., E. S. Harvey, B. M. Fitzpatrick, T. J. Langlois, and G. Shedrawi. 2010. Assessing Reef Fish Assemblage Structure: How Do Different Stereo-Video Techniques Compare? *Marine Biology***157**: 1237–50. doi:10.1007/s00227-010-1404-x.
- Watson, R. A., W. W. Cheung, J. A. Anticamara, R. U. Sumaila, D.,Zeller and D. Pauly,. 2013. Global marine yield halved as fishing intensity redoubles. *Fish and Fisheries*, **14**: 493-503.
- Webb, T. J. 2012. *Marine and Terrestrial Ecology: Unifying Concepts, Revealing Differences*. *Trends in Ecology and Evolution***27** (10). Elsevier Ltd: 535–41. doi:10.1016/j.tree.2012.06.002.
- Widder, E.A., B.H .Robison, K.R .Reisenbichler, and S.H.D. Haddock. 2005. Using red light for in situ observations of Deep-sea fishes.*Deep-Sea Res. I* **52**, 2077–2085.
- Wold, S., M., Sjostrom, and L. Eriksson 2001. PLS-regression: A basic tool of chemometrics. *Chemometrics and Intelligent Laboratory System*, **58**:109-130.
- Worm, B., R. Hilborn, J. K. Baum, T. A. Branch, J. S. Collie, C. Costello, M. J. Fogarty, E. A. Fulton, J. A. Hutchings, S. Jennings, O. P. Jensen, H. K. Lotze, P. M. Mace, T. R. McClanahan, C. Minto, S. R. Palumbi, A. M. Parma, D. Ricard, A. A. Rosenberg, R. Watson, D. Zeller 2009. Rebuilding global fisheries.*Science* **325**:578-585. DOI: doi:10.1126/science.1173146.
- Worm, B., and T. A. Branch. 2012. The future of fish. *Trends in ecology and evolution* **27**:594-599.
- Yeh, J., and J. C. Drazen. 2009. Depth Zonation and Bathymetric Trends of Deep-Sea Megafaunal

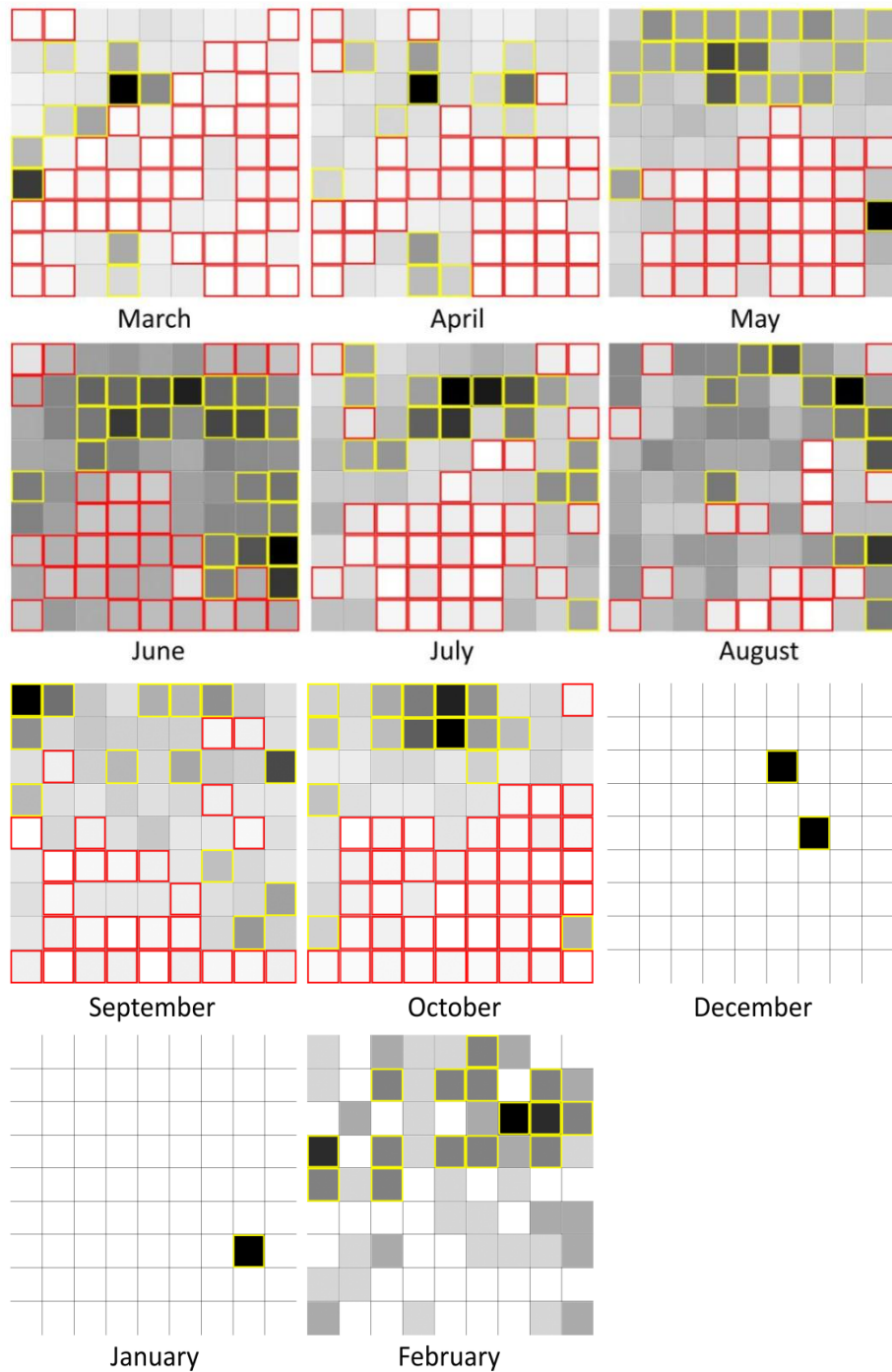
-
- Scavengers of the Hawaiian Islands. *Deep-Sea Research Part I: Oceanographic Research Papers* **56**: 251–66. doi:10.1016/j.dsr.2008.08.005.
- Yoshiyama, R.M., K.B. Gaylord, M.T. Philippart, T.R. Moore, J.R. Jordan, C.C. Coon, et al. 1992. Homing behavior and site fidelity in intertidal sculpins (Pisces: Cottidae). *Journal of experimental marine biology and ecology*. **160**: 115-130.
- Zar, J.H., 2010. *Biostatistical analysis*. 5th ed. Pearson Education International. 241-242.
- Zelditch, M.L., D.L. Swiderski, H.D. Sheets, and W.L. Fink. 2004. *Geometric morphometrics for biologists: A primer*. San Diego: Elsevier Academic. pp.443.
- Zinzen, V., K.M. Rogers., C.D. Roberts, A.L. Stewart, M.J. Anderson. 2013. Hagfish feeding habits along a depth gradient inferred from stable isotopes. *Mar. Ecol. Prog. Ser.* **485**: 223-234.

Appendix A. Annual Pearson's goodness of fit test for each of the three groups under the null hypothesis of equal probability of parcel occupation. Only significantly more occupied parcels (critical value ($p = 0.001$) = $\sqrt{X_{20.001, 80/81}} = 1.24$) are shown.

L. exilis		Large Munida		Small Munida	
Parcel	Pearson's residuals	Parcel	Pearson's residuals	Parcel	Pearson's residuals
B3	1.85	A4	6.24	B6	1.88
C3	3.14	A5	1.86	D1	2.41
D3	1.85	B8	2.69	D2	2.54
D4	6	B9	1.27	D7	16.18
D5	4.18	C6	4.23	D8	8.56
D6	2.88	C7	1.86	E1	9.23
D8	5.22	C8	3.75	E7	6.02
D9	2.62	C9	1.74	E8	41.18
E4	5.48	D7	18.91	E9	15.64
E5	3.66	D8	11.57	F2	6.15
E6	1.59	D9	2.92	F3	12.17
F5	2.62	E7	7.07	G4	16.58
F6	2.62	E8	12.99	G5	9.63
F7	2.37	E9	6.24	G7	4.55
F8	1.85	F7	1.74	G8	3.21
G3	1.33	F8	8.13	H4	2.01
G6	3.14	F9	3.87	H5	8.03
H6	1.59	G7	7.78	H6	6.82
I4	0.29	G8	3.99	H7	17.38
I5	1.33	H7	2.81	H8	7.49
I6	1.85	H8	3.28	I2	17.92
I7	1.85	I2	4.35	I3	5.89
		I3	9.44	I8	3.08
		I7	3.04		

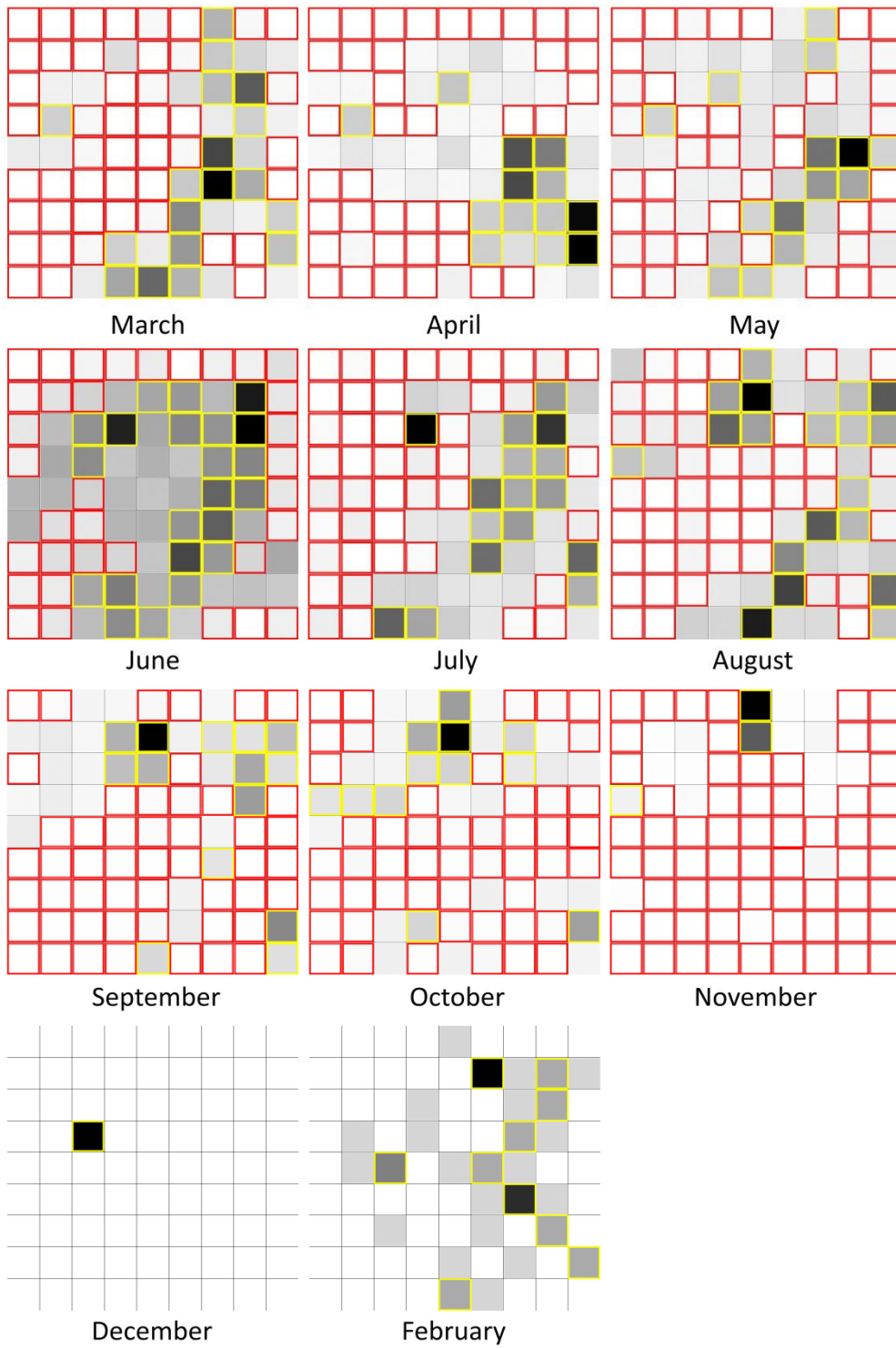
Appendix B. Monthly heat maps calculations for the three groups of benthic animals. See Figure 6 for specifications on grey scale (i.e. occupation) and on red and yellow outlining (occupation significance).

Large *Munida quadrispina*



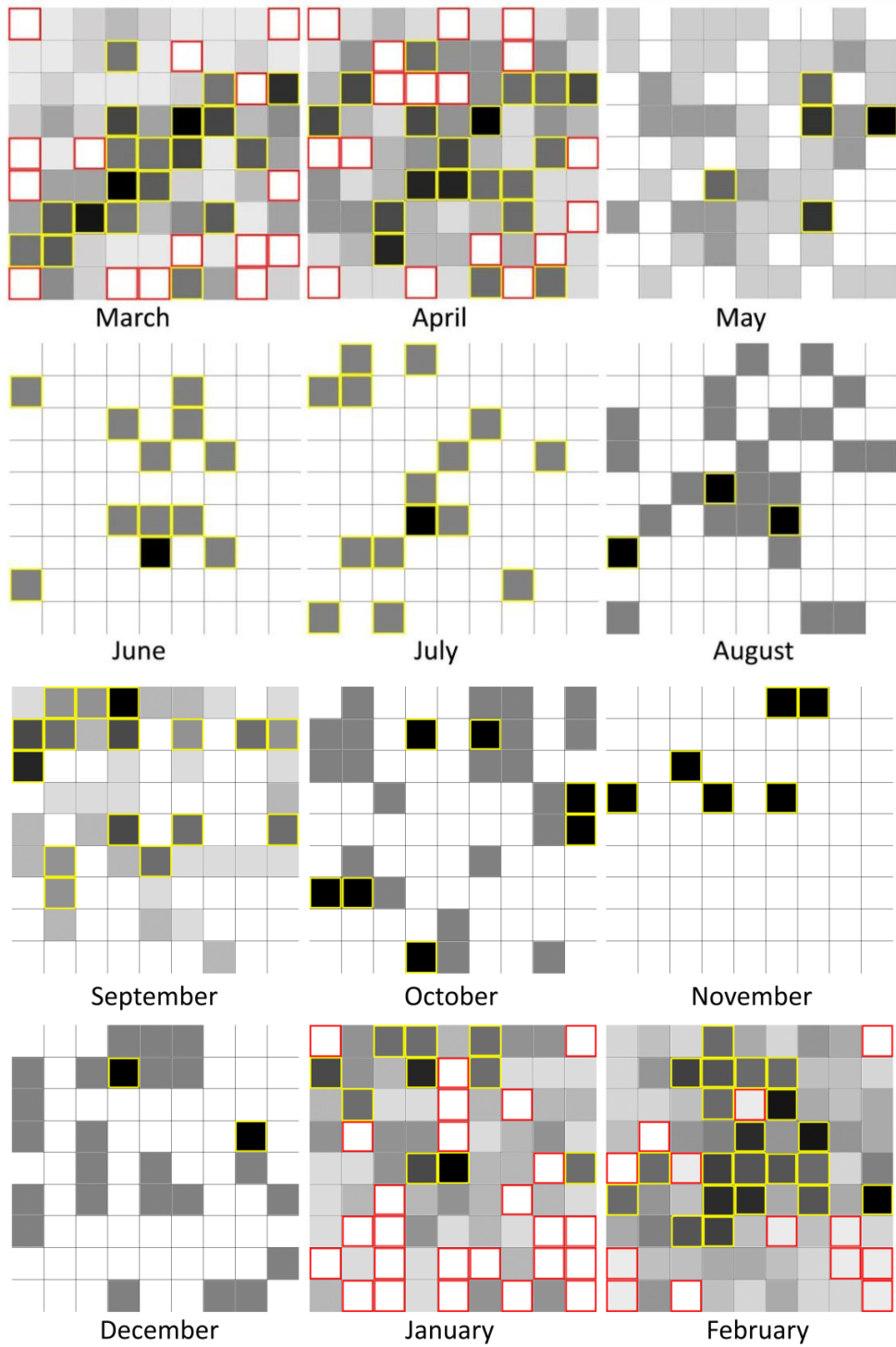
Appendix B. Prosecution.

Small Munida quadrispina



Appendix B. Prosecution.

Lyopsetta exillis



Appendix C. Monthly Segregation Index (S) values between pairs of groups (F, slender sole; L - S, large and small squat lobsters, respectively). Missing values occurred when one of the species was absent. In bold are reported intraspecific S values representing the degree of aggregation between conspecifics, whereas normal-text S values reports the degree of segregation between different groups

Comparisons		March		April		May		June		July		August				
From	To	Observed	Expected	S	Observed	Expected	S	Observed	Expected	S	Observed	Expected	S			
L	L	203	158.06	0.47	193	198	-0.05	394	408.01	-0.10	1624	1575.13	0.09	140	157.44	-0.19
	S	89	130.29	-0.53	111	113.5	-0.03	186	170.76	0.12	810	854.46	-0.08	251	249.79	0.01
	F	96	99.65	-0.05	93	85.5	0.11	47	48.23	-0.03	4	8.40	-0.74	6	7.82	-0.27
S	L	70	130.29	-0.90	78	113.5	-0.65	125	170.76	-0.72	641	854.46	-0.66	195	249.79	-0.44
	S	178	106.78	0.92	103	64.61	0.74	112	71.08	0.70	675	462.98	0.66	307	253.27	0.43
	F	71	81.93	-0.19	46	48.89	-0.08	25	20.15	0.24	6	4.56	0.28	9	7.95	0.13
F	L	66	99.65	-0.62	75	85.5	-0.25	26	48.23	-1.24	4	8.40	-1.41	7	7.82	-0.21
	S	75	81.93	-0.13	33	48.89	-0.52	28	20.15	0.49	9	4.56	1.43	6	7.95	-0.50
	F	103	62.41	0.75	63	36.61	0.76	20	5.62	1.51	0	0.04	-	3	0.23	2.75

Comparisons		September		October		November		December		February						
From	To	Observed	Expected	S	Observed	Expected	S	Observed	Expected	S	Observed	Expected	S			
L	L	116	148.55	-0.37	293	259.62	0.25	-	-	-	16	17.37	-0.10			
	S	248	217.48	0.31	225	254.23	-0.22	-	-	0	0.07	-	9	8.78	0.03	
	F	40	37.97	0.06	13	17.14	-0.28	-	-	1	0.93	-	67	65.85	0.06	
S	L	167	217.48	-0.39	199	254.23	-0.43	-	-	0	0.07	-	8	8.78	-0.11	
	S	385	317.07	0.48	304	248.01	0.44	185	183.1	0.50	-	-	13	4.29	1.34	
	F	38	55.45	-0.41	16	16.76	-0.05	3	4.9	-0.50	1	0.93	-	25	32.93	-0.75
F	L	35	37.97	-0.13	15	17.14	-0.25	5	4.9	-	1	0.93	0.08	56	65.85	-0.20
	S	55	55.45	-0.02	18	16.76	0.14	-	-	-	1	0.93	0.08	25	32.93	-0.30
	F	13	9.59	0.34	2	1.10	0.63	0	0.1	-	11	11.14	-0.09	264	246.22	0.27

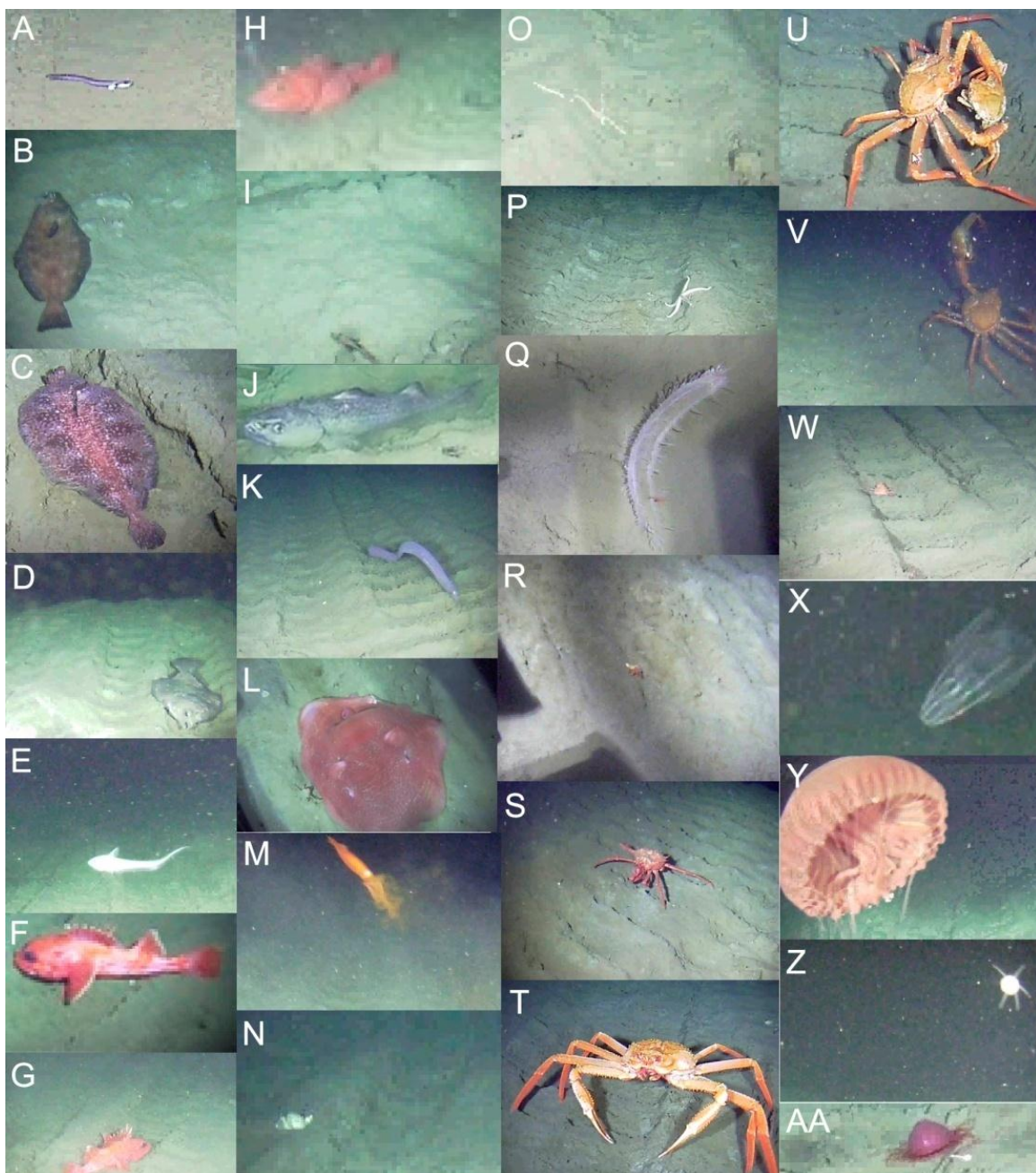
Appendix D. Monthly total visual counts and percentages for the different megafaunal species studied during the 14 months of video acquisition.

Morphotypes	Common name	N 2013												N 2014				Total	%
		Feb	Mar	Apr	May	Jun	Jul	Aug	Sept	Oct	Nov	Dec	Jan	Feb	Mar	Apr			
<i>Licenchelys</i> sp.	Eelpouts	8	13	17	15	10	4	27	6	8	10	4	2	18	20	162	2.09		
<i>Microstomus pacificus</i>	Dover sole	1	4	0	0	9	2	8	0	0	6	0	0	7	0	37	0.48		
<i>Embassichthys bathybius</i>	Deep sea sole	0	4	0	2	0	5	0	2	4	5	3	0	0	2	27	0.35		
<i>Hippoglossus stenolepis</i>	Pacific halibut	0	0	0	0	0	5	1	4	2	0	0	0	0	0	12	0.15		
<i>Coryphaenoides</i> sp.	Rattail	0	2	1	0	0	4	2	2	0	0	0	0	0	0	11	0.14		
Sebastidae	Rockfish	31	95	51	43	30	28	43	15	33	17	36	42	72	37	573	7.39		
<i>Bathygonus nigripinnis</i>	Blackfin poacher	0	1	0	0	0	0	0	0	0	0	0	0	0	0	1	0.01		
<i>Anoplopoma fimbria</i>	Sablefish	3	5	16	151	491	1018	299	19	13	146	23	10	2	18	2214	28.55		
<i>Eptatretus stoutii</i>	Hagfish	104	128	56	52	77	50	45	18	30	47	93	45	56	51	852	10.99		
Salpidae	Salp	0	0	0	0	0	0	0	0	0	0	0	0	2	0	2	0.03		
<i>Grimpoteuthis</i> sp.	Dumbo octopus	4	0	0	0	0	0	0	0	0	0	0	0	0	0	4	0.05		
<i>Gonapus</i> sp.	Squid	0	0	3	0	0	0	3	0	0	0	0	0	0	0	6	0.08		
Buccinoidea	Buccinid	69	116	104	112	56	42	76	15	12	33	49	4	550	80	1318	17.00		
Ophiuroidea	Brittle star	4	2	0	0	0	0	0	0	0	0	0	0	0	0	6	0.08		
Asteroidea	Starfish	0	0	2	6	2	0	2	2	0	0	0	18	0	6	38	0.49		
Zoroasteridae	Starfish	5	10	9	0	0	0	2	6	0	0	3	6	0	10	51	0.66		
<i>Hippasteria</i> sp.	Pincuchion star	0	2	4	6	0	0	0	10	7	0	2	0	0	0	31	0.40		
<i>Pannichia moseleyi</i>	Holoturian	3	0	0	0	0	3	0	0	0	0	0	0	0	0	6	0.08		
Diogenidae	Hermit crab	3	0	0	2	2	5	0	2	18	3	0	0	4	5	44	0.57		
<i>Lithodes couesi</i>	Scarlet king crab	6	2	12	0	2	0	0	0	0	0	0	2	0	0	24	0.31		
Not applicable	small crab	5	24	2	0	0	2	38	6	38	26	108	140	79	67	535	6.90		
<i>Chionectes tanneri</i>	Grooved tanner crab	16	76	49	15	45	86	13	6	6	18	11	5	9	30	385	4.97		
<i>Bolinopsis infundibulum</i>	Ctenophore	0	0	0	0	0	0	4	162	207	51	13	10	2	0	449	5.79		
<i>Poralla rufescens</i>	Scyphomedusa	20	103	84	83	59	58	53	24	39	68	71	34	67	35	798	10.29		
<i>Solmissus</i> sp.	Dinner plate jelly	3	7	3	1	12	8	4	0	0	11	4	2	12	0	67	0.86		
<i>Voragonema pedunculata</i>	Traquimedusa	1	3	8	5	21	1	10	13	0	14	6	5	3	15	105	1.35		
Total		286	597	421	493	816	1321	630	312	417	455	426	325	883	376	7754	100		
Number of transects		25	48	30	29	29	35	30	29	30	32	32	31	30	28	438			

Appendix E. Date and time of the reported ethological remarks. (A) Rockfish (Sebatiidae) agonistic display against the crawler (i.e. approaching the camera with the open mouth and then escaped). (B) Sablefish (*Anoplopoma fimbria*) swimming close to the crawler. (C) Male scarlet king crab (*Lithodes couesi*) feeding behavior and agonistic interaction with a grooved tanner crab. (D) Grooved tanner crab (*Chionnecetes tanneri*) agonistic display against the (i.e. an elevated body posture and chelipeds forward projection). (E) Grooved tanner crab reproduction behaviour. (F) Female grooved tanner crabs carrying eggs.

Ethological remark	Date (DD/M/YYYY)	Hour (UTC)
A	07/03/2013	3:28
B	04/03/2013	16:14
C	15/04/2013	16:45
D	06/03/2013	23:38
	05/03/2013	18:58
	19/03/2013	7:25
	20/03/2013	3:33
	20/03/2013	4:11
E	21/03/2013	7:05
	02/04/2013	3:30
	06/04/2013	11:30
	05/03/2013	18:58
	19/03/2013	7:27
	20/03/2013	3:15
F	20/03/2013	4:14
	21/03/2013	7:14
	03/04/2013	23:19
	06/04/2013	11:20

Appendix F. Photo-mosaic of all species portrayed with the camera installed on the crawler during the 14 months of video acquisition. Individuals in images are: (A) Eelpout (*Licenchelys* spp.). (B) Dover sole (*Microstomus pacificus*). (C) Deep sea sole (*Embassichthys bathybius*). (D) Pacific halibut (*Hippoglossus stenolepis*). (E) Rattail (*Coryphaenoides* spp.). (F) Rockfish (Sebastidae). (G) Rockfish (Sebastidae). (H) Rockfish (Sebastidae). (I) Blackfin poacher (*Bathyagonus nigripinnis*). (J) Sablefish (*Anoplopoma fimbria*). (K) Hagfish. (L) Dumbo octopus (*Grimpot euthis* spp.). (M) Squid. (N) Buccinids (*Neptunidae*). (O) Brittle star (*Ophiuroidea*). (P) Starfish (Asteroidea). (Q) Holoturian. (R) Hermit crab. (S) Scarlet king crab. (T) Grooved tanner crab (*Chionoecetes tanneri*). (U) Male (left) and female (right) of grooved tanner crab facing each other as a part of their reproduction behaviour. (V) Male (left) carrying out a female (right) of grooved tanner crab as a part of their reproduction behaviour. (W) Small crabs, probably small individuals of grooved tanner crab. (X) Ctenophore (*Bolinopsis infundibulum*). (Y) Scyphomedusa (*Poralia rufescens*). (Z) Dinner plate jelly (*Solmissus* spp.). (AA) Traquimedusa (*Voragonema pedunculata*).



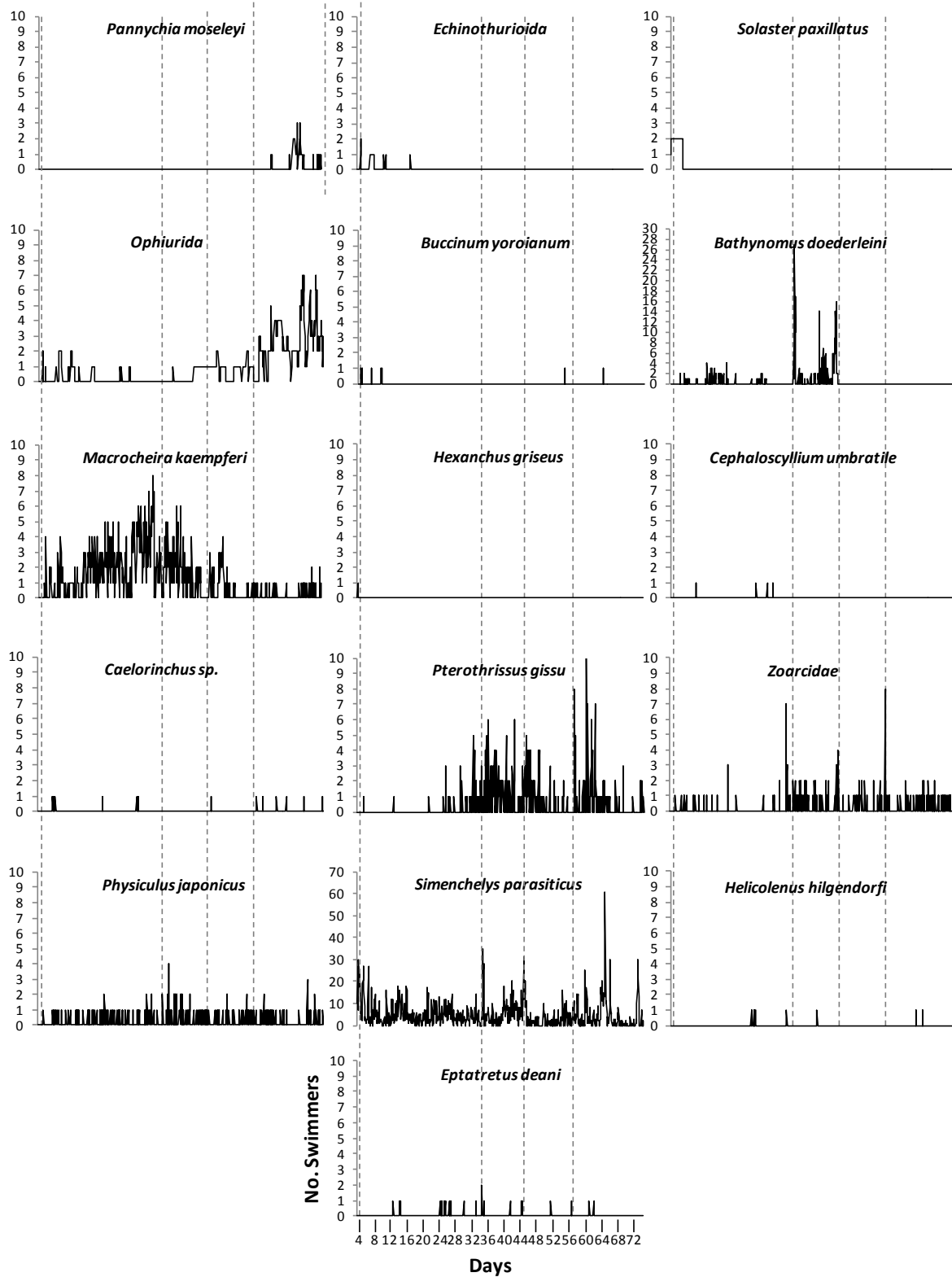
Appendix G. Taxonomical assemblage detected over 72 days starting on 14 June 2012 are hierarchically listed by phylogeny and grouped according to behavioral traits (type of movement and life habit as relationship with the seabed), along with bibliographic sources used to derive such an information. The number of individuals per species (N), their relative abundances (%), periodogram analysis outputs as significant ($p < 0.05$) periodicities (P) in minutes (min) and hours (hrs.) are reported along with periodogram peak variance (Var., %) as proxy of rhythm strength. In the periodicity column, we also reported in parenthesis significant sub-periodicities as a proxy of weak tidal patterning. Total animal abundance by functional groups with respect to the 3 trophic groups is also provided.

Taxonomical Unit	Movement	Life Habit	Trophic Habit	Source
<u>Echnodermata</u>				
<i>Pannychia moseleyi</i>	Walker	Epibenthic	Detritivore	Roberts et al. (2000); Gage (2003)
Echinothurioida	Walker	Epibenthic	Detritivore	Mortensen (1938)
<i>Solaster paxillatus</i>	Walker	Epibenthic	Scavenger (and predator)	Francour (1997)
Ophiuroidea	Walker	Endobenthic	Detritivore	Fujita and Otha (1990)
<u>Mollusca</u>				
<i>Buccinum yoroianum</i>	Walker	Epibenthic	Scavenger (and predator)	Aguzzi et al. (2010, 2012b)
<u>Arthropoda</u>				
<i>Bathynomus doederleinii</i>	Swimmer	Endobenthic	Scavenger	Matsui et al. (2011)
<i>Macrocheira kaempferi</i>	Walker	Epibenthic	Scavenger (and predator)	Park (1988); Okamoto (2001)
<u>Chordata</u>				
<i>Hexanchus griseus</i>	Swimmer	Nektobenthic	Scavenger (and predator)	Andrews et al. (2009)
<i>Cephaloscyllium umbratile</i>	Swimmer	Epibenthic	Predator	Taniuchi (1988)
<i>Caelorinchus</i> sp.	Swimmer	Epibenthic	Predator	Choen et al. (1990)
<i>Pterothrissus gissu</i>	Swimmer	Benthopelagic	Predator	Fujita et al. (1995); Balanov et al. (2009)
Zoarcidae	Swimmer	Epibenthic	Predator	Aguzzi et al. (2010)
<i>Physiculus japonicus</i>	Swimmer	Benthopelagic	Predator	Okamoto et al. (2007)
<i>Simenchelys parasiticus</i>	Swimmer	Nektobenthic	Scavenger	Anderson (2005)
<i>Helicolenus hilgendorfi</i>	Swimmer	Epibenthic	Predator	Fujiwara et al. (2007)
<i>Epiplatys dearni</i>	Swimmer	Epibenthic	Scavenger (and predator)	Zinzen et al. (2013); Doya et al. (2014)
<hr/>				
Assemblage (Total)				
<hr/>				
Scavengers (and predators)				
Detritivores				
Predators				

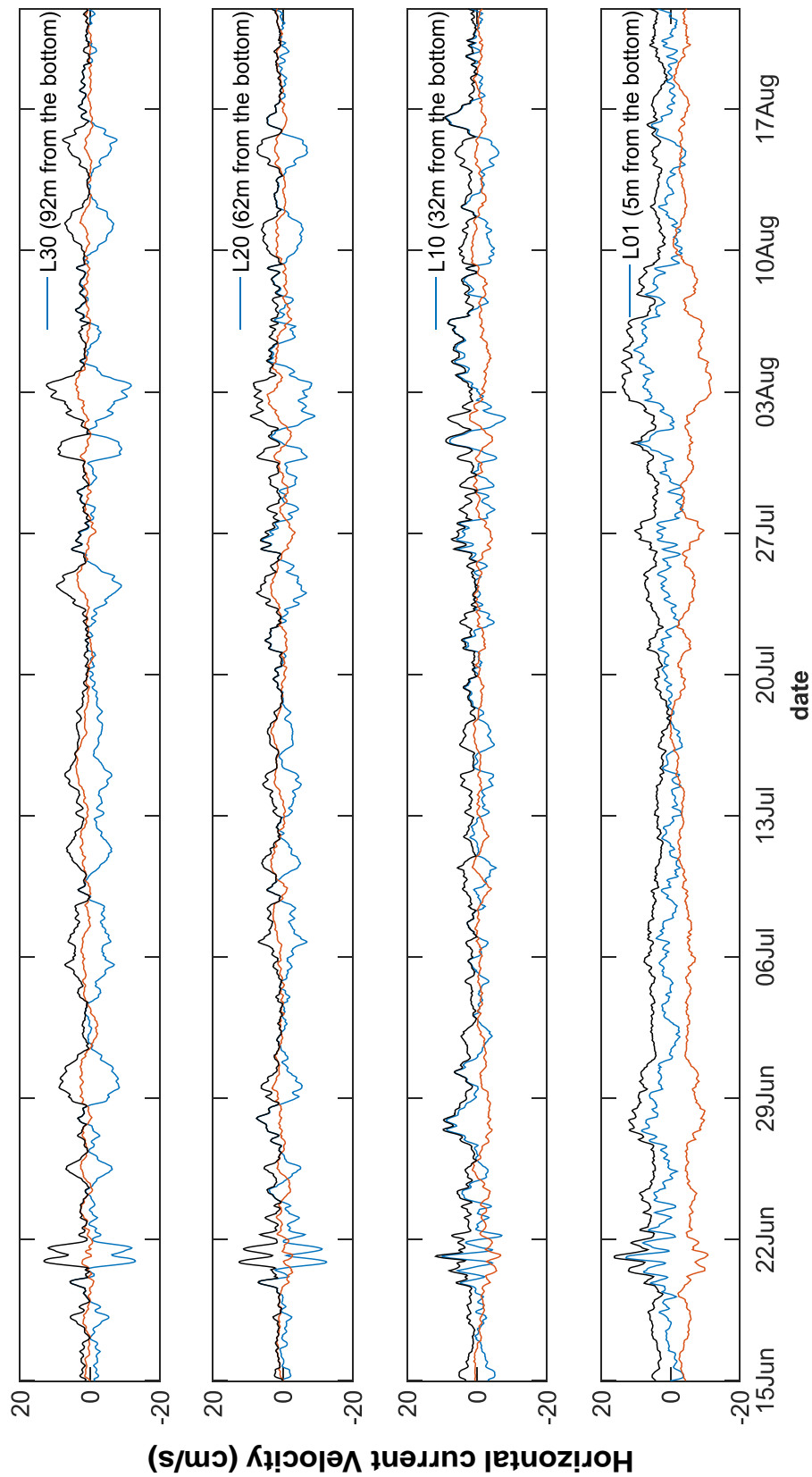
Appendix G. Prosecution.

Taxonomical Unit	N	%	P		
			min	hrs	Var
<u>Echnodermata</u>					
<i>Pannychia moseleyi</i>	62	0.86	-	-	-
Echinothurioida	21	0.29	-	-	-
<i>Solaster paxillatus</i>	73	1.02	-	-	-
Ophiuroidea	755	10.52	-	-	-
<u>Mollusca</u>					
<i>Buccinum yoroianum</i>	9	0.13	-	-	-
<u>Arthropoda</u>					
<i>Bathynomus doederleinii</i>	349	4.86	-	-	-
<i>Macrocheira kaempferi</i>	1002	13.96	1430	23.8	7.76
<u>Chordata</u>					
<i>Hexanchus griseus</i>	2	0.03	-	-	-
<i>Cephaloscyllium umbratile</i>	4	0.06	-	-	-
<i>Caelorinchus</i> sp.	16	0.22	1170	19.5	8.56
<i>Pterothrissus gissu</i>	390	5.43	1440	24	22.64
Zoarcidae	189	2.63	-	-	-
<i>Physiculus japonicus</i>	220	3.07	740	12.3	7.78
<i>Simenchelys parasiticus</i>	4052	56.46	1440 (1410)	24	15.79
<i>Helicolenus hilgendorfi</i>	9	0.13	-	-	-
<i>Eptatretus deani</i>	24	0.33	-	-	-
Assemblage (Total)	7177	100	1410 (1440)	23.5	11.06
Scavengers (and predators)	5511	76.8	1440 (1410)	24	12.92
Detritivores	838	11.7	-	-	-
Predators	828	11.5	1440	24	22.07

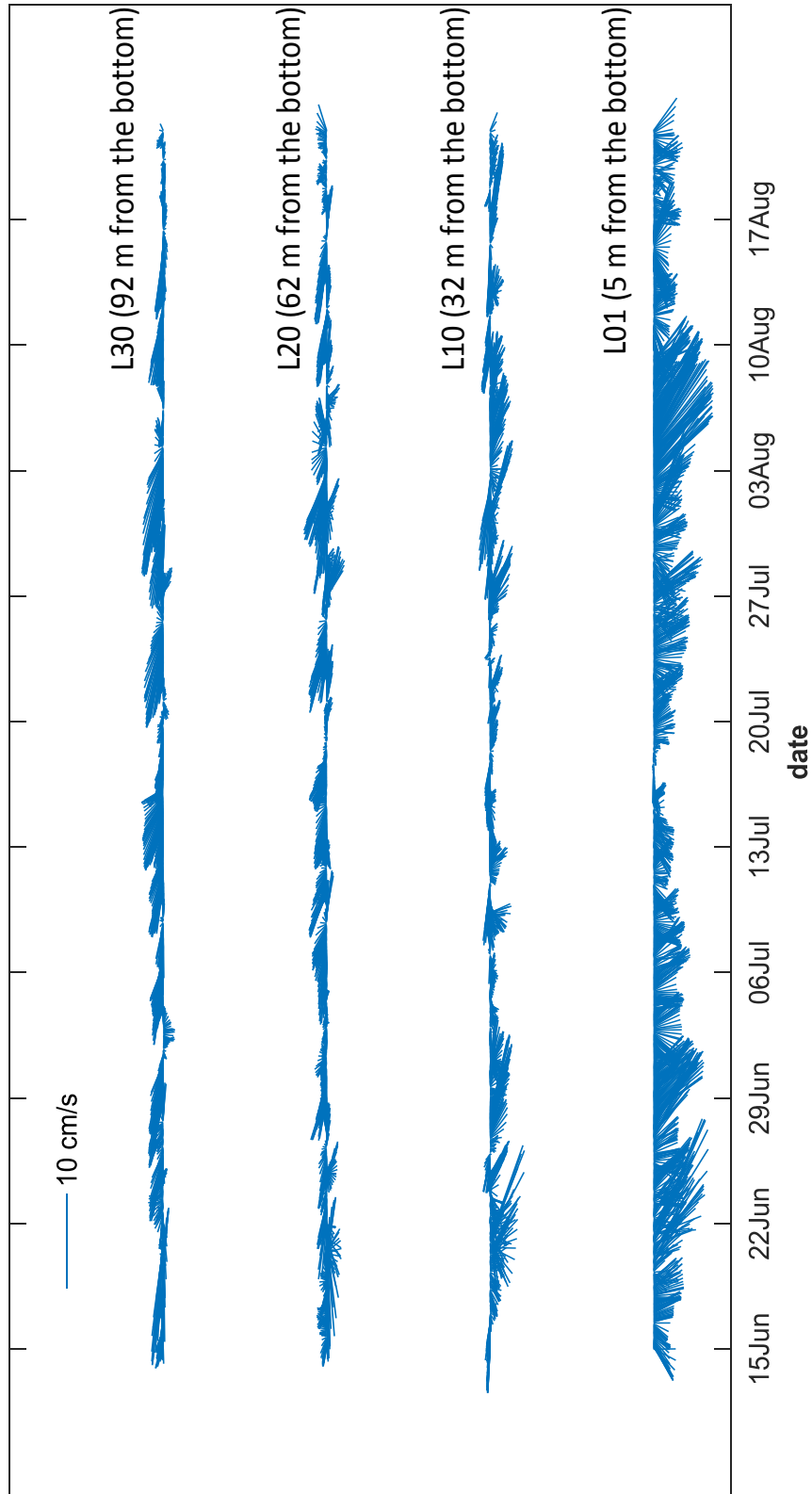
Appendix H. Seventy-two days-time series of visual counts for the different macrofauna taxonomical units identified during the scavenging process of the sunken whale carcass (following the same taxonomical order of Figure 2). Vertical dashed grey lines are the whale change positioning (see Figure 3).



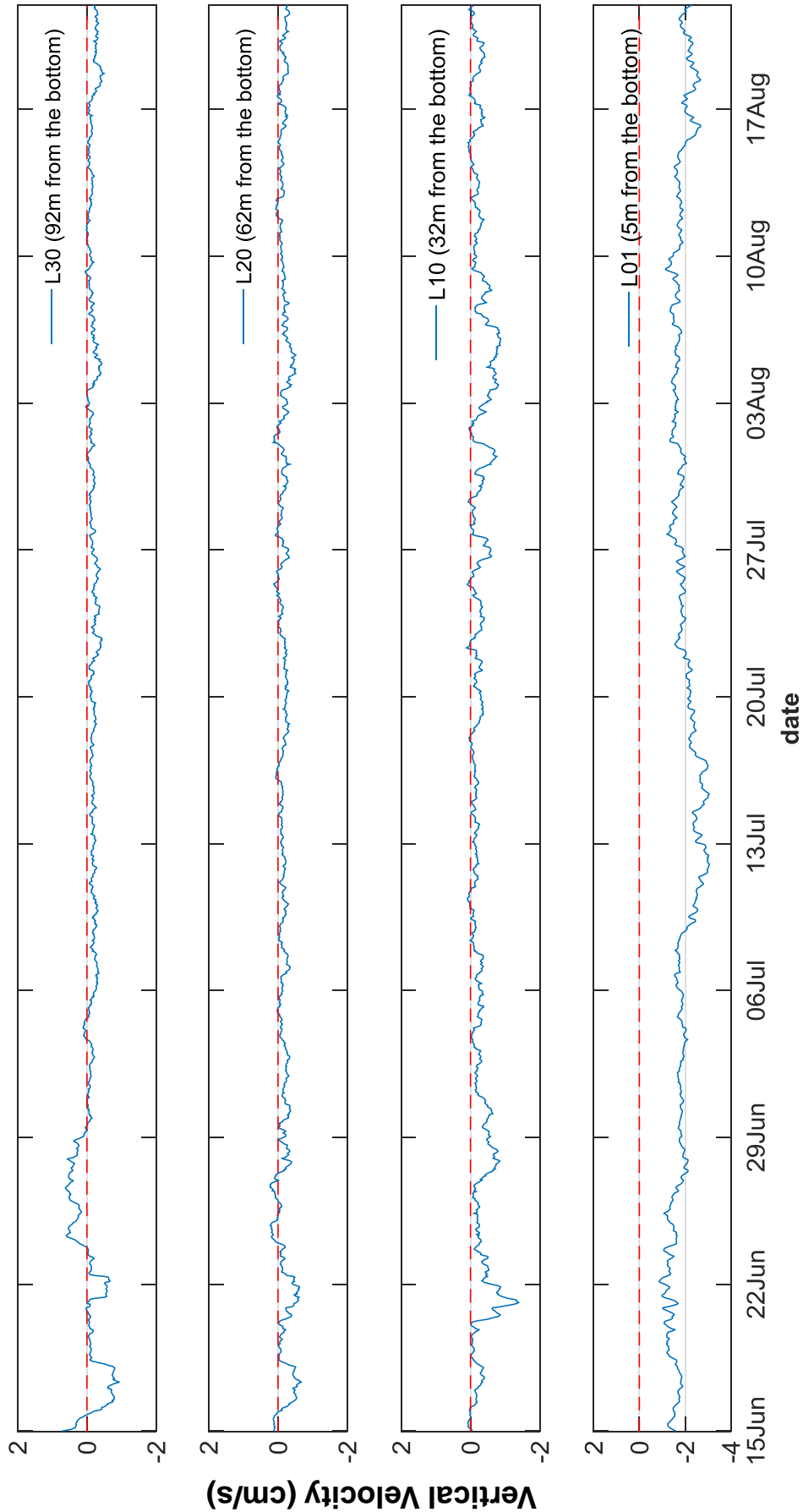
Appendix I. Time series of horizontal current data from the ADCP, at 5 m, 32 m, 62 m and 92 m above sea bottom, applying a 25 hrs. moving average window. Red and blue lines represent North-South and East-West component respectively. Black lines show the fluctuations of current velocity.



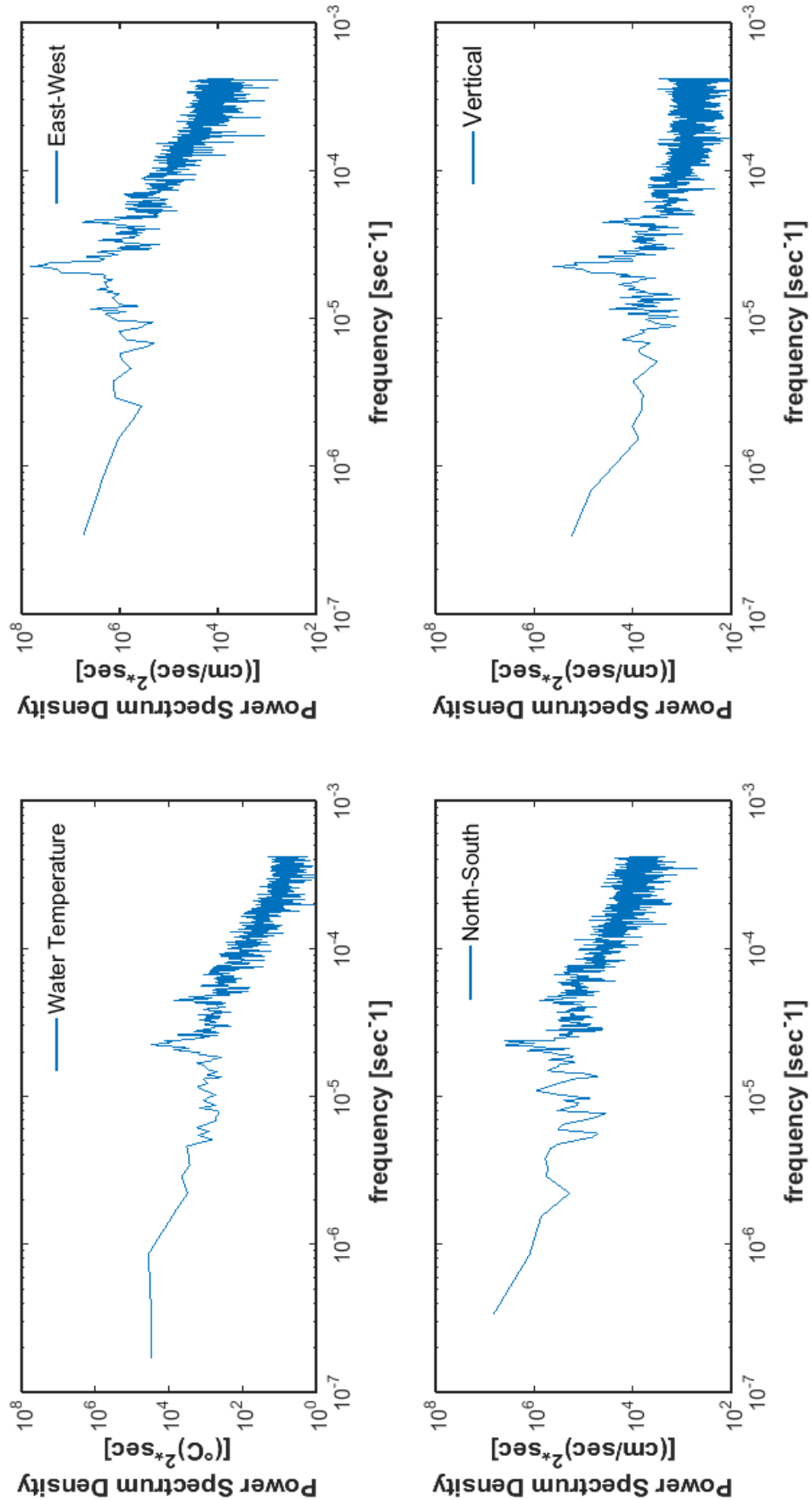
Appendix J. Stick diagrams of horizontal current data from the ADCP, at 5 m, 32 m, 62 m and 92 m above sea bottom, applying a 25 hrs. moving average window. Southeastward flows are dominant in the first 30 m above the sea bottom, whereas northwestward flow characterizes the water column from 32 m to 92 m above the sea bottom, creating a two-layer system.



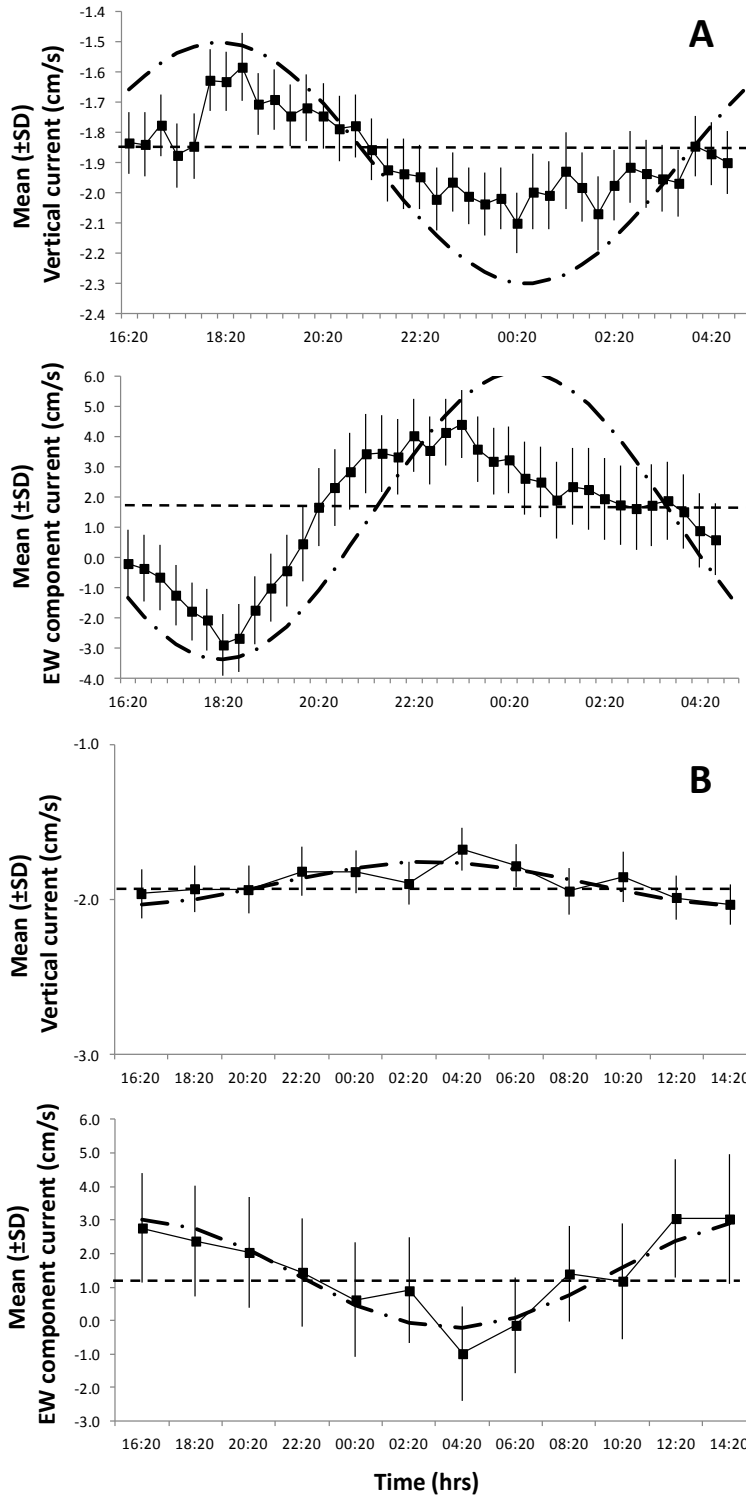
Appendix K. Time series of vertical current data from the ADCP, at 5 m, 32 m, 62 m and 92 m above sea bottom, applying a 25 hrs. moving average window. Dominant negative values indicate prominent downward flow in each layer, especially close to the bottom.



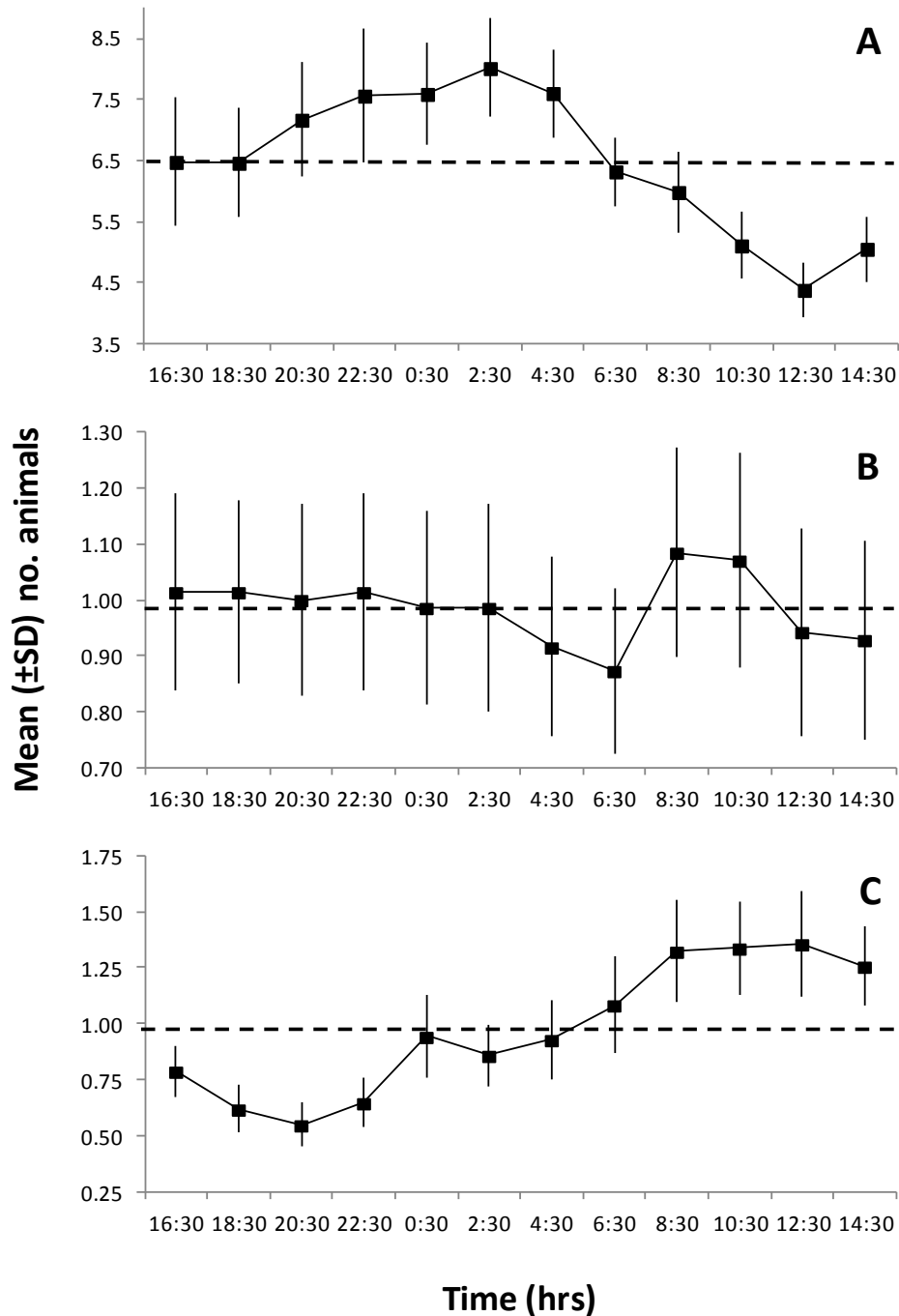
Appendix L. Power Spectra of water temperature, East-West, North-South and Vertical components of the velocity current data from the ADCP, at 5 m above sea bottom. Spectra of current data clearly show peak periods for 24, 12, and 6 hrs., whereas peaks for temperature data are only evident at 12 and 6 hrs. The flow near the sea bottom is affected by tidal periodicity. This rhythm may affect the behavior of marine organism



Appendix M. Waveform analysis outputs for ADCP data. Time series in A. have been partitioned in 12 hrs. segments, while time series in B. are at 24 hrs. length to show both diurnal and semidiurnal tides. The MESOR is the dashed horizontal line. The semidiurnal and diurnal Fourier component curves are superimposed for vertical and East-West current components (the dash-dotted lines), showing general accordance with the waveform analysis.



Appendix N. Waveform analysis outputs for visual counts time series of A. scavengers (and facultative predators), B. detritivores, and C. predators, indicating the occurrence of significant time shifted peaks (i.e. values above the MESOR; as horizontal dashed line) in the former (i.e. nocturnal) and the latter group (i.e. diurnal). Conversely, detritivores do not show any defined tendency (although a weak peaking occurs in the morning). MESORs are: A. 6.48; B. 0.99; C. 0.97.



Chapter 1. Diel behavioral rhythms in sablefish (*Anoplopoma fimbria*) and other benthic species, as recorded by the deep-sea cabled observatories in Barkley canyon (NEPTUNE-Canada).

Collaborators

María Pardo (ICM-CSIC, Spain)

Marjolaine Matabos (Ifremer Centre de Bretagne, REM/EEP, Laboratoire Environnement Profond, France)

Corrado Costa (CRA-ING, Italy)

S. Mihály (ONC, University of Victoria, Canada)

M. Canals (GRC, Spain)

Doya, C., Aguzzi, J., Pardo, M., Matabos, M., Company, J. B., Costa, C., & Canals, M. (2014).

Diel behavioral rhythms in sablefish (*Anoplopoma fimbria*) and other benthic species, as recorded by the Deep-sea cabled observatories in Barkley canyon (NEPTUNE-Canada). *Journal of Marine Systems*, 130, 69-78. I.F. 2.86 2014 <https://doi.org/10.1016/j.jmarsys.2013.04.003>

Chapter 2. The seasonal use of small-scale space by benthic species in a transiently hypoxic area

Collaborators

Damianos Chatzievangelou (Jacobs University, Germany)

Corrado Costa (CRA-ING, Italy)

Verena Tunnicliffe (University of Victoria, Canada)

Doya, C., Aguzzi, J., Chatzievangelou, D., Costa, C., Company, J. B., & Tunnicliffe, V. (2016). The seasonal use of small-scale space by benthic species in a transiently hypoxic area. *Journal of Marine Systems*, 154, 280-290. I.F. 2.174 2016 <https://doi.org/10.1016/j.jmarsys.2015.09.005>

Chapter 3. Seasonal monitoring of deep-sea megabenthos in Barkley Canyon cold seep by Internet Operated Vehicle (IOV)

Collaborators

Damianos Chatzievangelou (Jacobs University, Germany)

Nixon Bahamon (CEAB-CSIC, Spain)

Autun Purser (AWI, Germany)

Fabio C. De Leo (ONC, University of Victoria, Canada)

S. Kim Juniper (ONC, University of Victoria, Canada)

Laurenz Thomsen (Jacobs University, Germany)

Doya, C., Chatzievangelou, D., Bahamon, N., Purser, A., C. De Leo, Juniper, F. S. Kim, Thomsen L., Aguzzi J. Seasonal monitoring of deep-sea megabenthos in Barkley Canyon cold seep by Internet Operated Vehicle (IOV). PLoS One. <https://doi.org/10.1371/journal.pone.0176917>

Chapter 4. Faunal activity rhythms influencing early community succession of an implanted whale carcass offshore Sagami Bay, Japan

Collaborators

Emanuela Fanelli (ENEA, Italy)

Tiziana Ciuffardi

Antonio Schirone

Masaru Kawato (JAMSTEC, Japan)

Makoto Miyazaki (JAMSTEC, Japan)

Yoshihiro Furushima (JAMSTEC, Japan)

Corrado Costa (CRA-ING, Italy)

